# Cellular response to DNA damage after exposure to organophosphates *in vitro*.

A thesis submitted in accordance with the conditions governing candidates for the degree of

**DOCTOR OF PHILOSOPHY**

To Newcastle University


By

**Seth Eli Remington**

BSc (Hons) Medical Biochemistry (Birmingham University)

MSc Toxicology (Birmingham University)

October 2010

Institute of Cellular Medicine

The Medical Toxicology Research Centre

Wolfson Unit
Newcastle University
Newcastle Upon Tyne
NE2 4AA

## Cellular response to DNA damage after exposure to organophosphates *in vitro*

This study aimed to investigate the potential of dichlorvos (DCV), chlorpyrifos (CPF) and sarin (GB) to induce DNA damage in vitro. DNA damage was measured by the alkaline comet assay in the neuroblastoma SHSY-5Y and lymphoblastoid TK6 cells and corroborated using phosphorylation of H2AX. Cytotoxicity was measured using the MTT assay in TK6 cells. The activation of DNA damage signalling pathways was investigated using western blotting. TK6 cells were used to investigate p53 levels and cleaved PARP-1 after exposure to OPs. Cell cycle effects were investigated in A549 cells by measuring the phosphorylation of the retinoblastoma and cdc2. Whether a slowing of the cell cycle allowed for initiation of repair mechanisms was investigated in cells lacking the DNA repair pathways base excision repair (BER) and non homologous end joining (NHEJ) after DCV.

DCV induced DNA damage, the genotoxic potential was also corroborated by increased expression of γH2AX. DCV was cytotoxic at high concentrations. DCV results in increased p53 levels but no apparent phosphorylation on Ser15, which is known to be phosphorylated when exposed to other genotoxins. A G2/M block was found after exposure to dichlorvos as well as the possible initiation of DNA repair mechanisms NHEJ and BER.

CPF and CPF oxon induced DNA damage in TK6 cells with a decrease in cell viability. Western blot analysis did not show a p53 response to the DNA damage with CPF. A small p53 effect at 24hours was seen with chlorpyrifos oxon but p53 may have been induced at an earlier time point. It is possible that the DNA damage observed was due to both direct DNA damage and other cellular effects, as the cells undergo apoptosis or necrosis and subsequent DNA degradation.

Sarin caused low levels of DNA damage after 1 hour, which was partially repaired at 24 hours. This resulted in low level cytotoxicity and a rapid but transient increase in p53 levels and a G2/M cell cycle arrest.

## Table of Contents

**Acknowledgements**

I would first of all like to thank all my supervisors. Professor Faith Williams for her guidance and help throughout the PhD. thank you for teaching me how to think like a scientist. Dr Paul Jowsey, thank you for explanations, guidance and for teaching me how to conduct my studies. I would also like to thank my supervisor Professor Peter Blain, I was given a fantastic opportunity by you and thank you for all your support financial and academic throughout the study.

Everyone in the Medical toxicology research centre, for always being there with advice and friendly chats of encouragement.

To Craig Moore, for teaching me you can prove anything with facts, I always knew a PhD would be hard I never expected it to have been fun; It wouldn't have been the same without you.

And finally to my parents who have always supported me in whatever I have done I hope I have made you proud.

## List of Figures

## List of Tables

## List of Abbreviations

ACh – Acetylcholine
AChE – Acetylcholinesterase
AIF – Apoptosis inducing factor
APAF-1 – Apoptosis protease activating factor
AP – Apurinic/apyridimic
ATM – Ataxia telangiectasia mutated
ATP – Adenosine triphosphate
ATR - Ataxia telangiectasia related
BER – Base excision repair
CES – Carboxylesterase
CHK – Check point kinase
CHO – Chinese hamster ovary
COM – Committee on mutagenicity
CPD – Cyclobutane pyrimidine dimer
CPF - Chlorpyrifos
CPFO - Chlorpyrifos oxon
CYP – Cytochrome P450
DCV – Dichlorvos
DMEM – Dulbecco's Modified Eagles Medium
DMSO – Dimethyl sulfoxide
DNA – Deoxyribonucleic acid
DNA-PK – DNA dependent protein kinase
DSB – Double strand break
ECL- Enhanced Chemiluminescence
EPA – Environmental Protection Agency
EDTA - Ethylenediaminetetraacetic acid
ETOP- Etoposide
FADD – FAS associated death domain
FBS – Foetal bovine serum
FPG – Formamido –pyrimidine-DNA glycosylase
GB - Sarin
GSH – Glutathione
GST – Glutathione transferase enzymes
HR – Homologous recombination

HRP – Horseradish peroxidase

HSE – Health and Safety Executive

IMPA – Isopropyl methyl phosphonic acid

IPA – Isopropanol

IP – Intra peritoneal

IR – Ionizing radiation

LCMS – Liquid chromatography mass spectrometry

LDS – Lithium dodecyl sulfate

LMPA – Low melting point agarose

MN – Micro nucleus

MPA - Methyl phosphonic acid

MTT - 3-(4, 5-dimethylthiazol-2-yl)-2,5-diphenyl tetrazolium bromide

MTS - {3-(4,5-dimethylthiazol-2-yl)-5-(3-carboxymethoxyphenyl)-2-(4-sulfophenyl}-2*H*-tetrazolium

NAD – Nicotinamide adenine dinucleotide

NER – Nucleotide excision repair

NHEJ – Non homologous end joining

NTE – Neuropathy Target Esterase

OP – Organophosphate

OPIDP – Organophosphate Delayed Polyneuropathy

OTM – Olive Tail Moment

PARP-1 – Poly ADP(ribose) Polymerase

PBS – Phosphate buffered saline

PBS-T – PBS containing 0.2% Tween

PCE – Polychromatic erythrocytes

PON1 – Paraoxonase 1

Rb - Retinoblastoma

ROS – Reactive oxygen species

SCE – Sister Chromatid Exchange

SCGE – Single cell gel electrophoresis

SSB- Single strand break

TCPY - 3,5,6-trichloror-2 pyridinol

TNF-1 - Tumour necrosis factor

UV – Ultraviolet light

List of Abstracts and Presentations

British Toxicology Society – 2008 – Investigations into the genotoxic potential of dichlorvos

Society Of Toxicology – 2009 – Investigations into the genotoxic potential of organophosphates

British Toxicology Society - 2009 – Cellular response to DNA damage in A549 cells Student prize winner

**Investigations Into The Genotoxic Potential Of Dichlorvos**

Remington SE**,** Jowsey PA, Williams FM, Blain PG
Medical Toxicology Research Centre, Newcastle University, Newcastle upon Tyne NE2 4AA
Author's email s.e.remington@newcastle.ac.uk

Dichlorvos is an organophosphate pesticide which is a potent acetylcholinesterase (AChE) inhibitor in insects and in man. The effects of AChE inhibition are well documented but several studies suggest that dichlorvos is also able to cause DNA damage. The genotoxic potential of dichlorvos has been reviewed extensively with reports by the IARC (1991) and Mennear (1998) it is generally considered that Dichlorvos is DNA damaging *in vitro* (Booth 2007). In this study the potential of dichlorvos to cause DNA damage will be investigated by the comet assay in parallel with the measurement of DNA damaging signalling pathways.

Neuroblastoma (SH-SY5Y) cells were exposed to acetone (vehicle control), 2.7nM or 2.7µM dichlorvos for 10mins and DNA damage measured as Olive Tail Moment (OTM) was determined using the alkaline comet assay. Hydrogen peroxide (10µM) for ten minutes was used as a positive control, untreated cells were used as a control. DNA damage was also assessed in TK6 lymphoblastoid cells by the comet assay. The damage seen in initial experiments with SHSY-5Y cells was after a short exposure time at relatively low doses. Therefore, experiments were repeated using higher doses. TK6 cells were exposed to a range of dichlorvos concentrations (2, 20, 40, 60 and 100µM) for 24 hours and DNA damage measured. In parallel cytotoxicity was measured using the MTT assay and cell viability was expressed as a percentage of control. In order to establish whether dichlorvos initiated DNA signalling cascades or apoptosis in TK6 cells, Western blotting was used to investigate p53 induction and PARP-1 cleavage after exposure to 2, 20 or 100µM dichlorvos for 24 hours. Etoposide was used as a positive control for p53 induction and PARP-1 cleavage.

In SHSY-5Y cells, DNA damage was increased at both 2.7nM (p value = 0.0062) and 2.7µM (p value = 0.0002) when compared with control. TK6 cells displayed a dose-dependent increase in DNA damage after 24 hours exposure to dichlorvos (Table 1). 2µM dichlorvos had no effect on cell viability at 24 hours, however at 20 µM - 60 µM there was a loss of 20 % viability and 100 µM caused a 40% reduction in cell viability (Table1).

Table1. DNA damage and cell viability in TK6 cells by DDVP (2, 20, 40, 60 and 100µM) for 24 hours. DNA damage was measured as Olive Tail Moment (OTM) (P value =<0.0001*** Mann Whitney U). Cytotoxicity was measured as a percentage of control (MTT).

| | **Untreated** | **Acetone** | **2µM** | **20µM** | **40µM** | **60µM** | **100µM** | **$H_2O_2$ (10µM)** |
|---|---|---|---|---|---|---|---|---|
| **DNA damage (OTM)** | 0.47 | 0.34 | 2.04*** | 2.77*** | 3.91*** | 4.25*** | 6.72*** | 18.62*** |
| **Cytotoxicity (% viability)** | 100.00 | 93.7 | 82.6 | 80.2 | 82.6 | 78.8 | 63.2 | 3.3 |

Western blot analysis showed that the levels of full-length PARP-1 decreased only after 100µM dichlorvos and this is indicative of apoptosis. A background level of p53 was seen in the untreated and acetone treated cells with a high induction occurring with 20µM dichlorvos and etoposide which was indicative of DNA repair.

The comet assay has demonstrated that dichlorvos can cause DNA damage at low nM concentrations, after only 10 minute exposure. Induction of p53 provides further evidence of the ability of dichlorvos to bind to DNA *in vitro*.

*We acknowledge the UK Home Office for funding this research*

**References**

Booth ED, Jones E Elliot BM. Review of the in vitro and in vivo genotoxicity of dichlorvos. Regulatory Toxicology and pharmacology 49 (2007) 316-326.

## Investigations Into The Genotoxic Potential Of Organophosphates

**Remington SE,** Jowsey PA, Williams FM, Blain PG
Medical Toxicology Research Centre, Newcastle University, Newcastle upon Tyne NE2 4AA
Author's email s.e.remington@newcastle.ac.uk

Organophosphates (OP's) are used as pesticides which are a potent acetylcholinesterase (AChE) inhibitor in insects and in man. The effects of AChE inhibition are well documented but several studies suggest that OP's are also able to cause DNA damage. In this study the potential of DCV and chlorpyrifos (CPF) to cause DNA damage will be investigated by the comet assay in parallel with the measurement of DNA damaging signalling pathways.

SHS5Y Neuroblastoma cells and TK6 lymphoblastoid cells were exposed to a range of concentrations (0.01, 0.1, 1, 10 and 100μM) of both DCV and CPF. DNA damage was measured by the comet assay after exposure for 1 hour and 24 hours. Cytotoxicity was measured using the MTT assay and cell viability was expressed as a percentage of control. In order to establish whether the OP's initiated DNA signalling cascades or apoptosis in TK6 cells, Western blotting was used to investigate p53 induction and cleaved PARP-1 after exposure to (0.01, 0.1, 1, 10 and 100μM) for 1, 2, 4 and 24 hours.

The background DNA damage measured in olive tail moment in untreated and acetone treated cells (giving an OTM value of <1) was increased with an increase in dose of OP. Treatment with 100μM DCV gave an OTM value of 4.04 (±1.04) whilst CPF gave a value of 2.35 (±0.72) after 1 hour. A decrease in cell viability was seen with an increase in dose after 24 hours. A 40% and an 80% loss occurred with 100μM DCV and CPF respectively.

Western blot analysis showed that the levels of cleaved PARP-1 slightly increased after 100μM DCV and this is indicative of apoptosis after 24 hours. A background level of p53 was seen in the untreated and acetone treated cells with a maximum induction occurring with 100μM DCV after 4 hours.

The comet assay has demonstrated that DCV and CPF can cause DNA damage after exposure for an hour. 100μM DCV caused DNA damage without significant loss of cell viability or an indication of high apoptotic activity. Induction of p53 provides further evidence of the genotoxicity of DCV *in vitro*.

## Cell response in A549 cells after DNA damage caused by organophosphates

Remington SE**,** Jowsey PA, Williams FM, Blain PG
Medical Toxicology Research Centre, Newcastle University, Newcastle upon Tyne NE2 4AA
Author's email s.e.remington@newcastle.ac.uk

Organophosphates (OP's) are acetylcholinesterase inhibitors, although some studies have suggested that they are also able to damage DNA. The cellular response to genotoxic stress is initiated by the activation of the ATM (ataxia-telangiectasia, mutated) and ATR (ATM and Rad-3 related) protein kinases. These kinases phosphorylate various target proteins including p53, the checkpoint kinases Chk1 and Chk2, p53 and histone H2AX. These proteins along with many others act to slow the cell cycle progression, enhance the DNA repair capacity of cell or to direct cells to apoptosis. H2AX phosphorylation on serine 139 has been demonstrated in response to a range of DNA damaging agents and has been used as a sensitive indicator of genotoxic damage. This study aimed to investigate the potential of dichlorvos (an oxon) and chlorpyrifos (a thiosulphate) to induce DNA damage. Extensive H2AX phosphorylation occurs adjacent to DNA damage and can be detected by immunofluorescence resulting in individual foci within the cell nucleus that can be counted. Also the activation of DNA damage signalling pathways was investigated using western blotting. Finally cell cycle effects were investigated by measuring the phosphorylation of the retinoblastoma protein (hypophosphorylated when cell the cell cycle is arrested at the G1/S phase) and cdc2 (hyperphosphorylated during G2/M phase arrest).

The phosphorylation and cellular localisation of H2AX was investigated using immunofluorescence after exposure of cells to dichlorvos (0.01, 0.1, 1, 10 and 100μM) for 4 hours. Hydrogen peroxide (100μM) was used as a positive control. The induction of DNA damage signalling pathways was investigated using Western blotting. A549 cells were treated with dichlorvos (10μM and 100μM) and chlorpyrifos (10μM and 100μM) 24 hours. Etoposide (5μM and 50μM) was used as a positive control for phosphorylation of p53 and for cell cycle effects.

Dichlorvos showed clear phosphorylation of H2AX which formed nuclear foci after treatment in A549 cells after dichlorvos for 4 hours. These were not as clear or numerous in comparison with the hydrogen peroxide control. Western blot analysis showed that dichlorvos caused an induction of p53 after 4 hours but did not show a significant induction of p53 after 24hours although this was clear with etoposide. Dichlorvos did not cause a decrease in Rb phosphorylation after 4 or 24 hours. There was a clear decrease with etoposide after 24hours at both 5 and 50 μM etoposide. A G2-M phase block was indicated by an increase phosphorylation of cdc-2 this occurred after 4 hours with 5μM and 50μM etoposide but not dichlorvos. After 24r hours a decrease was seen in the phosphorylated cdc-2 protein with etoposide, other studies (Dan and Yamori, 2000) have confirmed this finding after the initial exposure. Chlorpyrifos does not show an induction of p53 or any cell cycle effects after 24 hours, the induction of p53 and cell cycle effects was clear after 24 hours after treatment with etoposide at both 5 and 50 μM.

Dichlorvos caused the formation of H2AX foci and this is an indication of the genotoxic potential of dichlorvos in A549 cells. The induction of p53 at 4 hours further suggests that dichlorvos is a genotoxin in vitro. No cell cycle effects were seen with either dichlorvos or chlorpyrifos.

# *Chapter 1*

# *Introduction*

# 1.0 Introduction

## 1.1 Organophosphates Compounds

The first organophosphates (OPs) were synthesised for use as insecticides in the 19th century and continue to be used as such today, with over 100 commonly used pesticides available worldwide. The extensive use of OPs as pesticides has led to an increase in poisonings, with 750,000 to 3,000,000 poisonings estimated worldwide per year. OPs cause a toxic effect by inhibiting the acetylcholinesterase (AChE) enzyme and disrupting neuromuscular transmission. This property led to a number of highly toxic compounds being developed and stockpiled for use as nerve agents, including sarin, soman and tabun. Nerve agents were used in the Iran-Iraq war in the mid-1980's (Holstege et al., 1997), leading to the exposure of many Iranian soldiers and civilians. More recently, in 1995 in Japan, the Aum Shinrikyo religious cult released Sarin into the Tokyo subway in a terrorist attack resulting in multiple fatalities and casualties (Vale., 2005). In addition to deliberate exposure there are a number of people exposed occupationally each year. For example pest control workers and farmers will come into close contact with pesticides that are often OPs. There is evidence that some OP pesticides may have in vivo genotoxic effects, suggesting a possible link to cancer with long term or repeated heavy exposures in farmers, who use sheep dip containing diazanon (Hatijan et al., 2000). Therefore a number of people worldwide can be exposed to OPs and it is important to understand if any toxicity occurs after exposure to OPs.

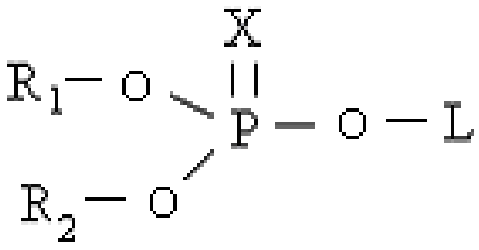


**Figure 1.1** General organophosphate structure. X = oxygen or sulphur, $R_1$ and $R_2$ = alkyl groups, L = leaving group Mutch et al. (1995).

Figure 1.1 shows that the OP is organised around a central phosphorous with a number of groups attached to it. Always present is the leaving group, represented by L, which is removed when the OP phosphorylates target proteins. Also present is either an oxygen or sulphur atom double bonded to the central phosphorous. The R1 and R2 groups vary from compound to compound but are generally alkoxy groups (Costa., 2006). In order for an OP compound to become effective, it is necessary for it to be in an oxon form. OPs that contain a sulphur molecule undergo bioactivation to remove the sulphur thus allowing for oxon formation.

### 1.2 Mechanisms of acute toxicity

Acetylcholine esterase (AChE) is the primary target of OP toxicity. This enzyme is classed as a B esterase whose major role is the hydrolysis of acetylcholine (ACh). ACh is a major neurotransmitter in the peripheral and central nerve system. Hydrolysis of ACh by AChE is essential for proper regulation of the nervous system. OPs with a P=O moiety are able to phosphorylate a hydroxyl group of a serine situated in the catalytic site of AChE. This disrupts the ability of the enzyme to bind to its normal substrate. The effects of OPs on the enzyme are long-lived because the bond between the carbonyl carbon of the acetylcholine (acetate component), is not as stable as the bond between the phosphorous of the OP oxon and the esteric site of the AChE (Costa et al., 2003). This is displayed nicely in that the carbon to enzyme bond is broken in a matter of seconds whereas the phosphorous to enzyme bond can take hours or days to be broken, dependent upon the chemical structure of the OP (Cho et al., 2004). The bond between OP and AChE is hydrolysed by water at a very slow rate. The rate can vary depending upon the R group of the OP compound (Worek et al., 2005). However this process can be altered by the use of oximes, containing a positively charged atom that is able to bind to the anionic site of AChE; this is then able to assist in the removal of the OP (Chunyuan et al., 1999). This is considered a therapy for nerve agent or OP poisoning but the administration of an oxime such as pralidoxime needs to be as soon as possible after exposure to the toxin due to the “aging effect” of the OPs, which render reactivation of a phosphorylated AChE impossible (Luo et al., 1999). Aging consists of the loss of one of the two R groups. The rate of aging depends mainly on the type of R group. (Costa et al., 2006). After an enzyme has become aged the only means of replacing the enzyme is through synthesis of new enzyme.

ACh is released from cholinergic nerves and is disposed of solely by the action of AChE. When this process is halted or slowed by the action of OPs it causes the accumulation of ACh at the presynaptic terminal. This build up causes a "cholinergic syndrome" which presents itself in an individual by increased sweating, bronchial secretion and salivation, miosis, bronchoconstriction, gastrointestinal motility is increased possibly causing vomiting, diarrhoea, muscle tremors and muscular twitching occurs along with other central nervous effects. Acute exposure can lead to death, likely due to respiratory failure caused by inhibition of respiratory centres in the brainstem, flaccid paralysis of the respiratory muscles and the other bronchial complications previously mentioned.

Another clinical manifestation of OP poisoning exists and this is known as the intermediate syndrome. This syndrome is characterised by weakness in respiratory, neck and proximal limb muscles. This does not occur as a direct effect of AChE inhibition and appears several hours after the beginnings of the cholinergic symptoms, but before the appearance of symptoms of organophosphate induced delayed polyneuropathy (OPIDP), hence the label intermediate (Yang et al., 2007). The actual mechanism for this syndrome is unknown but one likely hypothesis is that muscle weakness occurs due to receptor desensitisation, due to prolonged over stimulation.

Aside from the inhibition of AChE, OPs can cause another type of toxicity called organophosphate induced delayed polyneuropathy (OPIDP). Symptoms of this condition become apparent after 2-3 weeks and include swelling and a tingling sensation in the hands and feet, sensory loss, muscle flaccidity and ataxia (Moretto et al., 2006). The main nerve types affected are the larger or longer myelinated central and peripheral nerve fibres. The molecular target is an enzyme found in the nervous tissues called neuropathy target esterase (NTE). This enzyme is inhibited by OPs in a manner analogous to the inhibition of AChE. In order for OPIDP it is necessary for the NTE to become phosphorylated and aged by at least 70% (Moretto et al., 2006). The function of the enzyme is not clear, but it is found in the peripheral nerve system, brain and spinal cord. Neuropathy occurs after the NTE has aged, involving cleavage of the lateral side chain from the phosphorylated NTE. This occurs in the axon and the neuron cell body. These molecular changes are followed by

characteristic changes in the peripheral nerve, including the degeneration of long axons, with the loss of myelin and Schwann cell proliferation in the nerves.

## 1.3 Metabolism of OPs

OPs are metabolised by cytochrome P450s (CYPs) and a number of different esterases. These enzymes differ between individuals in their activity and this can greatly affect the toxicity of the OP, as some require bioactivation. Multiple forms of CYPs are responsible for the bioactivation of OPs by catalysing the desulfuration to form an oxon, for example CYPs 2D6, 3A5, 2B6 and 3A4 are responsible for the bioactivation of chlorpyrifos to chlorpyrifos oxon (Mutch and Williams., 2006) Additionally CYPs are also responsible for the detoxification of OPs. Further different isoforms of the CYPs can lead to different detoxification actions, for example, while CYP2B6 metabolizes chlorpyrifos primarily to the oxon, it metabolizes parathion primarily to p-nitrophenol (Buratti et al., 2002). In addition to being metabolised by CYPs OPs also undergo catalytic hydrolysis by phosphotriesterases or esterases. These enzymes are not inhibited by OPs and play an important role in the detoxification of OPs. The most documented example of these enzymes is Paraoxonase (PON1). This enzyme is known to hydrolyse the oxon form of chlorpyrifos (Mutch and Williams., 2006). The metabolically activated OPs also interact with serine esterases (B-esterases), examples include carboxylesterase and buturylcholinesterase. These enzymes are inhibited by OP's but they are unable to catalytically hydrolyse them and therefore act as scavenger molecules.

### 1.3.1 Genetic variation and metabolism of OPs

The polymorphisms that exist between individuals means that each individual has different enzyme activity and will therefore react differently in relation to the activation and detoxification after exposure to OPs. Whether these differences between individuals have any effect on OP metabolism and toxicity is not clear. For example, genetic variations exist between individual glutathione S-transferase enzymes (GSTs). GSTs contribute to the phase II biotransformation of xenobiotics. GSTs contribute to this type of metabolism by conjugating these compounds with reduced glutathione to facilitate excretion from the

body. These enzymes may be particularly important for those OPs with methyl groups in the side chains as these can form a potential nucleophile and glutathione is a very efficient nucleophillic scavenger (Costa et al., 2005). The polymorphisms that exist may be particularly important in an individual's ability to metabolise OPs effectively, as it has been found that dichlorvos is extensively metabolised by rats in the liver via two enzymic pathways, one which is glutathione-dependent, the other is glutathione independent. Therefore glutathione (GSH) availability can be a rate limiting factor for dichlorvos elimination (USEPA 1996). Glutathione predominantly exists in its reduced state in cells (termed GSH) which is also able to scavenge free radicals produced from reactive oxygen species, which OPs such as dichlorvos are believed to cause.

Esterases are able to hydrolyse the oxons of OPs directly to their constituent acid and alcohol, thereby detoxifying them and giving protection against the toxic effects of OPs. Paraoxonase 1 (PON1) is an example of an A esterase that is able to protect against OP toxicity (Furlong et al., 2002). It received its name from paraoxon; it was found to metabolise the active metabolites of parathion but not the parent compound, in addition PON1 is not able to metabolise several other OPs including malaoxon and dichlorvos (Furlong et al., 2010). PON1 is a high density lipid associated esterase, is calcium dependent and is predominantly synthesised in the liver. Early studies have indicated that there are differing levels of PON1 activity in the plasma in human populations and this demonstrates a polymorphic distribution (Costa et al., 2003) and this exhibits a large variation in activity and concentration amongst individuals. Currently two polymorphisms have been identified that can have an effect on the catalytic activity of PON1. These are found at position 192 where a Gln/Arg substitution occurs and at position 55 where Leu/Met occurs, both polymorphisms have been found to affect the catalytic activity of the enzyme (Sirivarasai et al., 2007).

One such protective biochemical mechanism arises from the family of nontarget serine esterases, which the inhibition of these esterases does not prove to be life threatening. These include the carboxylesterases, (CES1 found in monocytes and liver and CES2 found in the intestine and liver) and butyrylcholinesterase. Inhibition of these esterases serves as protection, because phosphorylation at the active site removes the OP molecule, thus accomplishing a stoichiometric detoxication (Chambers et al., 2003). Therefore the amount

of protection that nontarget esterases can provide is limited by the number of nontarget esterase molecules present and this will differ between individuals.

### 1.3.2 Metabolism of chlorpyrifos

Chlorpyrifos upon entering the body is rapidly metabolised and converted by CYPs to its oxon form. The oxon can then be spontaneously hydrolysed to form a dialkyl phosphate metabolite and a corresponding organic metabolite containing the leaving group portion of the original compound. For example chlorpyrifos is metabolised to diethylphosphate and 3,5,6-trichloror-2-pyridinol (TCPY). If chlorpyrifos is not converted to its oxon the compound is hydrolysed to its organic group metabolite (diethylthiophosphate) and dialkylthionate metabolites (TCPY) (Meeker et al., 2004; Nolan et al., 1984). Please refer to figure 1.2.

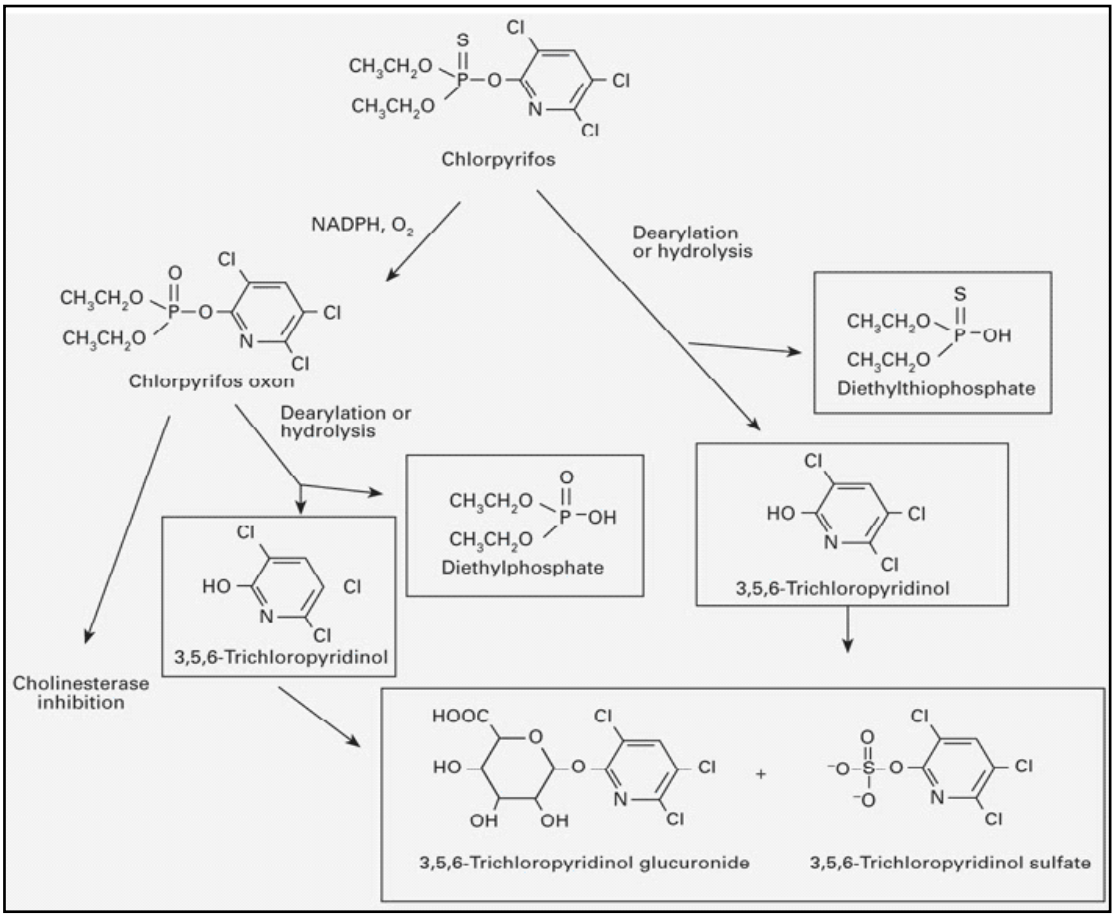


Figure 1.2. A schematic of the Metabolism of Chlorpyrifos taken from Wessels et al 2003

### 1.3.3. Metabolism of dichlorvos

As with previously mentioned chlorpyrifos and other OPs the liver is the main site of detoxification converting to dichlorvos to dimethyl phosphate. Several species have been evaluated in their ability to metabolise dichlorvos and each follows a similar path (Figure 1.3). The differences between species are generally attributed to the differing availabilities of enzyme and the rate at which these metabolic pathways occur. As previously mentioned dichlorvos is rapidly hydrolysed to dichloroacetaldehyde and dimethyl phosphate by PON1 (A esterase) and carboxylesterases mainly in the liver. Several species have been evaluated for their ability to metabolise dichlorvos and show qualitatively similar pathways with some quantitative differences. Also in the presence of glutathione, glutathione-S-transferase catalyses formation of desmethyl dichlorvos and methylglutathione but this pathway is minor. Desmethyldichlorvos is then a substrate for PON1. Dichloroacetaldehyde is unstable and is converted to dichloroethanol which forms dichloroethanol glucuronide. Dichloroacetaldehyde also undergoes dehalogenation (Wooder et al., 1977).

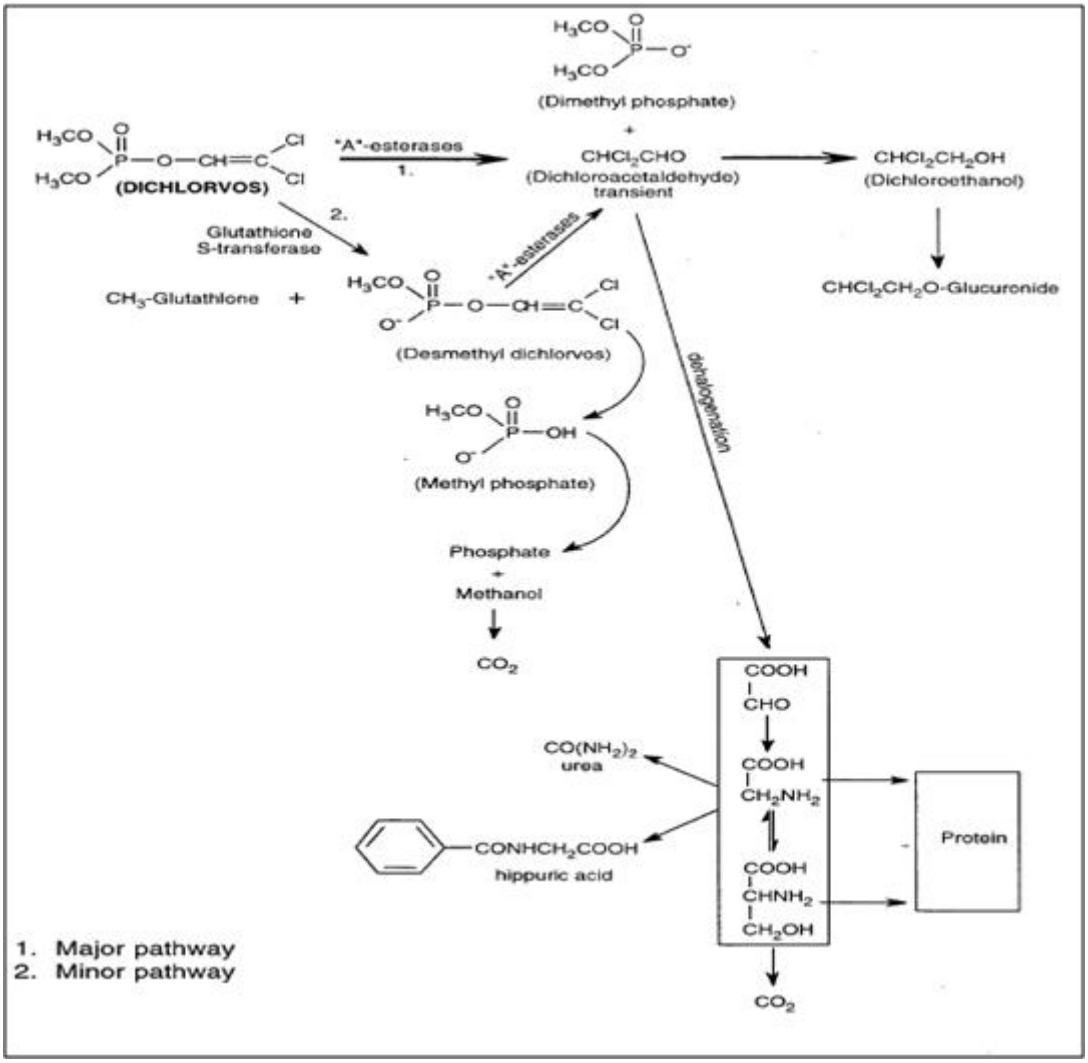


Figure 1.3. A schematic of the Metabolism of Dichlorvos. Adapted from Wooder et al., 1977.

### 1.3.4 Metabolism of sarin

Sarin will rapidly bind to AChE and other esterases. These nerve agents contain a C-P bond that is almost unique, for example, it is not found in OP pesticides; the C-P bond is very resistant to hydrolysis which is why they are effective as nerve agents (Munro et al., 1999). Esterase enzymes, such as paraoxonase, hydrolyze sarin to inactive metabolites (Davies et al., 1996) Isopropyl methyl phosphonic Acid (IMPA), which slowly undergoes further hydrolysis to the very stable methyl phosphonic acid (MPA) (figure 1.4). Matsuda et al. (1998) detected the sarin metabolite isopropyl methylphosphonic acid in the brains of victims of the Tokyo subway attack. Minami et al. (1997) found peak levels of the sarin

metabolite isopropyl methylphosphonic acid in human urine 10–18 h following the Tokyo subway attack. Esterase enzymes, such as paraoxonase, hydrolyze sarin to inactive metabolites (Davies et al., 1996).

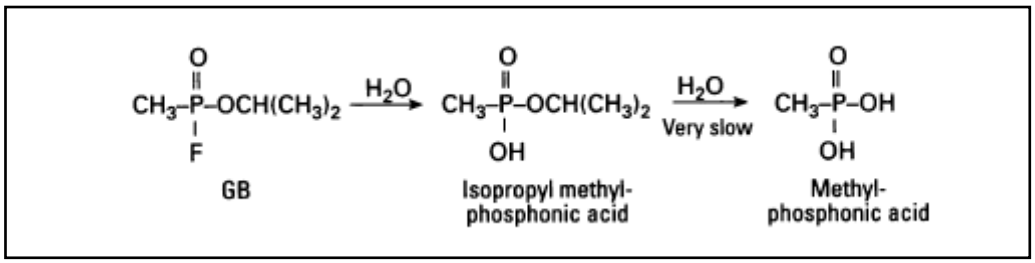


Figure 1.4 A diagram showing the hydrolysis of sarin. Taken from Munro et al. (1999).

## 1.4 Studies investigating the genotoxic effects of OPs

A number of studies have described an increase in certain cancers in occupationally exposed individuals, for example non-Hodgkins lymphoma in farmers exposed during treatment of crops with OP pesticides. (Dreiher et al., 2005). In addition, Atherton et al. (2006) have demonstrated the ability of OP insecticides to directly damage DNA in freshly isolated human lymphocytes in vitro utilising the comet assay. Additional studies are also being completed within our group to measure levels of DNA damage in lymphocytes from farm workers in Spain immediately after spraying of crops with OP pesticide (Atherton et al., 2009) and suggest an increase in oxidative stress. There was a increase in 8-oxodeoxyguanosine in OP-exposed individuals, correlated with increased levels of urinary OP metabolites though the sample number was low. Studies have also been performed on lymphocytes isolated from individuals occupationally-exposed to OPs as well as on cultured cells exposed to OPs during experimental procedures (Paz-y-Mino et al., 2002). Before describing specific studies, some background information will be provided on the type of tests currently employed to measure the genotoxic potential of a compound.

### 1.4.1 Genotoxicity tests

Before reviewing the genotoxic studies available for chlorpyrifos, dichlorvos and sarin, a brief overview of the most common types of genotoxic test is described below.

#### 1.4.1.1 Comet assay

Comet assay, also known as single cell gel electrophoresis (SCGE), is a micro gel electrophoresis technique which detects DNA damage and repair in individual cells. The principle of the comet assay is that single cells are embedded on a thin layer of agarose on a microscope slide. After exposure to a lysis buffer the cell is stripped of all cellular proteins and the remaining deoxyribonucleic acid (DNA) is allowed to unwind in alkaline (or neutral depending on type of DNA damage to be detected) conditions. Unwinding of the DNA and electrophoresis at neutral pH (7–8) predominantly facilitates the detection of double strand breaks and cross links; unwinding and electrophoresis at pH 12.1–12.4 facilitates the detection of single and double strand breaks, incomplete excision repair sites and cross-links; whereas unwinding and electrophoresis at a pH greater than 12.6 expresses alkali labile sites in addition to all types of lesions listed above (Kumaravel et al., 2007). The DNA is then electrophoresed. During this any broken or damaged DNA will migrate further away from the nucleus. The cells are then stained with a fluorescent dye for analysis under the microscope.

The comet assay can be conducted in both *in vitro* and *in vivo* test systems and is increasingly being used in genotoxic testing of industrial chemicals, agrochemicals and pharmaceuticals. Comet assay is rapid (results in days), simple to perform, requires small amounts of test substance (25-50 mg) and can be performed in almost any eukaryotic cell (different animal organs). Comet assay serves as an important tool in the early drug development compounds as a mechanistic and genotoxic predictor. In addition repair enzymes can be incorporated into the comet assay; these remove specific forms of DNA damage, and create a single strand break which results in a higher Olive Tail Moment (OTM). This allows for the identification of the type of damage occurred after exposure to a particular compound as the enzymes will be specific to a certain type of lesion.

#### 1.4.1.2 The Micronucleus assay

The micro nucleus assay (MN) is able to test the ability of a compound or chemical to cause a change in chromosome structure and or number. The size and shape and number of chromosomes are constant for each species therefore any disruption can therefore be detected. During cell division, the genetic material replicates and then divides equally between the two daughter cells that are produced. If this process is disrupted, or the chromosomes are broken or damaged by chemicals or radiation, the distribution of genetic material between the two daughter nuclei may become uneven and pieces or entire chromosomes may fail to be included in either of the two daughter nuclei. The genetic material that is not incorporated into a new nucleus may form its own "micronucleus" which is clearly visible with a microscope. Determining a chemical's ability to induce chromosomal damage is a useful indicator to observe whether a chemical can cause cancer, as a number of cancers are characterized by chromosomal changes.

#### 1.4.1.3 Sister Chromatid Exchange

Sister Chromatid Exchange (SCE) is the exchange of homologous stretches of DNA sequence between sister chromatids. SCE occurs normally in cells during S phase however the rate of SCE can be accelerated if a cell is exposed to genotoxic agents which are able to from DNA adducts or induce point mutations. It is thought that SCE is an attempt by the cell to fix the DNA damage caused by genotoxic agents and has been correlated with recombination repair; therefore, you would expect a more potent genotoxic agent to generate a higher rate of SCE.

#### 1.4.1.4 Chromosome aberration

Structural chromosome aberrations may be induced via DNA breaks by various types of mutagens. Such DNA breaks may rejoin such that the chromosome is restored to its original state, rejoin incorrectly or not rejoin at all. These last two cases may be observable on microscopic preparations of metaphase cells. Induced chromosomal aberrations can be divided into two main classes: chromosome-type aberrations, involving both chromatids of

a chromosome, and chromatid-type aberrations involving only one of the two chromatids. Ionizing radiation induces chromosome-type aberrations (symmetric aberrations), like dicentrics, inversions, ring chromosomes, in the G0 or G1 stage of the cell cycle (i.e. prior to replication), while chromatid type aberrations (asymmetric aberrations), like breaks and gaps, are produced during the S or G2 stage (i.e. during or after replication). Most chemical mutagens are S-dependent clastogens and therefore produce chromatid-type aberrations.

## 1.5: Genotoxic effects of OPs

Below is a review of the genotoxic data available for chlorpyrifos, dichlorvos and sarin.

### 1.5.1 Chlorpyrifos

Chlorpyrifos (chemical structure shown in figure 1.5) is listed by the Pesticides Safety Directorate for use in the UK (Environmental agency fact sheet) and is one of the most widely used organophosphate pesticides in America. It was used to control such pests as termites and was used in number of applications including residential and agricultural. In December 2000 it was decided by the Environmental Protection Agency (EPA) that all residential applications except for preconstruction termite applications were to be cancelled. In February 2001 residential formulation of chlorpyrifos was stopped and in December of the same year all retail sales for residential application were terminated (Barr et al., 2005).

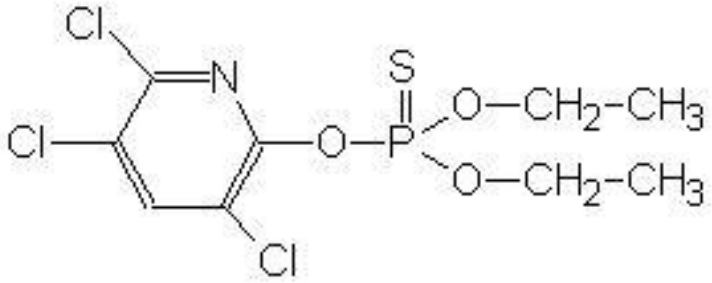


**Figure 1.5 The chemical structure of chlorpyrifos.**

Chlorpyrifos induces the same toxic effects as most pesticides caused by the inhibition of AChE (previously discussed) and is considered an EPA class II toxicant. In the literature there is conflicting data on the teratogenic, mutagenic effect or carcinogenic potential of chlorpyrifos.

In vitro results by Gollaupdi et al. (1995) reported that chlorpyrifos did not induce DNA damage in Chinese hamster cells or rat lymphocytes; this was measured by the chromosome aberration test, however the route of exposure and dose was not stated. Muscarella et al. (1984) exposed Chinese ovary cells to 1, 10 and 100mg/ml of chlorpyrifos and did not see any increase in the rate of SCE or chromosome aberration. A recent study by Cui et al. (2006) suggests that chlorpyrifos causes an increase in the incidence of micronuclei. In this study the potential of chlorpyrifos and cypermethrin to form DNA adducts in mouse hepatocytes was evaluated. It was found that chlorpyrifos was unable to form such adducts. Rahmann et al. (2002), in contrast to other reports, concluded that chlorpyrifos was able to cause DNA damage in mice leucocytes in a dose dependent manner, with DNA damage measured using the alkaline comet assay. The study also noted that the DNA was repaired 48hrs after exposure.

Studies with chlorpyrifos in the in vivo situation considers both the phosphorthioate and oxon form of chlorpyrifos as in animals chlorpyrifos is more readily metabolised to the active oxon form than in isolated cell lines. This is due to the abundance of cytochrome P450s in animals which can metabolise the chlorpyrifos to the active oxon. Amer et al. (1982) demonstrated that the repeated or dietary administration of chlorpyrifos induced significant incidence of micronuclei in mice bone marrow. The authors reported that mice, after receiving two injections of 45/mg/kg Body Weight (BW) over a period of one week (interval between dosing not specified), gave a mean of 23 micronuclei (MN) per 1000 polychromatic erythrocytes (PCE) in comparison with a background of 10.8 MN-PCE. This background has been questioned in the literature as being quite high, with a normal background being around 4 MN-PCE. In 1996 the same group reported that dosing mice with 4mg/kg of chlorpyrifos via Intra peritoneal (I.P) injection caused chromosomal aberrations after 24 hours. However the number of mice used was not stated. In contrast to these results Gollapudi et al. (1995) found no significant increase in MN in bone marrow

using 80% of an estimated LD 50 for chlorpyrifos (111mg/kg). Rahman et al. (2002) tested the DNA damaging capacity of chlorpyrifos in Swiss albino mice. The mice were administered orally doses ranging from 0.28 to 8.96 mg/kg and a alkaline comet assay was performed on whole blood samples at 24, 48 , 72 and 96 hours. Cyclophosphamide was used as a positive control. The group reported a statistically significant increase in DNA damage when compared to the positive control at 24 hours. The damage was also found to be dose related. The damage was seen to decrease over time and this was attributed to DNA repair pathways. Salazar-Arredondo et al. (2008) evaluated sperm DNA damage by several OPs including chlorpyrifos and chlorpyrifos oxon in human spermatozoa from healthy volunteers incubated with 50–750 µM chlorpyrifos and chlorpyrifos-oxon All concentrations were reported as not cytotoxic (evaluated by eosin-Y exclusion). Chlorpyrifos oxon was reported to be 15% more toxic to sperm DNA (evaluated by the Sperm Chromatin Structure Assay) than chlorpyrifos. Gupta et al. (2010) investigated the apoptosis and DNA damage inducing potential of chlorpyrifos in *Drosophila melanogaster*. Third instar larvae of Drosophila were treated with different concentrations of chlorpyrifos (0.015–15.0 µg/L) for 2–48 h. Reactive oxygen species (ROS) generation, oxidative stress markers, DNA damage and apoptotic cell death end points were measured in them. A significant increase in DNA damage was associated with apoptotic mode of cell death in 15.0 µg/L Chlorpyrifos-treated organisms for 24 and 48 h. Depolarization in mitochondrial membrane potential and increased casapase-3 and caspase-9 activities occurred after exposure to chlorpyrifos. The study suggested that ROS may be involved in inducing apoptosis and DNA damage in larvae of Drosophila after exposure to chlorpyrifos.

### 1.5.2 Dichlorvos

The use of dichlorvos (chemical structure shown in figure 1.6) has ceased in Great Britain. In 2002 the Health and safety executive (HSE) advised that dichlorvos stop being used as pest control agent. Dichlorvos is an OP and is effective as a pesticide as it is able to inhibit the AChE in insects. The effects of AChE inhibition are well documented but several studies suggest that dichlorvos is also able to cause DNA damage. The International Agency for Research on Cancer places dichlorvos in Group 2B (possibly carcinogenic to humans) based on what it considers to be sufficient evidence in animals, but inadequate evidence in

humans. The US Environmental Protection Agency classifies it in category 2B (possibly carcinogenic to humans) but the result of further testing is awaited and it may be reclassified.

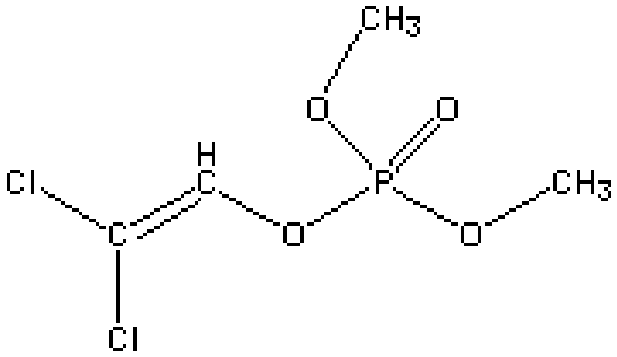


**Figure 1.6 The chemical structure of Dichlorvos.**

After a paper by Sasaki et al. (2000) the committee on mutagenicity (COM) reviewed the mutagenic data on dichlorvos. Here it was agreed that in vitro dichlorvos is a weak methylating agent, in comparison to Methyl Methanesuphonate (Green et al., 1974 and Bridges et al., 1973). Dichlorvos is able to induce strand breaks in isolated DNA (Griffin et al 1974) and methylate DNA (Lawely et al., 1974). Doherty et al. (1996) have also demonstrated that the incidence of micronuclei increases after exposure to dichlorvos in human lymphoblastoid cells. In addition to the previously mentioned studies, a recent study by Patel et al. (2007) demonstrated that dichlorvos is cytotoxic (measured by the MTT assay) and can cause DNA damage in Chinese hamster ovary (CHO) cells at a concentration from 0.01 µM – 10µM (measured by the comet assay). These findings were also backed up by previous work by Yamano et al. (1996) where CHO cells showed signs of DNA strand breaks using the alkaline elution assay. These findings were replicated in rat hepatocytes by the same group. These findings demonstrate that dichlorvos is genotoxic in vitro.

In vivo the results are very similar to the findings in vitro; possibly due to dichlorvos not requiring any metabolic activation, although, as with chlorpyrifos there is some conflicting data. Kligerman et al. (1985) injected mice with 5, 15, 25, 35 mg/kg dichlorvos. After 24

hours, the rate of SCE was measured in mouse peripheral blood lymphocytes. The group reported that there was not a significant increase in SCE above that of background levels during the study. Schop et al. (1989) exposed mice (topically exposed) to dichlorvos dissolved in dimethylsulfoxide (DMSO) and the genotoxicity was evaluated via the MN assay. The ability of DMSO to cause MN was assessed and found to be low. The paper concluded that dichlorvos was not able to cause MN. Yamano et al. (1996) showed that DNA is damaged in isolated rat hepatocytes analysed by the alkaline comet assay. However this was only witnessed at very high doses of dichlorvos, where rats were dosed with 160 mg/kg for 3 days and the DNA damage witnessed could be attributed to the depletion of glutathione by the detoxification of dichlorvos, as this may have drained glutathione reserves and leaving the liver susceptible to damage for example from ROS. Dichlorvos was able to induce micronuclei in keratinocytes in mice following topical application to the skin (Tungul et al., 1991). The approach used in this study had not been full validated but appropriate controls had been used which suggested a site of contact mutagenic effect. Nehez et al. (1994) treated male Wistar rats for 6 weeks with 5 treatment days per week at doses of 1/100, 1/75, and 1/50 of the $LD_{50}$. Following the final treatment, bone marrow cell chromosomes were prepared. The frequencies of cells revealing any aberrations as well as numeric and structural aberrations were evaluated. Dichlorvos demonstrated mutagenic effects following subchronic treatment of Wistar rats.

### 1.5.3 Sarin

Sarin was discovered in 1938 by German scientists attempting to develop more potent insecticides. Chemically, sarin is an OP compound, consisting of a central phosphate atom with a double bonded oxygen, a fluorine group, a methyl group and an alkoxy moiety as a leaving group (Figure 1.7). Due to the high acute toxicity of sarin, it was developed as a potential chemical warfare agent and has been used in both military conflict and acts of terrorism, most recently in the 1994 attack on the Japanese underground system (Abu-Qare et l., 2002).

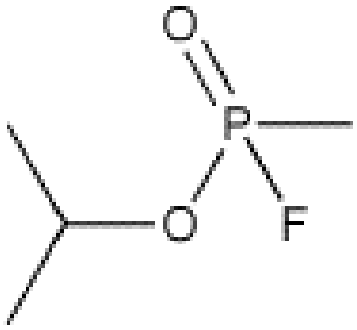


Figure 1.7 A schematic representation of sarin

There is very little information on the potential genotoxicity of sarin in humans with only a few studies being conducted after the previously mentioned release of sarin in Japan. A few animal studies are available and have conflicting results as to the genotoxic potential of sarin. Goldman et al. (1987) reported that sarin is not genotoxic or mutagenic based on both *in vivo* and *in vitro* assays. Negative results were obtained in the Ames *Salmonella* bacterial gene mutation assay using five revertant strains (TA135, TA100, TA98, TA1537, and TA1538) and a range of concentrations of sarin. Sarin and cyclosarin did not induce a significant increase in forward mutations in mouse L5178Y lymphoma cells at concentrations ranging from 50 to 200 µg/ml. Increases in SCE did not appear in CHO cells exposed *in vitro* to 200 µg/ml of sarin, nor did SCE in splenic lymphocytes significantly increase in mice receiving a maximally tolerated inter-peritoneal dose of 360 µg/kg of sarin (Klein et al 1987). Exposure of rat hepatocytes to sarin concentrations as high as 2.4 x $10^{-3}$ M decreased DNA repair synthesis. The authors conclude that sarin does not damage DNA directly but might inhibit DNA synthesis after endogenous DNA damage already had occurred (Klein et al., 1987; Opresko et al., 2001; Perrotta et al., 1996). In contrast to this Dave et al. (2007) determined levels of DNA fragmentation in blood leukocytes from guinea pigs following repeated low level exposure to sarin. Guinea pigs were injected subcutaneously once a day for 10 days with saline, or 0.1, 0.2, or 0.4 $LD_{50}$ (50% mean lethal dose) sarin dissolved in sterile physiological saline. Blood and parietal cortex was collected after injection at 0, 3, and 17 days and evaluated for DNA fragmentation. Repeated low-dose exposure to sarin produced a dose-dependent response in leukocytes at 0 and 3 days post-exposure. There was a

significant increase in all measures of DNA fragmentation at 0.2 and 0.4 $LD_{50}$, but not at 0.1 $LD_{50}$. There was no significant increase in DNA fragmentation in any of the groups at 17 days post-exposure. All measures of DNA fragmentation in leukocytes returned to control levels by 17 days post-exposure, indicating a small and non-persistent increase in DNA fragmentation following repeated low-level exposure to sarin. Li et al. (2000, 2003) reports that there is a positive correlation between the frequency of SCEs and the inhibition of serum cholinesterase activity in exposed subjects from the Tokyo sarin disaster recorded 2-3 months (Li et al,. 2000) and 3 years (Li et al., 2003) after the initial exposure. This report would suggest that an elevated frequency in SCE is related to sarin exposure. In addition to his report Bullman et al. (2005) have reported an increase in brain cancer death in veterans of the gulf war who were exposed to sarin during the March 1991 weapons demolitions at Khamisiyah Iraq. The cause-specific mortality of 100487 exposed US Army Gulf War veterans was compared with that of 224980 unexposed US Army Gulf War veterans. Exposure was determined with the Department of Defence 2000 Plume model. Relative risk estimates were derived from Cox proportional hazards models. The risk of brain cancer death was larger among those exposed 2 or more days than those exposed 1 day when both were compared separately to all unexposed veterans.

Although evidence exists demonstrating that dichlorvos, chlorpyrifos and sarin have genotoxic potential, there remains controversy within the literature, possibly due to different methods being used to assess the DNA damage. In addition, some studies simply use one genotoxicity test and do not look for relevant downstream effects of any DNA damage caused. This study aimed to investigate the ability of dichlorvos, chlorpyrifos and sarin to cause DNA damage using several genotoxic biomarkers, including the comet assay, the activation of DNA damage signalling pathways and cell cycle arrest. The regulation of these pathways and their relevance to this project are described in the following sections.

### 1.6. Types of DNA damage

DNA can be damaged in numerous ways. Spontaneous damage due to replication errors, deamination, depurination and oxidation is compounded in the real world by the additional

effects of radiation and environmental chemicals. The number of ways that DNA molecules can be damaged is very large. Examples of the types of DNA damage are shown in figure 1.8.

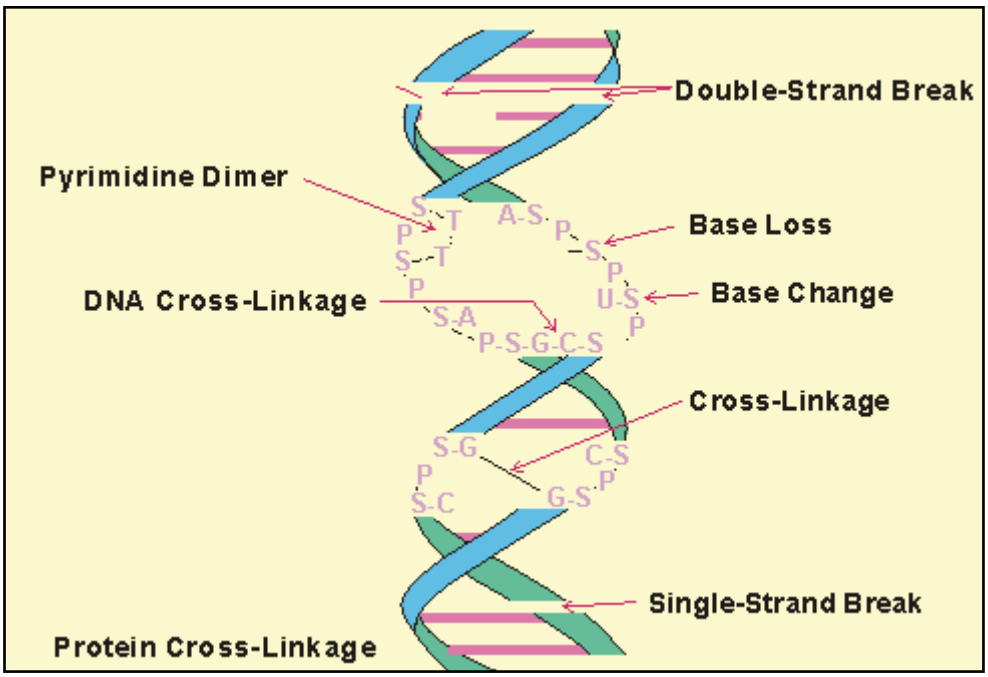


Figure 1.8 A representation of the different types of DNA damage that can occur after exposure to chemicals or radiation

### 1.6.1 Simple adducts

#### 1.6.1.1 Oxidation

Oxidative damage involves ROS damaging DNA and can produce a variety of lesions, including base adducts, single strand breaks (SSB) and double strand breaks (DSB) (Evans et al., 2004). For example the most reactive ROS is the hydroxyl radical. The hydroxyl radical can cause the oxidation of DNA bases, the most common adduct formed is 8-oxodeoxyguanosine (8-oxodG). The hydroxyl radical is also able to react with adenine in a

similar manner to guanine but this type of lesion is far less prevalent in DNA damage than 8-oxodG.

If the 8-oxodG lesion is not repaired, it results in guanine no longer pairing with cytosine but instead pairs with adenosine during DNA replication. This is due to the fact that the oxidised guanine bases no longer have three hydrogens available for hydrogen binding in cytosine and can only form two bonds and therefore binds preferably to adenosine. This results in guanine to thymine transition mutations if not repaired.

#### 1.6.1.2. Alkylation

Alkylation is the transfer of an alkyl group from one molecule to another, leading to a base adduct, with the simplest type of modification being methylation. Alkylation is accomplished by an alkyl electrophile, alkyl nucleophile or sometimes as alkyl radical. Undesired alkylation of DNA can lead to a possible mutation if unrepaired. An alkyl radical such as a methyl radical has only three out of four valency electrons of carbon bonded to hydrogen. This leaves one free unpaired electron which is free to interact with nucleophile groups on DNA. For example, alkylation of the O6 on a guanine can completely alter its ability to bind with cytosine resulting in it being read as deoxy-Adenine and therefore binding to thymine (Drablos et al., 2004). This is due to the molecule's ability to now only form two hydrogen bonds instead of three.

#### 1.6.1.3. Hydrolysis

The hydroxyl radical is also able to remove hydrogen from the deoxyribose-phosphate backbone. This results in DNA cleavage between the deoxyribose sugar and DNA base, leading to depurination and depyrimidation to form an apurinic or apyrimidinic site or AP site. If left unrepaired AP sites can lead to mutation during semi conservative replication as a random nucleotide base will be inserted into the strand synthesised opposite them.

### 1.6.2 Mismatches of DNA

Endogenous forms of DNA damage can occur through the mismatch of bases, due to errors in DNA replication, in which the wrong DNA base is stitched into place in a newly forming DNA strand, or a DNA base is skipped over or mistakenly inserted. Some genotoxins cause errors in DNA replication by inhibiting enzymes involved in the replication process. For example *mismatch* of bases, due to errors in DNA replication, in which the wrong DNA base is stitched into place in a newly forming DNA strand, or a DNA base is skipped over or mistakenly inserted.

### 1.6.3. Cross linkages

Bulky adducts can be produced by exposure to chemicals such as benzopyrene, leading to a large adduct on the N7 position of guanine. DNA crosslinks can be caused by various chemical agents but also by exposure to ultra violet light (UV). The main effect upon DNA is the formation of dimeric photoproducts between adjacent pyrimidine bases on the same DNA strand. These lesions are known as cyclobutane pyrimidine dimers (CPDs) (Ichashi et al., 2003). The presence of large DNA adducts or DNA crosslinks can cause major problems to the cell, in particular such lesions can impede the progression of DNA polymerases during replication and also interfere with chromosome segregation during mitosis.

### 1.6.4. Double strand breaks

Left unrepaired, DSBs can lead to genetic recombination and can cause the breakdown of DNA replication, leading to programmed cell death or apoptosis to stop a possible mutation being passed on during replication of the DNA. DSBs can be induced by ionizing radiation (IR) as well as various chemicals (in particular inhibitors of enzymes involved in DNA replication). IR causes DSB's through two mechanisms (Jackson et al., 2002). The first is a direct mechanism by which the radiation is able to directly cause the breakage of the phosphodiester backbone or through an indirect mechanism in which the ionizing radiation causes the production of free radicals thereby inducing oxidative stress in the cell. These

radicals can then react with the DNA and cause double strand breakage. DSBs can also be induced chemically by inhibitors of DNA polymerase and topoisomerase inhibitors such as etoposide.

### 1.7 Cellular response to genotoxic stress

Cells respond to genotoxic damage by initiating DNA damage signalling cascades and utilising specific DNA repair pathways to repair the DNA lesions. Activation of these pathways can be investigated to provide further evidence that cells have been exposed to a DNA damaging agent. In addition, by investigating specific components of these pathways it is possible to obtain information regarding the nature of the DNA damage being induced. DNA damage signalling is mediated by the ATM (ataxia telangiectasia mutated) and ATR (ataxia telangiectasia and Rad3 related) protein kinases). These kinases respond to different forms of DNA damage, for example ATM is normally activated in the presence of DNA double strand breaks (DSBs) (Jeggo et al., 2006), whereas ATR is activated by various forms of DNA damage, including DNA adducts and crosslinks (Cuadrado et al., 2006). Once activated, these kinases phosphorylate a wide range of target proteins, including the checkpoint kinases (Chk1 and Chk2), the tumour suppressor p53 and the histone variant H2AX (Paulsen et al., 2007). These target proteins, along with many others, act to cause cell cycle arrest, regulate transcription, enhance the DNA repair capacity of cells or to direct cells to die via apoptosis if the damage encountered is too great (Jowsey et al., 2009) (figure1.9). As well as mechanisms to arrest the cell cycle, thus preventing propagation of DNA damage, cells also possess a variety of DNA repair pathways that are able to respond to specific forms of DNA damage.

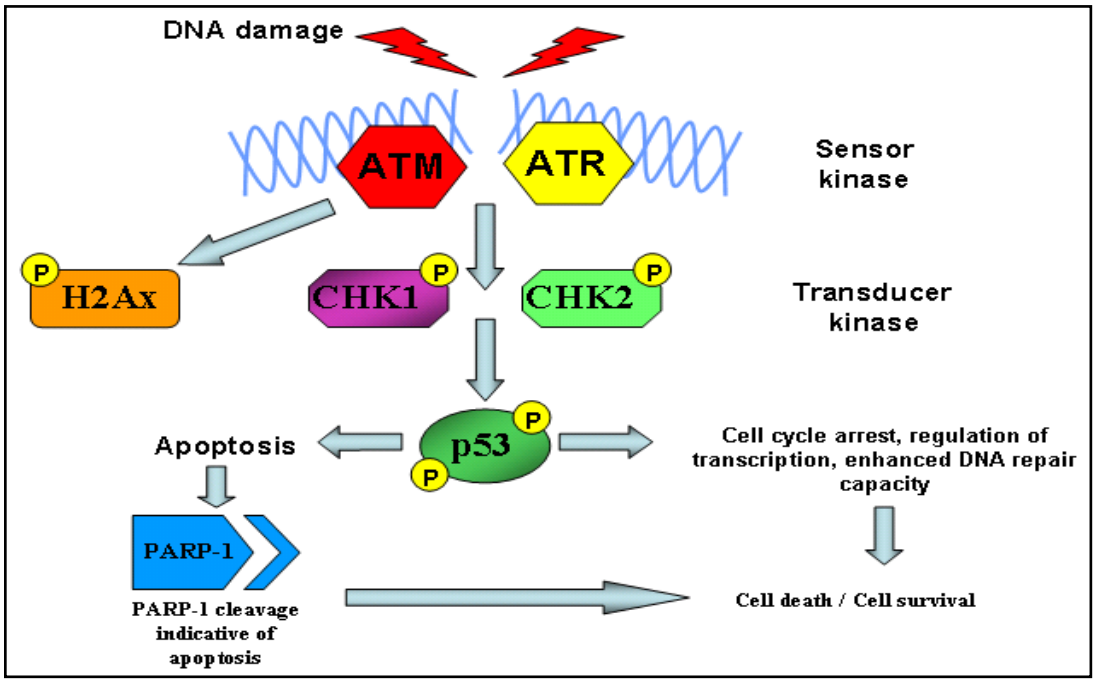


Figure 1.9 a schematic of cellular response to DNA damage via the ATM/ATR pathway

## 1.8 Cell cycle arrest

In response to DNA damage, a cell may arrest the cell cycle to allow for DNA repair. Damage response checkpoints have been identified at the G1/S and G2/M boundaries as well as during S phase and mitosis (Bartek et al., 2007). ATM and ATR are upstream activators of damage-inducible checkpoint arrest. The prevailing evidence suggests that in response to DNA damage, ATM phosphorylates p53 (either directly or via Chk2), which transcriptionally activates the Cdk2 inhibitor, p21, which serves to prevent progression from G1 into S phase (Ben-Yehoyada et al., 2007). P53 is an important tumour suppressor protein that regulates the cell cycle and progression to apoptosis. P53 can induce growth arrest at G1/S regulation point upon recognition of DNA damage allowing efficient repair. However if the damage is irreparable then p53 can initiate apoptosis. Entry into S phase requires the transcription factor E2F1 to be active. E2F1 is negatively regulated by binding of the tumour suppressor Retinoblastoma (Rb) protein. In cycling cells the interaction between E2F1 and Rb is prevented by the cdk2-mediated phosphorylation of Rb (Sherr et al., 1996). In the presence of DNA damage, p21 is induced which inhibits cdk2 resulting in reduced Rb phosphorylation (Knudsen et al., 1997). Rb is then able to bind and inhibit E2F1, preventing transcription of the genes required for progression into S-phase (figure 1.10).

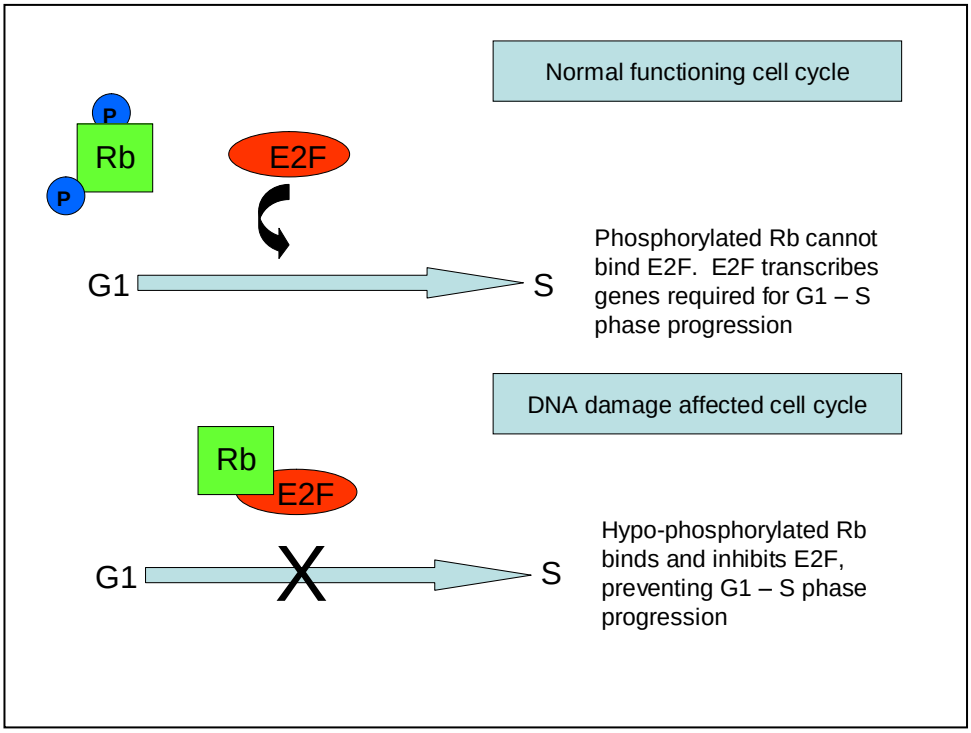


Figure 1.10 A schematic of cellular response after DNA damage in prevention of entry to S phase

The entry of eukaryotic cells into mitosis is regulated by cdc2 kinase activation, a process controlled at several steps including the binding of cyclin B to cdc2 and the subsequent phosphorylation of cdc2 at Thr161 (Atherton-Fessler et al., 1994). However, the critical regulatory step in activating cdc2 during progression into mitosis appears to be dephosphorylation of cdc2 at Tyr15. Phosphorylation at Tyr15, resulting in inhibition of cdc2, can be carried out by Wee1 and Myt1 protein kinases. The CDC25 phosphatases dephosphorylate Tyr15, resulting in the activation of cdc2 (figure 1.11) and progression into mitosis. After DNA damage, CDC25 phosphatases are phosphorylated by Chk1 and Chk2 (Reindhart et al., 2009). This results in inactivation of CDC25, increased phosphorylation of cdc2 on Tyr15 and reduced progression into mitosis.

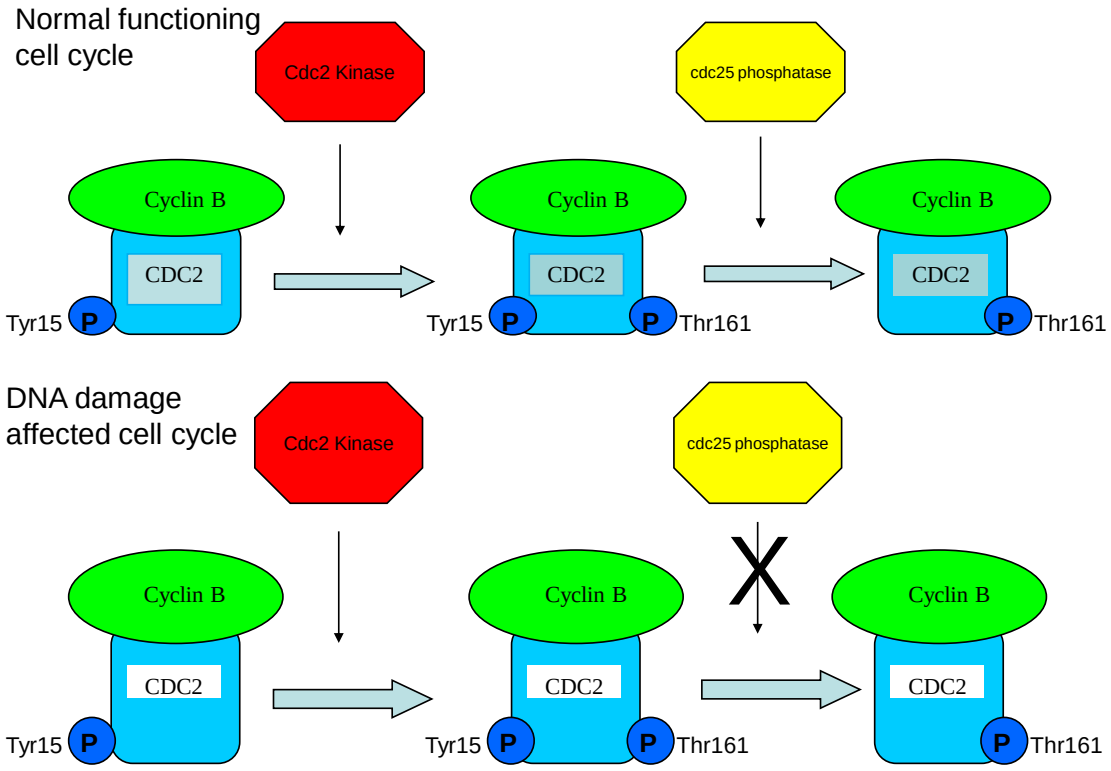


Figure 1.11 A schematic of cellular response after DNA damage in prevention of entry to M phase

## 1.9. DNA Repair pathways

As DNA can be damaged in different ways the cell employs a different repair pathway dependent on the type of damage. A brief description of the types of DNA repair pathways in mammalian cells is described below.

### 1.9.1 Base excision repair

The base excision repair (BER) pathway is involved in repairing simple DNA changes such as single strand breaks, and simple DNA adducts arising from oxidative and alkylating damage. BER is a multi stage process involving several proteins, outlined in figure 1.12. Briefly, a DNA glycosylase is responsible for recognition and removal of the damaged base, leaving an abasic or apurinic/apyrimidinic (AP) site. An AP endonuclease is then employed to nick the DNA backbone which causes a single strand break. This gap in the DNA is then filled by DNA polymerase B and ligated by DNA ligase I and III. As well as the basic pathway outlined here, several other proteins have roles in BER (Allinson et al., 2004). For example, the DNA repair enzyme poly(ADP-ribose) polymerase-1 (PARP-1) also plays a crucial role in BER, as part of a complex containing XRCC1 and DNA ligase III. Cells lacking PARP-1 protein or activity are hypersensitive to chemicals that induce alkylation or oxidative damage to DNA (Bolton at al., 1995; Bowman et al., 1999). Two different versions of BER exist within human cells. These are termed long patch or short patch repair BER which involve different polymerases and ligases. Various factors are thought to influence the decision of the cell as to which mechanism is employed; this includes the type of lesion being repaired in figure 1.12 illustrates long patch BER.

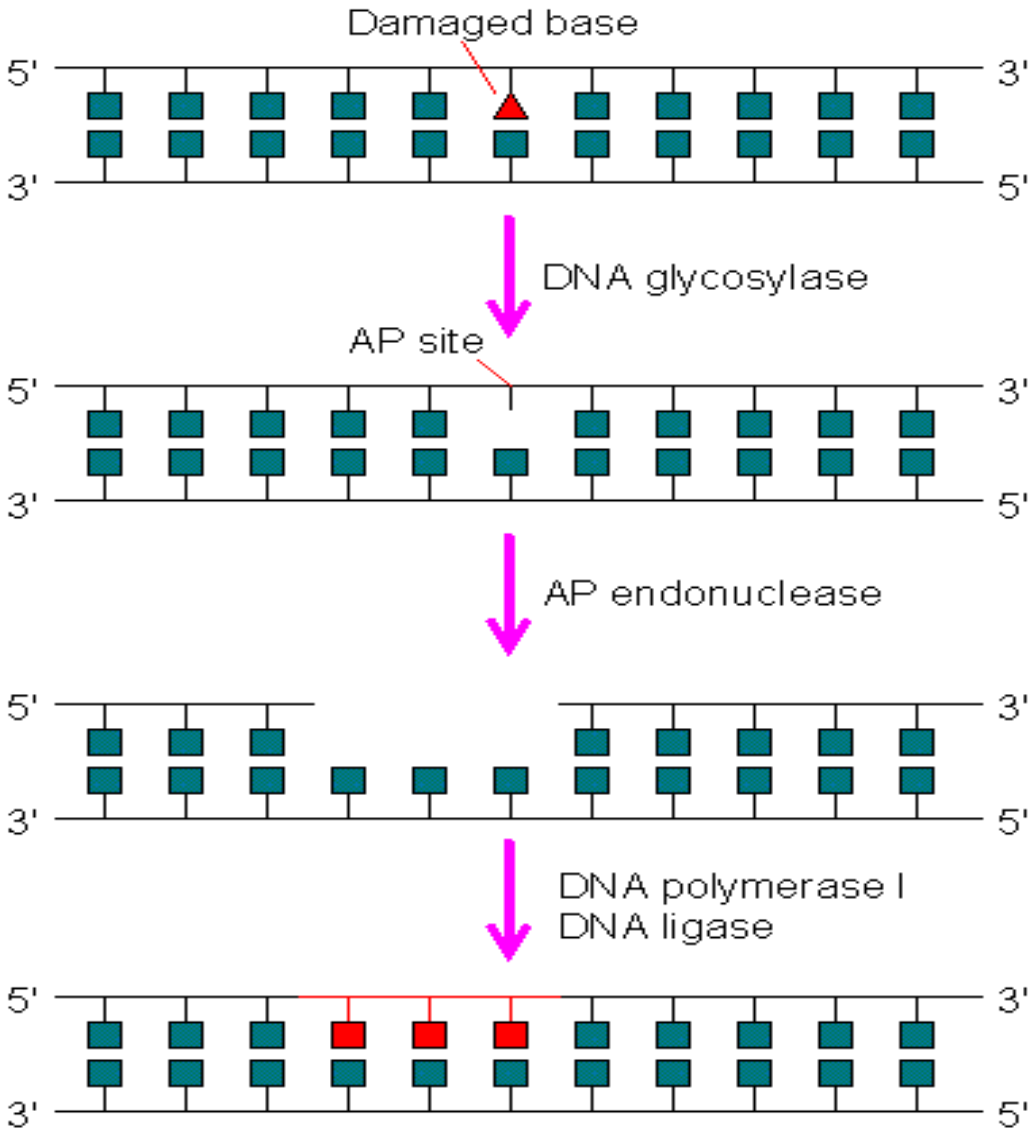


**Figure 1.12. Schematic representation of the base excision repair pathway** Diagram taken from http://www.web-books.com/MoBio/Free/Ch7G.htm adapted from Nilsen et al. (2000).

### 1.9.2 Nucleotide excision repair

The nucleotide excision repair (NER) pathway deals with larger and more bulky adducts and DNA crosslink. The NER pathway involves a number of proteins (around 30) and has been divided into 5 stages. The 1st involves recognition of the DNA lesion; 2nd single strand incision at both flanks of the lesion; 3rd excision of the single stranded nucleotides; 4th DNA repair synthesis replacing the now excised oligonucleotide; 5th ligation of the remaining single stranded nick (figure1.13). The whole process relies upon a family of proteins called XP proteins, which have been shown to be defective/mutated in the genetic condition Xeroderma Pigmentosum (Friedberg et al., 2004), characterised by an extreme sensitivity to sunlight and a predisposition to cancers, particularly of the skin. In addition, in vitro experiments have shown that cells isolated from individuals with XP are sensitive to UV radiation and have a defect in NER (Lehmann et al., 2003).

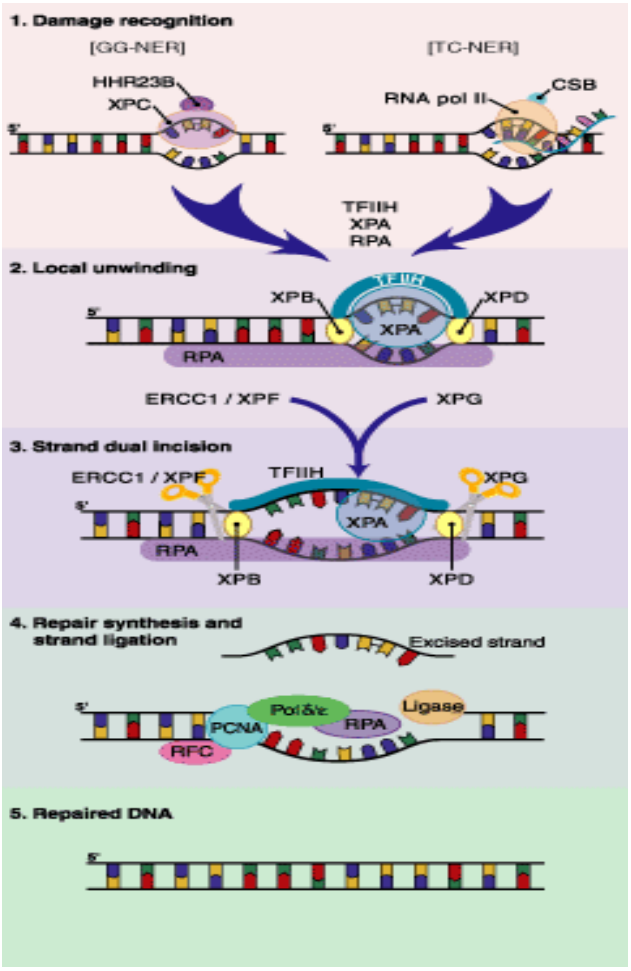


**Figure 1.13 Schematic representation of the nucleotide excision repair pathway.** Diagram taken from Batty et al. (2000)

### 1.9.3 Non-homologous end joining

Non-homologous end joining (NHEJ) is the major repair pathway for repairing DNA DSBs in human cells. NHEJ is a multi-stage process, mediated by the Ku70/80 and DNA dependant Protein kinase (DNA-PK) complex (figure 1.14). A possible three stage mechanism has been proposed, consisting of end binding and bridging, terminal processing and ligation.

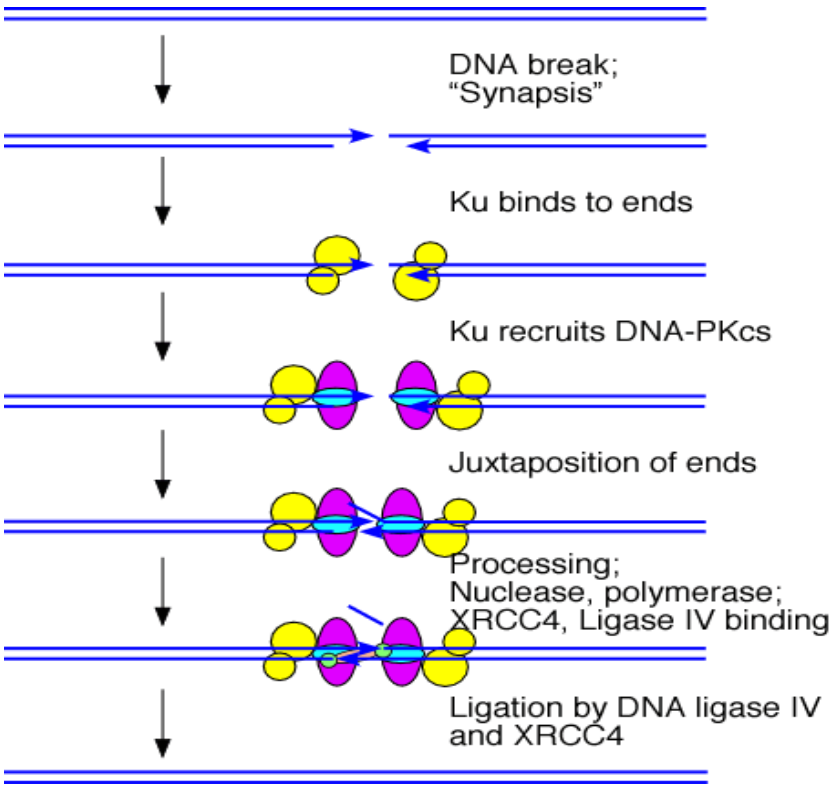


**Figure 1.14 Schematic representation of non homologous end joining.** Diagram taken from http://asajj.roswellpark.org/huberman/DNA_Repair/dsbreak.html

It has been suggested that the Ku protein is responsible for sensing the DNA damage due to its DNA binding ability (Burma et al., 2006). Upon sensing the damage, Ku binds the ends of the DNA and prepares the DNA by aligning the strands and protecting them from DNA degradation by nucleases. Ku is also responsible for recruiting the DNA-PK catalytic subunit, which phosphorylates XRCC4, leading to the recruitment of DNA ligase IV, allowing the DNA ends to be ligated. The fact that the DNA ends are processed, possibly leading to the loss of

genetic information and then directly ligated means that NHEJ is an error prone form of DNA repair.

### 1.9.4 Homologous Recombination

This pathway is the minor repair pathway for DSB in humans. Homologous recombination (HR) requires a homologous DNA sequence and therefore only occurs during late S and G2 phases of the cell cycle. The repair of the breakage is dependent upon the retrieval of genetic information from a sister chromatid or another undamaged homologue. This makes HR free from error when in comparison with NHEJ as an identical template is employed to resynthesise the DNA. In the initiation step of HR at the site of damage the double stranded DNA is exonucleolytically processed at both of the 5' ends of the DSB by a specific nuclease to 3' single stranded (ssDNA). One of the 3' ssDNA tails will invade an intact undamaged sister chromatid and causes the formation of a D loop structure. DNA strand exchange occurs and causes a joint molecule connecting sites of undamaged and damaged DNA (Dudass et al., 2004). DNA sequence information that is missing from the DSB is then resynthesised by DNA polymerase. Both of the 3' ends then act as primers for DNA synthesis using the intact duplex as a template. After ligation two holiday junctions (four stranded branched structures) are formed. In the last step of HR the holiday junctions are cleaved by the enzyme resolvase (figure 1.15).

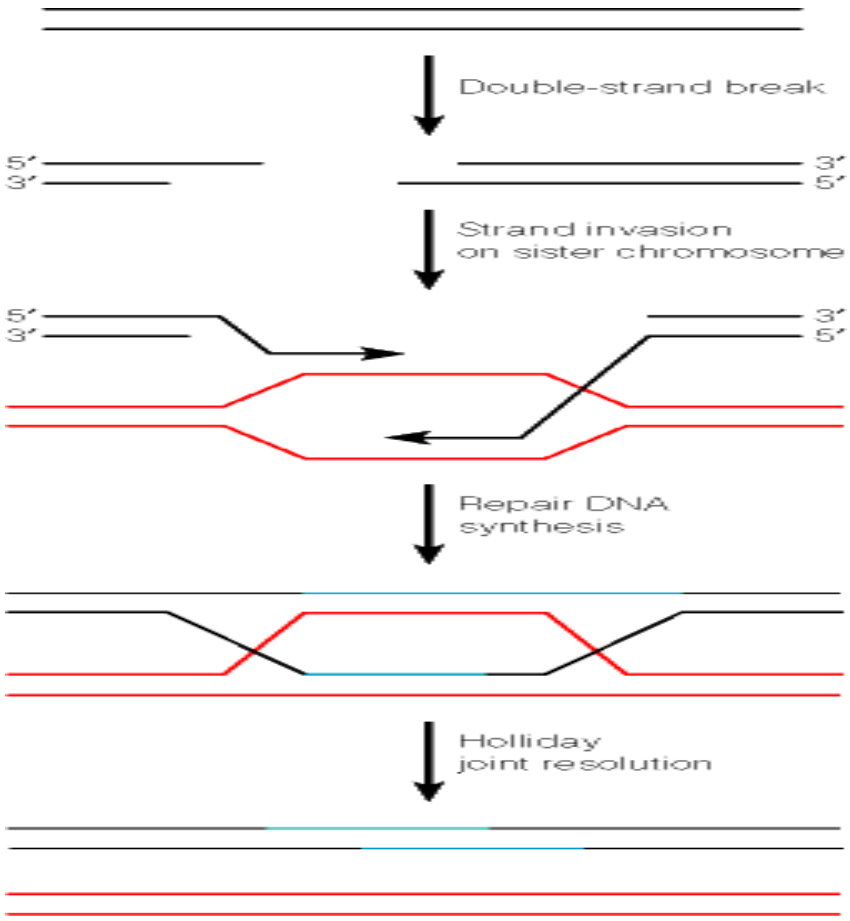


**Figure 1.15. Schematic representation of homologous recombination**. Diagram adapted from Dudas et al. (2004).

## 1.10 Cell death

Apoptosis and necrosis are two distinct forms of cell death, with clearly distinguishing morphological and biochemical features. Recently autophagy with cell death has been accepted as an alternative route of cell death, with distinct morphological features from that of apoptosis and necrosis.

### 1.10.1 Apoptosis

Apoptosis is a programmed form of cell death, characterised by nuclear condensation and fragmentation, cleavage of chromosomal DNA into internucleosomal fragments and packaging of the deceased cell into apoptotic bodies without plasma membrane breakdown

(Kitazumi et al., 2010). Apoptotic bodies are recognized and removed by phagocytes and thus apoptosis is also notable for the absence of inflammation around the dying cell. This is in contrast to necrosis where the cell membrane does breakdown and cellular constituents are released and cause further damage to surrounding cells. The morphologic features of apoptosis result from the activation of caspases (cysteine proteases) by either death receptor ligation or the release of apoptotic mediators from the mitochondria. Cell death via apoptosis requires energy in the form of adenosine triphosphate (ATP) (Leist et al., 1997) whereas death by necrosis is not an active process and therefore does not require energy and often occurs due to the cell becoming depleted of ATP. Cells will be directed to apoptosis if genotoxic stress has become too extensive, this pathway being mediated by the mitochondrial release of cytochrome c in either a p53-dependent or p53-independent manner. P53 dependent apoptosis involves the transcriptional activation of proapoptotic genes including Bax, Bix, Puma, Noxa and Bad (Yu et al., 2002). The resultant proteins function by either inhibiting the activity of the pro-apoptotic protein bcl-2 or by forming pores in the outer mitochondrial membrane causing the release of cytochrome C. Cytosolic cytochrome c induces the formation of the multisubunit apoptosome composed of apoptotic protease activating factor-1 (Apaf-1) and caspase 9 (Colin et al., 2009). Caspase 9 activates caspase 3 which mediates the apoptotic cascade (figure 1.16).

Apoptosis can also be activated in a p53 independent manner via the FAS receptor and FAS ligand Tumour necrosis factor (TNF-1), (Locksley et al., 2001). The receptor trimerizes and death adapter molecules are recruited on the cytoplasmic side of the membrane. Fas receptor recruits FADD (Fas-associated death domain protein) which in turn recruits the effector protein caspase-8. The activated caspase-8 can then cleave procaspase- 3 leading to apoptosis by caspase 3 activation. Caspase-8 also activates Bid, which translocates to mitochondria and leads to the release of cytochrome C.

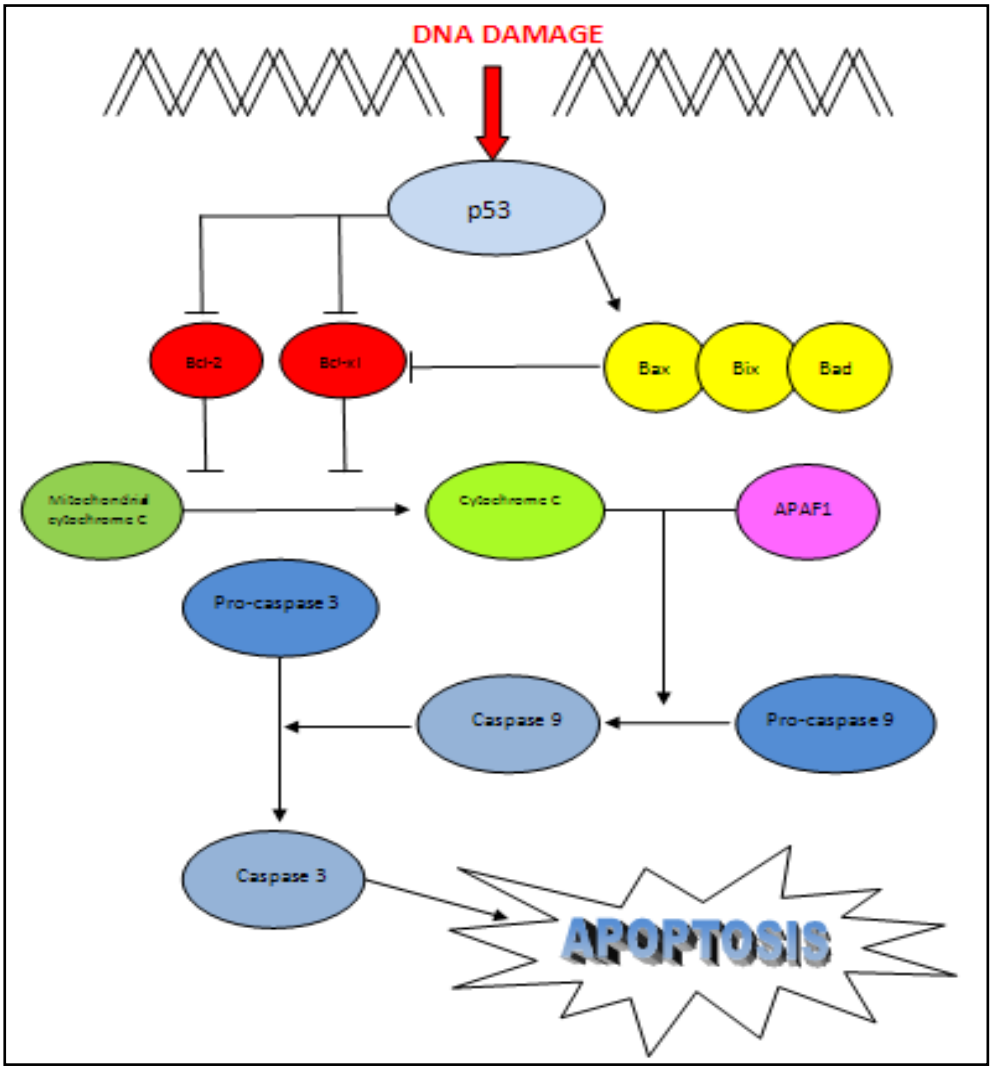


Figure 1.16 a schematic of cellular response after DNA damage in activating caspase induced apoptosis

This apoptotic cascade includes cleavage of a number of proteins including DNA repair enzymes such as PARP-1. Whilst being a very useful biomarker for apoptosis, PARP-1 cleavage is also functionally important (Bouchard et al., 2003). Specifically the cleavage of DNA during apoptosis would lead to massive hyper-activation of the strand break sensing enzyme PARP-1, which would in turn lead to the depletion of the PARP-1 substrate nicotinamide adenine dinucleotide (NAD) and subsequent depletion of ATP (Ha et al., 1999). As the process of apoptosis requires ATP, this would lead to a switch to the more damaging necrotic form of cell death, which does not require ATP. Cleavage of PARP-1 and resultant

inactivation of the enzymatic activity prevents the cell switching from apoptotic to necrotic cell death and thus prevents damage to neighbouring cells and tissues (figure 1.17).

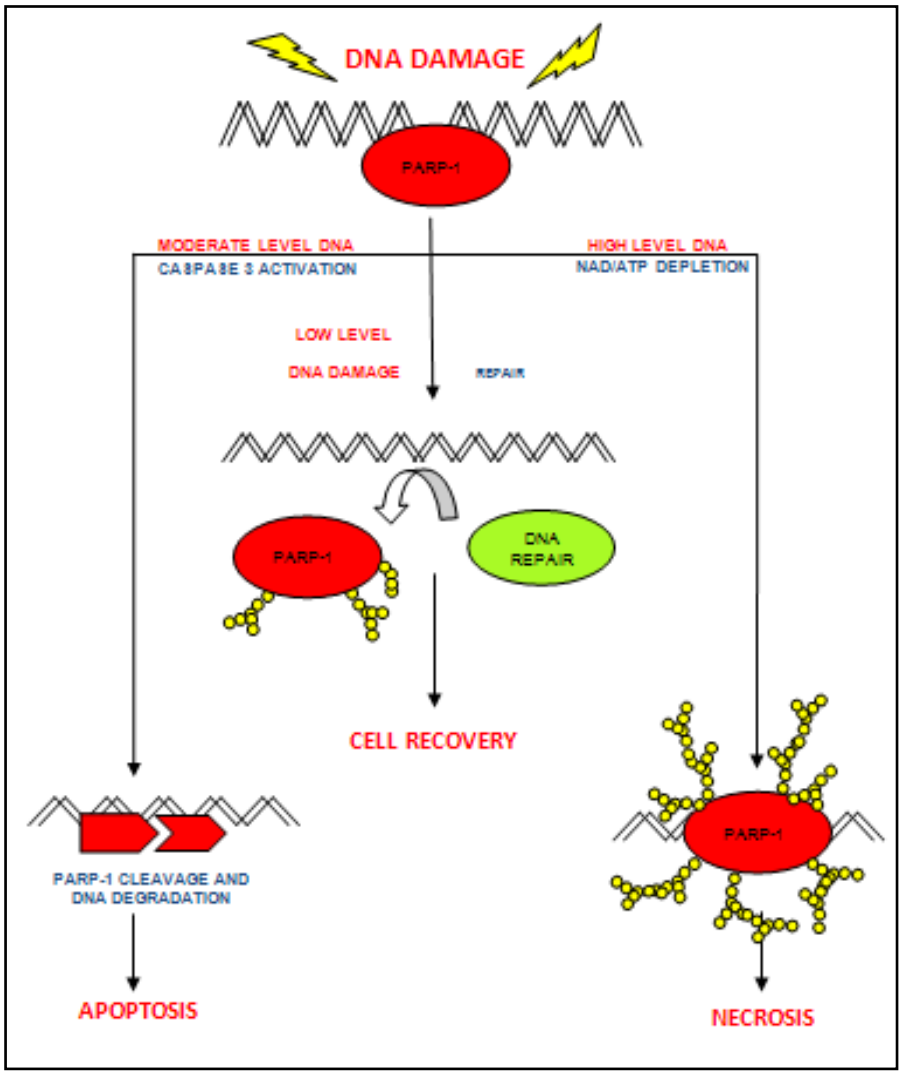


Figure 1.17 a schematic of cellular response after DNA damage deciding the fate of PARP-1 depending on the extent of DNA damage in the cell

### 1.10.2. Alternative modes of cell death

#### 1.10.2.1 Necrotic cell death

Since various stimuli induce both apoptotic and necrotic death, the mode of cell demise seems to be dependent on intracellular factors. One of these factors is the concentration of ATP. As previously mention over-activation of PARP depletes ATP and leads to the disorganised necrotic form of cell death rather than the cellular suicide route of apoptosis. Necrosis occurs in cases of severe physicochemical injuries such as chemical hypoxia (Eguchi et al., 1997). Necrosis typically begins with cell swelling, chromatin digestion, and disruption of the plasma membrane and organelle membranes. This causes the plasma membrane to burst, which results in release of the cytoplasmic contents into the surrounding area, causing an inflammatory response.

#### 1.10.2.2 Autophagy as a cell death mechanism

More recent studies have said that autophagy is a non apoptotic form of programmed cell death. There is confliction in the literature and the general understanding now seems to be that autophagy is a pro survival mechanism that occurs alongside cell death (Levine et al., 2005). Autophagy is a cellular mechanism for degrading long lived proteins and organelles. During autophagy, cytoplasmic constituents including organelles are enveloped into a double membrane autophagosome; this then fuses with liposomes allowing for the degradation of the cellular contents. This function as well as being implicated in cell death is also involved in cellular turnover and stress responses (Rami et al., 2009). Autophagic cell death is characterised by large scale seizure of the cytoplasmic constituents in autophagosomes. It is not fully understood what factors determine whether autophagy is cytoprotective or cytotoxic. When autophagy is not regulated autophagy can result in cell death either by selectively destroying key cell survival proteins or as a result over self digestion (Kroemer et al., 2008). Autophagy can also provide a source of ATP for the energy dependent apoptosis. In contrast with necrosis, both apoptotic and autophagic cell death are characterized by the lack of a tissue inflammatory response.

### 1.10.2.3 Parthanatos as a cell death mechanism

In addition to the roles of PARP-1 in apoptosis and necrosis outlined above, PARP-1 has been recognized in the recently identified form of cell death, parthanatos. Over activation of PARP-1 and excessive production of poly ADP ribose units (PAR) plays a role in the release of Apoptosis inducing factor (AIF), Andrabi et al. (2008) AIF is found in the inner mitochondrial space and like cytochrome c can play a protective role when localised in the correct compartment of mitochondria. In dying cells, AIF relocates from the mitochondria to the nucleus where its DNA binding activity is thought to mediate chromatin condensation and large-scale DNA fragmentation (Susin et al., 1999). PAR induced cell death (Parthantos) occurs due to rapid accumulation of PAR. This process shares many common features with necrosis and apoptosis but does not require ATP and is not mediated via caspases. PAR is key to initiating cell death by parthantos but is only one cog in multi protein dependent machinery leading to cell death. It is unclear how the precursor protein of AIF is cleaved by PAR molecules (Lorenzo et al., 2007).

### 1.11. Aims of project

The principal aim of this project is to investigate the ability of nerve agents and organophosphate surrogate compounds to induce DNA damage and subsequently investigate the cellular mechanisms that are used to repair this damage.

1) To assemble substantial evidence that OP compounds being studied does cause DNA damage in human cells.

2) To investigate how the cell responds to this damage, in terms of the DNA damage signalling pathways activated by exposure to the OPs.

3) To investigate the consequence of the activation of cell pathways, whether a cell will be directed to a slowing of the cell cycle allowing for repair and cell survival, or whether it is directed to apoptosis or cell death.

# *Chapter 2*

# *General methods*

## 2.0 Materials and methods

### 2.1 Cell culture

All cells were grown at 37$^{o}$C in a humidified atmosphere containing 5% $CO_2$.

#### 2.1.1 A549 lung epithelial cells

A549 cells are human alveolar basal epithelial carcinoma cells. They were grown in Dulbecco's Modified Eagles Medium (DMEM) supplemented with 10% fetal bovine serum (FBS), 100mM sodium pyruvate 10 U/ml penicillin/streptomycin and 2mM glutamine (all from Sigma). Cells were routinely cultured in T75 flasks (Corning) and maintained in the exponential growth phase by sub-culturing cells when approaching 75-80% confluence. Cells were split by removing media, rinsing cells in phosphate buffered saline (PBS, Sigma) and incubating with 2ml of warm 0.25% trypsin-EDTA (Sigma). When cells had detached from the plate the trypsin was neutralized with an equal volume of culture medium. Cells were re-seeded into fresh T75 flasks, at a split ratio of 1:4 - 1:10. When required for a specific experiment, cells were seeded at a known cell density in appropriate culture plates (see below).

#### 2.1.2 TK6 lymphoblastoid cells

TK6 cells (ECACC) are a B-lymphocyte cell line, transformed with Epstein Barr Virus to allow prolonged propagation in culture. The cells, which grow in suspension, were maintained in RPMI 1640 medium supplemented with 10% FBS and 10 U/ml Penicillin/Streptomycin (all from Sigma). TK6 cells were routinely grown in T75 flasks at a cell density of $1x10^5$/ml - $1x10^6$/ml until required for specific experiments.

#### 2.1.3 Neuroblastoma SHSY-5Y cells

SH-SY5Y is one of three serially isolated neuroblast clones (SH-SY, SH-SY5, and SH-SY5Y) of the human neuroblastoma cell line SK-N-SH which was established in 1970 from a metastatic bone tumour. SHSY-5Y cells were grown in Dulbecco's Modified Eagles Medium (DMEM) supplemented with 10% fetal bovine serum (FBS), 100mM sodium pyruvate 10 U/ml penicillin/streptomycin and 2mM glutamine (all from Sigma).

Cells were routinely cultured in T75 flasks (Corning) and maintained in the exponential growth phase according to the A549 method described above.

### 2.1.4 Preparation of isolated lymphocytes from human blood

Blood (12ml) was collected and fresh lymphocytes prepared using the Lymphoprep™ kit (Axis-Shield, UK). Briefly, blood was collected into a tube containing an anticoagulant (EDTA). The blood was diluted by addition of an equal volume of 0.9% NaCl. 6 ml of the diluted blood was carefully layered over 3 ml Lymphoprep™ in a 15ml falcon tube in duplicate. The prepared samples were then centrifuged at 800 x g for 20 minutes at room temperature. The isolated lymphocytes were then carefully removed and placed in a T25 flask with 10ml of TK6 media (15% serum) and left overnight at 37$^{o}$C in a humidified atmosphere containing 5% $CO_2$ before experimentation.

## 2.2 Chemicals

### 2.2.1 Dichlorvos

The OP compound dichlorvos was obtained from Greyhound Chromatography and Allied Chemicals. The neat agent was at a concentration of 6.4M. Subsequent dilutions were prepared in dry acetone (acetone containing an excess of sodium bicarbonate) to prevent hydrolysis of the dichlorvos. Neat dichlorvos was handled in a fume hood with external exhaust and dilute solutions were handled in a class II microbiological/chemical safety cabinet. Dichlorvos was inactivated by adding 10M NaOH to all waste prior to disposal.

### 2.2.2 Chlorpyrifos and chlorpyrifos oxon

The OP compounds chlorpyrifos and chlorpyrifos oxon was obtained from Sigma Aldrich. The agent was in powder form and was dissolved in DMSO to give a final concentration of 100mM. The 100mM stock of chlorpyrifos or chlorpyrifos oxon was handled in a fume hood with external exhaust and dilute solutions were handled in a class II

microbiological/chemical safety cabinet before application to cell lines. Chlorpyrifos and chlorpyrifos oxon were decontaminated in 10M NaOH prior to disposal.

### 2.2.3 Sarin

All studies with the nerve agent sarin were performed at the Defence Science and Technology Laboratories (DSTL, Porton Down). The nerve agent sarin was prepared from a 35.7mM (5mg/ml) stock solution diluted in isopropanol (IPA) by a trained agent handler to give a final concentration of 1mM. This dilution was conducted in a class III microbiological/chemical safety cabinet. All subsequent dilutions (into isopropanol) and cell treatments were handled in a class II microbiological/chemical safety cabinet. Sarin was decontaminated in 50% Chloros$^{TM}$ for 24 hours prior to disposal.

### 2.2.4 Etoposide

Etoposide is a chemotherapy agent whose mode of action is based on the induction of DNA damage and apoptosis, mediated by the inhibition of topoisomerase II and the generation of DNA strand breaks. Etoposide was therefore used as a positive control for the analysis of DNA damage signalling events and apoptosis. Etoposide was obtained from Sigma-Aldrich in powder form and diluted in DMSO to give a concentration of 50mM. The 50mM stock of etoposide was handled in a fume hood with external exhaust and dilute solutions were handled in a class II microbiological/chemical safety cabinet before application to cell lines. Waste etoposide was inactivated with 10% sodium hypochlorite prior to disposal.

### 2.2.5 Hydrogen peroxide

Hydrogen peroxide (Sigma-Aldrich) was used as a positive control for DNA damage. Hydrogen peroxide was in liquid from at a concentration of 9.8 Molar. This was diluted in a class II microbiological/chemical safety cabinet to the desired concentration using Phosphate Buffered Saline (PBS) immediately prior to experiments. Hydrogen peroxide was disposed of according to the same procedure as etoposide detailed above.

### 2.2.6 Solvent control

Each chemical described above was diluted in a different solvent. Therefore care was taken to ensure that the same amount of each solvent was applied to each of the cell lines in every experiment. In all cases the amount of solvent was kept constant at 0.1%.

## 2.3 Comet assay

The Comet assay, also known as single cell gel electrophoresis (SCGE), is a micro gel electrophoresis technique which measures DNA damage in individual cells. The principle of the comet assay is that single cells are embedded in a thin layer of agarose on a microscope slide. By exposure to a high salt lysis buffer the cell is stripped of all cellular proteins and the remaining nucleoid DNA is denatured by incubating the microscope slides in alkaline buffer. After the DNA is unwound, it is electrophoresed, with negatively charged DNA migrating towards the positive electrode. The extent of migration is determined by the level of DNA damage, with DNA ends or fragments being able to migrate further from the nucleoid. The cells are then stained with a fluorescent dye for analysis under a microscope. The comet assay can be modified to allow the measurement of a number of different types of DNA damage including double strand breaks, alkali labile sites, oxidative damage, and DNA crosslinks.

The figure 2.1 shows a representative comet image. The user selects the cell to be analysed by clicking the centre of the comet head. The cell is analysed using suitable analysis software, for example comet assay IV (INSTEM). Various parameters can be measured, including the proportion of DNA in the head, the proportion of DNA in the Tail and the length of the tail.

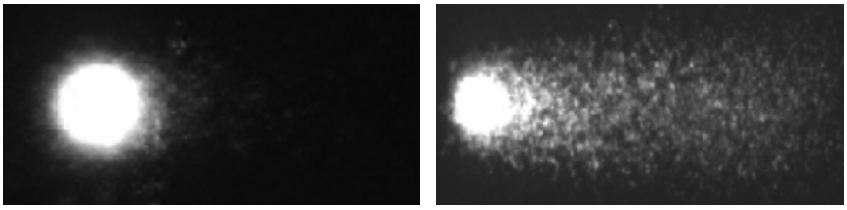

Normal DNA Damaged DNA

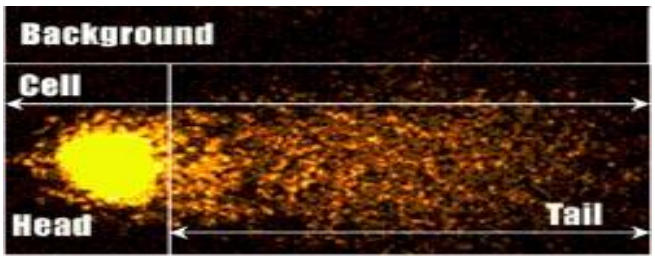


**Figure2.1 Analysis of a damaged cell by the comet assay, displays the difference between an intact cell and a damaged cell after a comet assay.** In the bottom diagram the "head" and "tail" of a cell which has been processed by the comet assay is defined

In this study a fluorescence microscope (Olympus CX41, 20x magnification) was used to view the prepared slides and Comet IV solution software (from Perceptive instruments distributed by INSTEM) was used to analyse the cells. A cell was selected by clicking on the "head" of a cell and the software derived a number of parameters including tail length and Olive tail moment (OTM) as indicators of DNA damage. OTM was derived from the product of the tail length and the fraction of total DNA in the tail. OTM was selected to define DNA damage in this study as it incorporates a measure of both the smallest detectable size of migrating DNA (reflected in the comet tail length) and the number of relaxed / broken pieces (represented by the intensity of DNA in the tail). A minimum of 50 cells were scored for each individual sample.

### 2.3.1Method

#### 2.3.1.1 Treatment of SHSY5Y cells and isolation prior to comet assay

SHSY-5Y cells were cultured on 6 well plates 48 hours prior to experiments. The cells were seeded at 2.5 x $10^5$ cells and allowed to grow to approximately 50% confluence. Two hours before treatment with dichlorvos the medium was replaced with serum free growth

medium. This was to prevent any dichlorvos binding to the FBS in the growth medium. Dichlorvos was added to the cells initially using low concentrations of 2.7nM and 2.7 µM for ten minutes. The study was expanded to include more concentrations (0.01, 0.1, 1, 10 and 100µM) for 1 hour. Control samples consisted of untreated cells and cells treated with acetone (0.1%). Hydrogen peroxide (10µM) was used as a positive control. The cells were incubated with the dichlorvos or solvent control for ten minutes or 1 hour before the media was removed and the cells washed with serum free media, removing all trace of the OP. To detach the SHSY-5Y cells 0.5ml of trypsin–EDTA was added to each well for thirty seconds. 1.5ml of serum free media was added to inactivate the trypsin. The cell suspensions were then transferred to Eppendorf tubes, placed on ice and cell number was determined using a haemocytometer before undergoing processing by the comet assay. Samples were prepared in dim light conditions and kept on ice to avoid any unwanted DNA damage.

#### 2.3.1.2 Treatment of TK6 cells and isolation prior to comet assay

TK6 cells were seeded in T25 flasks at a density of 2.x $10^5$ cells/m l (total volume 5 ml). Cells were treated with either: dichlorvos (2, 20, 40, 60 and 100µM), chlorpyrifos (0.01, 0.1, 1, 10 and 100µM), chlorpyrifos oxon (0.01, 0.1, 1, 10 and 100µM) or sarin (0.001, 0.01, 0.1 and 1 µM). Samples were isolated at 1 and 24 hours by transferring to 15 ml falcon tubes and centrifuging at 1000 RPM for ten minutes. The media was then removed and cells were washed in ice cold PBS and transferred to Eppendorf tubes. Samples were prepared in dim light conditions and kept on ice to avoid any unwanted DNA damage. Control samples consisted of untreated cells and an appropriate vehicle control (either 0.1% acetone, 0.1% DMSO or 0.1% isopropanol). Hydrogen peroxide (10µM final concentration) was used as a positive control to induce DNA damage.

#### 2.3.1.3 Alkaline Comet assay

A 2% solution of low melting point agarose (LMPA) was prepared in PBS (dissolved in water bath at 90$^{o}$C or heated up in microwave). The agarose was then transferred to a water bath at 42$^{o}$C and allowed to equilibrate to that temperature. Cell suspensions in serum free media were prepared. 70µl of cell suspension (containing 10000 cells) were mixed with 70µl LMPA and added to a Trevigen comet slide. Gels were spread evenly on the Comet Slide using the edge of a pipette tip and allowed to set by placing on an aluminium tray sat on a

bed of ice. After 5 minutes, slides were submerged in chilled lysis buffer (2.5M NaCl, 100mM EDTA and 10mM Tris, pH to 10). Immediately prior to use triton X-100 and DMSO were added to the lysis buffer at a final concentration of 1%. Slides were incubated for 1 hour at 4$^{o}$C before washing in cold PBS for 15 minutes. Slides were then placed in a horizontal electrophoresis tank filled with chilled alkali buffer (300mM NaOH, 2mM EDTA) for 30 minutes to allow unwinding of the DNA. After 30 minutes, electrophoresis was performed at a constant voltage of 22V and 500mA for 30 min. The slides were washed in cold neutralisation buffer (0.5M Tris pH 7.5) for 10 minutes followed by PBS for 15 minutes. DNA was then stained by adding 2ml of SYBR gold stain (diluted 1:10000 in 1xTE buffer) for 5 minutes. Excess stain was removed and gels allowed to dry overnight in the dark.

### 2.3.2 Comet assay with FPG enzyme

Formamido-pyrimidine-DNA-Glycosylase (FPG) initiates the repair of oxidised bases by excising them and cutting the sugar phosphate backbone of the DNA molecule, creating a single strand break (SSB). FPG can therefore be used in the comet assay for the specific detection of oxidative DNA damage. The enzyme is added after the lysis step and any oxidative damage will be recognised by the FPG, resulting in the production of a single strand break and further DNA relaxation and migration during electrophoresis.

#### 2.3.2.1 Method

SHSY-5Y cells were prepared on 6 well plates 48 hours prior to experiments. Cells were seeded at 2.5 x $10^5$ cells and allowed to grow to approximately 50% confluence. Two hours before treatment with dichlorvos the medium was replaced with serum free growth medium. This was to prevent any of the dichlorvos binding to the FBS in the growth medium. Initial experiments were carried out in order to optimise the assay and find the correct amount of enzyme needed for the experiment. Hydrogen peroxide (10µM) treated cells were incubated with different concentrations of enzyme to establish the required concentration for analysis by the alkaline comet assay. The methodology was identical to the standard comet assay expect for the addition of the following step subsequent to cell lysis: After lysis, the slides were washed with PBS and then treated with either 0.002 or 0.02

units of FPG enzyme (New England Biolabs). FPG enzyme is supplied in 400 units (8000 U/ml) a unit is defined as the amount of enzyme required to cleave 1ñmol of a 34-mer oligonucleotide duplex containing a single 8-oxogunaine base paired with a cytosine in 1 hour at 37$^{o}$C in a total reaction volume of 10 µl. The enzyme was diluted 1µl in 4000 µl (0.002 units) and 10 µl in 4000 µl (0.02 units) 1ml of each dilution was added to each slide. The slides were then incubated at 37$^{o}$C for 30 minutes in a humidified atmosphere prior to electrophoresis. It was found that 0.002 units was the amount of enzyme required for successful analysis. The experiment was repeated as above only using 0.002 units of enzyme and including a dichlorvos treatment of 2.7 µM.

### 2.3.3. Statistical analysis

The data shown in the results section are representative of 3 independent experiments. Kruskal Wallis analysis was used on the comet assay data which was not normally distributed. Dunn's post hoc test was used to compare concentration effects. The statistical relevance is indicated in a table next to the next to a figure of the mean OTM and of individual cell OTM values, levels of significance are as follows P value <0.05*, <0.01** <0.0001***.

## 2.4 Immunofluorescence microscopy of H2AX

Immunofluorescence is the detection of specific antigens using fluorescently labelled antibodies which can be visualised using fluorescence microscopy. Most commonly, immunofluorescence employs two sets of antibodies: a primary antibody is used against the antigen of interest; a subsequent, secondary, dye-coupled antibody is introduced that recognizes the primary antibody (known as indirect immunofluorescence).

### 2.4.1 Method

A549 cells were seeded at 1x10$^{4}$ per well on 8 well culture slides (BD Falcon) and allowed to adhere overnight. Cells were treated with dichlorvos for 4 h at 0.01, 0.1, 1, 10 or 100µM. Hydrogen peroxide (100µM) was used as a positive control. The medium was removed and cells were washed with cold PBS before they were fixed in 3.8% (v/v) formaldehyde for 5

minutes at room temperature. After two washes in ice cold PBS, cells were permeabilized with 0.2% Triton X-100 in PBS for 20 min at room temperature. After three washes in PBS, cells were incubated in blocking solution (PBS containing 5% goat serum and 0.2% Tween 20) for 1 hour. Cells were then incubated with primary antibody (anti-H2AX phospho-serine 139, New England Biolabs at 1:1000 dilution) in blocking solution for a minimum of 1 hour. After three 5 minutes washes in PBS-T (PBS containing 0.2% Tween 20), cells were incubated with the secondary antibody Alexa Fluor 594-conjugated goat anti-rabbit IgG secondary antibody (Invitrogen) for 45 minutes. Slides were washed thoroughly in PBS-T for 1 hour with fresh PBS-T being replaced every ten minutes before mounting with hydromount medium (National Diagnostics). Slides were viewed using a Carl Zeiss AxioCam MRc5 microscope.

### 2.5 MTT toxicity assay

The MTT [3-(4, 5-dimethylthiazol-2-yl)-2,5-diphenyl tetrazolium bromide] assay is a cytotoxicity test that allows the measurement of cell viability/proliferation. MTT is a yellow dye that is converted to formazone, an insoluble purple compound, by the activity of mitochondrial dehydrogenase. MTT is taken up into cells by endocytosis or a protein-facilitated mechanism where it is reduced to yield a purple formazan product which is largely impermeable to cell membranes, thus resulting in its accumulation within living cells (Figure 2.2). Solubilization of the cells results in the liberation of the purple product which can be detected using a colorimetric measurement. The MTT assay provides an indication of mitochondrial integrity and activity within the cells and of cell proliferation. Cells proliferating in culture will show an increase in retained formazan whereas following cytotoxicity proliferation is reduced and cell death leads to a reduced cell number and reduced formazan retention. A percentage loss of formazan retention compared to control is indicative of reduced viability (Fotakis et al., 2006).

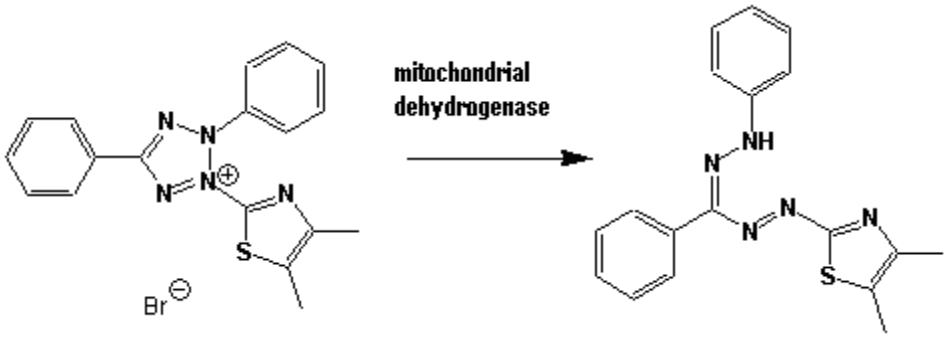


MTT Formazone

**Figure 2.2 Represents the cleavage of the tetrazolium ring of MTT to yield the purple formazone crystals by mitochondrial dehydrogenase**. (Adapted from Fotakis et al 2005)

### 2.5.1 Method

The MTT assay was performed using the TOX-1 in vitro toxicology kit (Sigma). A suspension of TK6 cells at a density of 2 x $10^5$/ml ml was prepared. 1ml aliquots of this suspension were incubated with with either: dichlorvos (0.01, 0.1, 1, 10 and 100µM), chlorpyrifos (0.01, 0.1, 1, 10 and 100µM), chlorpyrifos oxon (0.01, 0.1, 1, 10 and 100µM) or sarin (0.001, 0.01, 0.1 and 1µM). Controls for the experiment were untreated cells and a vehicle control which contained the appropriate concentration of 0.1% acetone, DMSO 0.1% or 0.1% isopropanol. Hydrogen peroxide (10µM) was used as a positive control. Samples were analysed at 1 and 24 hours. The cells were thoroughly resuspended by pipetting and 100µl of this suspension was added to a 96 well plate. 10µl of MTT dye (50µg/ml) was added to each well and cells incubated at 37$^{o}$C with 5% $CO_2$ for 2 hours. The cells were viewed under a microscope to observe if formazone had accumulated inside the cells. The cells were then lysed and the formazone crystals solubilized by adding 100µl of solubilization solution (10% triton X-100, 0.1 N HCl in anhydrous isopropanol) followed by gentle pipetting. The absorbance measured at wavelengths of 570nm and 690nm using a BIO-TEK synergy HT plate reader and KC4 software. The 690nm figure was subtracted from the figure at 570nm to give an absorbance reading giving an estimate of cell proliferation/viability.

### 2.5.2. Statistical analysis

The data shown in the results section are representative of 3 independent experiments. The data is displayed as a mean of three repeats within one experiment. A one way ANOVA test was performed on the MTT assay Tukey's multiple comparison test was used to compare concentration effects. The statistical relevance is indicated in a table next to the figure showing the mean of the three repeats within the experiment, displayed as a percentage of control. Levels of significance are as follows P value <0.05*, <0.01** <0.001***.

## 2.6 Western blotting

A Western blot is a method to detect and quantify one protein in a complex mixture of proteins. After lysis in appropriate buffer, cellular proteins are released. These proteins are denatured by adding a chemical such as lithium dodecyl sulfate (LDS), which coats proteins in a negatively charge causing them to unfold. Disulfide bonds need to be reduced and this is accomplished chemically using 2-mercaptoethanol. The samples are boiled at 95$^{o}$C to ensure all proteins are disaggregated and fully denatured. This means that when proteins are subsequently separated using polyacrylamide gel electrophoresis, this separation is solely according to size and not influenced by secondary/tertiary structure of the proteins. In electrophoresis the negatively charged protein molecules migrate through a polyacrylamide gel, with the smaller molecules able to migrate faster than the larger proteins. The proteins are therefore separated according to size and can be mapped by using protein markers of a known molecular weight. The proteins are then transferred onto nitrocellulose membrane by electrophoresis. After the proteins have been transferred specific antibodies are used to detect the protein of interest. To produce a primary antibody, animals are immunized with a specific antigen (for example a purified protein or specific peptide sequence). An immune response is initiated and specific antibodies can subsequently be purified from the blood of the animals. Depending upon the source of the primary antibody (e.g. mouse, rabbit etc), membranes are then incubated with appropriate secondary antibody that recognizes a species-specific portion of the primary antibody. The secondary antibody also contains a conjugated tag, commonly horseradish peroxidase (HRP). The secondary antibody will bind to the primary antibody, and this antibody complex

can be visualized by adding chemiluminescent reagents to the membrane followed by exposure to x-ray film. Enhanced chemiluminescence (ECL) is described as one of the most sensitive methods for blotting analysis. The light-emitting enzymatic reaction used in chemiluminescent detection is based on the oxidation of a luminol-based substrate by horseradish peroxidase. The oxidation of luminol causes light to be produced and this can be readily detected on photographic film.

### 2.6.1 Method

#### 2.6.1.1 Treatment of suspension cells and preparation of cell extract

5ml of TK6 cell suspension containing 4 x $10^5$ cells/ml were treated with either dichlorvos (0.01, 0.1, 1, 10 and 100µM) or chlorpyrifos (0.01, 0.1, 1, 10 and 100µM) or chlorpyrifos oxon (0.01, 0.1, 1, 10 and 100µM) or Sarin (0.1 and 1 µM) and incubated for up to 24 hours. Etoposide (50µM) was used as a positive control and 0.1% acetone, 0.1%DMSO or 0.1% isopropanol were used as vehicle control depending on the organophosphate used. At the indicated time points (see results) the media was removed and the cells were centrifuged for 10 min at 4000 rpm, the medium removed and the cell pellet washed in cold PBS. This suspension was centrifuged again for 5 min at 4000 rpm. The PBS was removed and 100µl of cold lysis buffer (50mM TRIS pH 7.4, 0.27M sucrose, 1% Triton X-100) added. Immediately prior to use the lysis buffer was supplemented with 1% Halt protease and phosphatase inhibitors (Thermo Scientific). The lysis buffer was previously used by the group at Dundee for immunoprecipitations (Munoz et al., 2007). They clearly showed the presence of nuclear proteins such as hPTIP and 53BP1 in cell extracts produced with this buffer indicating lysis of the nuclear membrane.

#### 2.6.1.2 Treatment of adherent cells and preparation of cell extract

A549 cells were seeded at 2x$10^5$ in 6 well dishes and allowed to adhere overnight before treatment with dichlorvos (10 and 100µM) or chlorpyrifos (10 and 100µM) or chlorpyrifos oxon (10 and 100µM) for 24 hours and etoposide (5 or 50 µM). At 4 and 24 hours the media

was removed and the cells were washed with ice cold PBS. Cells were scraped using a sterile cell scraper into 0.5ml of ice cold PBS. This cell suspension was then transferred to 1.5ml Eppendorf and centrifuged at 500 rpm for 5 minutes. The cell pellet was then washed in ice cold PBS before 50µl of ice cold lysis buffer (50mM TRIS-HCl pH 7.4, 0.27M sucrose, 1% Triton X100, supplemented with 1% protease inhibitors and phosphatase inhibitors) was added. The cells were resuspended in the lysis buffer. Samples were then stored in a freezer at -80$^{o}$C for future analysis.

For sarin studies, A549 cells were seeded at 2x10$^{5}$ in T25 flasks 24 hours before dosing with Sarin (0.1 or 1 µM) or chlorpyrifos oxon (10 and 100µM) and incubated for up to 24 hours. Etoposide (5 or 50 µM) was used as a positive control. At 4 and 24 hours the media was removed and the cells were washed with ice cold PBS. 0.5mls of trypsin was added to each flasks or well and incubated at 37$^{o}$C 5% $CO_2$ for 5 minutes. The trypsin was in activated by adding 1.5 ml of medium. This cell suspension was then transferred to 15ml tubes and centrifuged at 400 RCM for 10 minutes. The cell pellet was then washed in ice cold PBS before 50µl of ice cold lysis buffer (50mM TRIS-HCl pH 7.4, 0.27M sucrose, 1% Triton X100, supplemented with 1% protease inhibitors and phosphatase inhibitors) was added. The cells were resuspended and transferred to 1.5ml Eppendorf tubes. Samples were then stored in a freezer at -80$^{o}$C for future analysis.

### 2.6.2 Preparation of western blot and protein analysis

When required the samples were thawed and resuspended on ice. Samples were centrifuged in a pre-cooled centrifuge (4$^{o}$C) for 5 min at 13000rpm to remove cell debris. The supernatant (containing all protein) was transferred to fresh 1.5ml Eppendorf tubes on ice. The protein concentration was determined by the Coomassie Protein Assay (Thermo Scientific). Briefly, 1 µl of the lysed sample was added to 19 µl of water to which 1 ml of Coomassie reagent was added. The amount of protein was then determined by reading in a spectrophotometer at 595nm using lysis buffer to zero the samples. Absorbance readings were then compared to a standard curve of known bovine serum albumin concentrations.

Sample were then denatured by adding an equal volume of 2xLDS (lithium dodecyl sulphate, Invitrogen) containing 10% 2-mercaptoethanol. The samples were heated to 95$^{o}$C for 5 minutes and then frozen at -20$^{o}$C.

Prior to loading on gels, samples were thawed and again heated to 95$^{o}$C for 5mins. Equal amounts of protein (10-25µg) were separated on 4-12% bis-tris polyacrylamide gels (Invitrogen). Molecular weight protein markers (Seeblue plus2 pre-stained standard, Invitrogen) were loaded at 10µl at one end of the gel and 4µl at the other to allow for gel orientation after electrophoresis. The gels were run at 120-200 volts until the dye front had reached the bottom of the gel. Proteins were then transferred to nitrocellulose membrane (Hybond C Extra, GE Healthcare) either at 50V for two hours or 15V overnight.

The membrane was immersed in Ponseau S (Sigma) solution to check the quality of transfer and protein separation. The membrane was rinsed with TBST (50mM TRIS pH 7.6, 150mM NaCl, 0.2% tween-20) to remove the Ponseau S solution and incubated in 50ml of blocking solution (5% milk powder in TBST) for a minimum of 1hr. Blocking is required to reduce the amount of non-specific antibody binding.

The membrane was then probed using a primary antibody of interest; these include: Rabbit anti-cleaved PARP-1 (1:500), , rabbit anti-p53 Ser15 (1:1000), rabbit anti-Chk2 Thr68 (1:1000) rabbit anti-cdc2 Tyr15 (1:1000), rabbit anti-Rb Ser795 (1:1000), rabbit anti-Rb Ser 807/811 (1:1000), rabbit full length human specific pro-caspase 9 (1:1000) were all from Cell Signalling Technologies. In addition, mouse anti-p53 (DO7, Novocastra, 1:1000) and mouse anti-GAPDH (Abcam, 1:1000) and mouse anti C-2-10 PARP-1 (Biomol 1:1000). Primary antibodies were diluted in 5ml of blocking solution in 50ml Falcon tubes. The membrane was incubated with the primary antibody for a minimum of 4 hours before washing in three washes of TBST, each for 5mins. The membrane was incubated in appropriate HRP conjugated secondary antibody (1:5000 in blocking buffer) in a 50ml falcon tube for 1hour. The membranes were then thoroughly washed in TBST, with several changes of the buffer (at least 6) over the course of one hour.

The membrane was visualized using chemiluminescence (ECL plus, GE Healthcare). After adding the ECL reagents the membranes were sealed within plastic sheets and images

captured by a Syngene G:Box gel documentation system. Image analysis, including quantification of protein bands, was performed using Gene Tools software (Syngene).

### 2.6.3. Statistical analysis

The data shown in the results section is representative of 3 independent experiments. In some studies, samples were prepared in duplicate, quantified and data displayed as a mean ± standard error.

## 2.7 OP cytotoxicity in DNA repair-deficient cells

Specific DNA repair pathways were inhibited in TK6 cells using enzyme inhibitors. The cytotoxicity of dichlorvos was then investigated in DNA repair-proficient and -deficient cells using an MTS assay.

### 2.7.1 Inhibition of DNA repair pathways

DNA adducts such as methylated bases and those caused by oxidative damage to DNA are recognised and repaired by BER. This pathway utilises specific DNA glycosylases to detect DNA lesions before removing the damaged base. The DNA backbone is broken by an endonuclease to produce a single strand break, followed by DNA synthesis and ligation. The DNA repair enzyme PARP-1 plays a crucial role in BER, as part of a complex containing XRCC1 and DNA ligase III. The PARP-1 inhibitor NU1025 (Bowman et al 1998) was used to inhibit PARP-1 in TK6 cells. NU1025 was prepared at a stock concentration of 20mM in DMSO and added to cells at a final concentration of 200µM for 1 hr to allow for BER to become inhibited. Cells lacking PARP-1 protein or activity are hypersensitive to chemicals that induce alkylation or oxidative damage to DNA.

Non-homologous end joining (NHEJ) is employed to repair DSB in human cells. DSB's are directly ligated together by the action of the ku70/80 and DNA-dependent protein kinase (DNA-PK) complex, this is necessary for the phosphorylation of XRCC4 and subsequent recruitment of DNA ligase IV, which is responsible for the ligation and repair of the DNA DSB. The protein kinase inhibitor NU7026 (Boulton et al 1999) inhibits the formation of the DNA-PK complex. NU7026 was prepared at a stock concentration of 10mM and added to

cell culture to give a final concentration of 100 µM for 1 hour to allow sufficient time for NHEJ to become inhibited. Cells pre-treated with this inhibitor will not be able to form DNA-PK complex and will be more sensitive to chemicals that can cause DSB to DNA.

### 2.7.2 MTS assay

MTS assay is a similar assay to the MTT assay and is a related tetrazolium salt. MTS or {3-(4,5-dimethylthiazol-2-yl)-5-(3-carboxymethoxyphenyl)-2-(4-sulfophenyl}-2*H*-tetrazolium, inner salt) is converted into soluble formazan by mitochondrial dehydrogenase of viable cells, thus serving as an indicator of cell viability. The MTS compound is reduced by cells into a colored formazan product that is soluble in tissue culture medium. The quantity of formazan product as measured by the amount of 490nm absorbance is directly proportional to the number of living cells in culture. Cell viability can be determined by reading the resulting solution at 490nm and subtracting the average 490nm absorbance from a "no-cell" control.

### 2.7.3 Method

When investigating the effect of poly(ADP-ribose) polymerase-1 (PARP-1) or protein kinase inhibition in TK6 cells, $2x10^6$ cells (in a volume of 10ml) were incubated for one hour with either of the inhibitor's or 1% DMSO as a solvent control before 1ml aliquots (containing 2 x $10^5$ cells) were used for dosing with dichlorvos. The dichlorvos concentrations used were 0.01, 0.1, 1, 10 and 100µM, cells exposed for 24 and 48 hours prior to evaluation of cell viability by the MTS assay. Controls used were untreated cells as a negative control and hydrogen peroxide at 10 µM or etoposide 50 µM as a positive control. At 24 and 48 hours a 100µl aliquot of each treatment was taken in triplicate on a 96 well plate and 10µl of MTS dye (50µg/ml) was added to each well and cells incubated at 37$^{o}$C with 5% $CO_2$ for 3 hours. The cells were viewed under a microscope to observe if formazan salt had accumulated inside the cells and then read at 490nM in a BIO-TEK plate synergy HT plate reader and KC4 software to determine cell viability.

# *Chapter 3*

# *Cellular response to DNA damage and cytotoxicity after dichlorvos in vitro*

## 3.0 Dichlorvos

Organophosphates (OPs) are acetylcholinesterase inhibitors; although some studies have suggested that they are also able to damage DNA. The cellular response to genotoxic stress is initiated by the activation of the ATM (ataxia-telangiectasia, mutated) and ATR (ATM and Rad-3 related) protein kinases. These kinases phosphorylate various target proteins including p53, the checkpoint kinases Chk1 and Chk2 and histone H2AX. These proteins along with many others, to cause cell cycle arrest, regulate transcription, enhance DNA repair capacity of cells, or to direct cells to apoptosis. This study aimed to investigate the potential of dichlorvos (an oxon) to induce DNA damage using the alkaline comet assay. In addition, as a further indicator of DNA damage, the activation of DNA damage signalling pathways, including the phosphorylation of p53, Chk2 and H2AX was also investigated.

### 3.1 Cytotoxicity

In order to relate any DNA damage observed to the cytotoxic potential of dichlorvos TK6 cells were treated with dichlorvos and $H_2O_2$ for 1 or 24 hours and cell viability measured using an MTT assay. Figure 3.1 and Table 3.1, showed that dichlorvos shows no cytotoxic affect after 1 hour, but the effect with hydrogen peroxide was clear causing a 30% loss of cell viability. As shown in Figure 3.2 and Table 3.2, dichlorvos was cytotoxic to TK6 cells at higher concentrations after 24 hours. At 2-60µM, dichlorvos caused a 20% loss of cell viability over a 24 hour period, whereas 100µM caused a loss of 40 % viability.

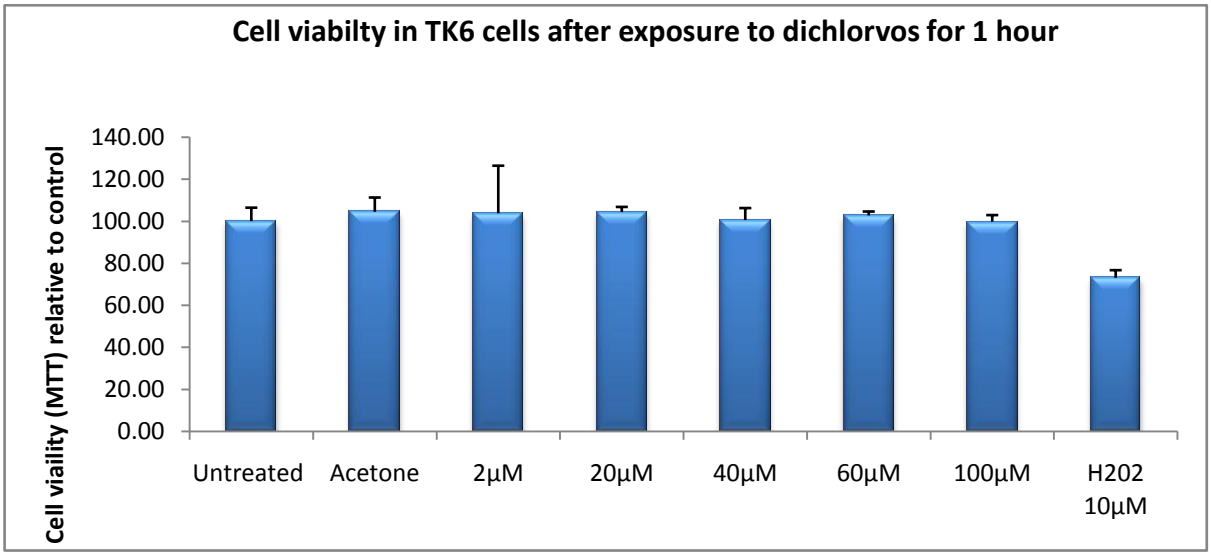


**Figure3.1 Cytotoxicity of dichlorvos in TK6 cells.** Cells were exposed to 2, 20, 40, 60 and 100µM dichlorvos or $H_2O_2$ for 1hour before cell viability was measured using an MTT assay. Results were expressed as mean % viability relative to untreated control (untreated cells designated 100% viability) ± standard deviation

| | Untreated | Acetone | 2µM | 20µM | 40µM | 60µM | 100µM | $H_2O_2$ 10 µM |
|---|---|---|---|---|---|---|---|---|
| Cytotoxicity (% viability) | 100.00 | 104.41 | 103.73 | 104.33 | 100.51 | 102.71 | 99.75 | 73.28* |

**Table3.1**. Cytotoxicity in TK6 cells after treatment with dichlorvos (2, 20, 40, 60 and 100µM) for 1 hour. Cytotoxicity was measured as a percentage of control. (P value * <0.05 **P value <0.01 ***P value <0.001 one way ANOVA)

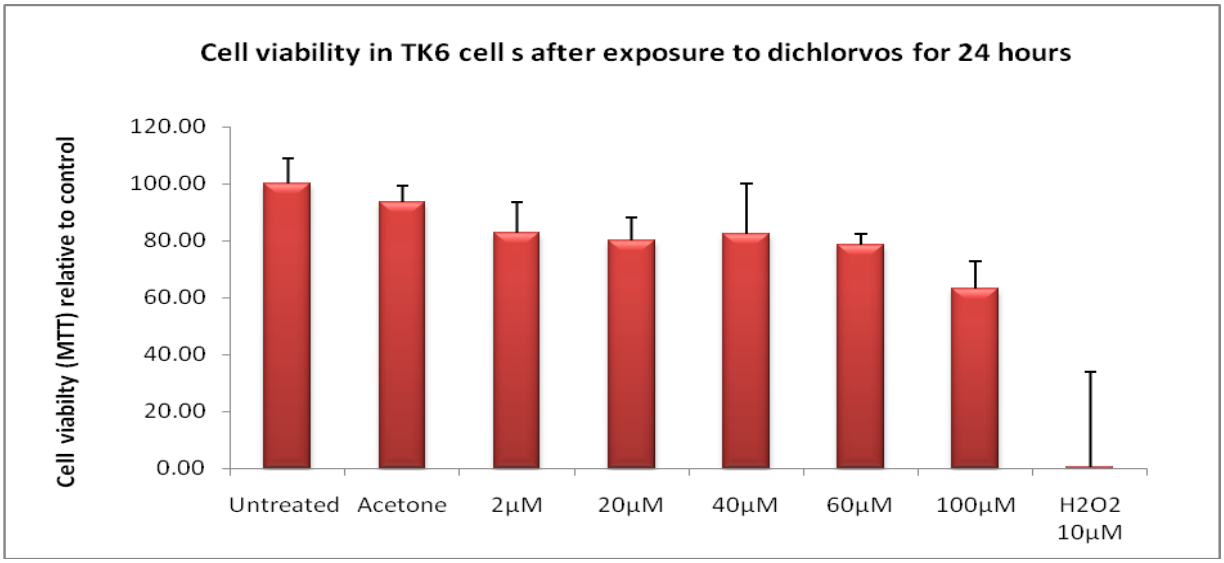


**Figure3.2 Cytotoxicity of dichlorvos in TK6 cells.** Cells were exposed to 2, 20, 40, 60 and 100µM dichlorvos or $H_2O_2$ for 24 hours before cell viability was measured using an MTT assay. Results were expressed as mean % viability relative to untreated control (untreated cells designated 100% viability) ± standard deviation

| | Untreated | Acetone | 2µM | 20µM | 40µM | 60µM | 100µM | $H_2O_2$ 10 µM |
|---|---|---|---|---|---|---|---|---|
| **Cytotoxicity (% viability)** | 100.00 | 93.71 | 82.61 | 80.23 | 82.55 | 78.75 | 63.23*** | 0.51*** |

**Table 3.2.** Cytotoxicity in TK6 cells after treatment with dichlorvos (2, 20, 40, 60 and 100µM) for 24hours. Cytotoxicity was measured as a percentage of control (P value * <0.05 **P value <0.01 ***P value <0.001 one way ANOVA)

## 3.2 DNA Damage

### *3.2.1 Comet assay*

DNA damage was measured by the alkaline comet assay in both SHSY-5Y neuroblastoma cells and TK6 lymphoblastoid cell lines. To test whether dichlorvos was able to cause DNA damage, SH-SY5Y cells were exposed to different doses of dichlorvos and DNA damage was estimated by the alkaline comet assay. In the initial study, SHSY-5Y cells were exposed to 2.7 nM and 2.7 µM as it had previously been established by Atherton et al. (2006) that 2.7nM caused complete inhibition of AChE in SHSY-5y cells. DNA damage was increased at both 2.7nM and 2.7µM when compared with untreated cells (Figure 3.3 and Table 3.3).

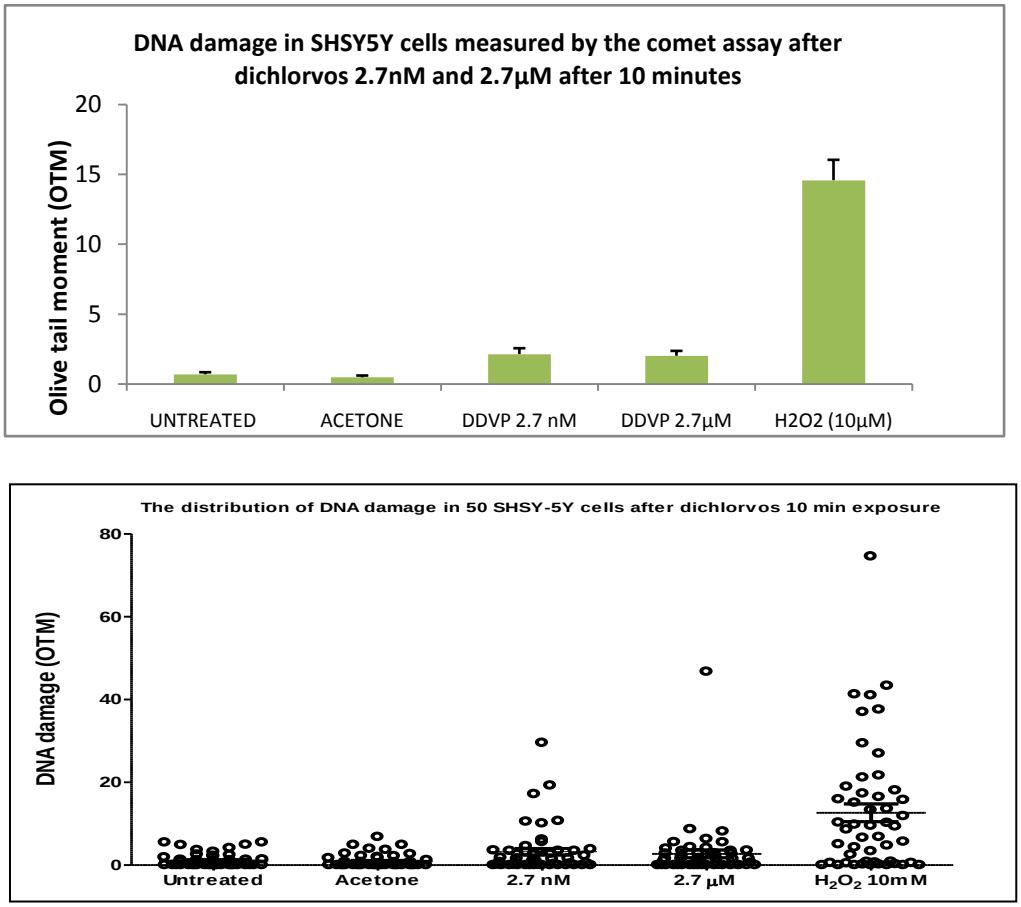


**Figure 3.3. DNA damage in SH-SY5Y cells after Dichlorvos (2.7nM and 2.7µM).** The exposure time for the experiment was ten minutes. The upper graph shows the mean olive tail moment of 50 cells± S.E. Positive control hydrogen peroxide 10µM (value 17.8 OTM) has been excluded from the upper graph. Acetone was used as a vehicle control. The lower graph shows the distribution of damage between the 50 cells scored.

| | Untreated | Acetone | 2.7nM | 2.7µM | H2O2 10µM |
|---|---|---|---|---|---|
| **DNA damage (OTM)** | 1.08 | 0.92 | 3.24* | 2.71 | 12.63*** |

**Table3.3 DNA damage in SHSY5Y cells by dichlorvos (2.7nM and 2.7µM) and for ten minutes**. DNA damage was measured as OTM (P value * <0.05 **P value <0.01 ***P value <0.001 Kruskal-Wallis)

Figure 3.3 and Table 3.3 demonstrates that dichlorvos was able to rapidly damage DNA in a short exposure time of just ten minutes. The damage is slightly higher with the 2.7nM than 2.7µM. This is due to approximately 6 cells displaying a much higher than expected OTM value. The 2.7µM has one outlandish figure but the majority of cells have an OTM of 2. The untreated and acetone treated SHSY5Y cells have a figure of around 1 OTM. This value was

higher than expected with Collins et al. (1997) describing OTM of less than 1 to be undamaged.

The study described in figure 3.3 shows that dichlorvos was able to cause DNA damage after a short exposure time. The study was expanded to include a wider range of dichlorvos doses (0.01, 0.1, 1, 10, 100µM) and a longer time point of one hour (Figure 3.4 and Table 3.4). The values represented are OTM (arbitrary units). At all concentrations an increase in DNA damage in comparison with control (untreated sample) was observed with an increase in dose. 100µM caused the largest increase in DNA damage giving a mean OTM value of 4.04 when compared to 0.59 of untreated cells. The distribution of damage in SHSY5Y is interesting as the majority of cells have a low OTM value, with a minority of cells showing high OTM value. This trend is seen at all concentration's, after 0.01µM 10% of cells have an OTM greater than 5 and this increases with dose to approximately 30% of cells displaying an OTM greater than 5 after 100µM dichlorvos.

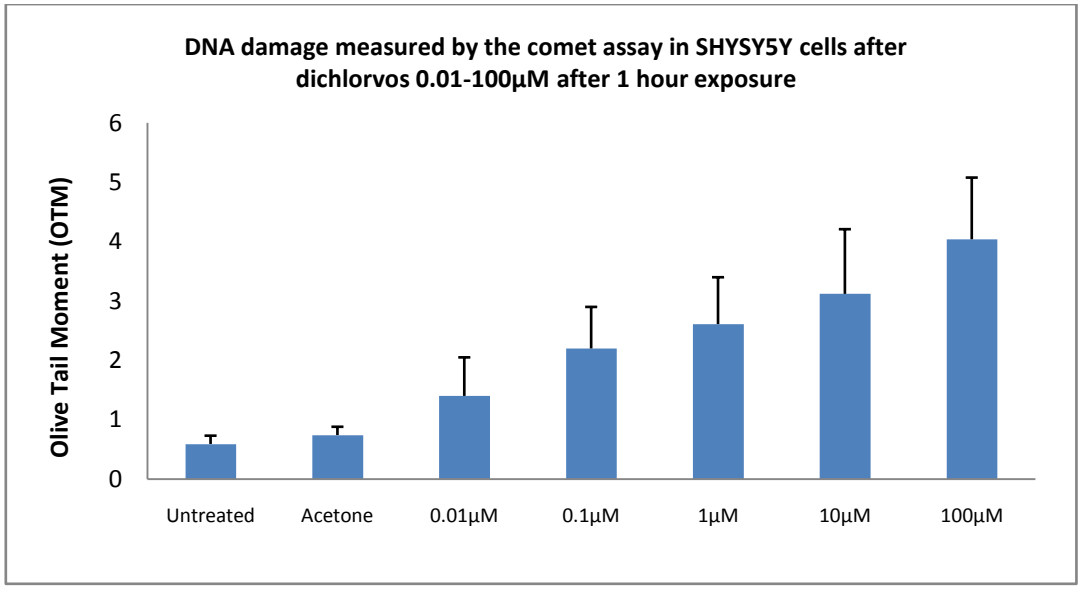


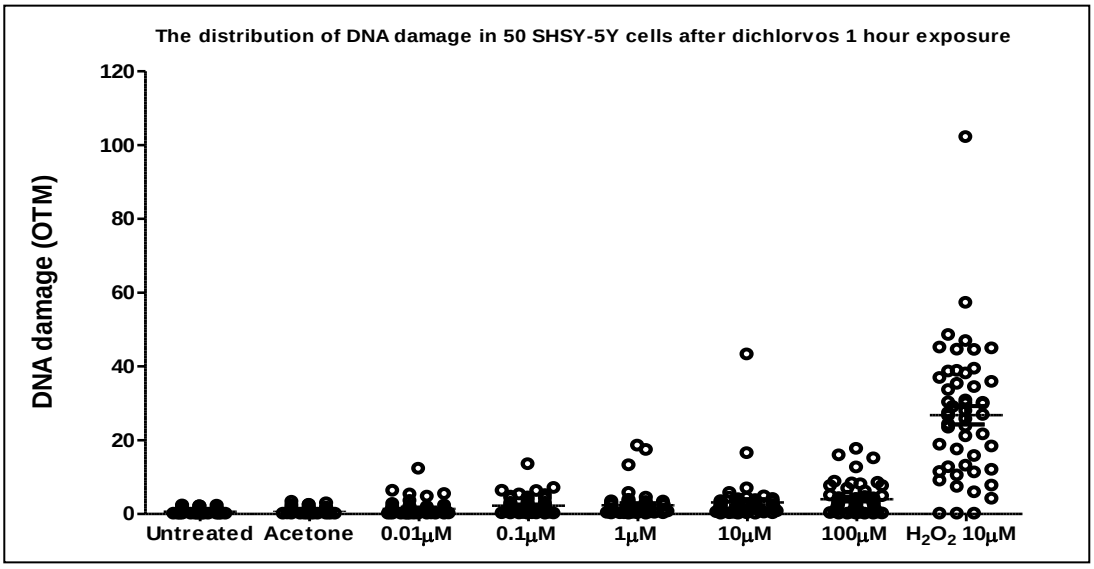


**Figure 3.4. DNA damage in SH-SY5Y cells after Dichlorvos (0.01-100µM).** The exposure time for the experiment was 1 hour. The upper graph shows the mean olive tail moment of 50 cells ± S.E. Positive control hydrogen peroxide 10µM (value 30.5 OTM) and has been excluded from the upper graph. Acetone was used as a vehicle control. The lower graph shows the distribution of damage between the 50 cells scored.

| | Untreated | Acetone | 0.01µM | 0.1µM | 1µM | 10µM | 100µM |
|---|---|---|---|---|---|---|---|
| **DNA damage (OTM)** | 0.59 | 0.74 | 1.4 | 2.2** | 2.61* | 3.12*** | 4.04*** |

**Table 3.4. DNA damage in SHSY5Y cells by dichlorvos (0.01, 0.1, 1, 10, 100 µM) for 1 hour**. DNA damage was measured as Olive Tail Moment (OTM) (P value * <0.05 **P value <0.01 ***P value <0.001 Kruskal-Wallis)

To corroborate the findings in SH-SY5Y cells, experiments were repeated in a different cell line, this being TK6 lymphoblastoid cells. TK6 cells were exposed to a range of dichlorvos concentrations over 24 hours. An increase in dose caused an increase in OTM at both 1 and 24 hours (Figures 3.5 and 3.6; Tables 3.5 and 3.6), though the levels of DNA damage were greater at 24 hours. The largest difference in damage was observed between acetone treated cells and the 100µM with the OTM increasing from 0.34 to 6.72. It is also worth noting the distribution of DNA damage after exposure to dichlorvos for one hour, almost all cells have an OTM value less than 5 with the majority of cells displaying low level DNA damage (<2 OTM). After 24 hours the majority of the cells have a similar value between 2-3 OTM with a few cells that displayed high OTM values >5.

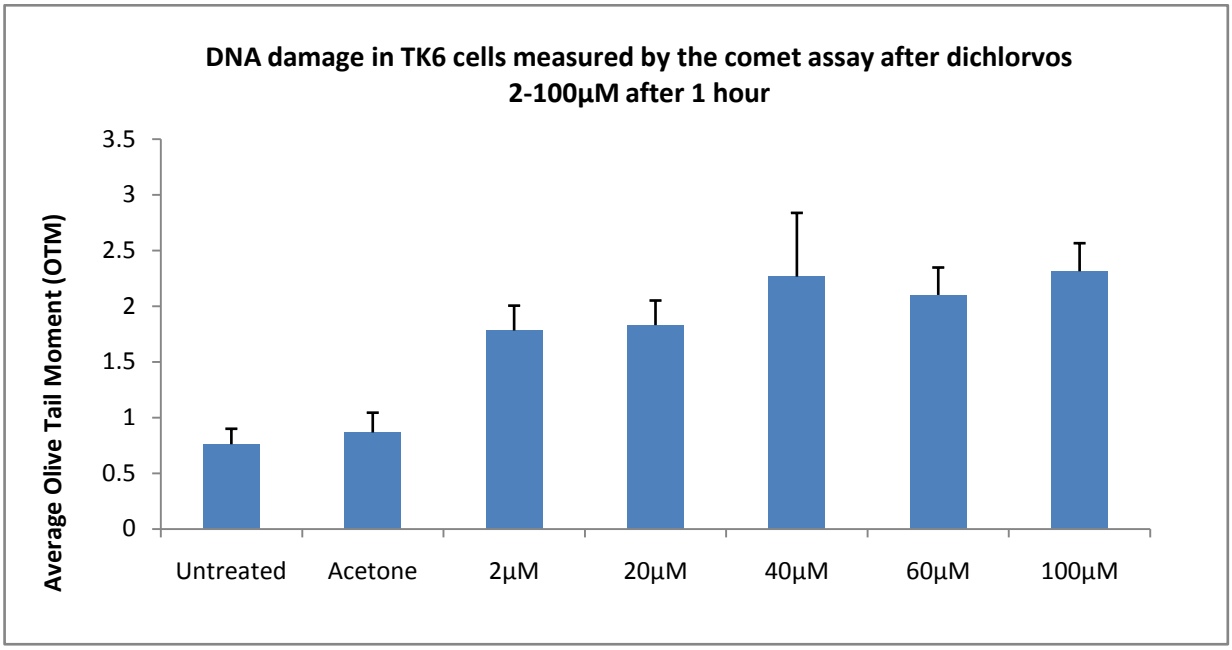


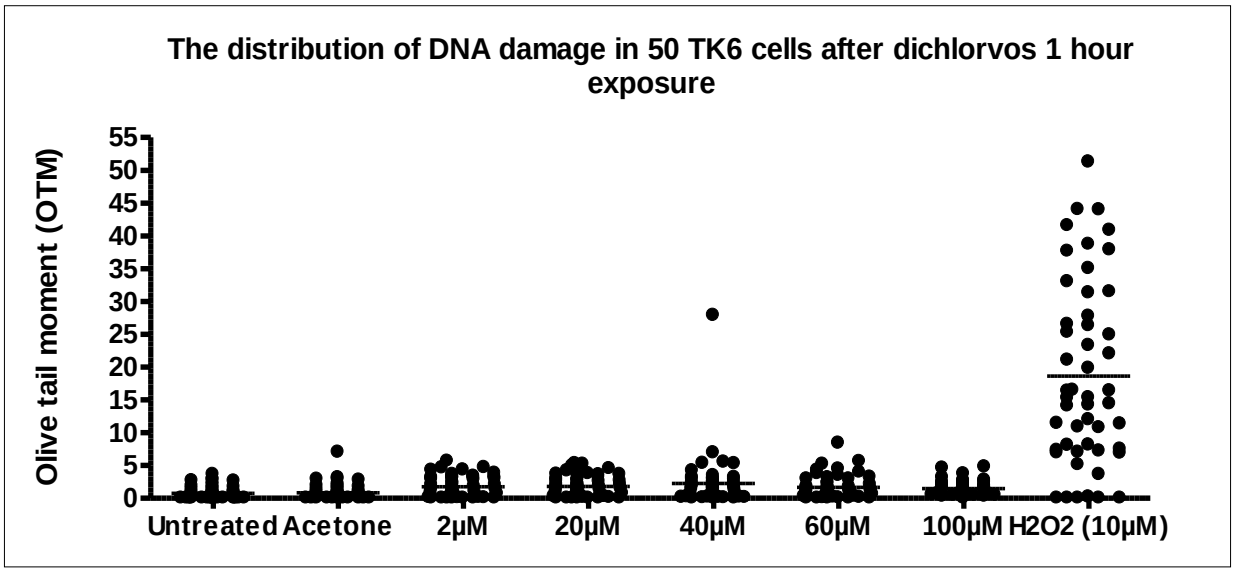


**Figure 3.5. DNA damage in TK6 cells after Dichlorvos.** TK6 cells were exposed to the indicated doses of dichlorvos or hydrogen peroxide for 1 hour prior to measurement of DNA damage using the alkaline comet assay. The upper graph shows the mean olive tail moment of 50 cells ± S.E. Hydrogen peroxide 10µM (value 19.8 OTM) has been excluded from the upper graph. The lower graph shows the distribution of damage between the 50 cells scored.

| | Untreated | Acetone | 2µM | 20µM | 40µM | 60µM | 100µM |
|---|---|---|---|---|---|---|---|
| DNA damage (OTM) | 0.76 | 0.87 | 1.78* | 1.83** | 2.27** | 2.10* | 2.31** |

**Table 3.5. DNA damage in TK6 cells by Dichlorvos (2, 20, 40, 60 and 100µM) for 1 hours**. DNA damage was measured as Olive Tail Moment (OTM) (P value * <0.05 **P value <0.01 ***P value <0.001 Kruskal-Wallis)

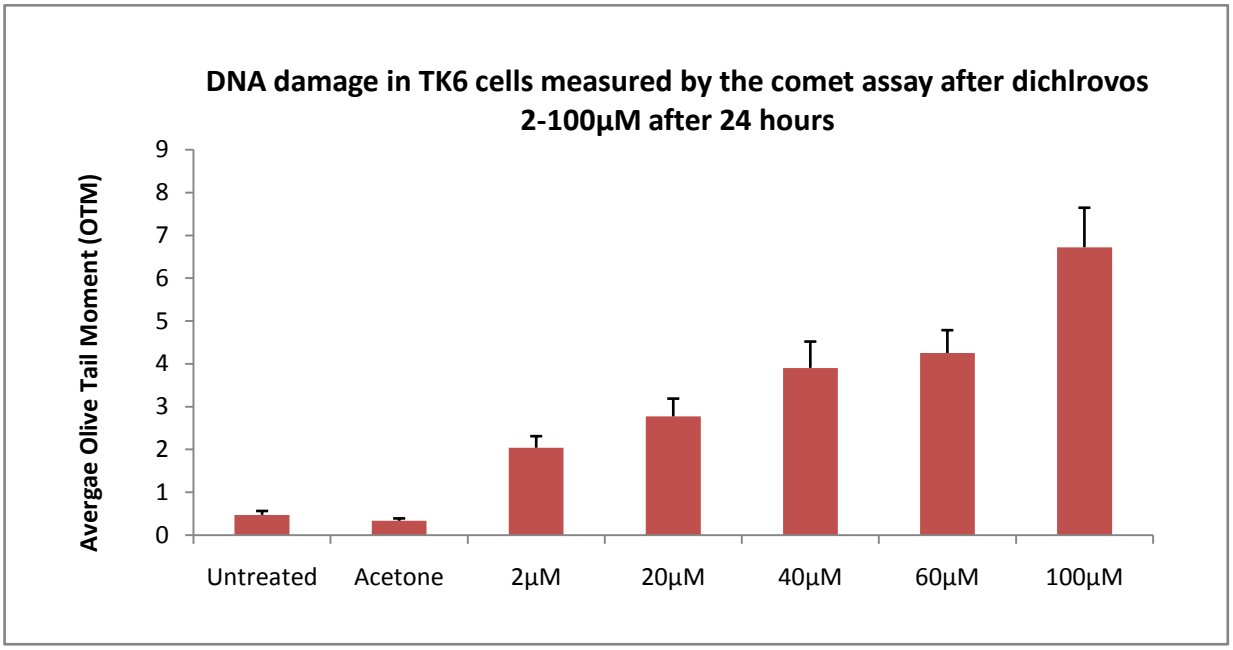


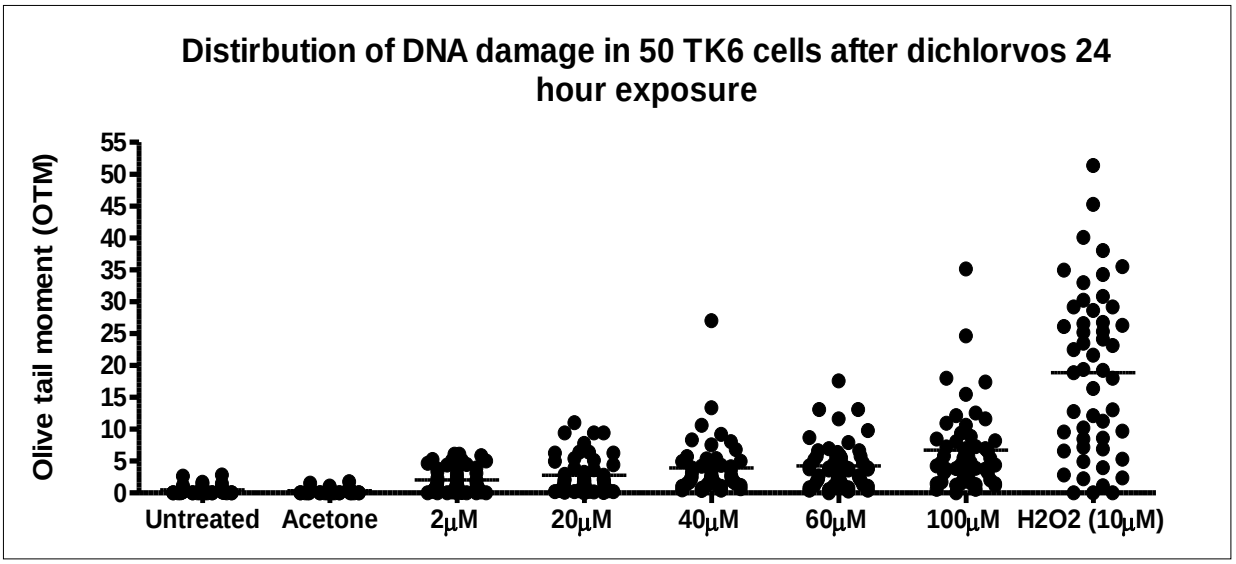


**Figure 3.6. DNA damage in TK6 cells after Dichlorvos.** TK6 cells were exposed to the indicated doses of dichlorvos or hydrogen peroxide for 24 hours prior to measurement of DNA damage using the alkaline comet assay The upper graph shows the mean olive tail moment of 50 cells ± S.E. Hydrogen peroxide 10µM (value 21.8 OTM) has been excluded from the upper graph. The lower graph shows the distribution of damage between the 50 cells scored.

| | Untreated | Acetone | 2µM | 20µM | 40µM | 60µM | 100µM |
|---|---|---|---|---|---|---|---|
| DNA damage (OTM) | 0.47 | 0.34 | 2.04*** | 2.77*** | 3.91*** | 4.25*** | 6.72*** |

**Table 3.6. DNA damage in TK6 cells by dichlorvos (2, 20, 40, 60 and 100µM) for 24 hours**. DNA damage was measured Olive Tail Moment (OTM) ) (P value * <0.05 **P value <0.01 ***P value <0.001 Kruskal-Wallis)

After 24 hours the level of DNA damage is greater than after 1 hour. This may be due to dichlorvos causing more damage over time though it could also be due to the cytotoxic potential of dichlorvos. The alkaline comet assay does not have the ability to demonstrate the type of DNA damage occurring within the cell. Therefore it is possible that the increase in OTM after 24 hours is not entirely due to dichlorvos directly damaging the DNA. Dichlorvos has been proven to be cytotoxic to cells in culture, after exposure for 24 hours some apoptotic or necrotic stress pathways may have been triggered and one indication of these pathways is DNA degradation. This degradation of DNA would be included in the analysis by the comet assay. However DNA damage is still seen at non-cytotoxic doses, suggesting that dichlorvos is able to induce DNA damage independent of cytotoxicity.

In order to see if similar concentrations of dichlorvos would cause similar levels of DNA damage in a primary cell line, a preliminary study was conducted using freshly isolated lymphocytes; lymphocytes were isolated from blood and placed in TK6 medium for 24 hours prior to experimentation. These lymphocytes were used to assess DNA damage by the alkaline comet assay after dichlorvos (0.01, 0.1, 1, 10, 100 µM) for 1 hour (Figure 3.7 and Table 3.7).

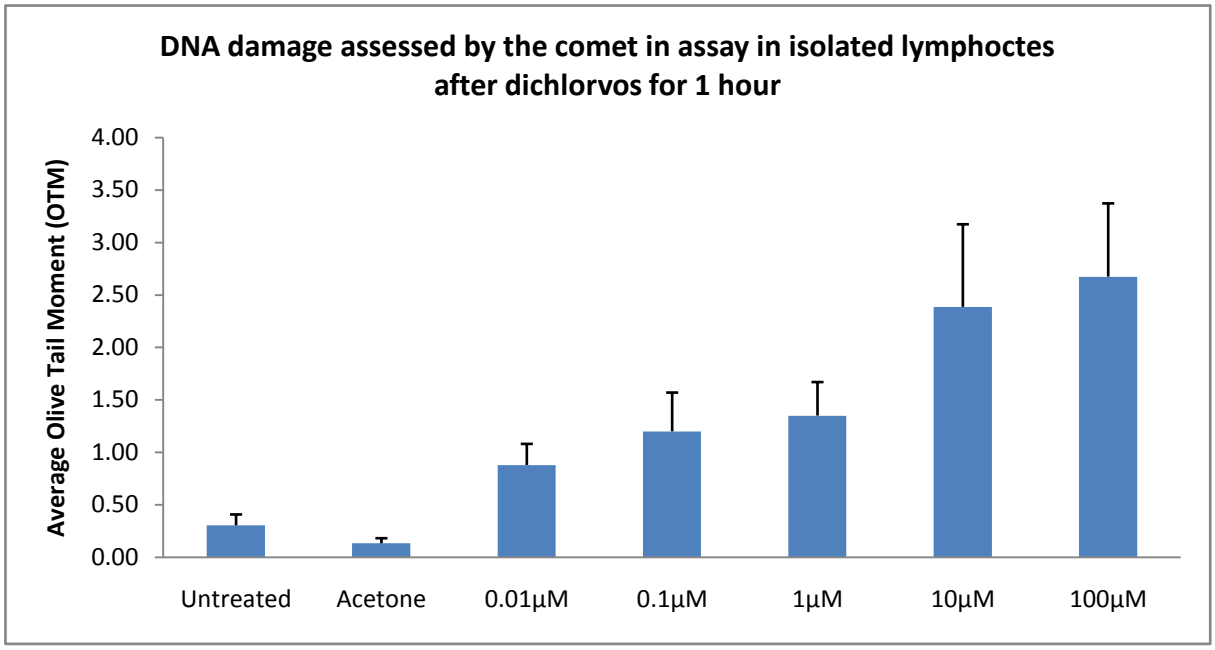


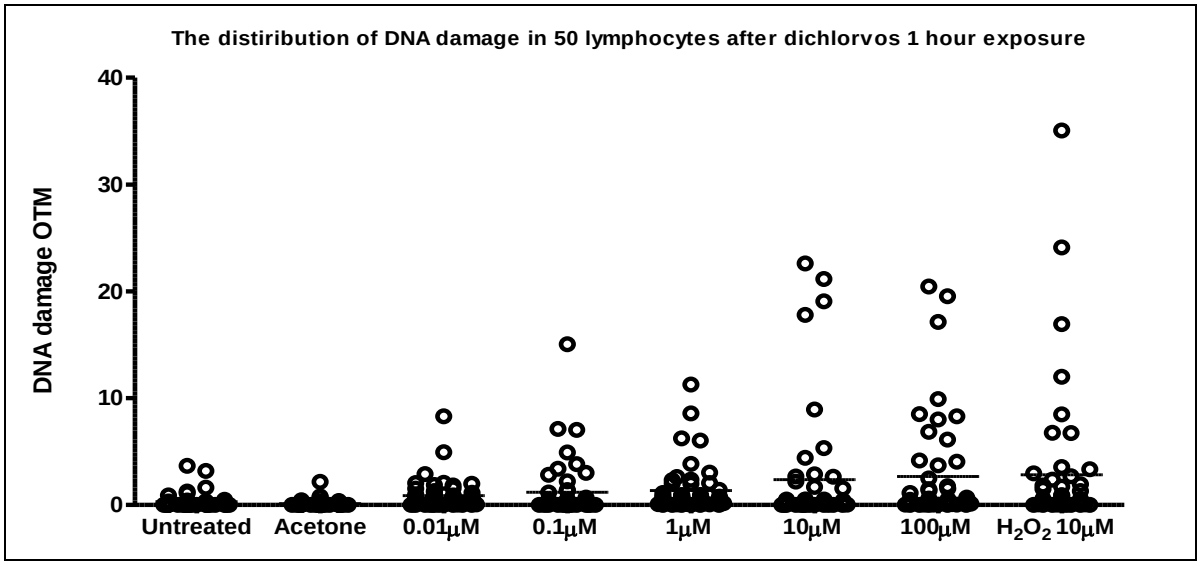


**Figure 3.7. DNA damage in primary lymphocyte cells after Dichlorvos.** Lymphocytes were exposed to the indicated doses of dichlorvos or hydrogen peroxide for 1hour prior to measurement of DNA damage using the alkaline comet assay. The upper graph shows the mean olive tail moment of 50 cells ± S.E. Hydrogen peroxide 10µM (value 3.8 OTM) has been excluded from the upper graph. The lower graph shows the distribution of damage between the 50 cells scored.

| | Untreated | Acetone | 0.01µM | 0.1µM | 1µM | 10µM | 100µM |
|---|---|---|---|---|---|---|---|
| DNA damage (OTM) | 0.30 | 0.13 | 0.88** | 1.20 | 1.35*** | 2.38* | 2.67*** |

**Table3.7 DNA damage in lymphocytes by dichlorvos (0.01, 0.1, 1, 10, 100 µM) for 1 hour**. DNA damage was measured as OTM (P value * <0.05 **P value <0.01 ***P value <0.001 Kruskal-Wallis)

Dichlorvos was able to cause DNA damage in freshly isolated lymphocytes in a dose dependent manner. The damage seen after 1 hour with dichlorvos in isolated lymphocytes is similar to that seen in the established cell line TK6 cells. The greatest damage caused was with 100µM in both cell types but in isolated lymphocytes the mean damage for 50 cells was 2.67 and in TK6 cells 2.31. These values are less than those obtained in SHSY-5Y cells where 100µM gave an average OTM of 4.04, this may be due to the shape of the neuroblastoma cell as it is an uneven shape and can be difficult to analyse using the comet assay. This result suggests that the alkaline comet assay may be a useful genotoxic biomarker to monitor DNA damage in individuals exposed to dichlorvos. This experiment is preliminary but it is useful as the cell lines respond in a similar manner with regards to DNA damage after dichlorvos. When comparing the distribution of DNA damage in Lymphocytes with TK6 cells after 1 hour, lymphocytes at all concentrations of dichlorvos showed a higher proportion of cells displaying OTM greater than 5.

### 3.2.2. Comet assay with lesion specific endonucleases

The comet assay can be modified to include purified DNA repair enzymes that detect specific DNA lesions. The standard alkaline method gives limited information on the type of DNA damage being measured as it is not possible to determine whether these are a consequence of direct effects of the damaging agent, or of indirect effects, such as oxidative damage, apurinic/pyrimidinic (AP) sites or DNA repair intermediates. The sensitivity and specificity of the assay can be improved by incubating the lysed cells with lesion-specific endonucleases, which recognize particular damaged bases and create additional breaks which can then be analysed by the alkaline comet assay. Information about oxidative DNA damage and its repair can be obtained by including Formamidopyrimidine glycosylase (FPG). FPG recognises and repairs the damaged bases including the mutagenic 8-oxodeoxyguanosine (8-oxodG), 2,6-diamino-4-hydroxy-5-formamidopyrimidine (FapyG), 4,6-diamino-5-formamidopyrimidine (FapyA), and 8-oxo-7,8-dihydroadenine (8-oxoA) (Perlow-Poehnelt et al., 2004).

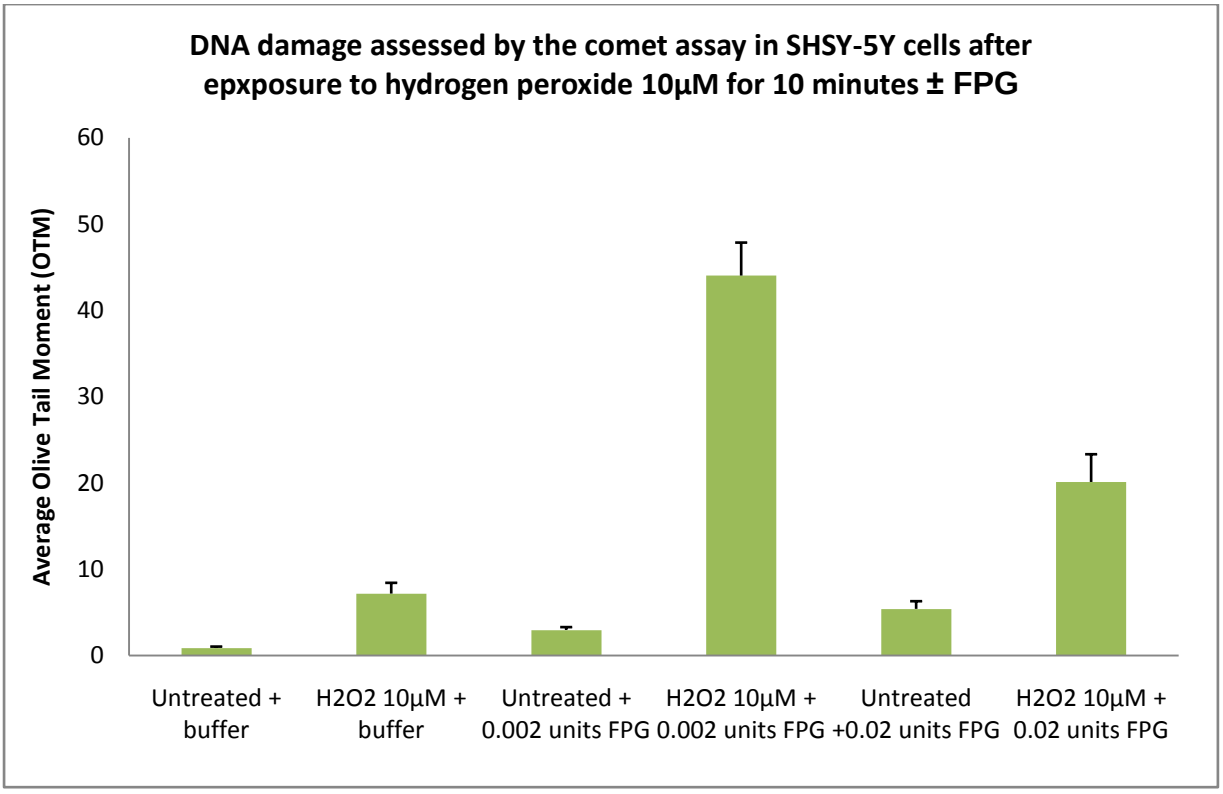


**Figure 3.8 DNA damage in SY5Y cells after hydrogen peroxide (10µM) treatment with and without FPG enzyme for ten minutes**. The buffer by itself was included to establish that this did not cause any increase in DNA damage and then two concentrations of enzyme were chosen 0.002 units and 0.02 units. Olive Tail Moment (OTM). Values are the mean of 50 cells ± standard error.

A preliminary study was conducted using alkaline comet assay with FPG to assess whether oxidative damage occurred after exposure to dichlorvos. Initial studies were performed to test the appropriate amount of enzyme required. Untreated and hydrogen peroxide treated samples, in the presence, and absence of FPG, were compared. SH-SY5Y cells were exposed to hydrogen peroxide (10µM) for two minutes and then processed as in materials and methods. The results can be seen in figure 3.8. The result at 0.002 units provided the greatest increase in OTM with an increase from 2.94 to 44.05. Increasing the amount of enzyme to 0.02 units actually led to a smaller increase in OTM, possibly due to the fact that many cells were rendered unreadable as the tails were so large that they overlapped with each other. For this reason 0.002 units of enzyme was used in subsequent studies.

To analyse whether the type of DNA damage caused by dichlorvos was oxidative in nature, SH-SY5Y cells were treated with dichlorvos and the DNA damage was measured by the modified comet assay (Figure 3.9 and Table 3.8).

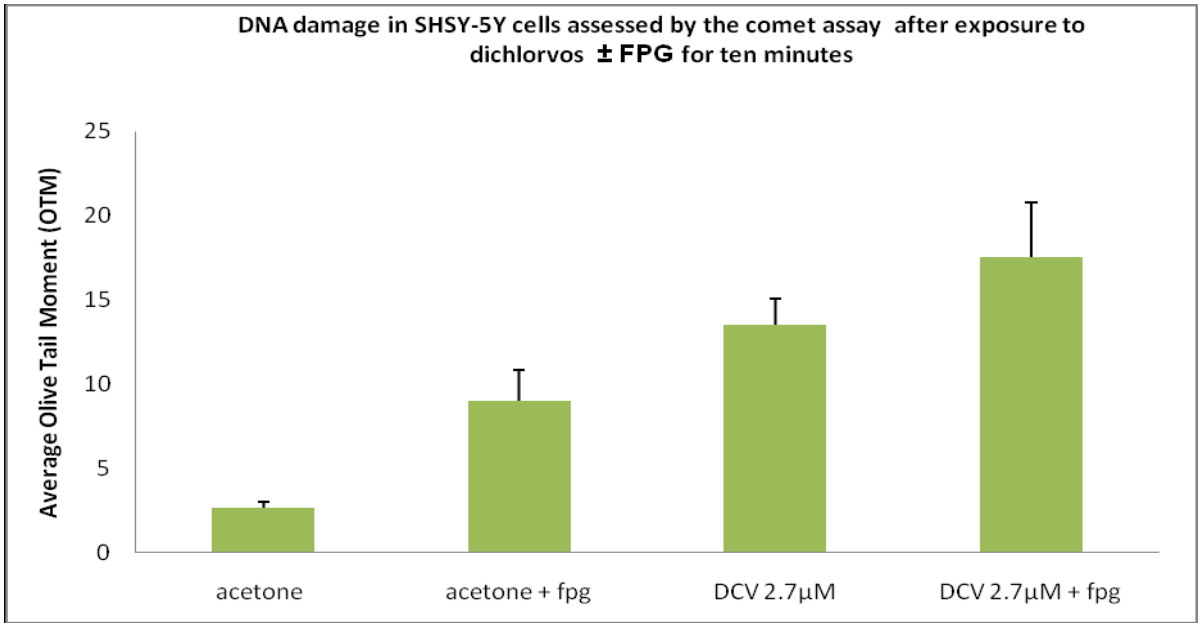


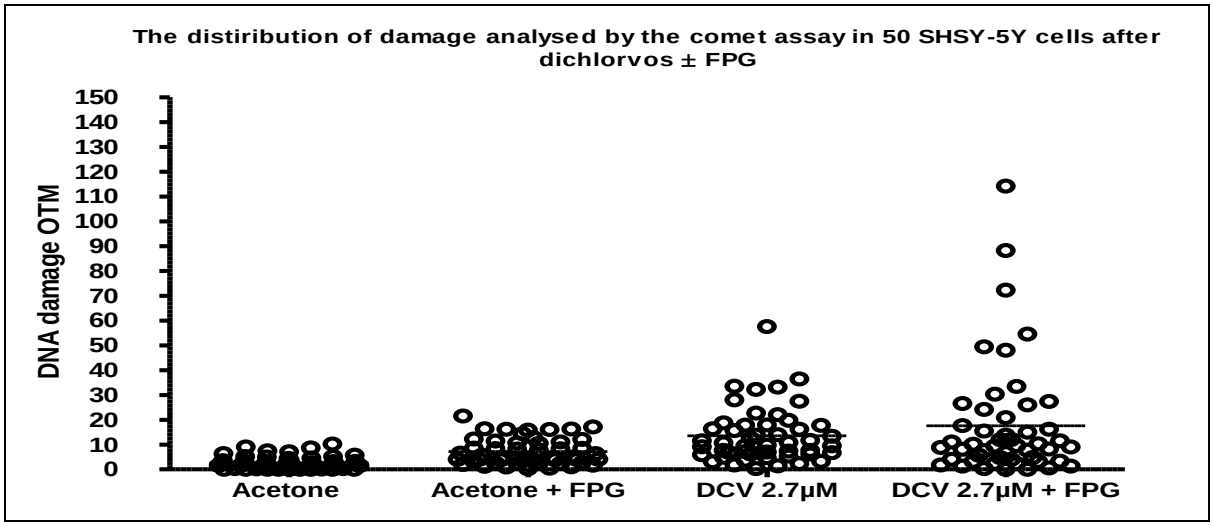


**Figure 3.9 DNA damage in SH-SY5Y cells after 2.7µM dichlorvos ± FPG for 10 minutes.** DNA damage was measured as Olive Tail Moment (OTM). Positive control hydrogen peroxide 10µM (value 41.5 OTM) has been excluded from the upper graph, values are mean of 50 cells ± S.E. The lower graph shows the distribution of damage between the 50 cells scored.

| | Acetone | Acetone + FPG | 2.7µM | 2.7µM + FPG |
|---|---|---|---|---|
| DNA damage (OTM) | 2.65 | 7.37*** | 13.53 | 17.58$^{ns}$ |

**Table 3.8. DNA damage in SHSY-5Y cells by DCV (Acetone, Acetone +FPG, 2.7µM DCV and 2.7µM DCV +FPG) for 10 minutes**. DNA damage was measured as Olive Tail Moment (OTM) (P value <0.001*** Kruskal-Wallis).

The change in OTM with and without FPG was then compared to give an estimate of oxidative DNA damage present. As in Figure 3.3, dichlorvos at 2.7µM caused an increase in DNA damage (Figure3.9). The OTM values for this experiment are much higher than previously recorded. It is possible that this was due to the processing step but is unlikely. The acetone treated samples had a much higher OTM than previously recorded and this suggests that the cells were not in optimum condition for experimentation. There was an increase in OTM between acetone treated cells and acetone + FPG and is statistically significant ($p$ value<0.001). There was an increase in OTM between dichlorvos treated cells and dichlorvos +FPG treated sample, though this is not statistically significant. This preliminary study should be repeated including an alternative oxidative damage-specific enzyme.

### 3.2.3 H2AX immunofluorescence

As a further marker for DNA damage, the phosphorylation of histone H2AX was investigated. In response to DNA DSBs, induced by Ionising radiation, histone H2AX is rapidly phosphorylated to form discreet nuclear spots or foci, termed γ-H2AX. Several studies have also demonstrated phosphorylation of this protein after other forms of DNA damage, including ultra violet radiation and alkylating agents (Heacock et al., 2010), although nuclear foci do not always form (Kinner et al., 2008). A549 Cells were grown on 8 well culture slides and treated with dichlorvos for 4 hours at 0.1, 1, 10, 100 µM and hydrogen peroxide 100 µM was used as a positive control.

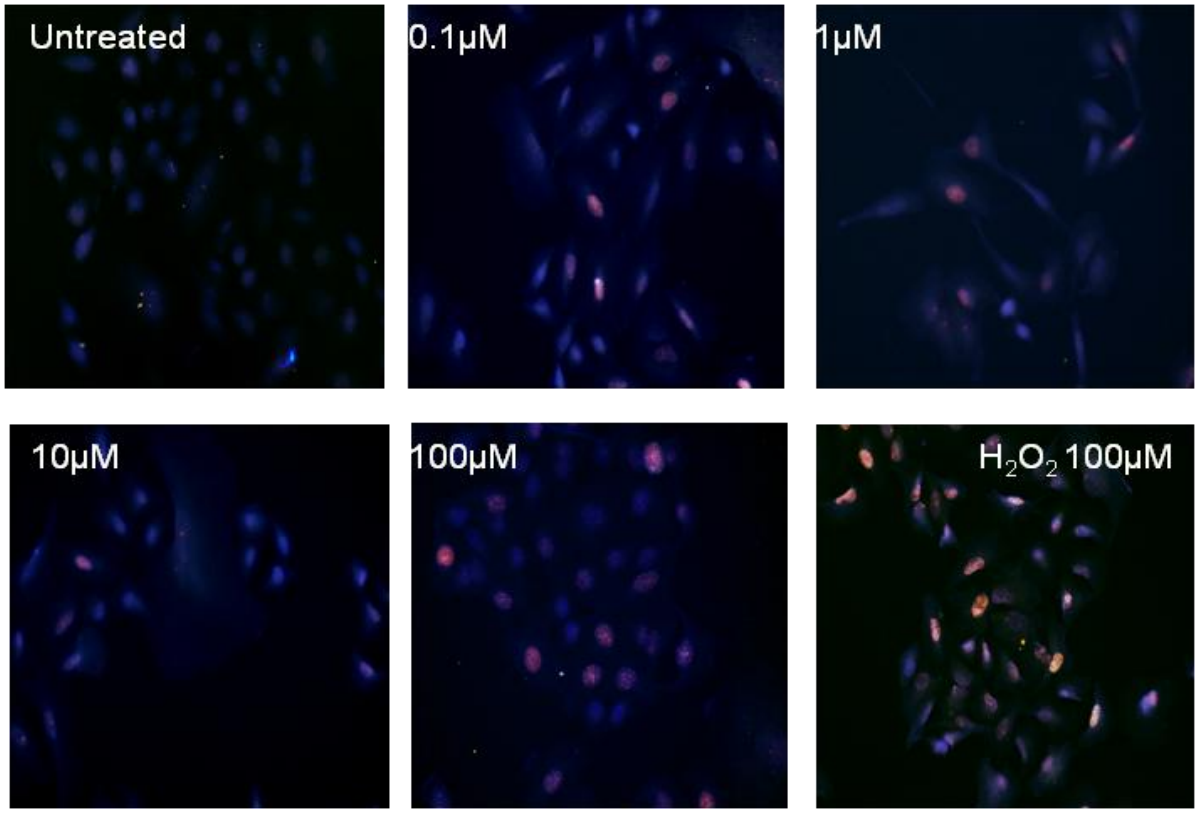


**Figure 3.10. Immunofluorescent detection of γ-H2AX in A549 cells exposed to dichlorvos.**

Studies with DCV showed clear phosphorylation of H2AX (Figure 3.10), which appeared to form foci, when viewed at a higher magnification (Figure 3.11). From the above images it is clear that dichlorvos caused the phosphorylation of H2AX at all concentrations after 3 hours incubation. The images show that dichlorvos did not phosphorylate H2AX in every cell and some showed no sign at all of phosphorylation of H2AX. This data is in agreement with the DNA damage, seen with the comet, in that some cells displayed a greater degree of damage than other cells. With hydrogen peroxide 100µM it is clear that most cells show clear phosphorylation and the fluorescence is far brighter and intense than that seen with dichlorvos, suggesting that the damage seen with hydrogen peroxide is far greater than with dichlorvos. This also supports the results seen with the comet assay. The formation of γ-H2AX is putatively a marker for DNA DSBs although further experiments will be required to confirm the nature of the DNA damage after dichlorvos. This data, together with the comet assay data provide strong evidence that dichlorvos is able to induce DNA damage *in vitro*.

**Figure 3.11. High magnification immunofluorescent detection of γ-H2AX in A549 cells exposed to dichlorvos.**

## 3.3 Response to DNA damage

### 3.3.1 p53 response

If dichlorvos is damaging DNA, then DNA damage signalling pathways should also be activated, this would result in p53 induction and cell cycle arrest or apoptosis if repair does not occur. In order to establish whether dichlorvos caused the initiation of DNA signalling cascades or apoptosis, cells were treated with a range of dichlorvos concentrations prior to western blot analysis. Samples were analysed for the expression of p53, phosphorylated p53 (Ser15), phosphorylated chk2 (Thr68), PARP-1 or the cleaved PARP-1 fragment as a marker of apoptosis. Etoposide is a chemotherapy agent whose specific action is based on the induction of DNA damage and apoptosis, mediated by the inhibition of topoisomerase II and the generation of DNA strand breaks. Etoposide was therefore used as a positive control for the induction of DNA damage signalling events and apoptosis

The initial study conducted was a dose range study at 24 hours. Figure 3.12 shows that PARP-1 is cleaved after 100µM DCV and 50µM etoposide, consistent with apoptotic cell death. A background level of p53 can be seen in the untreated and acetone treated cells

with a high increase in levels of p53 occurring with 50µM etoposide and a slight increase of p53 occurring with dichlorvos treated cells. GAPDH was used as a loading control.

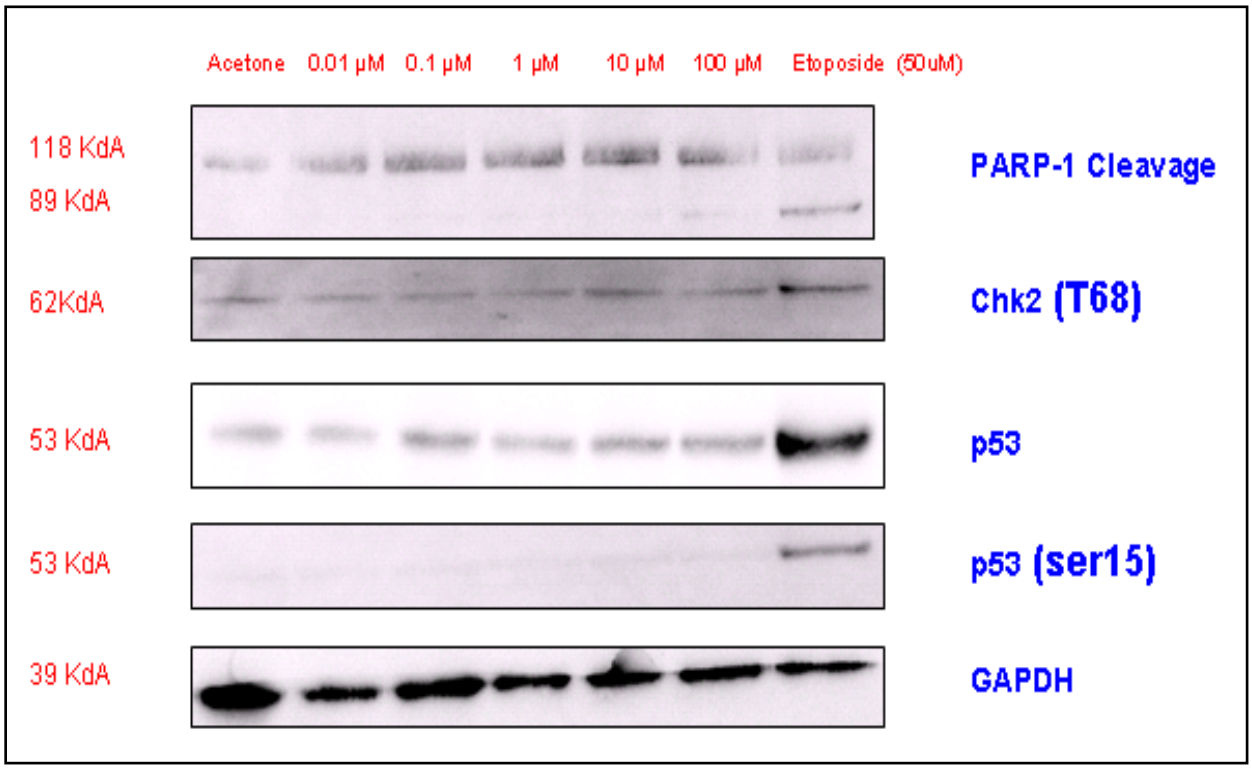


**Figure 3.12. Western blot of TK6 cells after 24 hours exposed to Dichlorvos.** Cells were exposed to the indicated concentrations of dichlorvos for 24 hours prior to western blot analysis. Etoposide was used as a positive control for the activation of DNA damage signalling/apoptotic pathways

A small increase of p53 protein levels was seen after 24 hours with 100µM dichlorvos. This dose was used for a time course experiment. Figure 3.13 shows that the maximal levels of p53 were observed at 2 and 4 hours, although, there was no increase in the phosphorylated p53 after dichlorvos, as seen with etoposide (A 24 hour exposure with etoposide was used as a control)

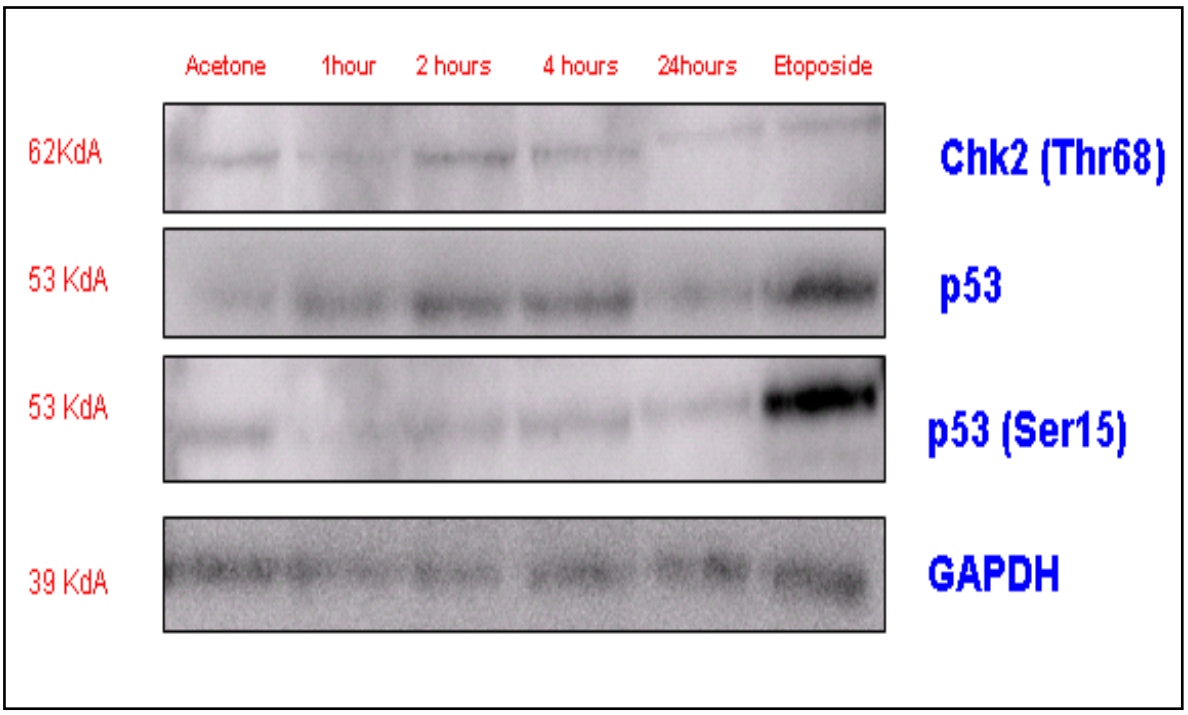


**Figure 3.13. Western blot of TK6 cells after exposure to Dichlorvos.** Cells were exposed to 100µM dichlorvos for the indicated times prior to western blot analysis. Etoposide (24hours) was used as a positive control for the activation of DNA damage signalling/apoptotic pathways.

In order to understand the kinetics of the cell signalling events after treatment with 100µM dichlorvos, a time course experiment was repeated, comparing treatment with dichlorvos (100µM) to that of treatment with Etoposide (50µM). Figure 3.14 depicts that Etoposide caused an increase in protein levels of p53 over the 24 hours, whereas dichlorvos displayed a maximum increase in levels of p53 after 4 hours. After dichlorvos, p53 levels were increased without phosphorylation of ser15, whereas etoposide caused both an increase of p53 and p53 Ser15.

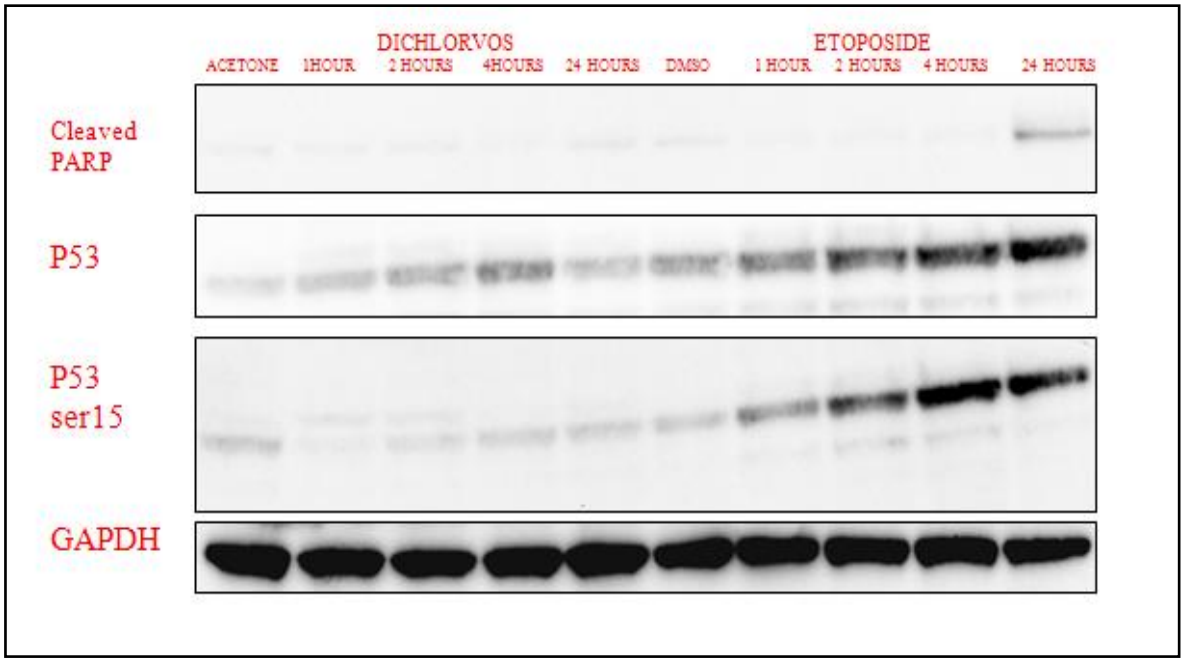


**Figure 3.14. Western blot of TK6 cells after Dichlorvos or etoposide.** Cells were exposed to 100μM dichlorvos or 50μM Etoposide for the indicated times prior to western blot analysis.

The protein expression in figure 3.14 was quantified using Syngene GeneTools software. The values obtained for p53, p53 Ser15induction and cleaved PARP-1 were normalised against GAPDH. From figure 3.15 it is clear that the highest increase of p53 occurred after 4 hours causing approximately a 4 fold increase. Etoposide causes maximum induction at 24 hours causing a 4 fold increase in p53 expression. However this result is misleading as in figure 3.11 the p53 result is much stronger for etoposide than with dichlorvos. Dichlorvos and etoposide are being compared to their respective controls; acetone for dichlorvos, DMSO for etoposide. The p53 levels in DMSO-treated cells are markedly higher than the acetone treated cells, which obviously influences the fold change in Figure 3.15. Dichlorvos did not produce a marked increase in p53-Ser15, however maximal levels of this protein did occur after 4 hours, but this is not appreciably higher than the control sample. There was a clear increase of p53-Ser15 with etoposide with maximal levels occurring at 4 hours with a 12 fold increase. This increase in protein levels of p53-Ser15 is present over 24 hours with etoposide. A small amount of cleaved PARP-1 is present after 24 hours dichlorvos with a 0.5 fold increase compared to the acetone treated sample. Etoposide caused a much more considerable increase of 7 fold after 24 hours. No noteworthy increase of the cleaved PARP-1 fragment was seen with either treatment after 2 or 4 hours.

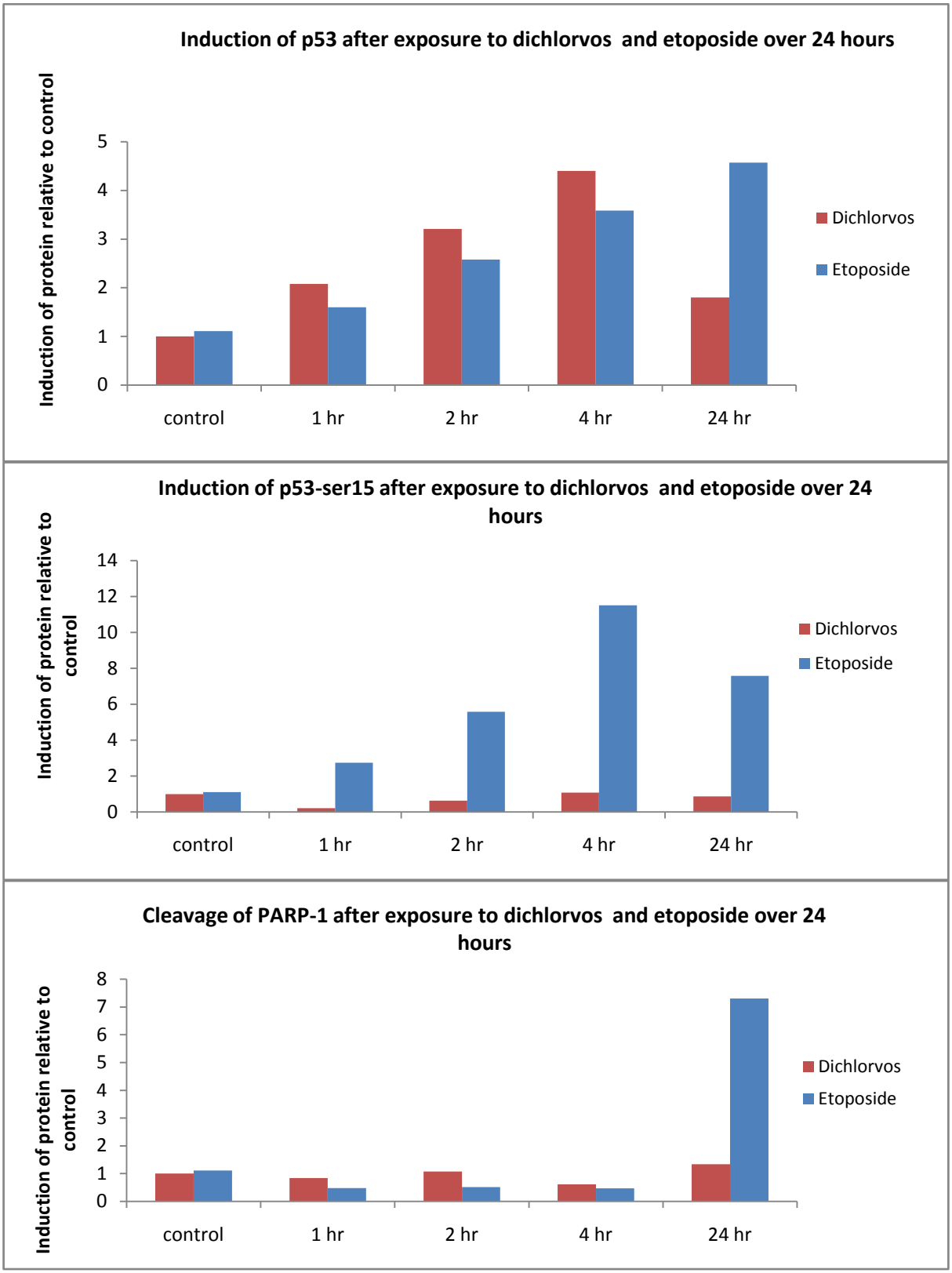


Figure 3.15. **A graph of the change in expression of cleaved PARP-1, p53 and p53 ser 15 in TK6 cells after dichlorvos or etoposide over 24hours.** Cells were exposed to 100μM dichlorvos or 50μM Etoposide for the indicated times prior to western blot analysis.

The time course indicated that after 4 hours incubation with dichlorvos caused maximal increase in p53 protein levels. Figure 3.16 shows a dose range experiment conducted at 4 hours. The analysis was expanded to include duplicates of samples to allow for accurate quantification of the western blot. At 4 hours there is no cleavage of PARP after any treatment besides a very faint band with etoposide but this is not clear. There is a clear increase with 100µM dichlorvos and after 50µM etoposide of p53. There is a slight increase of p53 with 1 and 10µM dichlorvos and this is consistent with the lower levels of DNA damage caused at these concentrations (as suggested by the comet assay and H2AX immunofluorescence data). No clear increase in phosphorylation of p53 is seen except with etoposide.

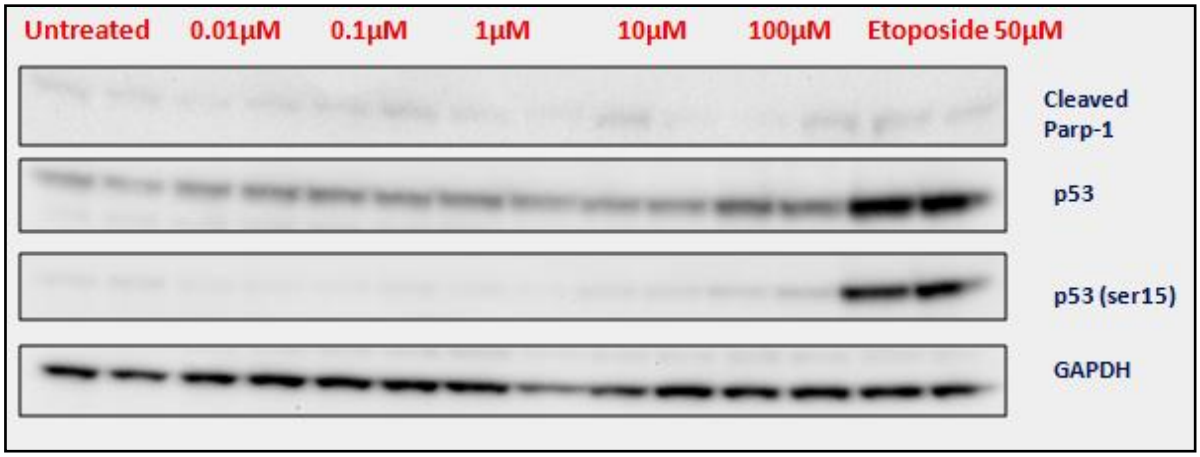


**Figure 3.16. Western blot of TK6 cells after 4 hours Dichlorvos.** Cells were exposed to the indicated concentrations of dichlorvos for 4h prior to western blot analysis. Etoposide was used as a positive control for the activation of DNA damage signalling/apoptotic pathways.

Figure 3.17 shows a dose range experiment conducted at 24 hours the analysis has also been expanded to include duplicates of samples to allow for accurate quantification. After 24 hours there are clear bands of the cleaved PARP-1 fragment after 100µM dichlorvos and after 50µM etoposide. There is a clear increase with 50µM etoposide of p53. There is a slight increase of p53 after 100µM dichlorvos. No clear increase in phosphorylation of p53 is seen except with etoposide.


**Figure 3.17 Western blot of TK6 cells after 24hours exposed to Dichlorvos.** Cells were exposed to the indicated concentrations of dichlorvos for 24hours prior to western blot analysis. Etoposide was used as a positive control for the activation of DNA damage signalling/apoptotic pathways

The western blots in figures 3.16 and 3.17 were quantified using Syngene Gene tools software. The values obtained for PARP-1 cleavage and the increases in p53 and p53-Ser15 protein levels were then normalised against GAPDH. Each sample was completed in duplicate and the results are displayed as a mean, ± standard error. In figure 3.18 it is clear that PARP-1 cleavage only occurred after 100µM dichlorvos and 50µM etoposide after 24 hours. Dichlorvos causes only a small 2 fold increase in p53 induction at 4 hours and then at 24 hours decreases almost to background levels. Etoposide shows a clear increase of p53 at both 4 and 24 hours with a 7 fold increase of p53 expression. Treatment with dichlorvos did not cause a significant phosphorylation of p53-Ser15 however there was clear phosphorylation after treatment with etoposide. This confirms the previous cell signalling data with dichlorvos.

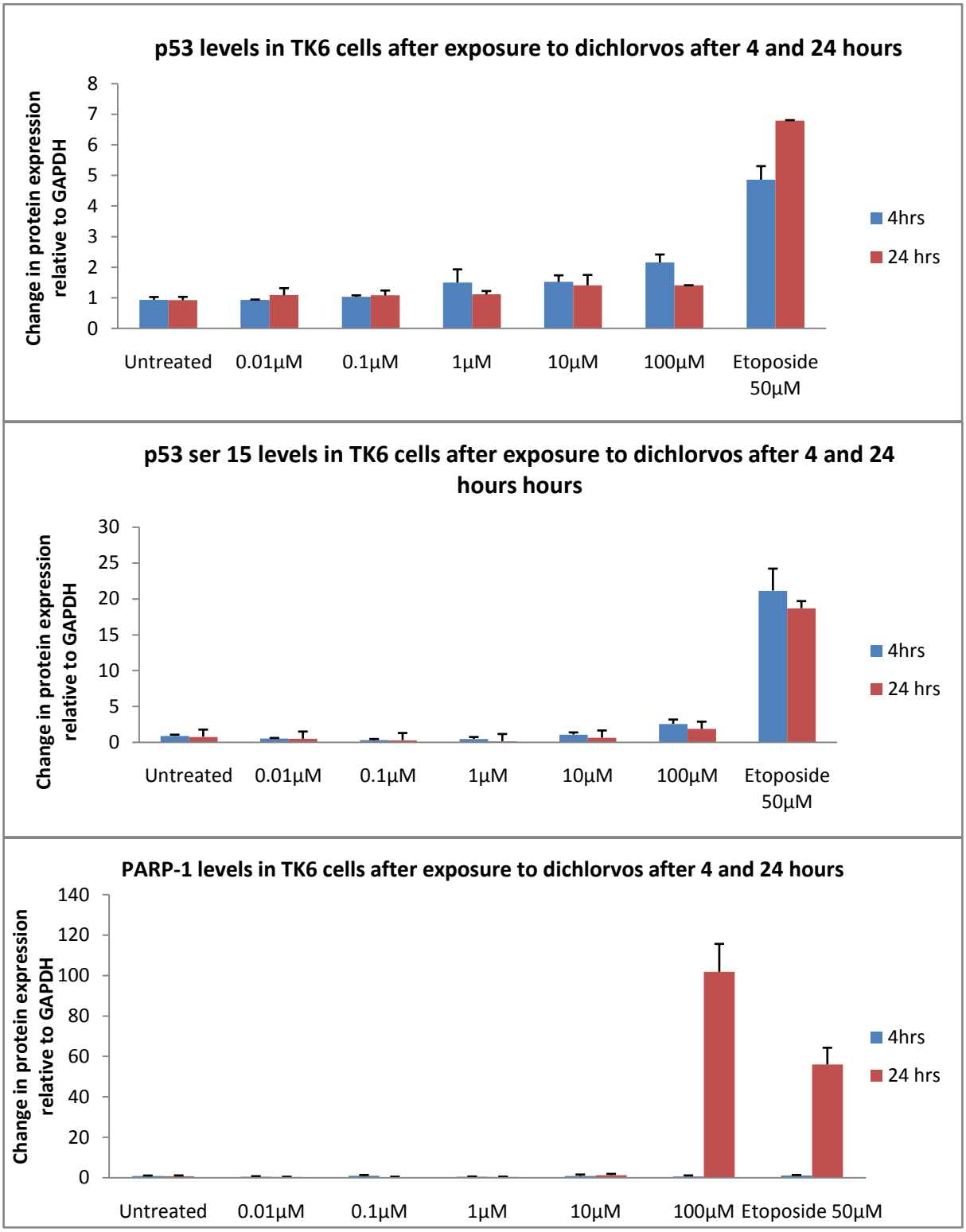


**Figure 3.18. A graph of the change in expression of cleaved PARP-1, p53 and p53 ser 15 in TK6 cells after dichlorvos.** Cells were exposed to the indicated concentrations of dichlorvos for 4 and 24h prior to western blot analysis. Etoposide was used as a positive control for the activation of DNA damage signalling. Values have been calculated using Syngene software and normalised against GAPDH levels. Error bars are ± STD error

### 3.3.2 Cell cycle effects of dichlorvos

Our initial studies in TK6 cells demonstrated inconsistent results in response to a variety of DNA damaging agents (including ionizing radiation, $H_2O_2$, etoposide and the alkylating agent methyl methane sulphonate, data not shown). The literature was searched for readily available cells that can be used for the study of cell cycle regulation. Several papers were found demonstrating intact G1/S and G2/M phase cell cycle arrest in A549 lung carcinoma cells. As well as being appropriate for the study of cell cycle effects, these cells are also an appropriate model system as inhalation of nerve agent/OP pesticides is a common route of exposure. A549 cells are carcinoma human alveolar basal epithelial cells. In order to test the suitability of A549 cells to assess cell cycle effects after exposure two positive control treatments were used. One was etoposide a topoisomerase inhibitor and the second was ionizing radiation (IR) known to cause DNA double strand breaks. These controls should allow for testing of the cell cycle as both cause sufficient DNA damage to increase p53 levels and cause cell cycle arrest to allow for efficient DNA repair or apoptosis.

A549 cells were seeded at $2x10^5$ and left overnight to give an approximate confluence of 60%. Cells were either left untreated or treated with 5µM Etoposide or Ionizing radiation (I.R.) at 5 Gray for 5 minutes. Cells were left for 24 hours prior to western blot analysis.

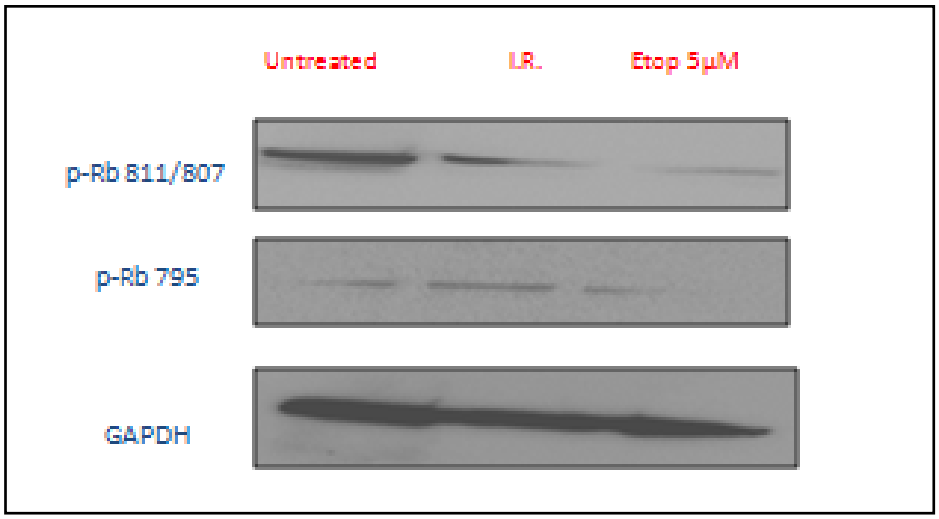


Figure 3.19. Western blot of A549 cells 24 hours after treatment with IR or etoposide.

As shown in Figure 3.19, both treatments resulted in decreased phosphorylation of Rb (Ser 807/11), with decreased phosphorylation of Ser795 also evident after 5μM etoposide. Therefore, to investigate whether dichlorvos exposure resulted in cell cycle arrest, A549 cells were used for the analysis of cell cycle regulated proteins, with etoposide as a positive control.

After establishing that A549 cells were suitable to study changes in cell cycle effect after genotoxins, these cells were used to view any cell cycle effects after 10μM and 100μM dichlorvos for 24 hours. During cell cycle arrest at the G1/S phase, phosphorylation of Rb decreases, allowing this protein to bind to and inactivate the E2F transcription factor, preventing transcription of the genes required for progression into S-phase. In addition, phosphorylation of cdc2 (Tyr15) was investigated. When phosphorylated on this site, cdc2 is inactive and is unable to drive progression of the cell cycle from G2 to mitosis. In normal cycling cells, to allow cell cycle progression, this phosphate group is removed by the action of the cdc25 phosphatase. After DNA damage, this phosphatase is phosphorylated and inactivated by the checkpoint kinases Chk1 and Chk2. This results in increased phosphorylation of cdc2 and reduced progression into mitosis. Eventually, this phosphorylation appears to decrease relative to untreated cells, possibly due to degradation of the cdc2 protein. In order to confirm that the p53 response was the same as seen with TK6 cells, samples were also probed for p53 and p53 Ser15, in addition to cdc2 (Tyr15) and Rb (Ser 795).

Figure 3.20 show that dichlorvos does show an increase in p53 protein levels after 4 hours, although this is smaller than previously seen in TK6 cells. The lower p53 response could be due to differences in DNA repair capacities between the cell lines. At 24 hours p53 has returned to back ground levels and this was the same as seen with TK6 cells. The comet assay should be performed in A549 cells after treatment with dichlorvos so the p53 response can be related to levels of DNA damage. The increase in p53 and phosphorylated p53 was clear after 24 hours after treatment with etoposide (5 and 50 μM).

Dichlorvos (10 μM) did not cause a decrease in Rb phosphorylation; however 100μM caused a clear decrease in p-RB-Ser795 at 4 hours, which returned to similar levels as untreated cells after 24 hours, this suggests dichlorvos caused a G1/S block at 4 hours which was lifted

after 24 hours. There was a clear decrease in p-Rb-Ser795 with etoposide after 4 and 24hours at both 5 and 50µM concentrations, suggesting a G1/S block that was persistent for 24 hours. There was a small increase in the phosphorylated cdc2 protein with 10µM dichlorvos and a clear increase with 100µM dichlorvos and etoposide (5 and 50µM) after 4 hours. Cdc-2 phosphorylation increased at 4 hours and then decreased at 24 hours, these observations are consistent with a G2/M block according to Dan and Yamori (2000).

4 HOURS

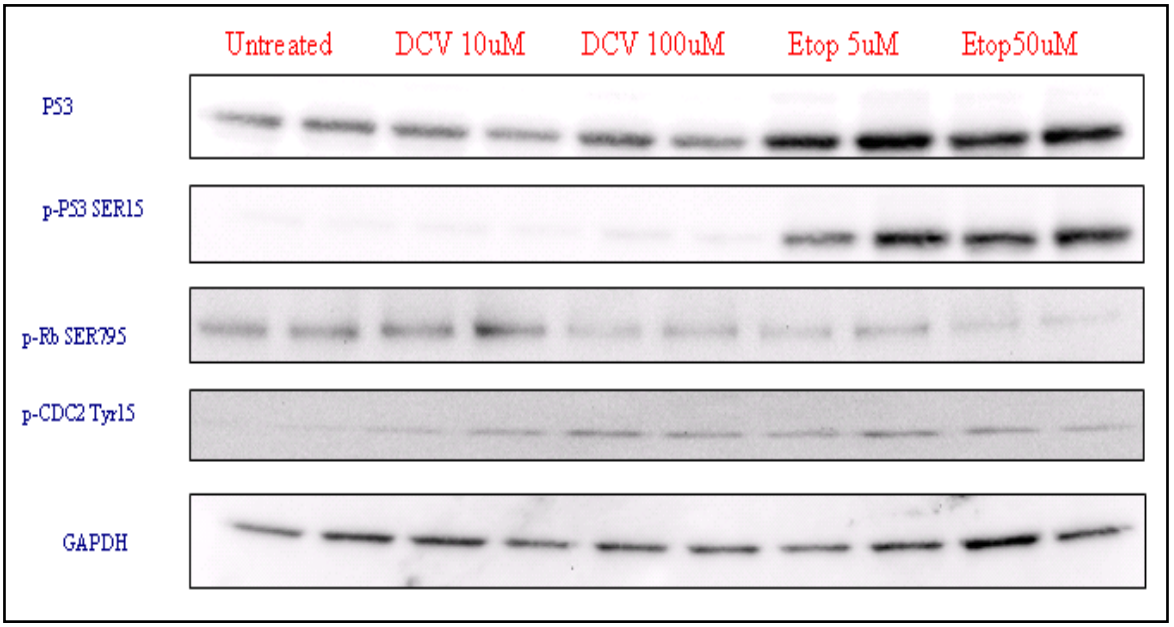


24 HOURS

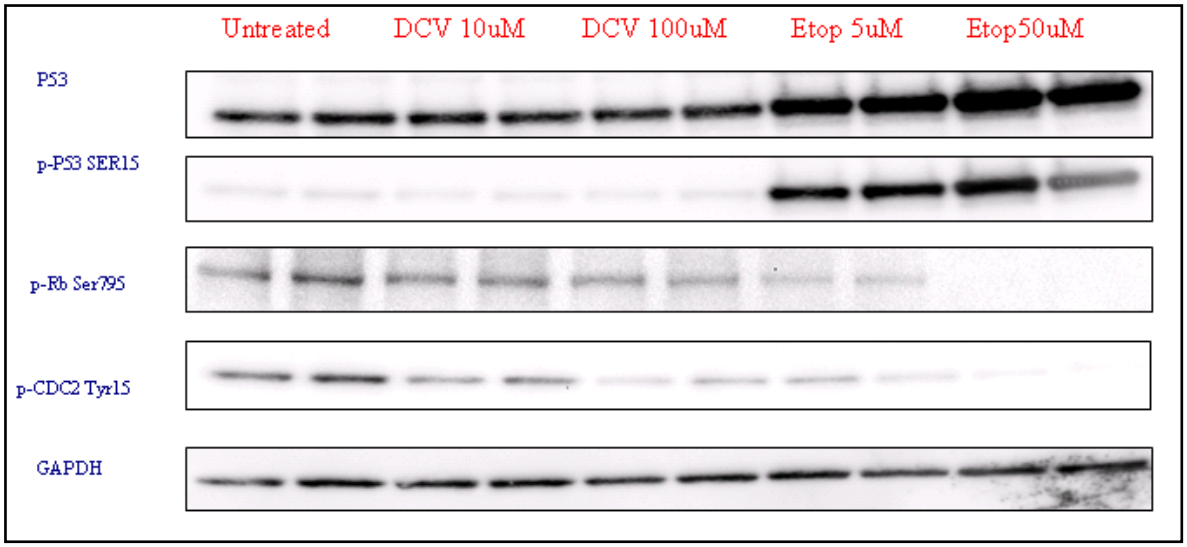


**Figure 3.20 Western blot of the change in expression of p53 p53 (ser15), p-cdc2 (tyr15), p-Rb (ser795) and GAPDH in A549 cells after dichlorvos.** Cells were exposed to the indicated concentrations of dichlorvos for 4 and 24 hours prior to western blot analysis. Etoposide was used as a positive control for the cell cycle effects.

The western blot in figure 3.20 was quantified using Syngene GeneTools software. The values obtained for p53, p53-Ser15 induction were then normalised against GAPDH. In figure 3.21, dichlorvos (100µM) caused a 50% increase in p53 protein levels after 4 hours and returned back to background levels after 24 hours. No affect on p53 was seen after 10µM dichlorvos. Etoposide (5 and 50µM) caused clear p53 induction at both 4 and 24 hours the greatest change in protein expression occurred with a 3 fold increase of p53 at 5µM. Dichlorvos did not have any effect on p53-Ser15 levels at either 10 or 100µM. Treatment with etoposide at both 5 and 50µM resulted in a significant increase in p53ser15 levels casing around a 25 fold increase after 4 hours. The findings in A549 cells were consistent with the finding in TK6 cells.

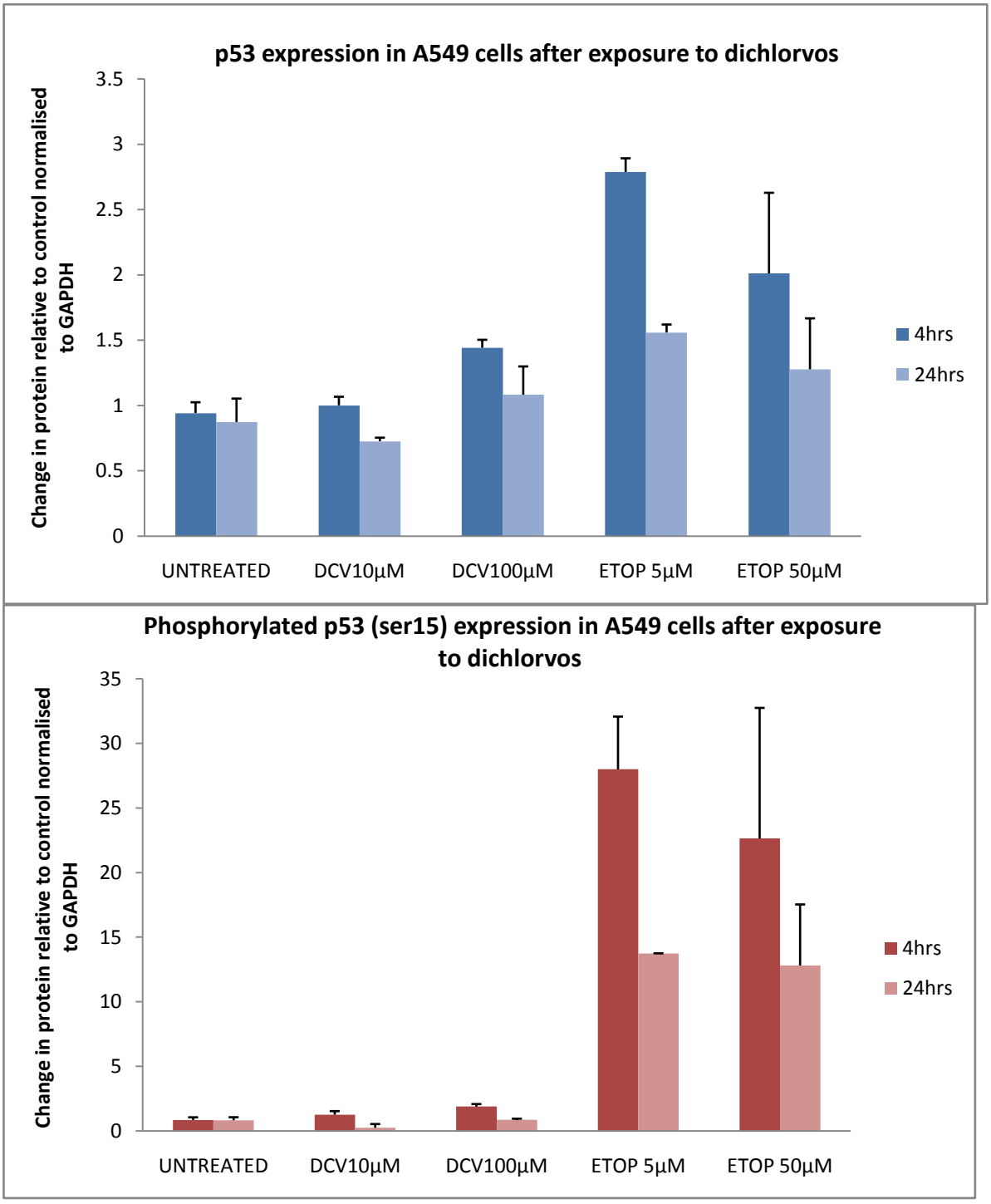


**Figure 3.21. Differing levels expression of p53 and p53 (ser15) in A549 cells.** Cells were exposed to the indicated concentrations of dichlorvos for 4 and 24h prior to western blot analysis. Etoposide was used as a positive control for the activation of DNA damage signalling and cell cycle effects. Values have been calculated using Syngene software and normalised against GAPDH levels. Error bars are ± STD error

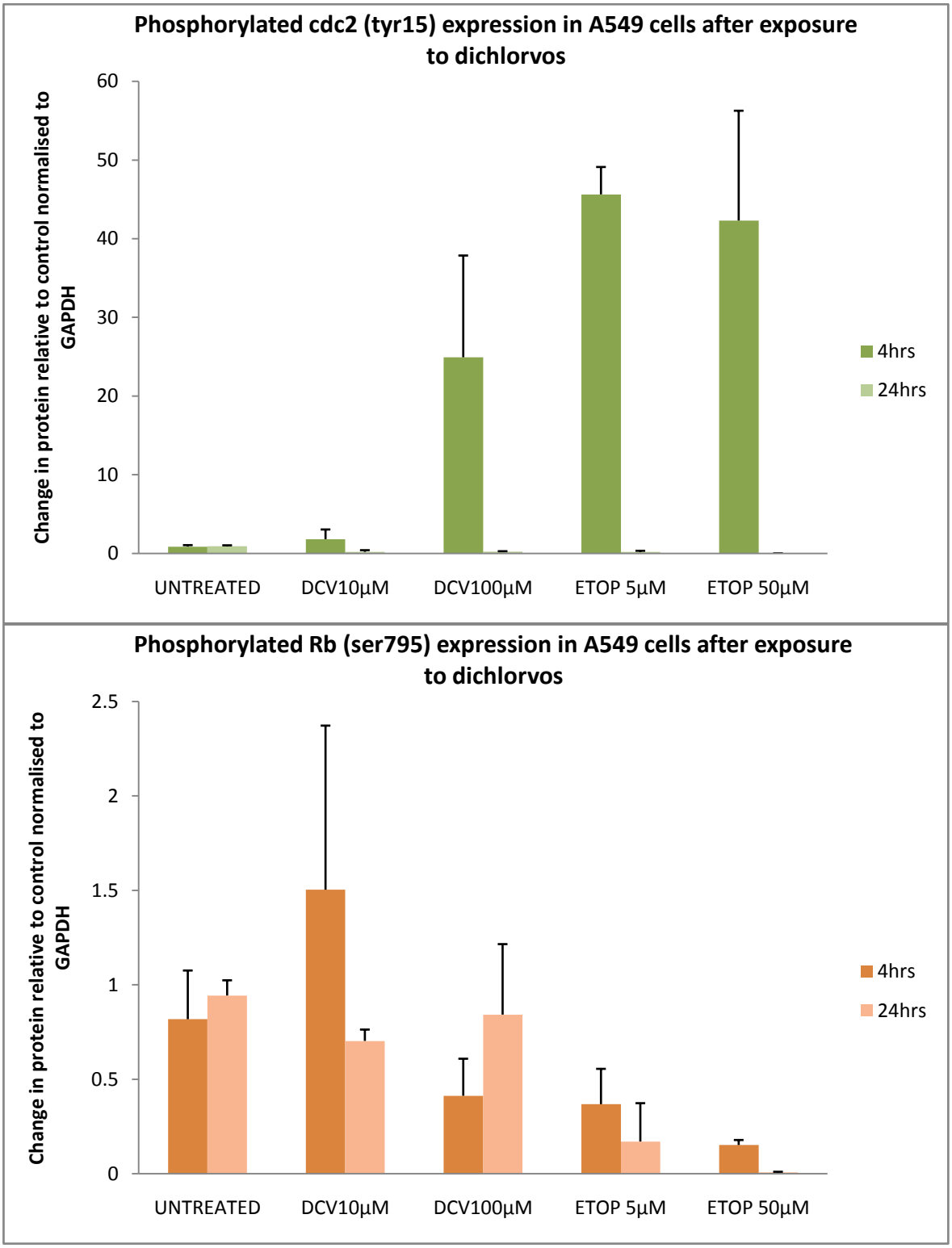


**Figure 3.22. Differing levels expression of p-cdc2 (tyr15) and p-Rb (ser795) in A549 cells.** Cells were exposed to the indicated concentrations of dichlorvos for 4 and 24 hours prior to western blot analysis. Etoposide was used as a positive control for the activation of DNA damage signalling and cell cycle effects. Values have been calculated using Syngene software and normalised against GAPDH levels. Error bars are ± STD error

The western blot in figure 3.20 was quantified using Syngene GeneTools software. The values obtained for p-Rb-Ser795 and p-Cdc2-Tyr15 were then normalised against GAPDH. Figure 3.22 indicates that dichlorvos 10µM caused a 2 fold increase in the expression of Cdc-2-Tyr15 and 100µM dichlorvos caused a 24 fold increase after 4 hours. This is indicative of the initiation of a G2/M block. After 24 hours the levels have fallen below back ground levels. Etoposide has similar affect on the profile of cdc2-tyr15 induction although etoposide causes a 45 fold increase at 5µM and 42 fold increase at 50 µM after treatment for 4 hours before falling below background levels. Dichlorvos 10µM has no affect on Rb phosphorylation at 4 or 24 hours with the levels staying close to back ground levels. There is a clear decrease in Rb phosphorylation at 4 hours after 100µM dichlorvos which then returns to back ground levels at 24 hours. After 5µM etoposide there was a drop in expression by 66% after 4 hours decreasing to 75% at 24 hours. 50µM etoposide caused nearly a 75% drop in expression of p-Rb-Ser795 after 4 hours falling further to nearly 90% loss in comparison with untreated cells after 24 hours. These findings are consistent with a G1/S block.

## 3.4. Initiation of DNA repair pathways after DNA damage by dichlorvos

The data in this chapter clearly shows that dichlorvos is able to induce DNA damage in vitro. The nature of this DNA damage remains unclear. By investigating the role of specific DNA repair pathways it is possible to obtain some information regarding the type of DNA damage being induced. For example, if dichlorvos is methylating DNA, then BER is likely to be involved in repairing these lesions. Therefore, cells lacking BER would have higher levels of DNA damage after dichlorvos, which would result in greater cytotoxicity. The sections below describe preliminary data investigating the role of BER and NHEJ in the cellular response to dichlorvos.

### 3.4.1 Base excision repair

BER repairs simple DNA adducts such as oxidative DNA damage and methylation damage. To investigate the role of BER in response to dichlorvos, the PARP-1 inhibitor NU1025 was

used. Whilst PARP-1 is a multi-functional protein, it has an important role in the BER pathway and cells treated with PARP-1 inhibitors are hypersensitive to simple alkylating agents and hydrogen peroxide. If BER is required to repair the DNA damage induced by dichlorvos, then cells lacking BER would be expected to be more sensitive to dichlorvos toxicity.

TK6 cells ($2x10^6$in a volume of 10ml) were incubated for one hour with NU1025 or 1% DMSO as a solvent control before dosing with dichlorvos. The dichlorvos concentrations used were 0.01, 0.1, 1, 10 and 100µM, cells exposed for 24 and 48 hours prior to MTS assays. Controls used were untreated cells as a negative control and hydrogen peroxide at 10µM as a positive control.

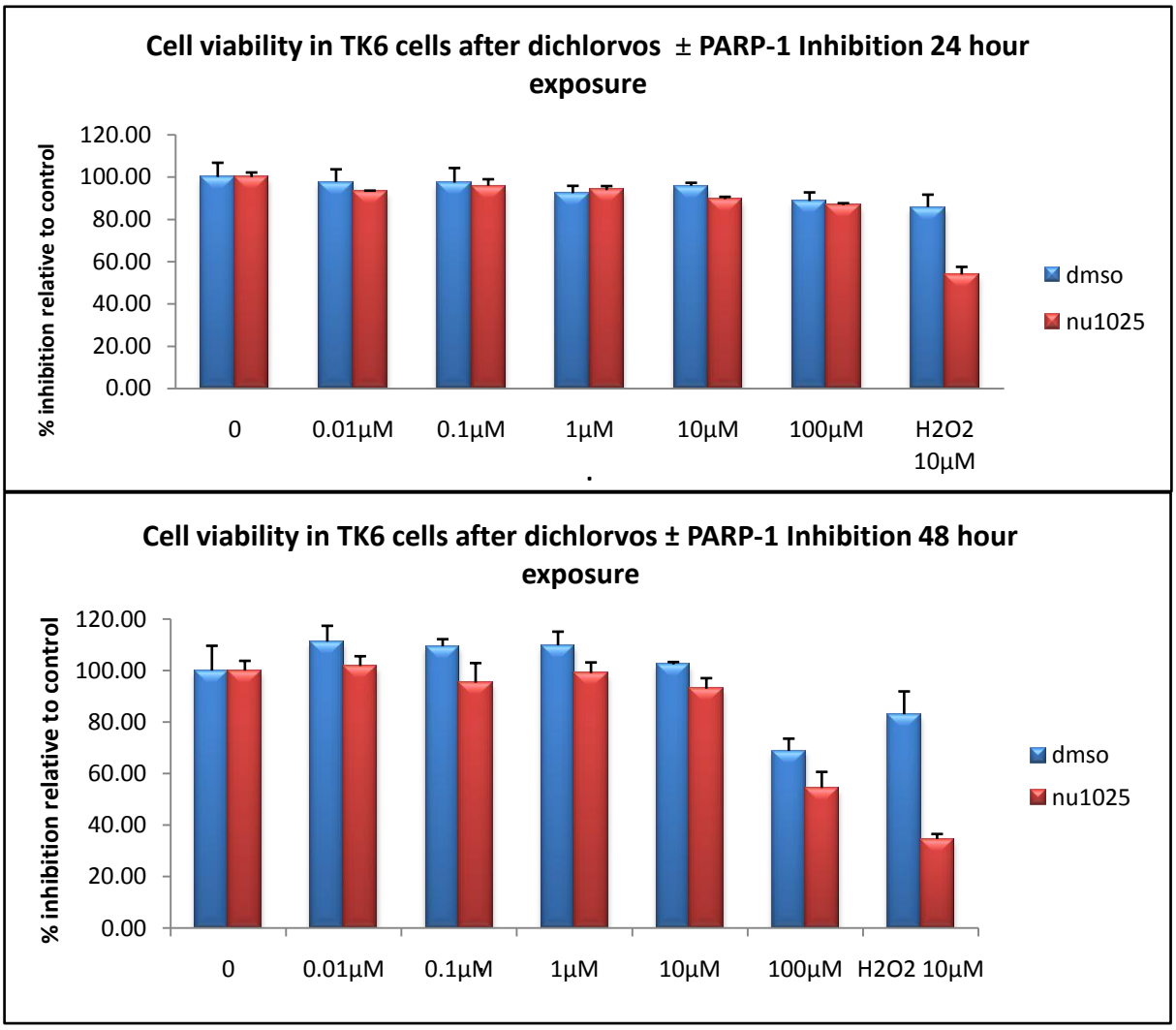


**Figure 3.23. Change in cell viability measured by the MTS assay after 24 and 48 hours in TK6 cells after exposure to dichlorvos with and without PARP-1 function.** Results were expressed as mean % viability relative to untreated control (untreated cells designated 100% viability) ± standard deviation.

There is little cytotoxicity as measured by the MTS assay after 24 hours treatment with dichlorvos at all concentrations. This is surprising as at the same time point and same concentrations using the MTT assay to measure cell viability, dichlorvos demonstrated a higher cytotoxic potential. This finding is not restricted to dichlorvos as hydrogen peroxide has previously demonstrated a higher cytotoxicity at 24 hours using the same concentration. This may be due to differences in the sensitivity of MTT and MTS assays or may be due to the experiments being performed at different periods in time (with possible differences in the batch of dichlorvos and hydrogen peroxide used as well as different batches of TK6 cells).

Hydrogen peroxide was used as a positive control. As shown in Figure 3.23, cells lacking BER were more sensitive to hydrogen peroxide than BER-proficient cells. After 24 hours TK6 cells with and without PARP-1 function displayed a 20% loss in viability, PARP-1 inhibition had no effect on dichlorvos cytotoxicity after 24 hours. However, after 48hours, cells lacking BER (NU1025-treated) were more sensitive to dichlorvos than DMSO-treated cells at all doses, for example, a further 15% decrease in cell viability occurred after 100µM dichlorvos in cells without PARP-1 function. Hydrogen peroxide at 48 hours caused a decrease of approximately 50% of cell viability in cells lacking PARP-1 activity. These preliminary studies suggest that there is some evidence for BER being required for the repair of dichlorvos induced DNA damage. The small differences between repair proficient and deficient are likely due to low levels of damage that dichlorvos is able to induce. The positive control of hydrogen peroxide, an agent which is known to cause oxidative stress showed clearly that cells without PARP-1 function were more sensitive to damage by hydrogen peroxide. The data presented in this section is preliminary and further repeats of the experiment are required to confirm the findings presented here.

### 3.4.2. Non homologous end joining

NHEJ is the major pathway used by human cells to repair DNA DSBs. To investigate the role of NHEJ in the response to dichlorvos, the DNA-PK inhibitor NU7026 was used. Cells treated with NU7026 are hypersensitive to agents that induce DSBs, including ionising radiation and

etoposide. If NHEJ is required to repair the DNA damage induced by dichlorvos then cells lacking NHEJ would be expected to be more sensitive to dichlorvos toxicity.

TK6 cells ($2x10^6$in a volume of 10ml) were incubated for one hour with NU7026 or 1% DMSO as a solvent control before dosing with dichlorvos. The dichlorvos concentrations used were 0.01, 0.1, 1, 10 and 100 µM. Samples were taken at 24 and 48 hours to assess cell viability via the MTS assay. Controls used were untreated cells as a negative control and etoposide 50 µM as a positive control.

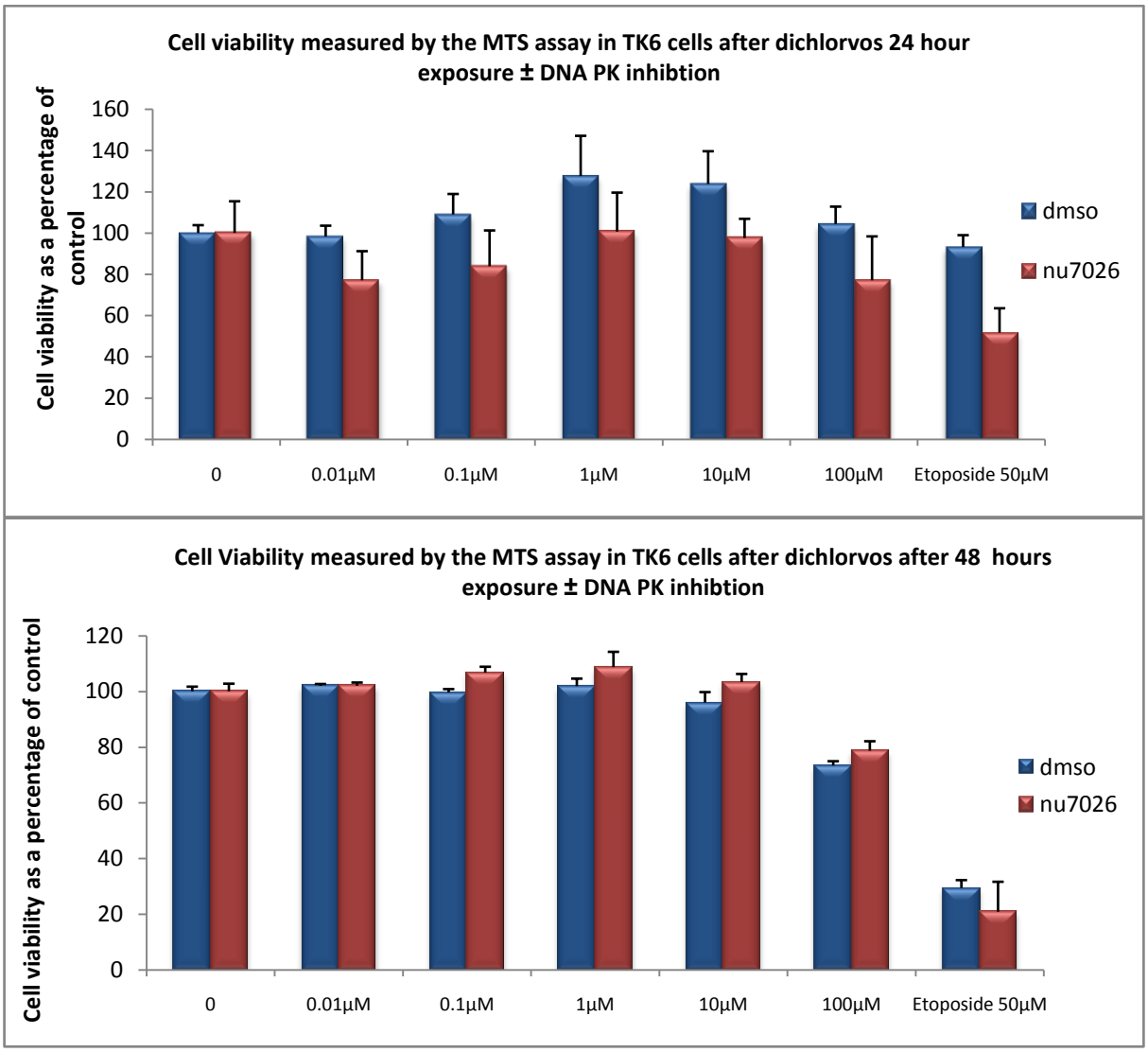


**Figure 3.24. Change in cell viability measured by the MTS assay after 24 and 48 hours in TK6 cells after exposure to dichlorvos with and without DNA PK function**. Results were expressed as mean % viability relative to untreated control (untreated cells designated 100% viability) ± standard deviation.

As observed in the BER studies, the dichlorvos appeared less cytotoxic when using the MTS assay (Figure 3.24) instead of the previously used MTT assay. After 24 hours, cells treated with NU7026 were more sensitive to dichlorvos than DMSO-treated cells. This would suggest that NHEJ is involved in the cellular response to dichlorvos and that the mechanism of dichlorvos-mediated genotoxicity may involve the generation of DNA DSBs. However, after 48 hours, there is no real difference in dichlorvos toxicity between NHEJ-proficient and deficient cells (Figure 3.24, lower graph). At both 24 hours and 48 hours, cells lacking NHEJ were more sensitive to etoposide than cells with an intact NHEJ pathway. It is important to further investigate the potential generation of DSBs after dichlorvos as these lesions are highly cytotoxic and mutagenic. These preliminary cytotoxicity studies using NU7026 should be repeated. In addition, neutral comet assays should be performed, which specifically detect DSBs.

### 3.5 Discussion

The comet assay demonstrated that dichlorvos induced DNA damage in TK6 cells in a dose-dependent manner. There was an increase in DNA damage in TK6 cells relative to control; the extent of DNA damage had increased after 24 hours. In general, OTM values <1 are classed as 'undamaged' and values of 1-2 are classed as low level damage (Collins et al 1997), the majority of cells treated with 100µM dichlorvos were above 5 OTM. In addition DNA damage was observed after only ten minutes in SHSY-5Y neuroblastoma cells at low concentrations, suggesting that dichlorvos is able to modify DNA relatively quickly. After 24 hours, the levels of DNA damage had increased compared to the values at 1 hour after high µM treatments. It is possible that dichlorvos is able to directly bind to and modify DNA and Wooder et al. (1977) and Lawley et al. (1974) have suggested that dichlorvos can directly methylate DNA and other proteins. The observation of DNA damage measured by the comet assay does not provide information on the type of DNA damage and as there is a loss in cell viability the DNA damage could be attributed to cell death mechanisms such as apoptosis. During apoptosis the cell undergoes morphological changes, such as cell shrinkage, fragmentation of nuclei and blebbing of the plasma membranes (Nagata et al., 2003). This process is accompanied by the degradation of chromosomal DNA. This degradation of DNA could be detected by the comet assay. Attempts were made to identify the type or types of lesion after exposure to dichlorvos in SHSY5Y cells. The procedure of adding the FPG

endonuclease was problematic and provided data that was much higher in levels of damage than had been seen previously with dichlorvos. It is possible that this is due to the extra processing during the comet and the introduction of artefactual DNA damage. However, the data when used as a preliminary tool suggests that the lesion created by dichlorvos is unlikely to be oxidative in nature. Yamano et al. (2000) reports that dichlorvos (250, 500 and 1000µM) does cause oxidative damage in rat hepatocytes but states that the oxidative damage is confined to lipid peroxidation and therefore only plays a significant role in its cytotoxicity but not in its genotoxicity, which corroborates the preliminary study.

Damage to DNA should result in the activation of DNA damage signaling pathways, mediated by the activity of the ATM/ATR and Chk1/2 protein kinases. Central to this signaling cascade is the tumour suppressor protein p53, which is induced and activated after DNA damage. In TK6 cells exposure to 100µM dichlorvos resulted in an increase in p53 protein levels after 1 hour, with maximum levels measured at 4 hours but at 24 hours a similar expression to the untreated samples was seen. This would suggest that 100µM dichlorvos caused a rapid and transient increase in p53 as a result of the moderate and rapid DNA damage detected by the comet assay. Whilst the increase in p53 protein levels was clear, there was no evidence for phosphorylation of p53 at serine 15. A range of genotoxins have been shown to induce serine 15 phosphorylation (reviewed in Dumaz et al 1999) and it has been shown that phosphorylation of p53 at Ser15 is necessary to activate p53 but it is not increased p53 expression. The increased expression of p53 may not due to an effect at the transcriptional level but to protein stabilization (Blattner et al., 1999) To better understand the mechanism of p53 activation after exposure to dichlorvos further investigation is required and other post translational modifications should be measured, for example, other phosphorylation sites on p53. In addition the levels of mdm2 should be measured to assess whether p53 is no longer being targeted for degradation thus allowing for its stabilization (Jacobberger et al., 1999). It is also possible that dichlorvos which is an organophosphate has covalently phosphorylated p53 at Ser 15 kinase mediated phosphorylation is blocked. To test this theory TK6 cells should be pre-treated with dichlorvos and then with an agent known to cause phosphorylation of p53 at Ser15 such as Etoposide. If phosphorylation still occurs then this would indicate that dichlorvos is not preventing kinase mediated phosphorylation.

Cytotoxicity studies showed that dichlorvos has cytotoxic potential even at low µM concentrations. The cytotoxicity of dichlorvos, demonstrated in the MTT assay, was investigated further by analysing the cleavage of PARP-1 as an indicator of apoptotic cell death. Dichlorvos (100µM) caused an increase in full length PARP-1 and the cleaved fragment of 89kDa after 24 hours. Further investigation is required to confirm the mode of cell death is apoptosis. To confirm that apoptotic cell death is occurring, other apoptotic markers would need to be investigated, for example, the use of AnnexinV assays that detects the expression of phosphatidylserine on the outer leaflet of the plasma membrane (occurs early in apoptosis) and caspase activation by western blotting should also be examined.

A549 cells were used to study any cell cycle effects seen after exposure to dichlorvos. Dichlorvos did cause a slight induction of p53 at 4 hours and this returned to background levels after 24 hours as seen with TK6 cells. Dichlorvos did cause a decrease in Rb phosphorylation after 4 hours this returned to background levels at 24 hours, this suggested that dichlorvos, does cause cell cycle arrest at G1/S phase but the block is lifted after 24 hours. There was an increase in the phosphorylated cdc2 protein with both 10 and 100µM dichlorvos at 4 hours. This would suggest a G2/M block in the cell cycle. These affects would allow for the slowing of the cell cycle and allow for repair of the DNA damage unless the damage was too high and the cells would be directed to apoptosis.

Preliminary studies were conducted in TK6 cells on the role of specific DNA repair pathways after dichlorvos treatment. These studies involved treatment of TK6 cells with specific enzyme inhibitors to inhibit BER and NHEJ followed by treatment with dichlorvos and measurement of cell viability after 24 and 48 hours. An initial observation was that dichlorvos appeared less cytotoxic compared to previous studies. Slightly different methods were used to measure cytotoxicity previously the MTT assay had been used, in the repair studies cytotoxicity was measured using the MTS assay. These preliminary studies differed in levels of cytotoxicity found with the MTT assay. Although these are two different methods for measuring cytotoxicity and a difference would be expected, the difference in cell viability is quite large. At 24 hours dichlorvos has caused nearly a 20% loss of cell viability with the MTS assay compared to a 40% loss recorded with the MTT assay. It is worth noting that these results were not restricted to dichlorvos and the positive control

hydrogen peroxide 10µM did not cause similar levels of cytotoxicity seen with MTT assay either. This could possibly be attributed to a different batch of dichlorvos and hydrogen peroxide as well as a different consignment of TK6 cells used. The preliminary data suggested that TK6 cells at 24 hours were showing signs of repair by non homologous end joining, cells devoid of this repair mechanism showed a larger decrease in cell viability. This data is corroborated by the phosphorylation H2AX in A549 cells and formation of nuclear foci. γ-H2AX is rapidly phosphorylated to form discreet nuclear spots or foci in response to double strand breaks. Some studies have suggested that dichlorvos can methylate DNA. If this was the case then the BER pathway would be expected to be involved in the repair of this type of lesion. After 48 hours cells that were devoid of BER were showing a slight (15%) increase in cell death. These preliminary studies suggest that two different repair pathways may be involved in the response to dichlorvos-induced DNA damage. These pathways repair different forms of DNA damage, suggesting that dichlorvos was able to cause more than one type of lesion. These lesions may be attributed to either a direct effect by dichlorvos and/or due to dichlorvos initiating cell death. These results along with the comet assay data certainly indicate that dichlorvos is able to damage DNA, which the cell responds to by initiating DNA repair mechanisms. Dichlorvos caused DNA damage with an increase in cytotoxicity, the results presented here suggests that some cells were directed to repair and others were directed to cell death with evidence to suggest apoptosis as a mechanism of cell death.

### 3.6 Summary

Dichlorvos induced DNA damage, even at nM levels and after only a short exposure time, in two cell lines TK6 lymphoblastoid cells and SH-SY5Y neuroblastoma cells. The genotoxic potential has also corroborated by increased expression of γ-H2AX. Dichlorvos was cytotoxic at high concentrations. Dichlorvos results in p53 induction but no apparent phosphorylation on Ser15, in contrast to etoposide which causes both p53 induction and phosphorylation. This may suggests a different mechanism in response to DNA damage induced by dichlorvos rather than that seen with etoposide. A G2/M block was found after exposure to dichlorvos as well as the possible initiation of DNA repair mechanisms NHEJ and BER.

# *Chapter 4*

# *A comparison of the genotoxic potential of a phosphorothioate and an oxon*

# 4.0 Chlorpyrifos

Previous studies had been conducted using dichlorvos which is a stable oxon. These were compared with chlorpyrifos, a phosphorothioate and its unstable metabolite chlorpyrifos oxon. Chlorpyrifos, without undergoing biotransformation by cytochrome P450s to chlorpyrifos oxon, does not bind AChE. The ability of chlorpyrifos and chlorpyrifos oxon to cause DNA damage and cytotoxicity was compared, this allowed for the evaluation of AChE binding in the genotoxic potential of an organophosphate.

## 4.1 Cytotoxicity

DNA damage activates cellular signalling pathways that may ultimately lead to cell death, if the damage encountered is too great or not repaired. The cytotoxicity of chlrpyriofos and chlorpyrifos oxon was tested in TK6 cells using the MTT assay. Cells were exposed to 0.01, 0.1, 1, 10 and 100µM of either chlorpyrifos or chlorpyrifos oxon and tested for cytotoixicty after 1 and 24 hours.

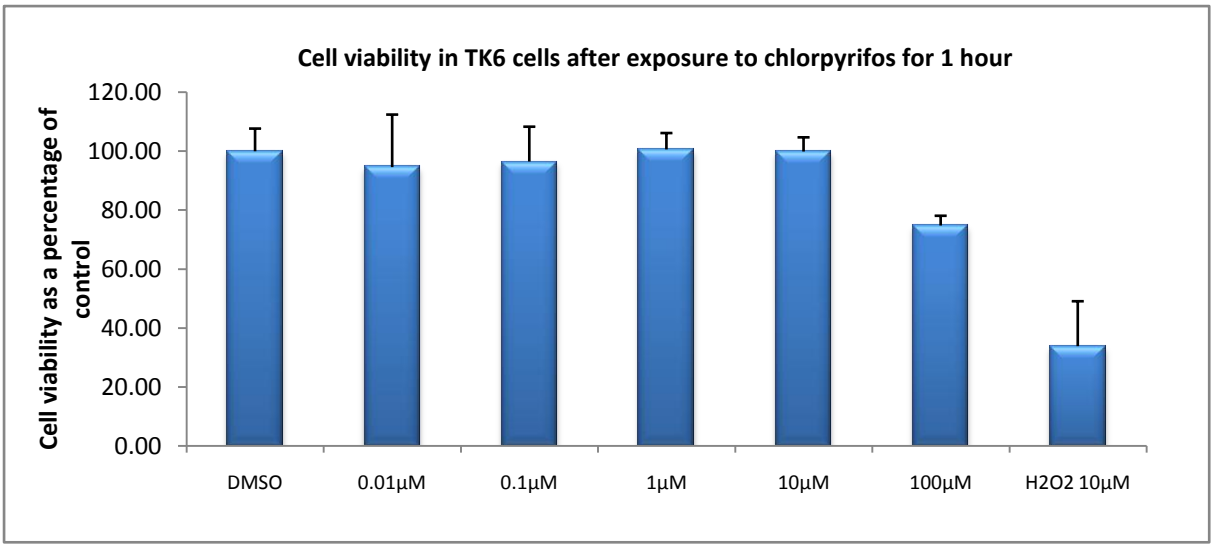


**Figure 4.1. Cytotoxicity of chlorpyrifos in TK6 cells.** Cells were exposed to the indicated doses of chlorpyrifos or $H_2O_2$ for 1 hour before cell viability was measured using an MTT assay. Results were expressed as mean % viability relative to untreated control (untreated cells designated 100% viability) ± standard deviation

| | DMSO | 0.01µM | 0.1µM | 1µM | 10µM | 100µM | $H_2O_2$ 10µM |
|---|---|---|---|---|---|---|---|
| **Cell viability (%)** | **100.00** | **94.62** | **96.53** | **100.64** | **99.92** | **74.81*** | **33.87***** |

**Table 4.1. Cytotoxicity in TK6 cells after treatment with chlorpyrifos (0.01, 0.1, 1, 10 and 100µM) for 1 hour**. Cytotoxicity was measured as a percentage of control. (P value * <0.05 **P value <0.01 ***P value <0.001 one way ANOVA)

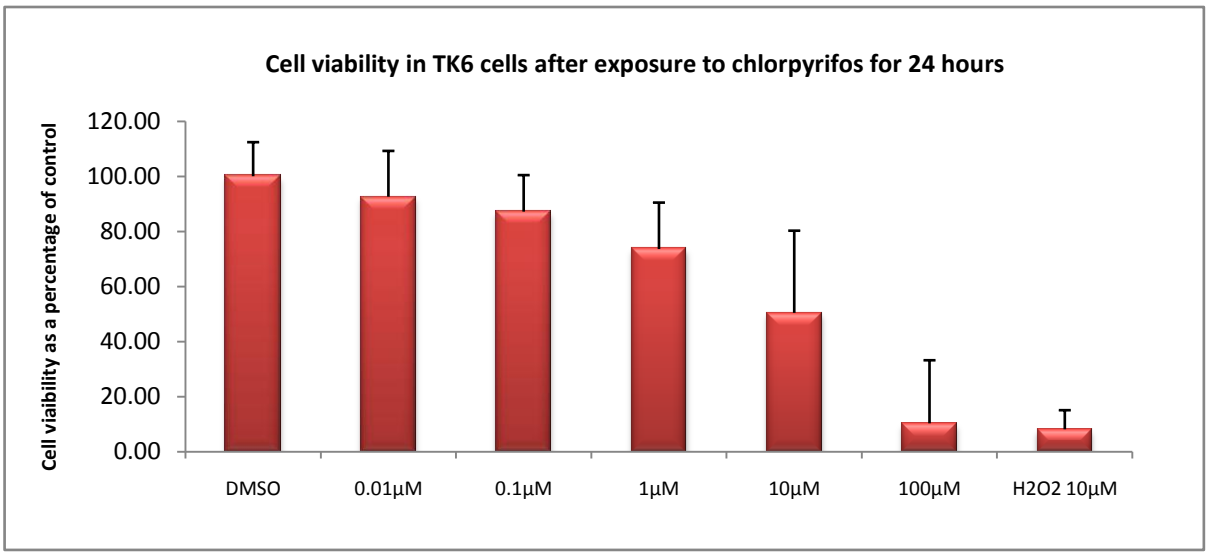


**Figure 4.2. Cytotoxicity of chlorpyrifos in TK6 cells.** Cells were exposed to the indicated doses of chlorpyrifos or $H_2O_2$ for 24 hours before cell viability was measured using an MTT assay. Results were expressed as mean % viability relative to untreated control (untreated cells designated 100% viability) ± standard deviation

| | DMSO | 0.01µM | 0.1µM | 1µM | 10µM | 100µM | $H_2O_2$ 10µM |
|---|---|---|---|---|---|---|---|
| **Cell viability (%)** | **100.00** | **92.57** | **87.15** | **73.55** | **50.37**** | **10.25***** | **8.10***** |

**Table 4.2. Cytotoxicity in TK6 cells after treatment with chlorpyrifos (0.01, 0.1, 1, 10 and 100µM) for 24 hours**. Cytotoxicity was measured as a percentage of control. (P value * <0.05 **P value <0.01 ***P value <0.001 one way ANOVA)

Figure 4.1 and Table 4.1 shows that chlorpyrifos did not cause cytotoxicity in TK6 cells between doses of 0.01 and 10µM after 1 hour, but 100µM chlorpyrifos caused a 20% loss of cell viability. Hydrogen peroxide 10µM, used as a positive control, caused a 66% loss in cell viability after 1 hour. A Longer incubation period with chlorpyrifos proved to be cytotoxic even at low µM concentrations. At doses of 0.01 and 0.1µM, cytotoxicity was not observed even after 24 hours whereas 1µM chlorpyrifos caused a 20% loss in cell viability and 100µM caused a loss of more than 80% viability (Figure 4.2 and Table 4.2).

The experiment was repeated but using chlorpyrifos oxon and the results are described below.

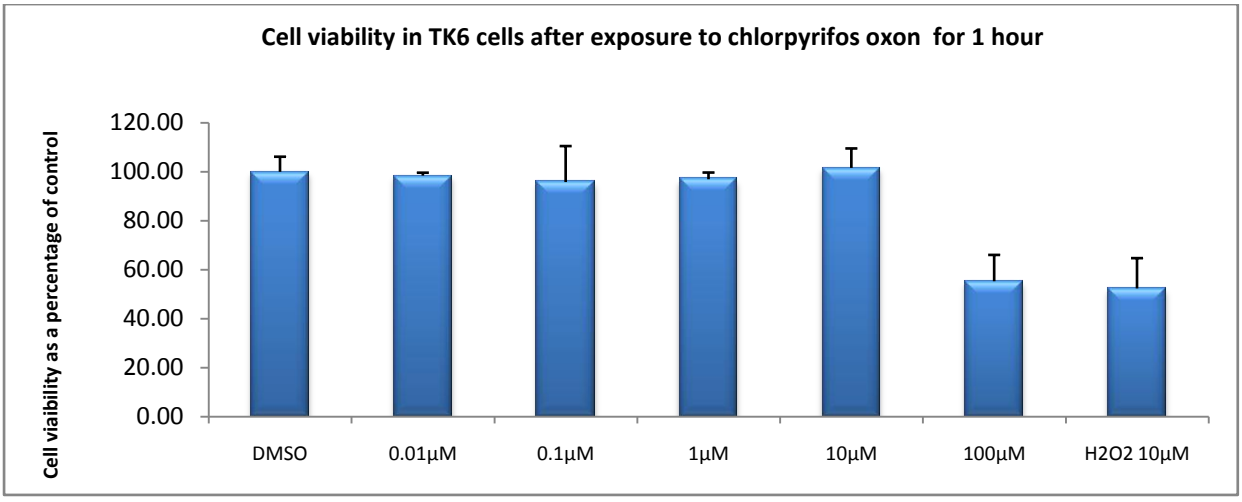


**Figure 4.3. Cytotoxicity of chlorpyrifos oxon in TK6 cells.** Cells were exposed to the indicated doses of chlorpyrifos or $H_2O_2$ for 1 hour before cell viability was measured using an MTT assay. Results were expressed as mean % viability relative to untreated control (untreated cells designated 100% viability) ± standard deviation

| | DMSO | 0.01µM | 0.1µM | 1µM | 10µM | 100µM | $H_2O_2$ 10µM |
|---|---|---|---|---|---|---|---|
| **Cell viability (%)** | 100.00 | 98.46 | 95.81 | 96.97 | 101.60 | 55.32*** | 52.40** |

**Table 4.3. Cytotoxicity in TK6 cells after treatment with chlorpyrifos oxon (0.01, 0.1, 1, 10 and 100µM) for 1 hour.** Cytotoxicity was measured as a percentage of control. ((P value * <0.05 **P value <0.01 ***P value <0.001 one way ANOVA)

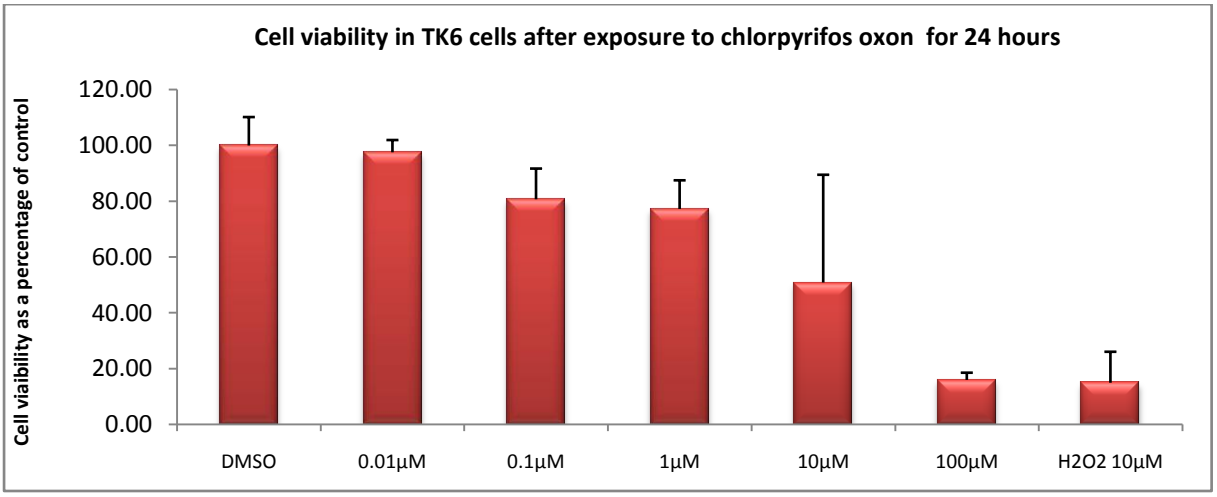


**Figure 4.4. Cytotoxicity of chlorpyrifos oxon in TK6 cells.** Cells were exposed to the indicated doses of chlorpyrifos or $H_2O_2$ for 24 hours before cell viability was measured using an MTT assay. Results were expressed as mean % viability relative to untreated control (untreated cells designated 100% viability) ± standard deviation

| | DMSO | 0.01µM | 0.1µM | 1µM | 10µM | 100µM | $H_2O_2$ 10µM |
|---|---|---|---|---|---|---|---|
| **Cell viability (%)** | 100.00 | 97.58 | 80.74* | 77.27* | 50.91*** | 15.96*** | 14.97*** |

**Table 4.4. Cytotoxicity in TK6 cells after treatment with chlorpyrifos oxon (0.01, 0.1, 1, 10 and 100µM) for 24 hours.** Cytotoxicity was measured as a percentage of control. (P value * <0.05 **P value <0.01 ***P value <0.001 one way ANOVA)

Chlorpyrifos oxon showed a very similar profile of cytotoxicity to the parent phosphorothioate form. After 1 hour, no cytotoxicity was observed with the concentrations 0.01 to 10µM but 100µM caused nearly a 50% loss of cell viability (Figure 4.3 and Table 4.3). The oxon was slightly more toxic than the phosphorothioate form which only caused a 33% loss in cell viability. After 24 hours, lower concentrations of chlorpyrifos oxon, as with the parent compound, proved to be cytotoxic as 0.1 and 1µM caused a 20% loss of cell viability after 24 hours. 10µM caused a 50 % loss in cell viability and 100µM caused approximately an 85% loss of cell viability (Figure 4.4 and Table 4.4). After 1 hour the oxon form was slightly more toxic at 100µM but overall on a molar basis there is no difference between the phosphorothioate and oxon form after 24 hours.

## 4.2 DNA Damage

### 4.2.1 Comet assay

To test the ability of chlorpyrifos to damage DNA, TK6 cells were exposed to a range of concentrations (0.01, 0.1, 1, 10 and 100µM) for 24 hours following which DNA damage was assessed by the alkaline comet assay. An increase in dose caused an increase in OTM at both 1 and 24 hours with chlorpyrifos (Figure 4.5 and Table 4.5; Figure 4.6 and Table 4.6).

Chlorpyrifos caused a dose dependent increase in DNA damage after 1 hour exposure. The highest amount of damage occurred at 100µM with an OTM of 2.35 compared to a control value of 0.62. After treatment with chlorpyrifos for 1hour there was an uneven distribution of damage in the 50 cells analysed, about 80% of cells had low OTM values of less than 1, however increasing the dose caused an increase in cells displaying higher OTM values. After 24 hours there was a decrease in DNA damage compared with the 1hour sample after treatment with the lowest doses of chlorpyrifos (0.01 and 0.1 µM). In contrast, at higher doses (1, 10 and 100µM) an increase in DNA damage was observed, these concentrations have increased approximately by 1 OTM unit (when considering the mean) between 1 and 24 hours. The distribution of the DNA damage in the 50 cells analysed for 1, 10 and 100µM showed there was a marked increase in the number of cells displaying damage between 5 and 10 OTM. After treatment with 100µM there is also an increase in the number of cells showing damage with an OTM value greater than 10. At 24 hours with 10 and 100µM there

is a massive loss in cell viability and this makes interpretation of these results difficult due to the extensive cell death.

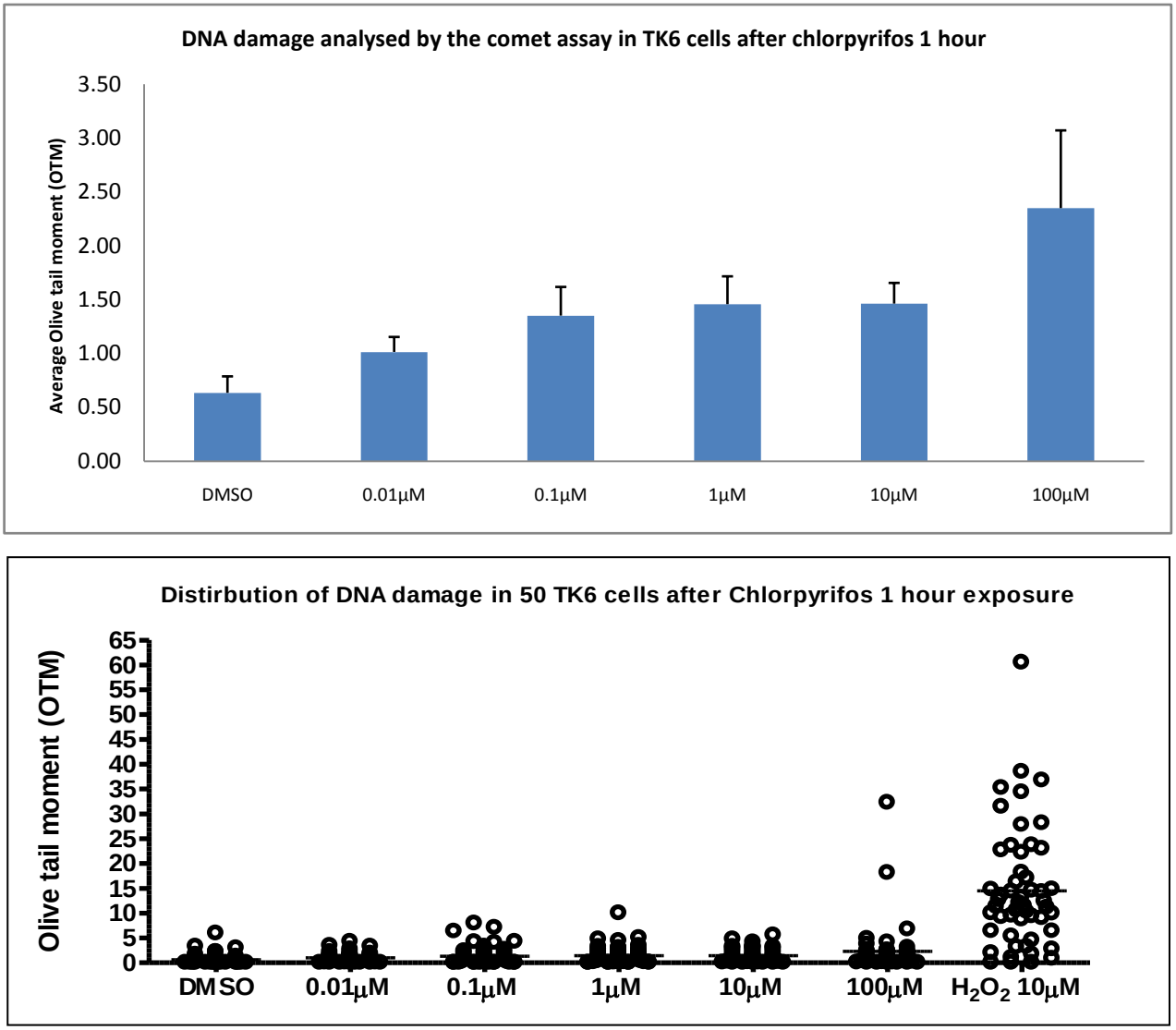


**Figure 4. 5. DNA damage in TK6 cells after chlorpyrifos** TK6 cells were exposed to the indicated doses of chlorpyrifos or hydrogen peroxide for 1 hour prior to measurement of DNA damage using the alkaline comet assay. The upper graph shows the mean olive tail moment of 50 cells ± S.E. Hydrogen peroxide 10µM (value 14.8 OTM) has been excluded from the upper graph. The lower graph shows the distribution of damage between the 50 cells scored.

| | DMSO | 0.01µM | 0.1µM | 1µM | 10µM | 100µM | $H_2O_2$ 10µM |
|---|---|---|---|---|---|---|---|
| **DNA damage (OTM)** | 0.63 | 1.01 | 1.35 | 1.46 | 1.46** | 2.35** | 14.76*** |

**Table 4. 5. DNA damage in TK6 cells by chlorpyrifos (0.01, 0.1, 1, 10 and 100µM) for 1 hour**. DNA damage was measured as OTM (P value * <0.05 **P value <0.01 ***P value <0.001 Kruskal-Wallis)

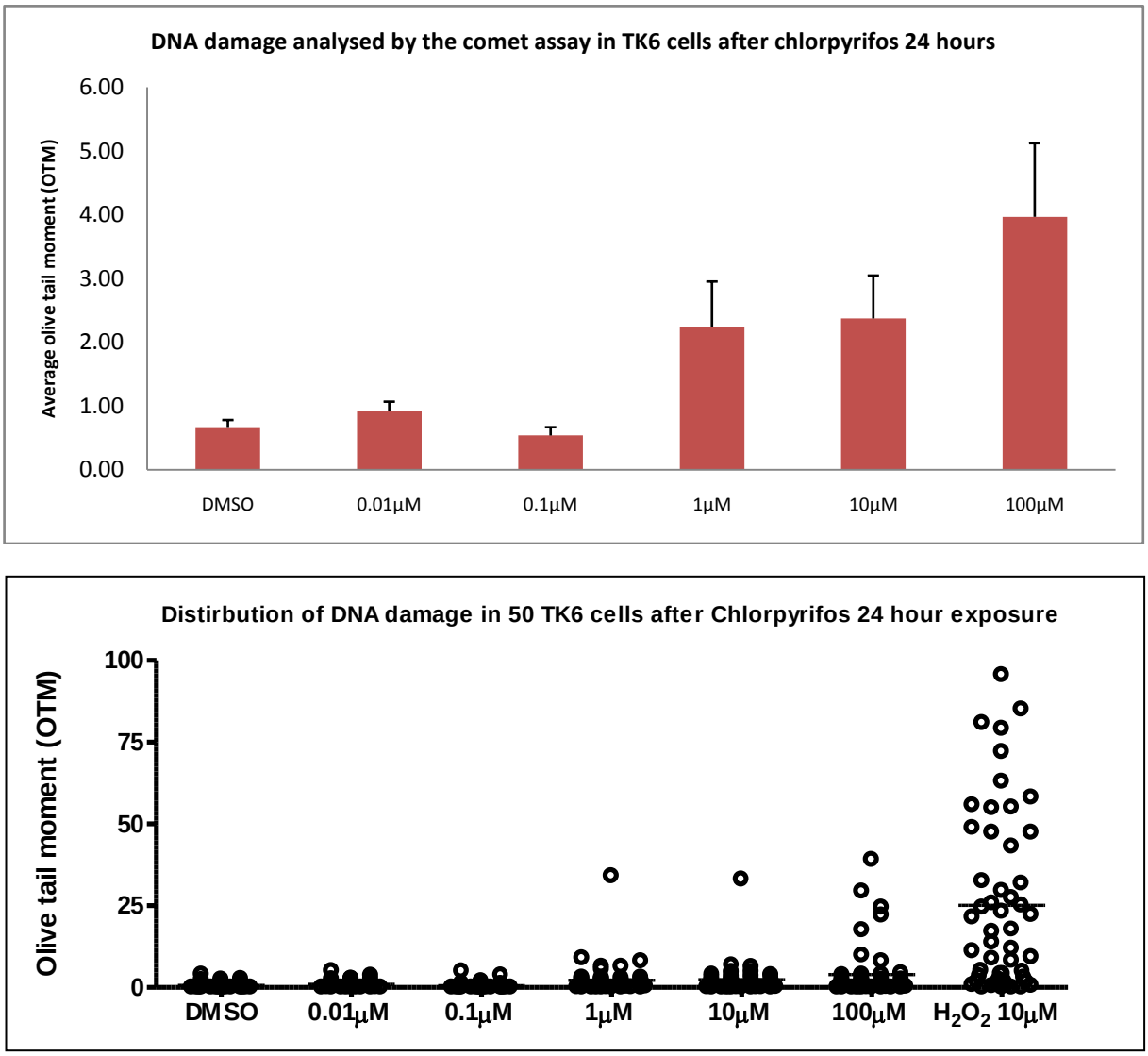


**Figure 4.6. DNA damage in TK6 cells after chlorpyrifos** TK6 cells were exposed to the indicated doses of chlorpyrifos or hydrogen peroxide for 24 hours prior to measurement of DNA damage using the alkaline comet assay. The upper graph shows the mean olive tail moment of 50 cells ± S.E. Hydrogen peroxide 10µM (value 25.2 OTM) has been excluded from the upper graph. The lower graph shows the distribution of damage between the 50 cells scored.

| | DMSO | 0.01µM | 0.1µM | 1µM | 10µM | 100µM | $H_2O_2$ 10µM |
|---|---|---|---|---|---|---|---|
| **DNA damage (OTM)** | 0.66 | 0.92 | 0.54 | 2.24 | 2.37* | 3.97 | 25.16*** |

**Table 4.6. DNA damage in TK6 cells by chlorpyrifos (0.01, 0.1, 1, 10 and 100µM) for 24 hours**. DNA damage was measured as OTM (P value * <0.05 **P value <0.01 ***P value <0.001 Kruskal-Wallis)

To test the ability of chlorpyrifos oxon to damage DNA, TK6 cells were exposed to a range of concentrations (0.01, 0.1, 1, 10 and 100µM) for up to 24 hours. At 1 and 24 hours DNA damage was assessed by the alkaline comet assay and displayed an increase in dose caused an increase in OTM at both 1 and 24 hours (Figure 4.7 and Table 4.8; Figure 4.8 and Table 4.8).

Chlorpyrifos oxon caused a dose dependent increase in DNA damage after 1 hour exposure. The highest amount of damage was after 100µM with a rise from an average 1.09 OTM with the DMSO treated cells, to 11.27. The distribution of DNA damage in the 50 cells analysed after treatment with 100µM showed that roughly half the cells had an OTM value greater than 20, with the other half displaying an OTM of less than 5. After treatment with 0.01, 0.1, 1 and 10µM the majority of the cells have an OTM value of less than 5, however there is an increase in the number of cells (approx 20%) showing damage between 5 and 10 OTM, with some cells showing damage above 10 OTM. An increase in DNA damage was seen at 24h compared to 1h, with an increase in DNA damage after 0.01, 0.1 and 10 µM. These values have approximately doubled in OTM values when considering the mean compared to the 1 hour sample. When considering the distribution of damage in the 50 cells analysed for each of these concentrations, the majority of cells displayed damage between 5 and 10 OTM with a number of the cells showing OTM values over 10 OTM with some as high as 50 OTM. After treatment with 100µM, the majority of cells showed extremely high OTM levels. When considering the spread of DNA damage within the 50 cells some displayed damage well above 100 OTM with the majority of cells showing extensive damage, similar to the profile seen with hydrogen peroxide a known reactive oxygen species producer. After 24 hours there was a decrease in DNA damage compared with the 1hour sample after treatment with 1µM, however the error bar at 1hour is quite large due to a few high OTM values of a few cells, this has obscured the mean. When comparing the distribution of damage of 1µM chlorpyrifos at 1 and 24 hours, it is clear that at 24 hours there is an increase in the proportion of cells showing greater damage than after 1 hour. After 24 hours with 100µM there is low cell viability measured by the MTT assay this makes interpretation of results difficult due to the excess of cell death at this time point.

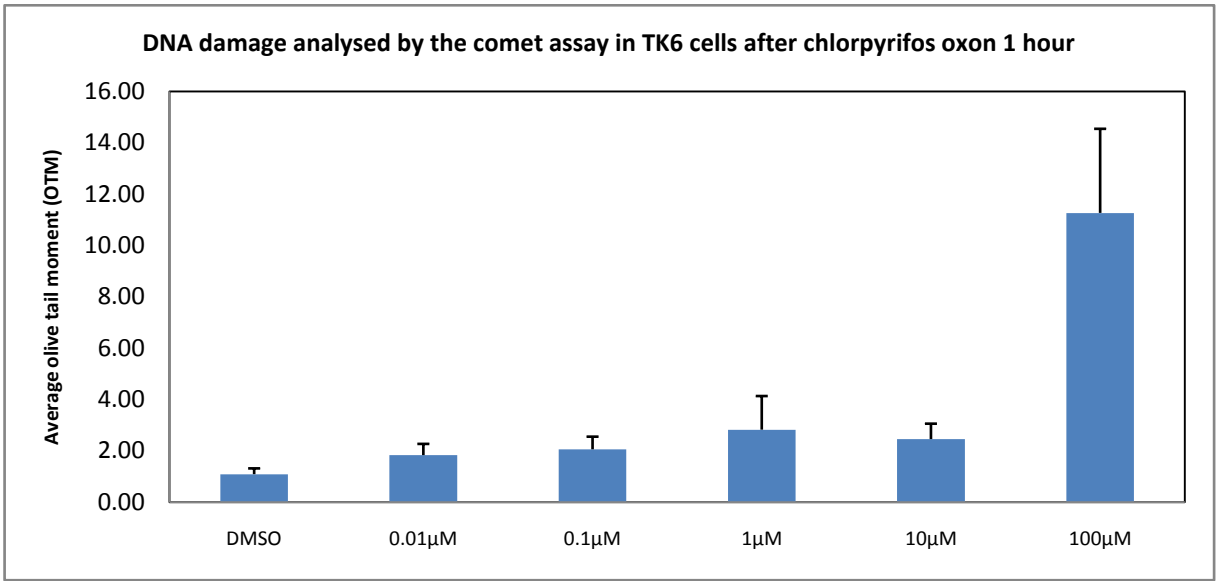


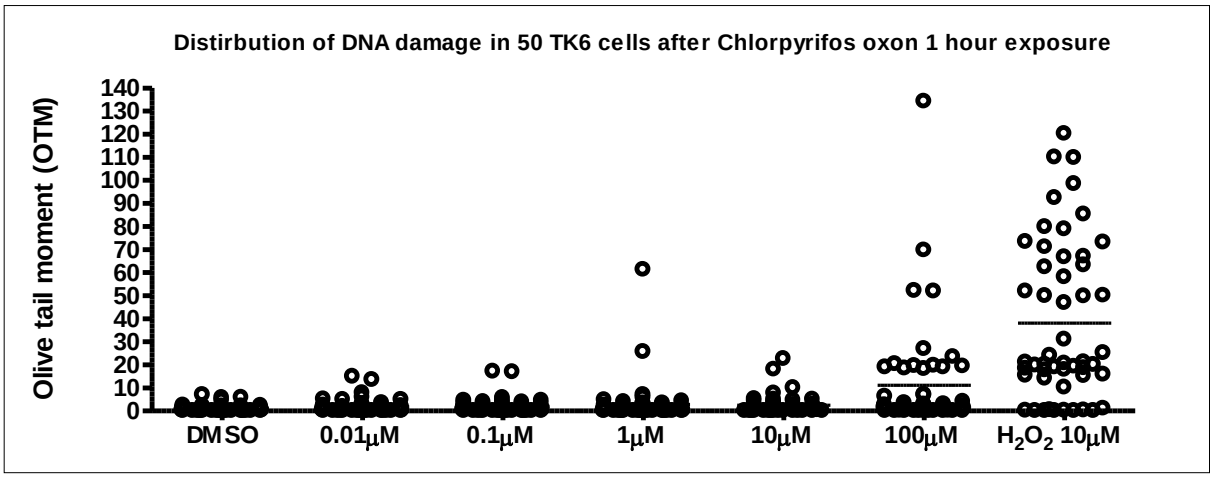


**Figure 4.7. DNA damage in TK6 cells after chlorpyrifos oxon** TK6 cells were exposed to the indicated doses of chlorpyrifos oxon or hydrogen peroxide for 1 hour prior to measurement of DNA damage using the alkaline comet assay. The upper graph shows the mean olive tail moment of 50 cells ± S.E. Hydrogen peroxide 10µM (value 38.4 OTM) has been excluded from the upper graph. The lower graph shows the distribution of damage between the 50 cells scored.

| | DMSO | 0.01µM | 0.1µM | 1µM | 10µM | 100µM | $H_2O_2$ 10µM |
|---|---|---|---|---|---|---|---|
| **DNA damage (OTM)** | 1.09 | 1.83 | 2.06 | 2.82 | 2.45 | 11.27* | 38.37*** |

**Table 4.7. DNA damage in TK6 cells by chlorpyrifos oxon (0.01, 0.1, 1, 10 and 100µM) for 1 hour**. DNA damage was measured as OTM (P value * <0.05 **P value <0.01 ***P value <0.001 Kruskal-Wallis)

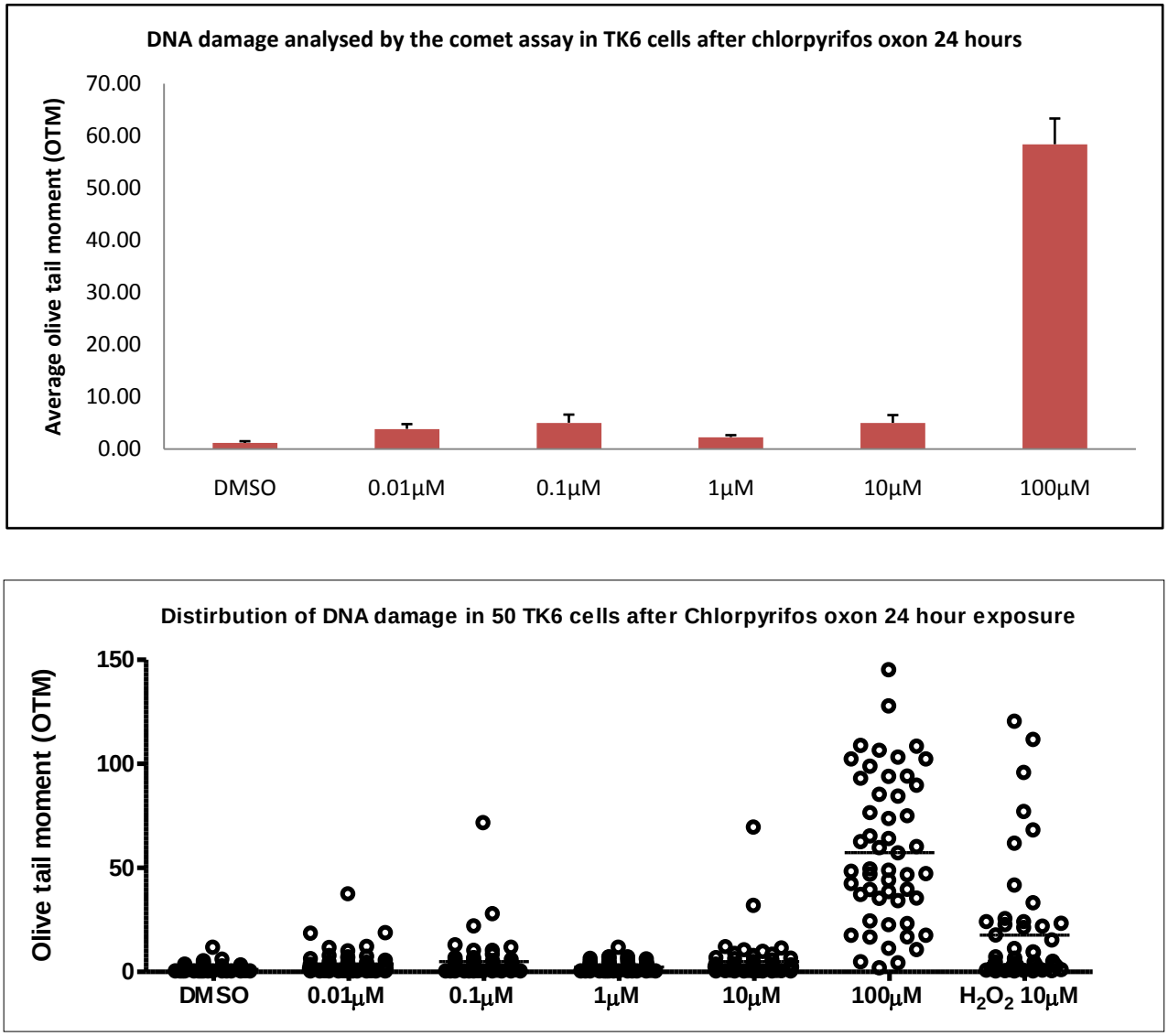


**Figure 4.8. DNA damage in TK6 cells after chlorpyrifos oxon** TK6 cells were exposed to the indicated doses of chlorpyrifos oxon or hydrogen peroxide for 24 hours prior to measurement of DNA damage using the alkaline comet assay. The upper graph shows the mean olive tail moment of 50 cells ± S.E. Hydrogen peroxide 10µM (value 17.5 OTM) has been excluded from the upper graph. The lower graph shows the distribution of damage between the 50 cells scored.

| | DMSO | 0.01µM | 0.1µM | 1µM | 10µM | 100µM | $H_2O_2$ 10µM |
|---|---|---|---|---|---|---|---|
| **DNA damage (OTM)** | 1.20 | 3.84 | 5.02* | 2.27 | 4.99 | 58.40*** | 17.52*** |

**Table 4.8. DNA damage in TK6 cells by chlorpyrifos oxon (0.01, 0.1, 1, 10 and 100µM) for 24 hours**. DNA damage was measured as OTM (P value * <0.05 **P value <0.01 ***P value <0.001 Kruskal-Wallis)

## 4.3 Response to DNA damage

### 4.3.1. p53 response

Chlorpyrifos and chlorpyrifos oxon caused significant DNA damage and cytotoxicity, particularly at higher doses. If these compounds are damaging DNA, then DNA damage signalling pathways should also be activated in response to this damage. TK6 cells were treated with 0.01µM, 0.1µM, 1µM, 10µM and 100µM chlorpyrifos and chlorpyrifos oxon for 4 and 24hrs. Samples were collected for western blot analysis and analysed for the expression of p53, phosphorylated p53 (Ser15), and PARP-1 or the cleaved PARP-1 fragment as a marker of apoptosis (already described in a previous chapter). Etoposide was used as a positive control for the induction of DNA damage signalling events and apoptosis.

Figure 4.9 shows that there was no evidence of PARP-1 cleavage at doses 0.01-10µM or etoposide 50 µM at 4 hours. However there was evidence of PARP-1 cleavage after 100µM chlorpyrifos after 4 hours, suggesting apoptosis has been induced. No band was seen at 4 hours with etoposide as this is a topoisomerase inhibitor and primarily exerts a toxic effect during S phase, therefore cells will need to enter S phase before any significant toxic effect occurs. After 24 hours treatment with etoposide a clear band of cleaved PARP-1 can be seen. There is no band at 24 hours after treatment with chlorpyrifos. A possible reason for this is due to an early initiation of apoptosis. After 24 hours a high number of cells are no longer viable as seen with the MTT assay and this may account for no band being seen at 24 hours with chlorpyrifos.

A background level of p53 and phosphorylated p53-Ser15 can be seen in the DMSO treated cells with elevated levels of both p53 and the phosphorylated p53 occurring with 50µM etoposide. No increase in protein levels of p53 or p53-Ser15 occurred with chlorpyrifos after 4 or 24 hours, suggesting that DNA damage signalling events are not being activated.

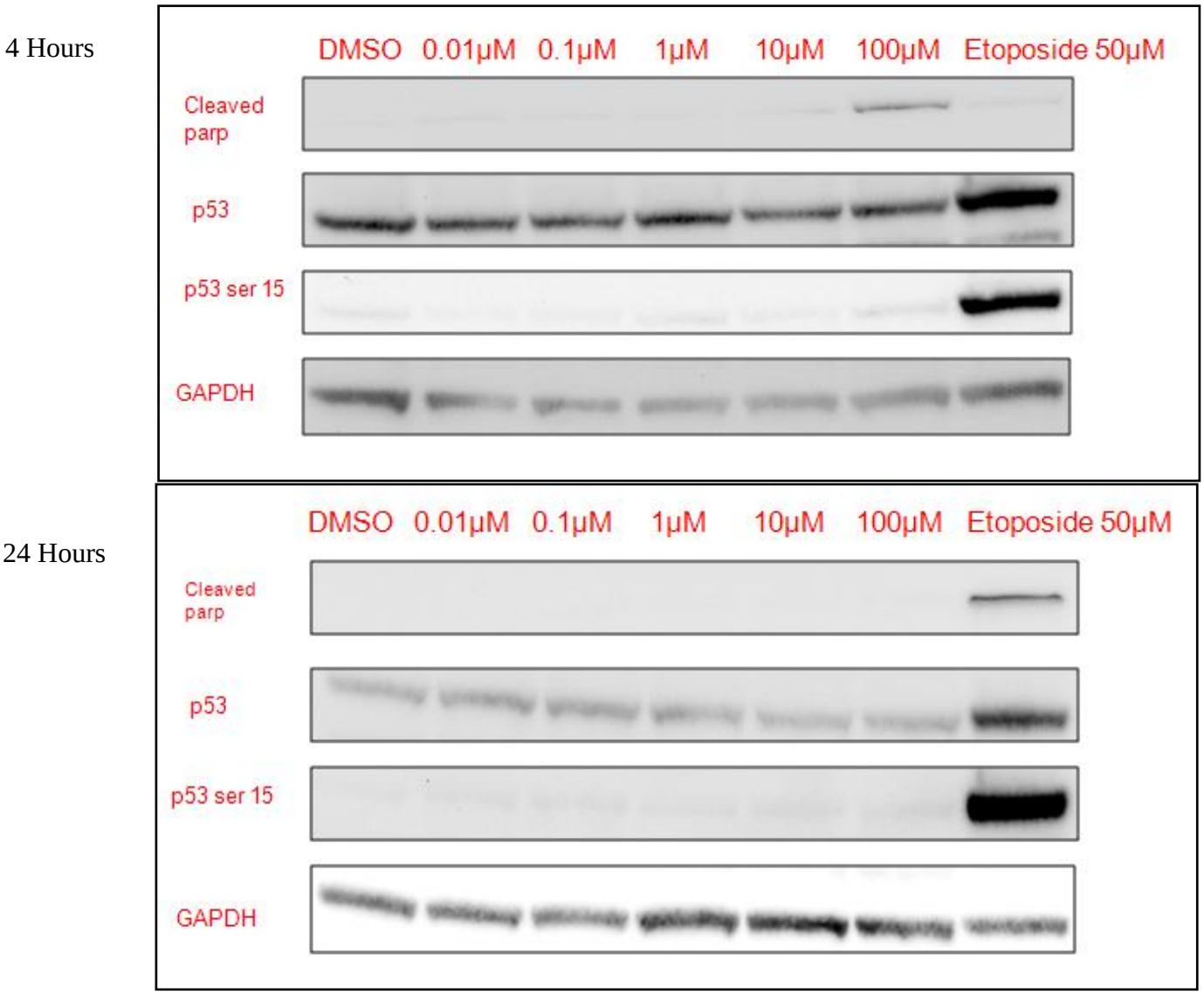


**Figure 4.9. Western blot of TK6 cells after chlorpyrifos or etoposide.** Cells were exposed to the indicated doses of chlorpyrifos or 50µM etoposide for 4h or 24h prior to western blot analysis.

A similar study was conducted to see if DNA damage signalling cascades were initiated after exposure to 10 or 100µM chlorpyrifos oxon in TK6 cells. Samples were prepared in duplicate to allow for more accurate analysis. Etoposide (50 µM) was used as a positive control for the initiation of DNA signalling cascades.

Figure 4.10 shows that PARP-1 is cleaved after 24 hours with chlorpyrifos oxon (100µM) and etoposide. No band for cleaved PARP-1 was observed at 4 hours following exposure to chlorpyrifos oxon but a band can be seen after 24 hours indicating apoptosis. This differs to chlorpyrifos and may indicate that the phosphorothioate and oxon form of chlorpyrifos exert a cytotoxic effect via different mechanisms. There is no increase in p53 after 4 hours

but a small increase of p53 can be seen after 24 hours at both 10µM and 100µM chlorpyrifos oxon.

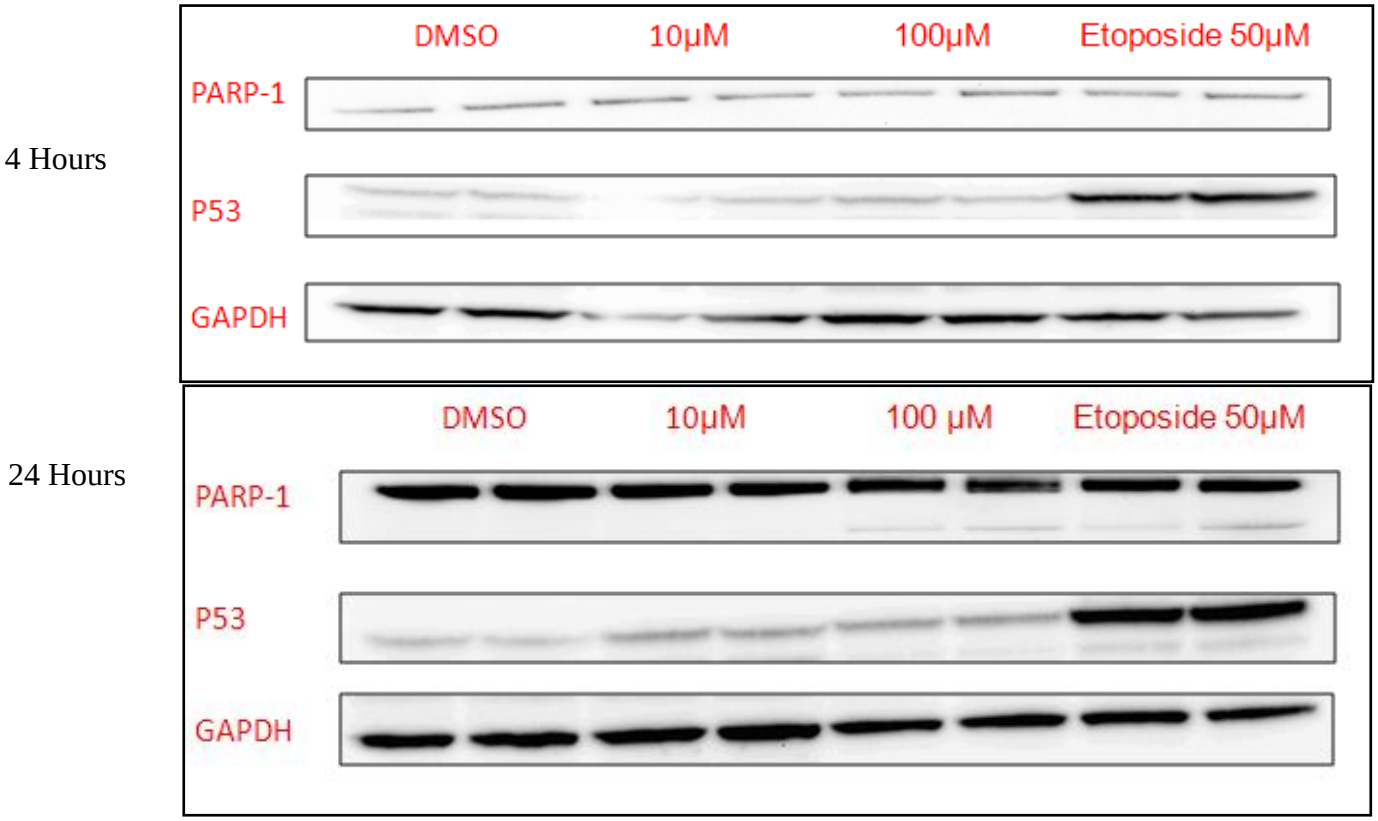


**Figure 4.10. Western blot of TK6 cells after chlorpyrifos oxon or etoposide.** Cells were exposed to the indicated doses of chlorpyrifos or 50µM etoposide for 4h or 24h prior to western blot analysis

The western blot in Figure 4.10 was quantified using Syngene Gene tools software. The values obtained for the increase in p53 protein levels were then normalised against GAPDH. Each sample was completed in duplicate and the results are displayed as a mean +/- standard error. Figure 4.11 demonstrates that chlorpyrifos oxon does not cause an increase of p53 after 4 hours. However, p53 levels approximately doubled after 100µM chlorpyrifos oxon for 24 hours.

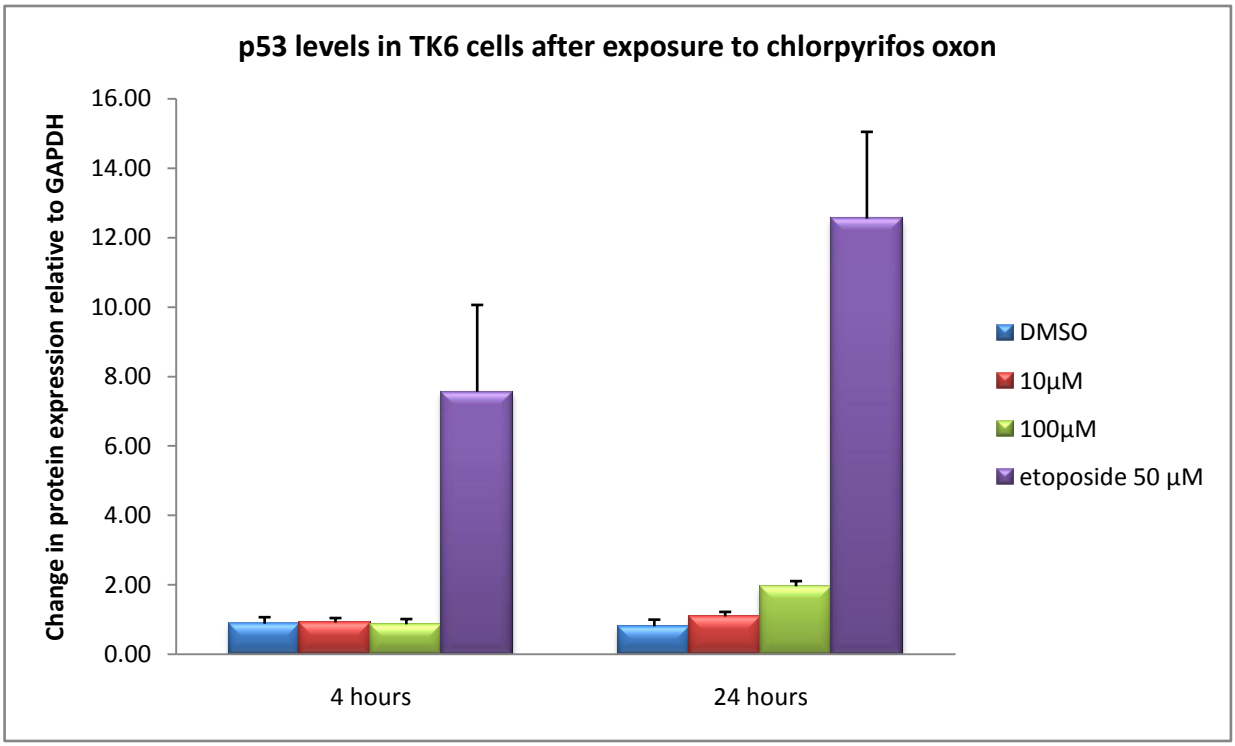


**Figure 4.11. Change in expression of p53 in TK6 cells after chlorpyrifos oxon.** Cells were exposed to the indicated concentrations of chlorpyrifos oxon for 4 and 24h prior to western blot analysis. Etoposide was used as a positive control for the activation of DNA damage signalling. Values have been calculated using Syngene software and normalised against GAPDH levels. Error bars are ± STD error

### 4.3.2 Cell cycle effects

A549 cells had previously been established as suitable to study cell cycle effects after genotoxins and were used to view any cell cycle effects after 10µM and 100µM chlorpyrifos for 24 hours. In order to confirm that the p53 response was the same as seen with TK6 cells, the expression of p53 and p53-Ser15, in addition to phosphorylated cdc2-Tyr15 and phosphorylated Rb-Ser795 were also investigated.

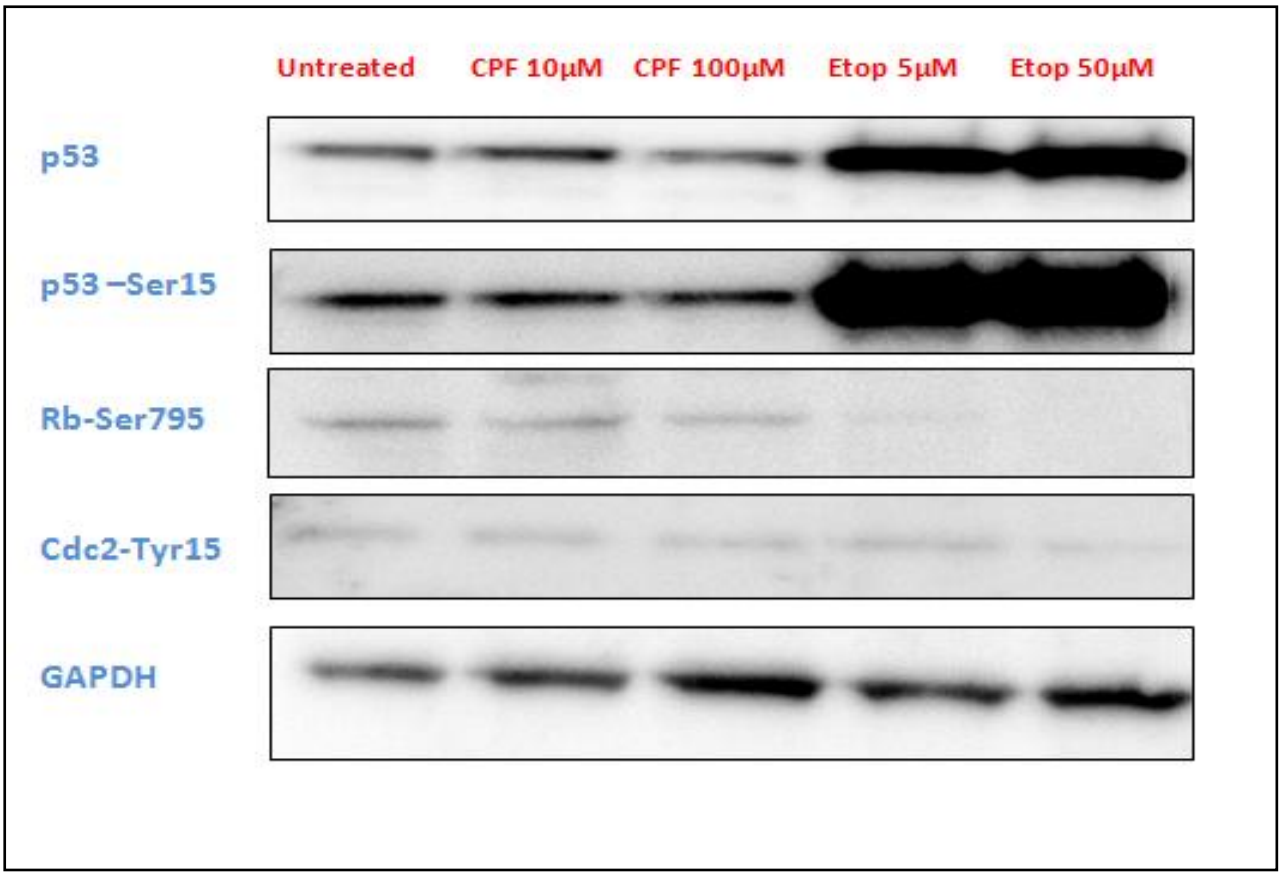


**Figure 4.12. Western blot of A549 cells after chlorpyrifos or etoposide.** Cells were exposed to the indicated doses of chlorpyrifos or 50µM etoposide for 24h prior to western blot analysis

Chlorpyrifos does not show an increase in p53 protein levels after 24 hours and this was the same as seen with TK6 cells. The increase of p53 protein levels and the phosphorylation of p53 is clear after 24 hours after treatment with etoposide at both 5 and 50µM (Figure 4.12). Chlorpyrifos does show a decrease in Rb (Ser 795), in contrast to the marked decrease with etoposide at both 5 and 50 µM concentrations (Figure 4.12). A small decrease can be seen in the p-cdc2-Tyr15 protein after chlorpyrifos (10 and 100µM) and etoposide (5 and 50µM) which would indicate a G2/M block.

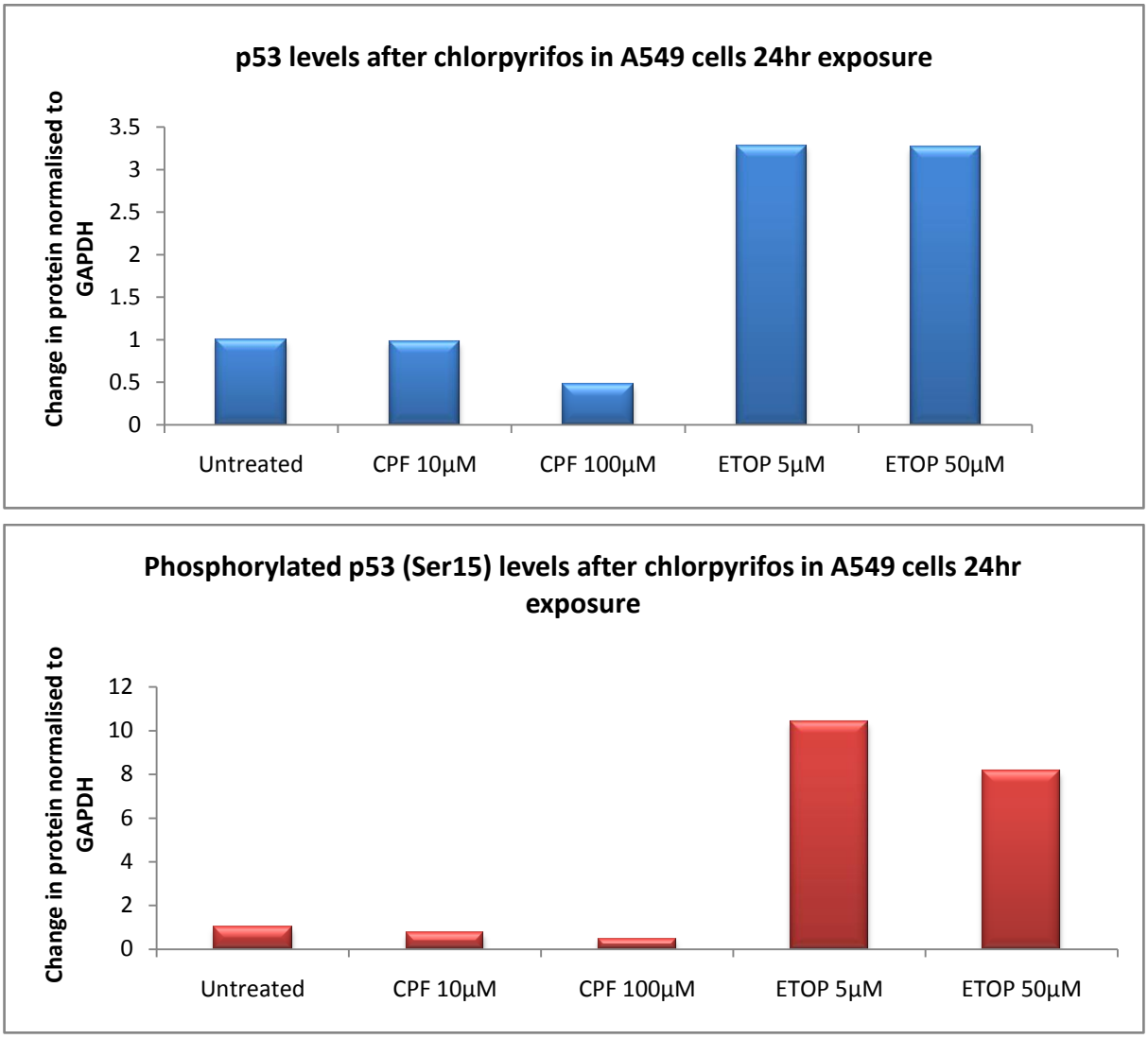


**Figure 4.13. Change in expression of p53 and p53 Ser15, in a549 cells after chlorpyrifos.** Cells were exposed to the indicated concentrations of chlorpyrifos 24h prior to western blot analysis. Etoposide was used as a positive control for the activation of DNA damage signalling. Values have been calculated using Syngene software and normalised against GAPDH levels. Error bars are ± STD error

The western blot in figures 4.12 was quantified using Syngene Gene tools software. The values obtained for the increase in protein levels of p53 and p53-Ser15 were then normalised against GAPDH. Figure 4.13 confirms that there was no increase in p53 or p53-Ser15 levels after treatment with chlorpyrifos after 24 hours. However etoposide was able to cause a 3 fold increase after 24 hours after both 5 and 50µM treatments for p53, this was coupled with an 8 fold increase in phosphorylation of p53 at Ser15.

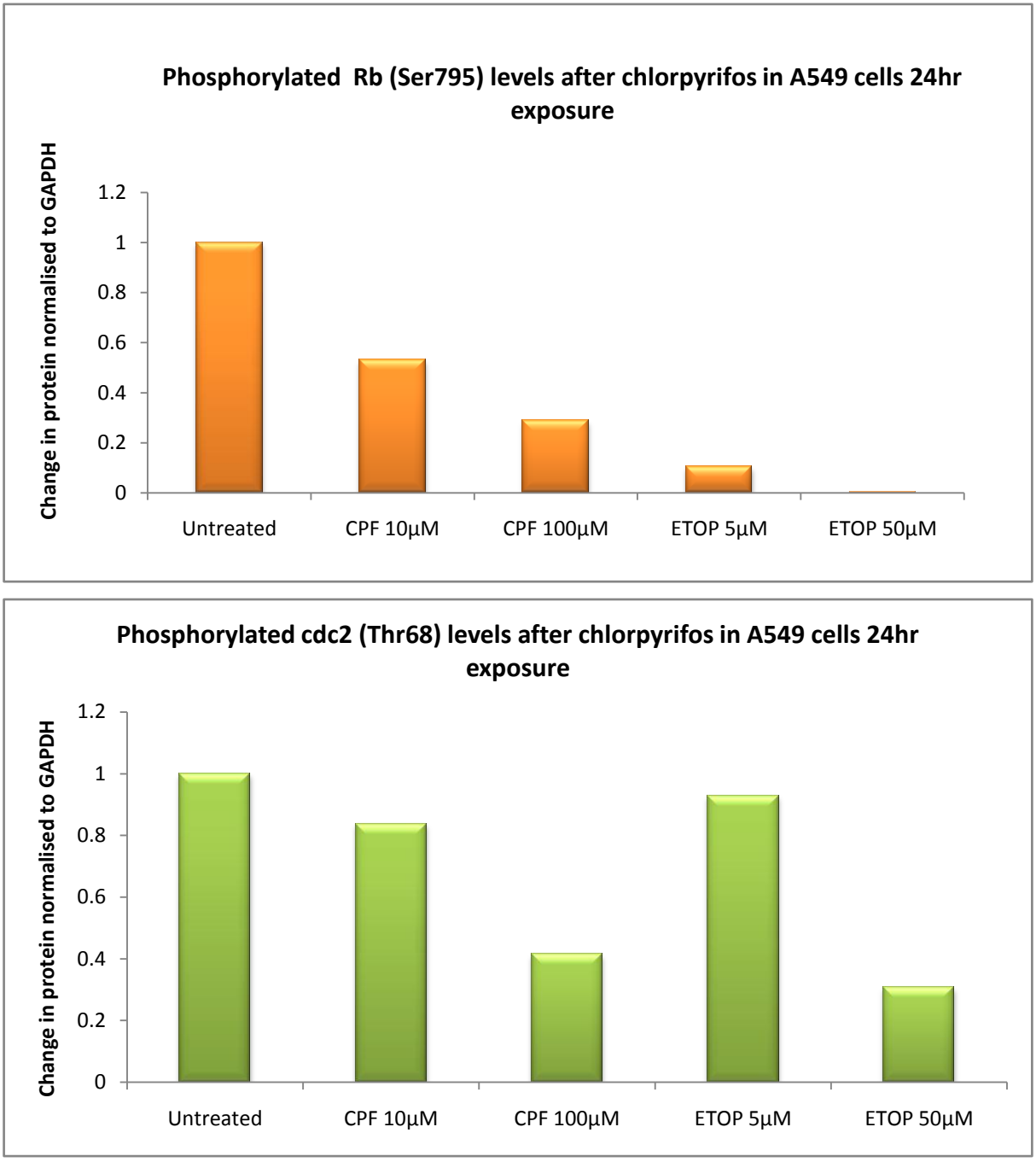


**Figure 4.14. Change in expression of, p-Rb ser795 and p-cdc2 (Tyr15) in a549 cells after chlorpyrifos.** Cells were exposed to the indicated concentrations of chlorpyrifos 24h prior to western blot analysis. Etoposide was used as a positive control for the activation of DNA damage signalling. Values have been calculated using Syngene software and normalised against GAPDH levels. Error bars are ± STD error

The western blot in figure 4.12 was quantified using Syngene Gene tools software. The values obtained for p-Rb-ser795 and p-cdc2-thr68 were then normalised against GAPDH. After 24 hours, chlorpyrifos was able to cause a 50% decrease in p-Rb-ser795 expression with 10µM and a 65% decrease with 100µM; this is consistent with a G1-S block. Etoposide decreased p-Rb-ser795 levels almost to zero causing a >90% reduction in expression with both 5 and 50µM concentrations. Chlorpyrifos (100µM) and etoposide (50µM) caused a decrease in cdc2 phosphorylation (Tyr15) at 24 hours; this is consistent with a G2-M block according to the findings of Dan and Yamori. (2000). Initiation of a G2-M block is mediated initially by increased phosphorylation of cdc2, due to the inactivation of cdc25 phosphatase; the phosphorylated protein then diminishes at 24 hours as regulation of the check point is maintained by down regulation of cyclin B1. This does not allow for the formation of the cyclinB1-cdc2 complex and therefore cannot progress into mitosis. The results presented here are consistent with cell cycle arrest at G1/S and G2/M although it is surprising that there is no p53 effect. Further experiments are required to verify the cell cycle effects and also to investigate the mechanism of cell cycle arrest.

Due to time restraints, it was impossible to perform cell cycle studies in A549 cells using chlorpyrifos at earlier time points of 4 hours and repeating the study using chlorpyrifos oxon.

## 4.4 Discussion

### 4.4.1 Chlorpyrifos

Chlorpyrifos caused DNA damage at 0.01 and 0.1µM after one hour in TK6 cells, however this increase in DNA damage returned to normal background levels after 24 hours. This may suggest that at lower doses cells were able to repair the DNA damage induced by chlorpyrifos. It is also possible that after 24 hours damaged cells had expired by completed apoptosis (or another cell death mechanism) and were no longer available for detection by the comet assay. At higher concentrations of chlorpyrifos (1, 10 and 100µM) the damage increased after 24 hours. After exposure to chlorpyrifos there was no significant p53 response after 4 and 24 hours, despite DNA damage occurring after 1 hour. It is possible

that the p53 response was transient and at earlier time points of ten minutes or 1 hour is where it might be detected. A similar effect is observed when using sarin where p53 protein levels were increased at 1 hour but returned to basal levels at 4 hours (Chapter 5), unfortunately the sarin studies were the final studies performed and there was insufficient time to allow for repeats of the chlorpyrifos experiments at earlier time points. A very early transient p53 response would be consistent with the early PARP-1 cleavage as there is no p53 response observed at 4 hours. It is also possible that the observed DNA damage is an artefact of cytotoxicity due to apoptosis and subsequent DNA cleavage, the observation of cleaved PARP-1 fragment at 4 hours supports this theory. This hypothesis is corroborated by the findings of Wellman et al. (2003) that suggest that chlorpyrifos and its oxon are not able to directly bind to DNA below 1mM. However, chlorpyrifos was able to cause DNA damage at concentrations that had little or no cytotoxicity.

Cleavage of PARP-1 was used as a marker of apoptosis and was seen after exposure to 100µM at 4 hours. However, there was no evidence of PARP-1 cleavage after 24 hours. After the early induction of apoptosis, it may be that there is further protein degradation within apoptotic bodies, resulting in loss of cleaved PARP-1. An alternative to this is that the cells have switched from apoptotic cell death at 4 hours to necrotic cell death at 24 hours. Further experiments would be required to determine the mechanism of cell death, such as staining with Annexin v and ethidium homodimer which can separate cells undergoing apoptosis and necrosis. There was a decrease in Rb phosphorylation and a decrease in cdc-2 phosphorylation at 24 hours with chlorpyrifos. It is possible that earlier effects had been missed by 24 hours and at earlier time points should be included to get a complete profile of the changes that occur in a slowing of the cell cycle. At a concentration of 100µM the phosphorothioate caused an 85% loss of cell viability after 24 hours. It is not clear how chlorpyrifos causes cell death, Crumpton et al. (2000) have suggested that chlorpyrifos can generate ROS; this would damage nucleic acids and proteins in the cell causing cytotoxicity through a culmination of different mechanisms. In addition Bagchi et al. (1995) have used lipid peroxidation and the formation of single strand breaks in DNA as evidence that chlorpyrifos is able to generate ROS. ROS are often mediators of apoptosis which is consistent with results presented here.

### 4.4.2. Chlorpyrifos oxon

Chlorpyrifos oxon caused an increase in DNA damage after 1 hour and this increased in all cases (except 1µM where it remained the same) at 24 hours. The damage seen with chlorpyrifos oxon (100µM) is extremely high and this corresponded with an 85% loss in cell viability. After 24 hours there is an increase in PARP-1 cleavage which is indicative of apoptosis. The 85% loss of cell viability and the cleavage of PARP-1 may indicate that the increase in DNA damage observed at 24 hours is due to apoptosis and the subsequent DNA degradation during this cellular process. Chlorpyrifos oxon showed no increase in p53 levels at 4 hours despite high levels of DNA damage being detected at 1 hour, but a small increase in p53 was seen after chlorpyrifos oxon at 24 hours. However if the level of damage is compared to dichlorvos, it was far greater with 100µM chlorpyrifos oxon than 100µM dichlorvos at both 1 and 24 hours. Dichlorvos caused an increase of p53 at 2 and 4 hours associated with less DNA damage and cytotoxicity than chlorpyrifos oxon. It is likely that the high levels of DNA damage after 100µM chlorpyrifos oxon are a consequence of cytotoxicity and DNA degradation. However, there is also evidence that DNA damage is increased at chlorpyrifos oxon concentrations causing little or no cytotoxicity. Whilst there is no evidence for an increase in p53 protein levels at 4 hours (after 10 and 100µM), this may be due to the p53 response being rapid and transient (as seen for sarin in chapter 5).

### 4.4.3. Comparison of chlorpyrifos and its metabolite chlorpyrifos oxon

Chlorpyrifos was able to cause the cleavage of PARP-1 much earlier than chlorpyrifos oxon, but chlorpyrifos oxon was able to cause greater DNA damage than chlorpyrifos. There is confliction in the literature whether chlorpyrifos or chlorpyrifos oxon is the most effective at producing reactive oxygen species. Crumpton et al. (2000) suggest that when PC12 cells were exposed to chlorpyrifos *in vitro* there was greater production of ROS than its oxon. However, Giordano et al. (2007) when using granule neurons from mice with and without glutathione deficiency suggest that the oxon produced more ROS at a faster rate than the parent compound. However, in both studies ROS was measured over ten minutes and not at 1 hour. Giordano et al. (2007) have reported similar levels of cell death with both chlorpyrifos and chlorpyrifos oxon after 24 hours exposure at 100µM. A possible reason for both of these observations may be due to availability of compounds. If chlorpyrifos and

chlorpyrifos oxon is causing a toxic affect due to reactive oxygen species, then the compound with greater availability will produce more ROS. Chlorpyrifos oxon will bind rapidly to esterases in TK6 cells; chlorpyrifos will not bind and remain in the cell causing more damage. Alternatively chlorpyrifos is more stable than chlorpyrifos oxon and this may degrade to 3,5,6-trichloro-2-pyridinol (TCP), in the in vitro environment (Brzak et al., 1998; Meikle et al., 1983). Either of the previous scenarios would allow for chlorpyrifos showing earlier signs of apoptosis at 4 hours. The lower damage seen with chlorpyrifos compared to the oxon maybe a misnomer as chlorpyrifos treated cells are too extensively damaged and are no longer measured in the comet assay and are lost during the lysis period of the comet assay. The oxon however is not as available, and exerts a toxic effect by producing reactive oxygen species via the same mechanism, but at a slower rate. The oxon therefore demonstrates a slower mechanism of cell death, which allows for extensive damage to be registered by the comet assay at 24 hours with the oxon but not with chlorpyrifos, as these cells were too damaged to be measured by the comet assay.

### 4.5 Chapter summary

Chlorpyrifos induced DNA damage in TK6 cells, but not to the same extent as chlorpyrifos oxon. DNA damage occurred in parallel with a decrease in cell viability. Western blot analysis did not show a p53 response to the DNA damage with chlorpyrifos, a small p53 effect at 24 hours was seen with chlorpyrifos oxon, but p53 may have been induced earlier, as for sarin (see chapter 5). This may suggest that the damage seen in the comet assay with chlorpyrifos and its oxon is due to cytotoxic potential at higher doses; however, at lower doses chlorpyrifos was able to cause DNA damage without loss of cell viability. It is possible that the DNA damage seen after treatment with chlorpyrifos and chlorpyrifos oxon is due to both direct DNA damage and other effects, as the cells undergo apoptosis or necrosis and subsequent DNA degradation.

# *Chapter 5*

# *The genotoxic potential of sarin*

## 5.0 Sarin results

The cytotoxic and genotoxic potential of sarin (GB) was investigated by using TK6 lymphoblastoid cells, as a model for systemic exposure. Cytotoxicity was measured using the MTT assay and DNA damage measured using the alkali comet assay.

### 5.1 Cytotoxicity

DNA damage activates DNA damage signalling pathways that may ultimately lead to cell death, if the damage encountered is too great or cannot be repaired. Therefore, sarin was tested for cytotoxicity in culture using the MTT assay after 1 hour and 24 hours exposure (Figures 5.1 and 5.2). A one way ANOVA test was performed on the cytotoxicity data, the treated samples were compared with the untreated sample and the statistical relevance is shown in Table 5.1 and Table 5.2

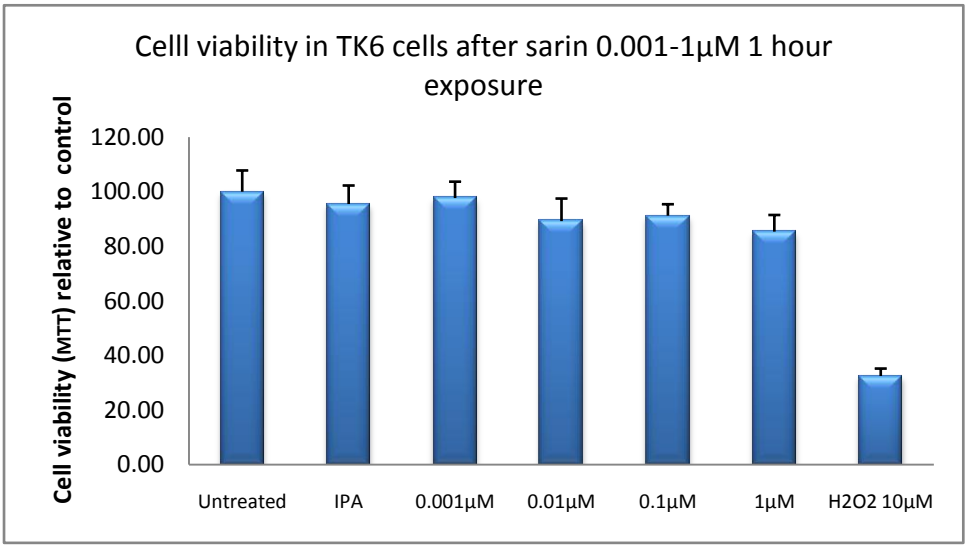


**Figure 5.1 Cytotoxicity of sarin in TK6 cells.** Cells were exposed to the indicated doses of sarin or $H_2O_2$ for 1 hour and cell viability was measured using an MTT assay. Results were expressed as mean % viability relative to untreated control (untreated cells designated 100% viability) ± standard deviation.

| | UNTREATED | IPA | 0.001µM | 0.01µM | 0.1µM | 1µM | $H_2O_2$ 10µM |
|---|---|---|---|---|---|---|---|
| **Cell viability relative to control (%)** | 100.00 | 98.54 | 97.67 | 89.22 | 91.21 | 85.38 | 32.49*** |

**Table5.1. Cytotoxicity in TK6 cells after treatment with sarin (0.001, 0.01, 0.1 and 1µM) for 1 hour**. Cytotoxicity was measured as a percentage of control (P value * <0.05 **P value <0.01 ***P value <0.001 one way ANOVA)

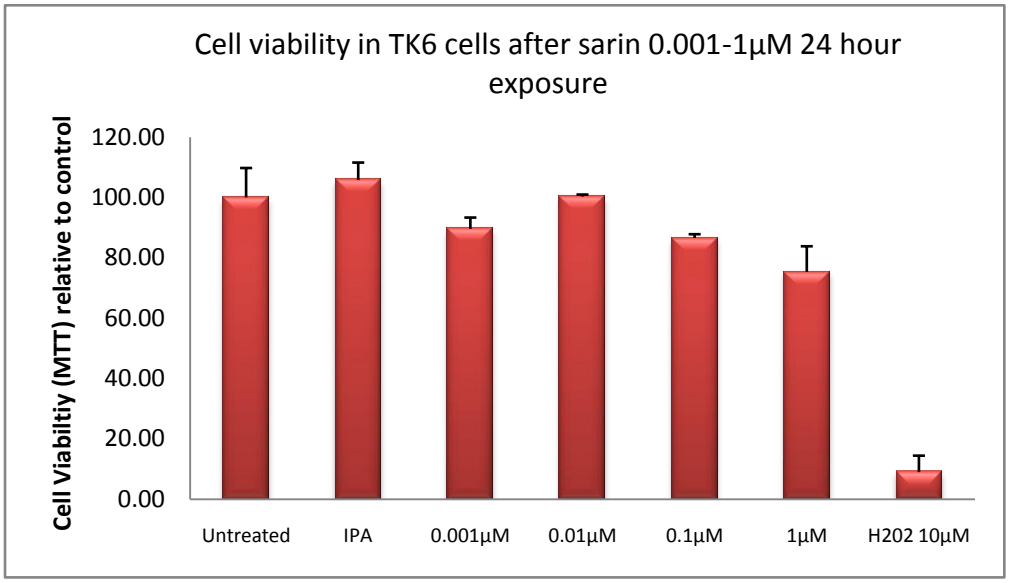


**Figure 5.2 Cytotoxicity of sarin in TK6 cells.** Cells were exposed to the indicated doses of sarin or $H_2O_2$ for 24 hours and cell viability was measured using an MTT assay. Results were expressed as mean % viability relative to untreated control (untreated cells designated 100% viability) ± standard deviation.

| | UNTREATED | IPA | 0.001µM | 0.01µM | 0.1µM | 1µM | $H_2O_2$ 10µM |
|---|---|---|---|---|---|---|---|
| **Cell viability relative to control (%)** | 100.00 | 105.75 | 89.54 | 100.29 | 86.58 | 75.33*** | 8.97*** |

**Table 5.2 Cytotoxicity in TK6 cells after treatment with sarin (0.001, 0.01, 0.1 and 1µM) for 24 hours**. Cytotoxicity was measured as a percentage of control (P value * <0.05 **P value <0.01 ***P value <0.001 one way ANOVA)

Sarin was shown to be cytotoxic to TK6 cells at low µM concentrations. At 1µM, sarin caused a 15% loss in cell viability after 1 hour and this increased to a 20% loss in cell viability after 24 hours. Hydrogen peroxide was used as a positive control and caused a 70% loss in cell viability after an hour and nearly 100% loss of cell viability after 24 hours.

## 5.2 DNA damage

### 5.2.1 Comet assay

TK6 cells were exposed to a range of Sarin concentrations over 24 hours. An increase in dose caused an increase in OTM at both 1 and 24 hours, though the increase was small (Figures 5.3 and 5.4). A Kruskal-Wallis test was performed on the comet assay data, the treated samples were compared with the untreated sample using Dunn's post hoc test and the statistical relevance is shown in Table 3.1 and Table 3.2

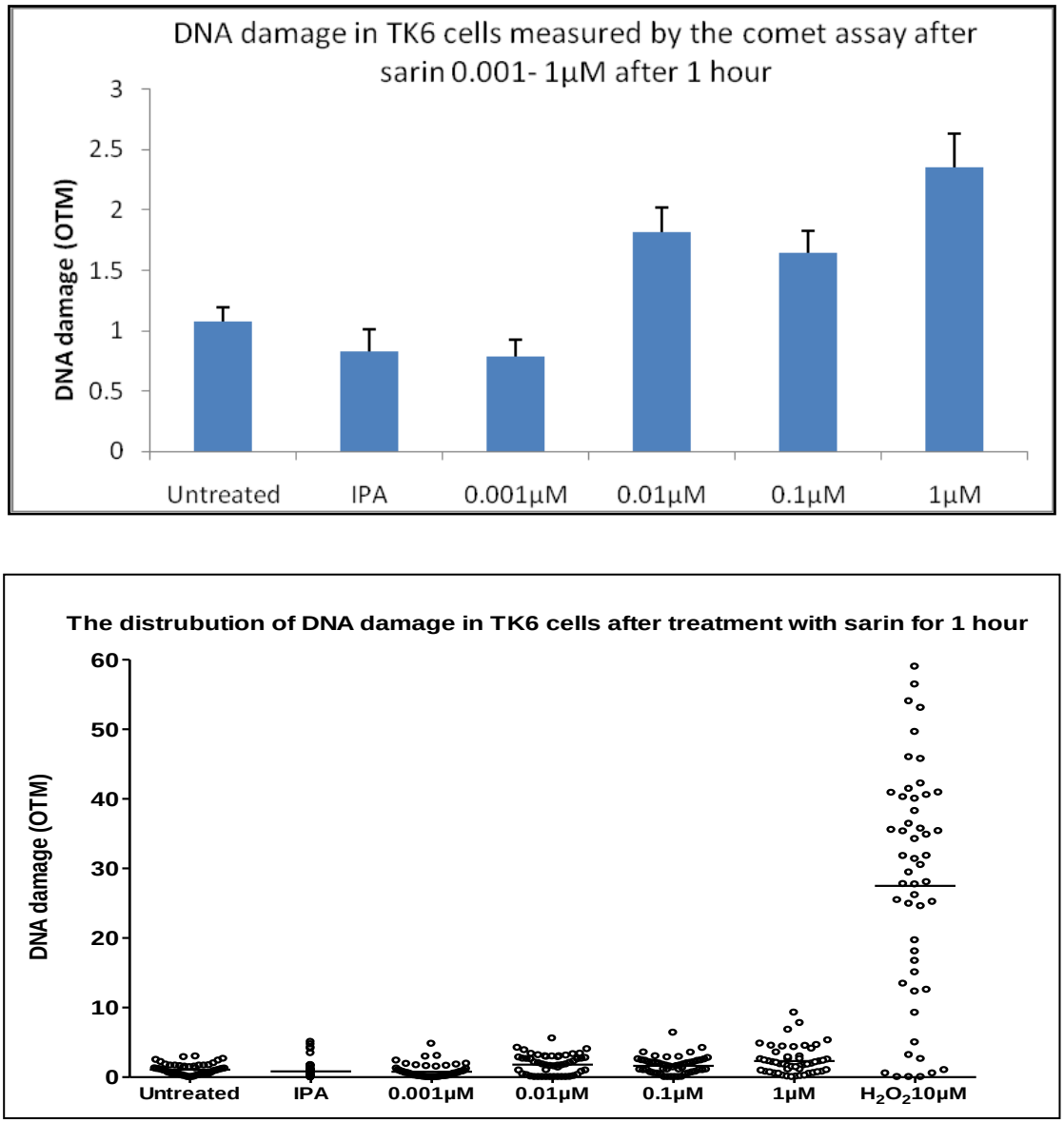


**Figure 5.3. DNA damage in TK6 cells after sarin.** TK6 cells were exposed to the indicated doses of sarin or hydrogen peroxide for 1 hour prior to measurement of DNA damage using the alkaline comet assay The upper graph shows the mean olive tail moment of 50 cells ± S.E. Hydrogen peroxide 10µM (value 28.0 OTM) has been excluded from the upper graph. The lower graph shows the distribution of damage between the 50 cells scored.

| | UNTREATED | IPA | 0.001µM | 0.01µM | 0.1µM | 1µM | $H_2O_2$ 10µM |
|---|---|---|---|---|---|---|---|
| **DNA damage (OTM)** | 1.08 | 0.83 | 0.79 | 1.82 | 1.65 | 2.35 | 28.02*** |

**Table 5.3. DNA damage in TK6 cells after sarin (0.001, 0.01, 0.1 and 1µM) for 1 hour**. DNA damage was measured as OTM (P value * <0.05 **P value <0.01 ***P value <0.001 Kruskal-Wallis)

There was an increase in OTM after treatment with 0.01, 0.1 and 1µM sarin after 1 hour, though the increase was relatively small. The maximum damage was observed after 1µM

sarin with an average OTM of 2.35 compared to the untreated sample of 1.08. There was a decrease in DNA damage with the IPA treated and 0.001µM sarin. When considering the distribution of DNA damage in the 50 cells scored, around 20% of cells have a DNA damage of >5 OTM. This is quite a high proportion of cells displaying high damage after only one hour exposure.

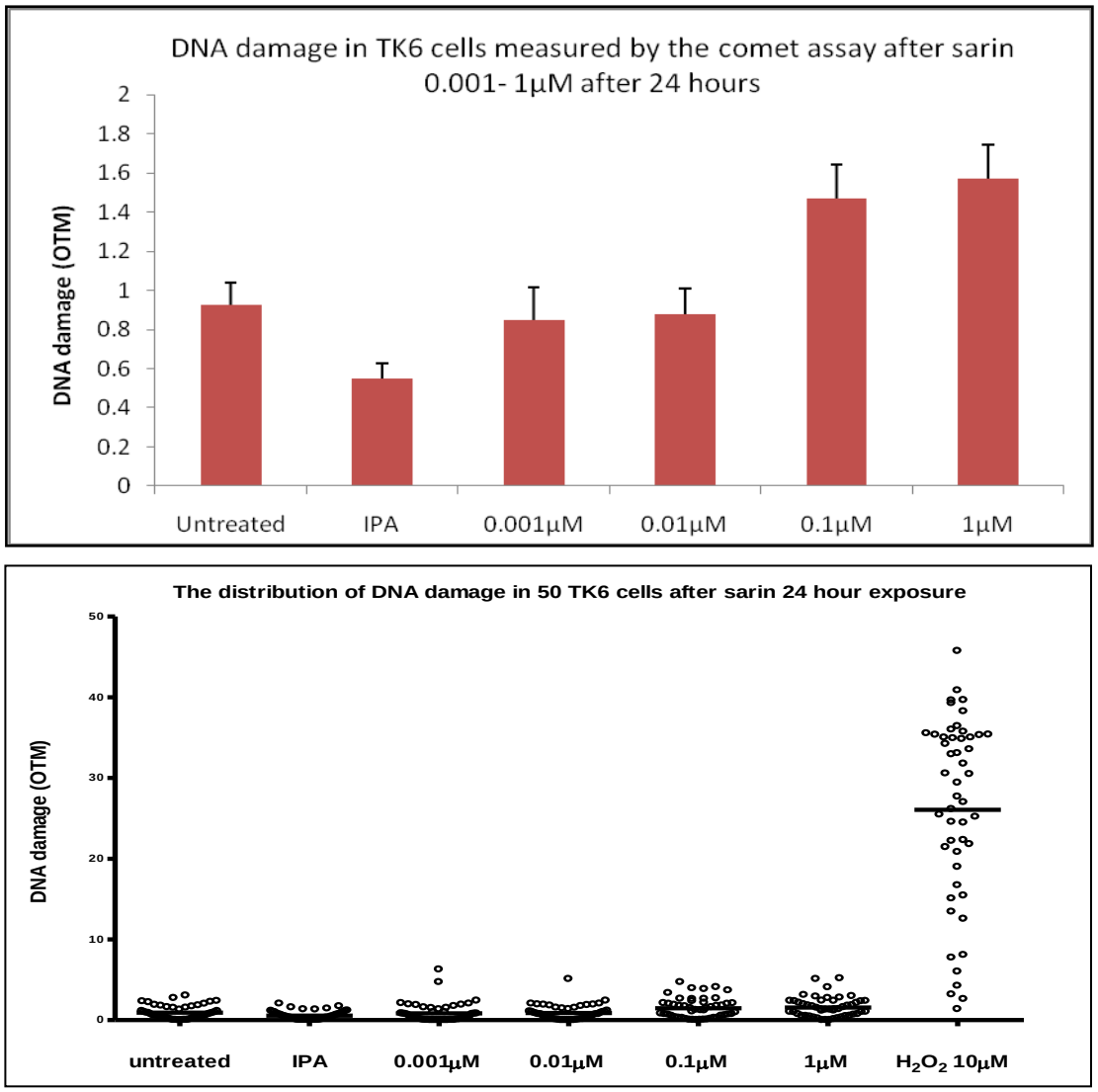


**Figure 5.4 DNA damage in TK6 cells after sarin.** TK6 cells were exposed to the indicated doses of sarin or hydrogen peroxide for 24 hours prior to measurement of DNA damage using the alkaline comet assay. The upper graph shows the mean olive tail moment of 50 cells ± S.E. Hydrogen peroxide 10µM (value 26.06 OTM) has been excluded from the upper graph. The lower graph shows the distribution of damage between the 50 cells scored.

| | UNTREATED | IPA | 0.001µM | 0.01µM | 0.1µM | 1µM | $H_2O_2$ 10µM |
|---|---|---|---|---|---|---|---|
| **DNA damage (OTM)** | 0.93 | 0.55 | 0.85 | 0.88 | 1.47 | 1.57 | 26.06*** |

**Table 5.4 DNA damage in TK6 cells after sarin (0.001, 0.01, 0.1 and 1µM) for 24 hours**. DNA damage was measured as OTM (P value * <0.05 **P value <0.01 ***P value <0.001 Kruskal-Wallis)

There was an increase in OTM after treatment with 0.1 and 1µM sarin after 24 hours, though the increase was relatively small, with untreated cells having a value of 0.93 and 1µM a value of 1.57. There is a high level of DNA damage with hydrogen peroxide after 1 hour and 24 hours, there was a decrease in OTM with the IPA treated, 0.001µM and 0.01µM sarin compared to untreated cells. However due to the level of damage being relatively low it is not possible to conclude whether this is due to repair or whether the decrease is due to the variability in the comet assay.

The observed DNA damage after sarin was higher after 1 hour compared to 24 hours. This could be due to the DNA damage being repaired after the initial exposure to sarin. It is possible that sarin acts very rapidly when coming into contact with the cell and causes DNA damage. The alkali comet assay cannot assess the means by which this damage is caused or the type of lesion that occurs. Sarin is known to be very unstable in aqueous solution and therefore could rapidly degrade in the in vitro system. It is possible then that as the sarin level depletes so too does its ability to cause DNA damage, allowing the cell to repair the small levels of DNA damage induced. Hydrogen peroxide has previously been established as a positive control and gave a very high OTM value, consistent with previous findings.

### 5.3 Response to DNA damage

In order to establish whether sarin caused the initiation of DNA signalling cascades or apoptosis, duplicate samples of cells were treated with the two highest concentrations of sarin used in the MTT and comet assay studies. Samples were analysed for the expression of p53, cleavage of PARP-1 and for cleavage of pro-caspase 9 (both markers of apoptosis) using western blotting. Etoposide is a chemotherapy agent whose specific action is based on the induction of DNA damage and apoptosis, mediated by the inhibition of topoisomerase II and the generation of DNA strand breaks. Etoposide was therefore used as a positive control for the analysis of DNA damage signalling events and apoptosis.

### 5.3.1 p53 response

A background level of p53 can be seen in the IPA treated cells with an increase in p53 protein levels at 1 hour with 0.1 and 1µM sarin (GB) but returning to similar levels to the IPA treated cells at 4 and 24 hours. Elevated levels of protein occurred with 50µM etoposide at 1, 4 and 24 hours. GAPDH was used as a loading control (figure 5.5).

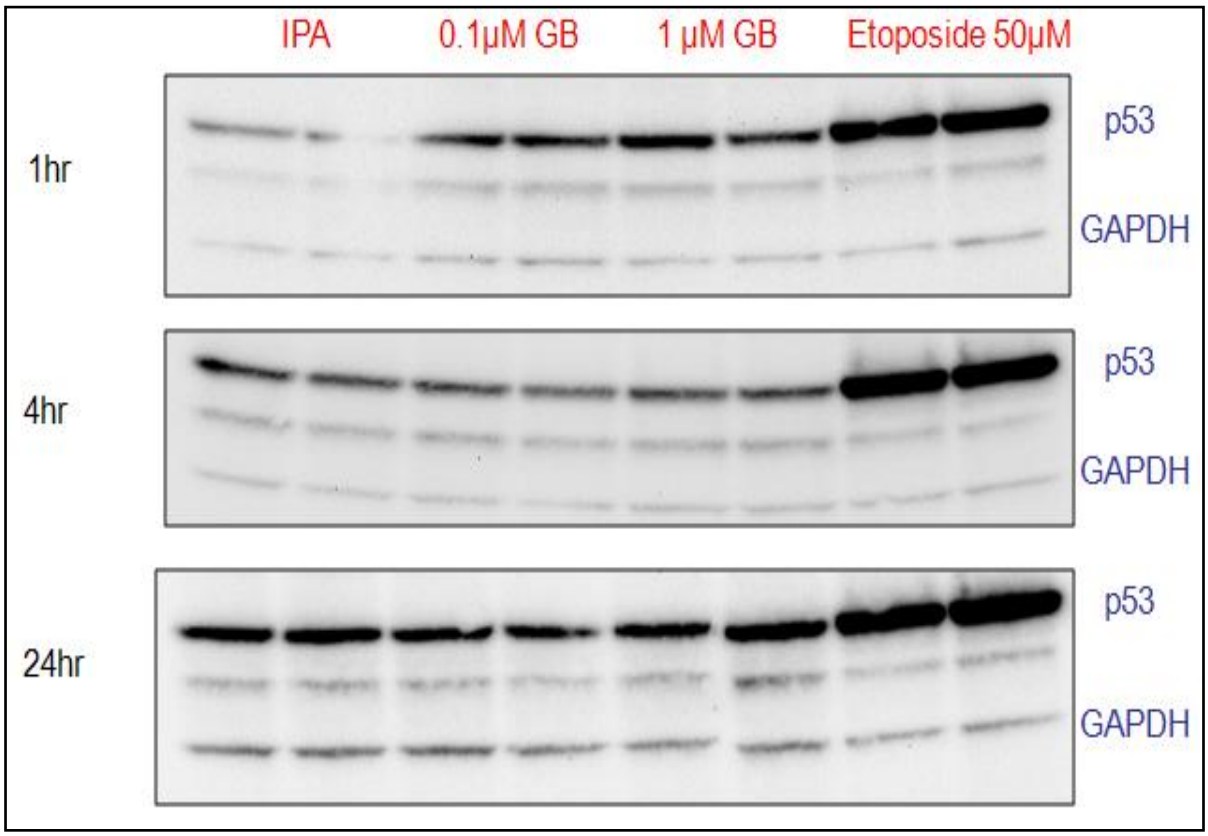


**Figure 5.5. Western blot of the expression of p53 in TK6 cells after sarin (GB).** Cells were exposed to the indicated concentrations of Sarin for 1, 4 and 24 hours prior to western blot analysis. Etoposide was used as a positive control for the activation of DNA damage signalling.

The western blot in figure 5.5 was quantified using Syngene GeneTools software. The values obtained for increases in p53 were then normalised against GAPDH. Each sample was completed in duplicate and the results are displayed as a mean with +/- standard error.

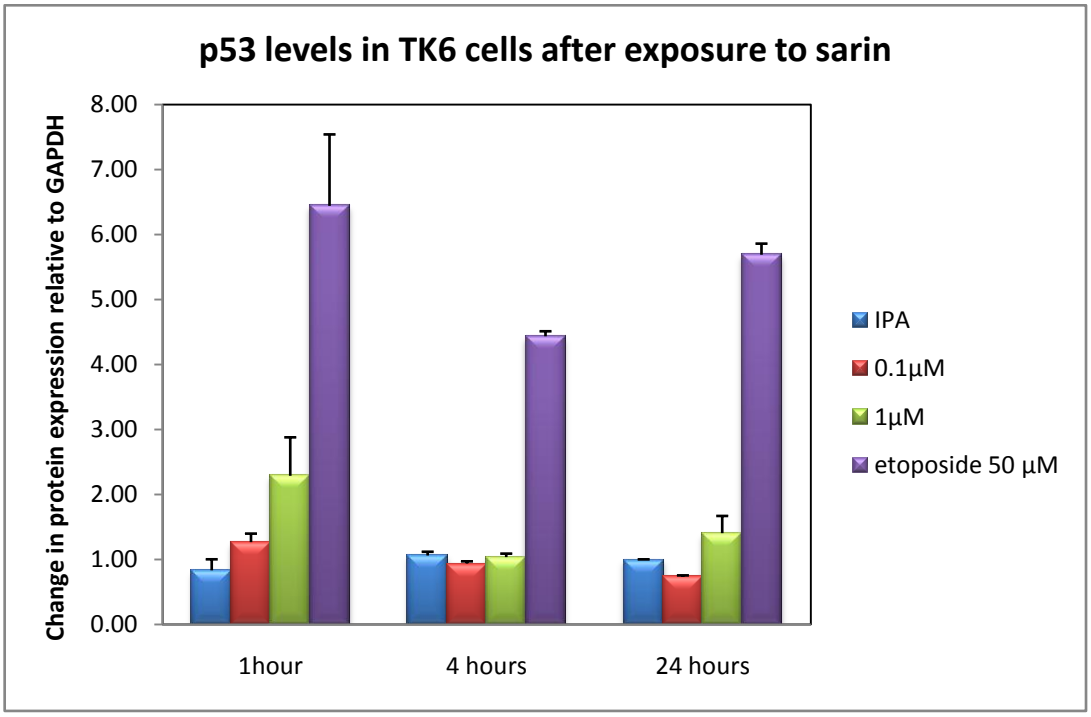


**Figure 5.6. A graph of the change in expression of p53 in TK6 cells after Sarin.** Cells were exposed to the indicated concentrations of Sarin for 1, 4 and 24 hours prior to western blot analysis. Etoposide was used as a positive control for the activation of DNA damage signalling. Values have been calculated using Syngene software and normalised against GAPDH levels. Error bars are ± STD error

An increase in p53 was seen after sarin at 1 hour, returning to background levels at 4 and 24 hours. In figure 5.6 it is clear that the kinetics of p53 levels after exposure to sarin compared to etoposide is very different. Sarin causes an increase of p53 protein levels very rapidly at 1 hour with a doubling of p53 when compared to untreated sample. At 4 and 24 hours, p53 levels then return to background levels. Etoposide however causes an increase of p53 protein levels over the entire 24 hours. The rapid but transient increase in p53 after sarin is consistent with the comet assay data and would further support the conclusion that low levels of DNA damage are rapidly induced but then repaired over the course of 24 hours.

### 5.3.2 PARP-1

PARP-1 is cleaved from its full length form at 116kDa to a 89kdA fragment during apoptosis, figure 5.7 shows full length PARP-1 at 1, 4 and 24 hours after treatment with sarin and

etoposide. The IPA treated cells show that PARP-1 does not become cleaved at 1, 4 or 24 hours with a clear band shown at 116kDa. The sarin treated cells (both 0.1 and 1 μM) show a clear increase in the full length PARP-1 fragment and a small increase in the cleaved PARP-1 fragment. The increase in the cleaved PARP fragment at 1 hour is most likely due to the increase in the full length fragment and occurs due to a higher turnover of the enzyme rather than an early induction of apoptosis. Etoposide shows no PARP-1 cleavage at 4 or 24 hours but very clear PARP-1 cleavage at 24 hours. GAPDH was used as a loading control.

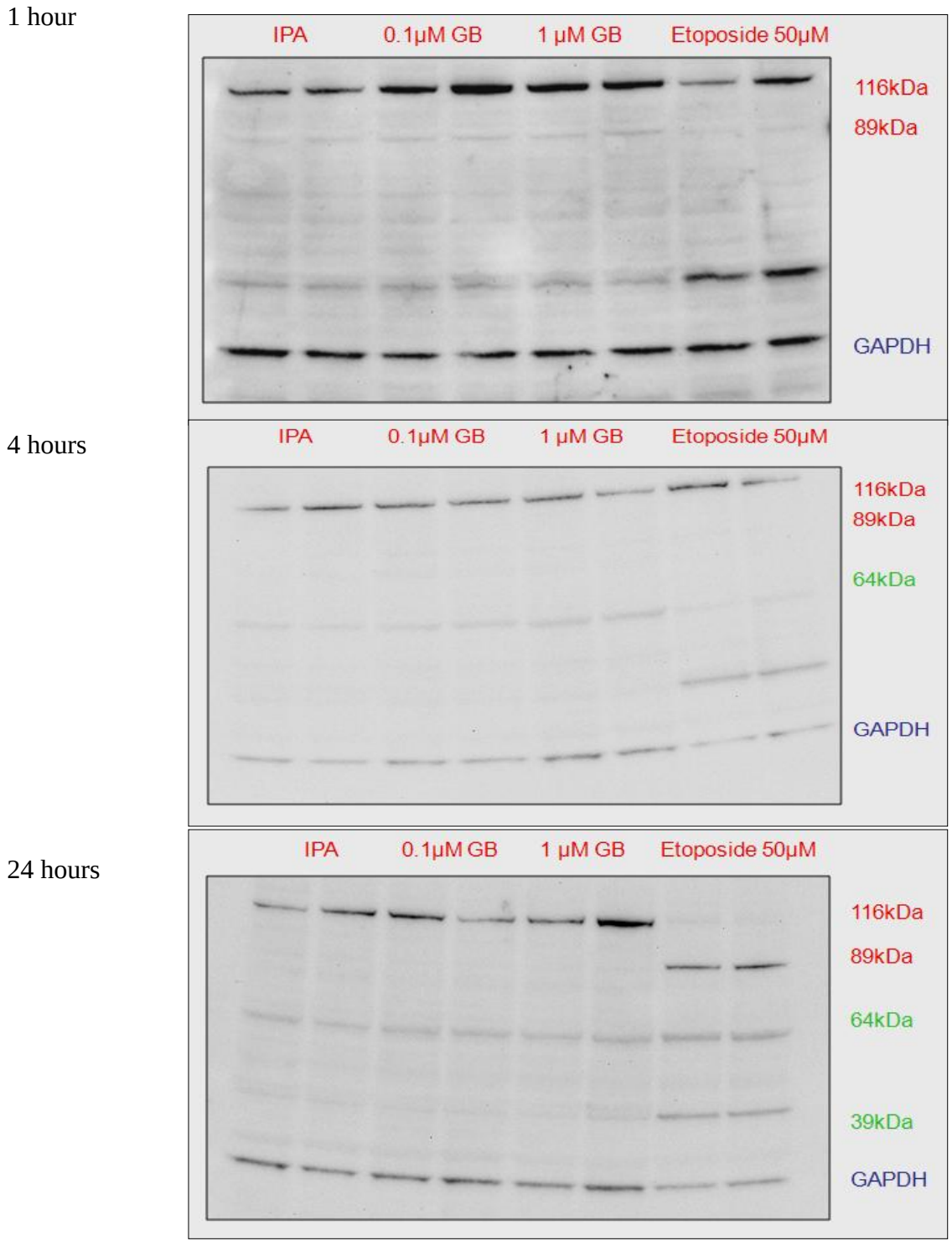


**Figure 5.7. Western blot of the expression of full length PARP in TK6 cells after Sarin (GB).** Cells were exposed to the indicated concentrations of Sarin for 1, 4 and 24 hours prior to western blot analysis. Etoposide was used as a positive control for the Cleavage of PARP1.

The western blots in figure 5.7 have been quantified using Syngene Genetools software as previously described. Sarin caused an induction of full length PARP-1 and PARP-1 cleavage fragment at 1 hour causing a 3 fold induction of both proteins compared to the untreated sample and then returned to background levels at 4 and 24 hours. Etoposide however displays a classic profile of PARP-1 cleavage showing no cleavage at 1 and 4 hours, with strong bands of the 89kDa fragment at 24 hours. As described earlier, it is likely that the increase in cleaved PARP-1 is an artefact, caused by increased levels of full length PARP-1. To clarify, cleaved PARP-1 is present in untreated cells due to a background level of PARP-1 cleavage. If the full length protein increases then the levels of cleaved PARP-1 will increase accordingly. This is exactly the pattern observed in figure 5.8 with sarin. The increase in full length PARP-1 is an interesting observation that will be discussed further at the end of the chapter. Etoposide shows no PARP-1 cleavage at 1 and 4 hours, with strong bands of the 89kDa fragment at 24 hours, consistent with the induction of apoptosis.

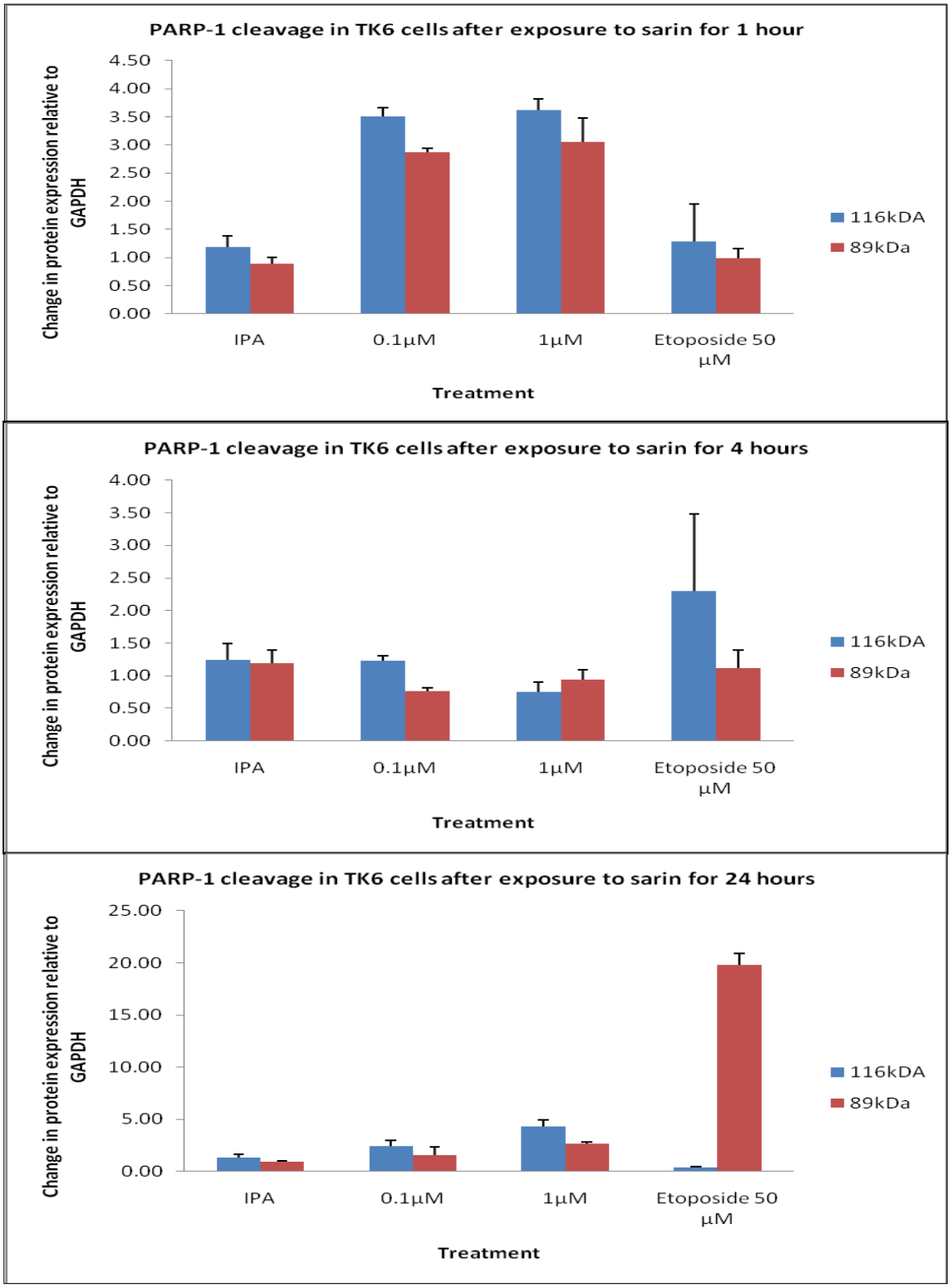


**Figure 5.8. The expression of PARP1 in TK6 cells after sarin.** Cells were exposed to the indicated concentrations of Sarin for 1, 4 and 24 hours prior to western blot analysis. Etoposide was used as a positive control for the activation of DNA damage signalling. Values have been calculated using Syngene software and normalised against GAPDH levels. Error bars are ± STD error.

### 5.3.3. Apoptosis

During apoptosis pro-caspase 9 is cleaved from 45kDa to 35kdA and 10kdA fragments; Figure 5.9 shows the levels of full length pro-caspase 9 and cleaved caspase 9 after treatment with sarin and etoposide at 4 and 24 hours. At 4 hours it is clear that there is no sign of pro-caspase 9 cleavage, whereas at 24 hours there is clear cleavage of pro-caspase 9 with etoposide, but not with sarin.

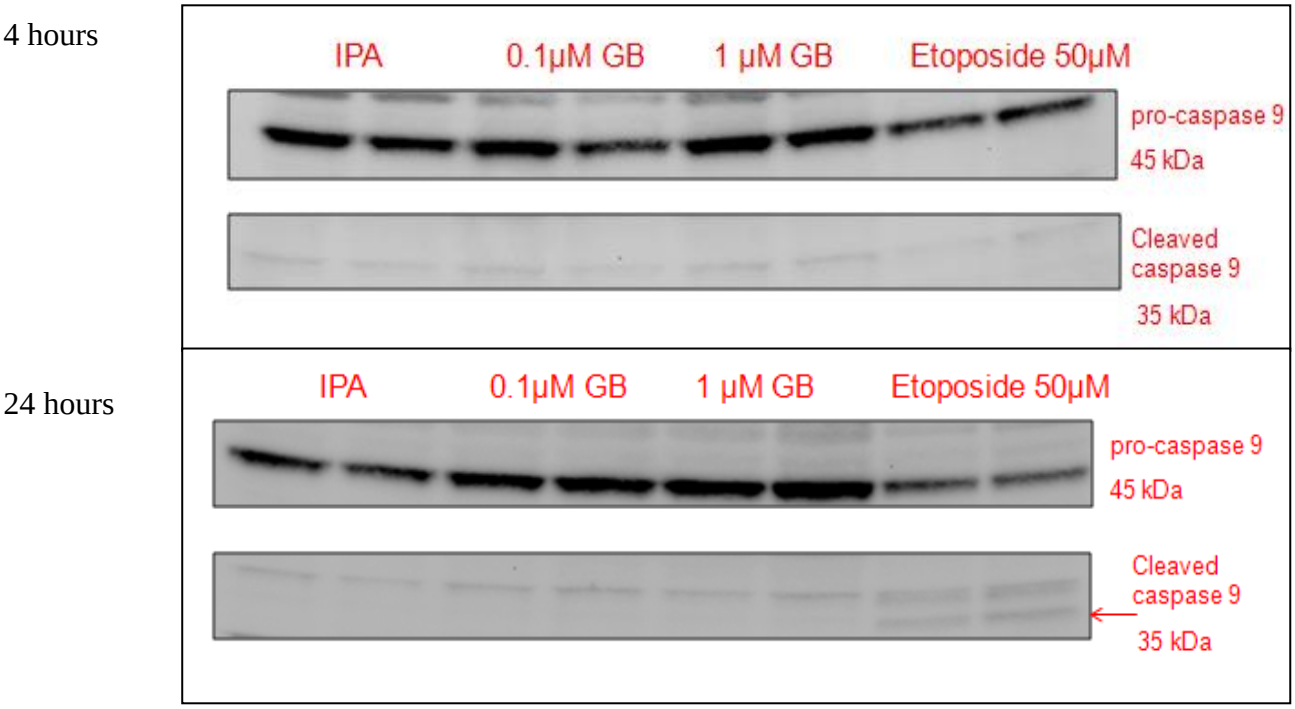


**Figure 5.9 Western blot of the expression of full length caspase 9 in TK6 cells after Sarin.** Cells were exposed to the indicated concentrations of Sarin for 4 and 24 hours prior to western blot analysis. Etoposide was used as a positive control for the Cleavage of caspase 9

The data in figure 5.9 has been quantified as previously explained. It is clear that cleavage of pro-caspase 9 did not occur with sarin as levels of cleaved fragment remain at background levels of 1. Pro-caspase 9 cleavage did occur with etoposide after 24 hours, with a 5-fold increase in comparison with IPA treated cells. Sarin did cause an induction of the full length pro-caspase 9 in comparison with IPA treated cells causing an increase in expression from 1 to 1.5 in the full length fragment after treatment with 0.1µM and an increase from 1 to 2 after 1µM at 24 hours.

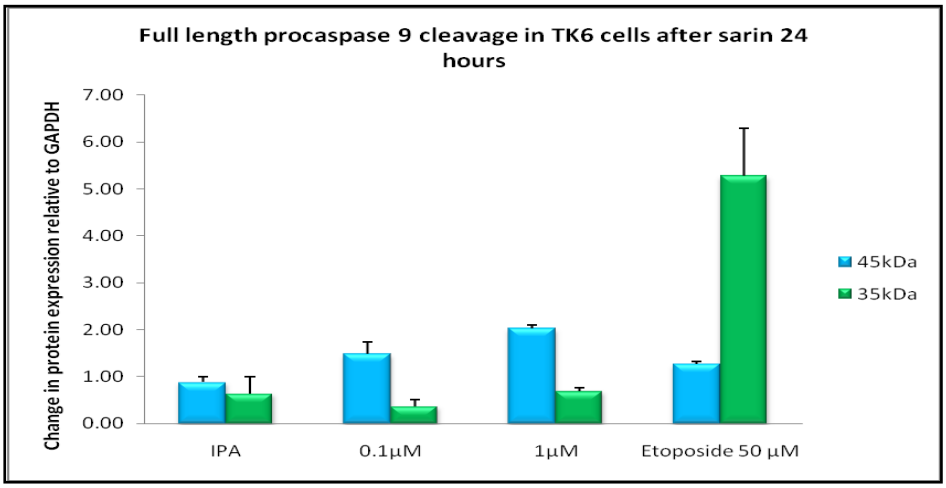


**Figure 5.10. The change in expression of Pro-caspase 9 in TK6 cells after sarin.** Cells were exposed to the indicated concentrations of sarin for 24 hours. Etoposide was used as a positive control for the induction of apoptosis and cleavage of caspase 9. Values were calculated using Syngene software and normalised against GAPDH levels. Error bars are ± STD error.

### 5.3.4 Cell cycle effects

A549 were used to investigate cell cycle effects after 0.1µM and 1µM sarin for 4 and 24 hours. The membranes were probed for cdc2 (Tyr15) and Rb (Ser 795). In addition, the levels of p53 were investigated for two reasons. Firstly, to corroborate our findings in TK6 cells and secondly, p53 induction is required for G1/S phase arrest, via induction of p21 and subsequent inactivation of cdk2.

Sarin does not show a significant increase of p53 after 4 or 24 hours, consistent with the previous studies in TK6 cells. The increase of p53 protein levels is clear after 4 and 24 hours after treatment with etoposide (5 and 50µM). Sarin does not cause a decrease in Rb phosphorylation after 4 or 24 hours, suggesting that a G1/S phase cell cycle arrest is not occurring. However, there was a clear decrease in Rb phosphorylation with etoposide after 24hours at both 5 and 50 µM concentrations (Figure 5.11). The antibody detects two bands in the region of interest, likely corresponding to different phospho-forms of Rb (phosphorylation can affect protein migration during gel electrophoresis).

There is an increase in the phosphorylated cdc2 protein with both 0.1 and 1µM sarin, particularly at 4 hours and, to a lesser extent, at 24 hours. A clear increase can be seen at 4 hours with both concentrations of etoposide (5 and 50µM) in comparison with the untreated sample (Figure 5.11). A decrease in the phosphorylated cdc2 protein at 24 hours was seen with etoposide, consistent with a previous study demonstrating G2/M arrest after Adriamycin (Dan and Yamori., 2000). This data suggests that sarin is able to cause a G2/M block at 4 hours, this block is still present at 24 hours, but to a lesser extent.

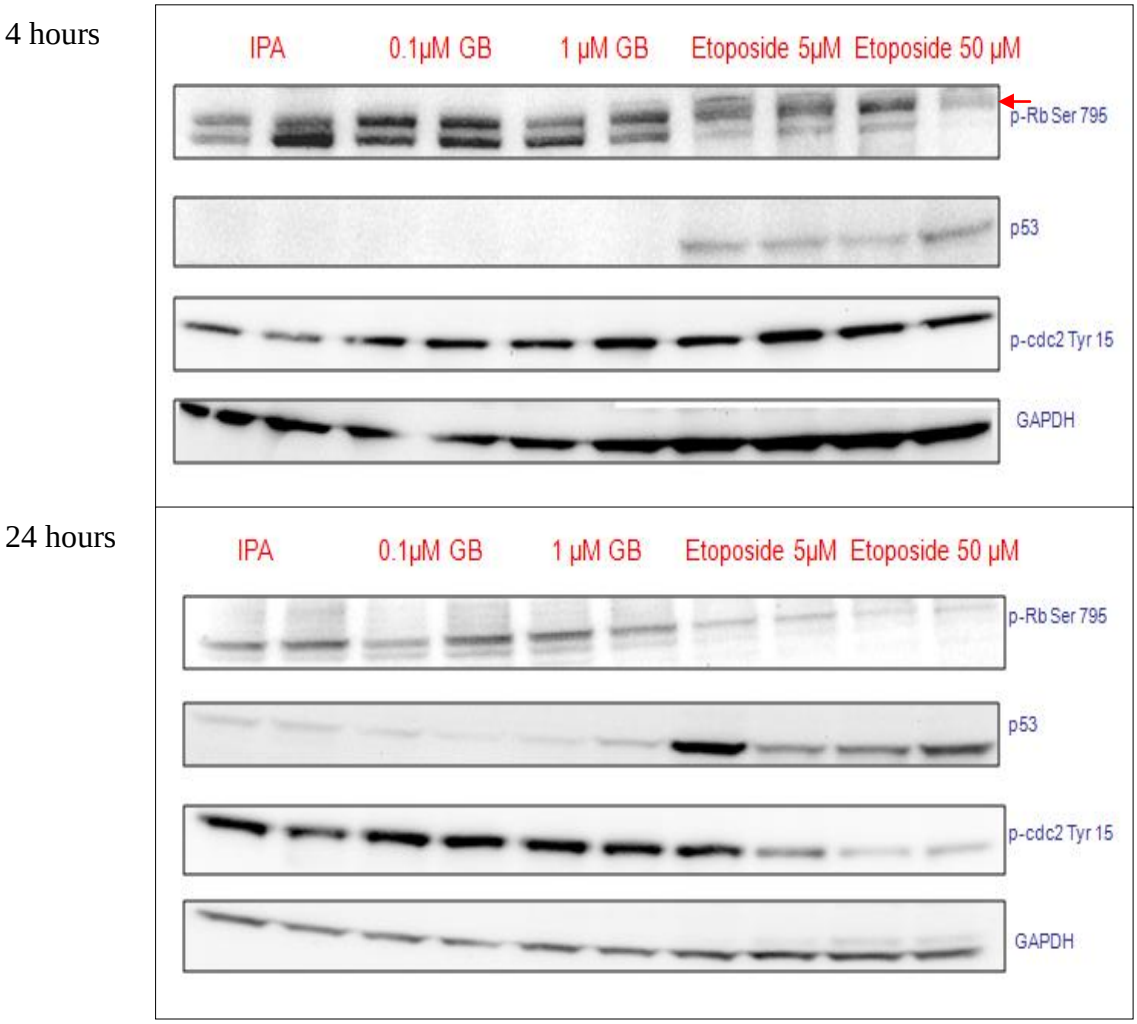


**Figure 5.11. Western blot of the change in expression of p53, p-cdc2 (tyr15), p-Rb (ser795) and GAPDH in A549 cells after sarin.** Cells were exposed to the indicated concentrations of Sarin for 4 and 24 hours prior to western blot analysis. Etoposide was used as a positive control for the cell cycle effects.

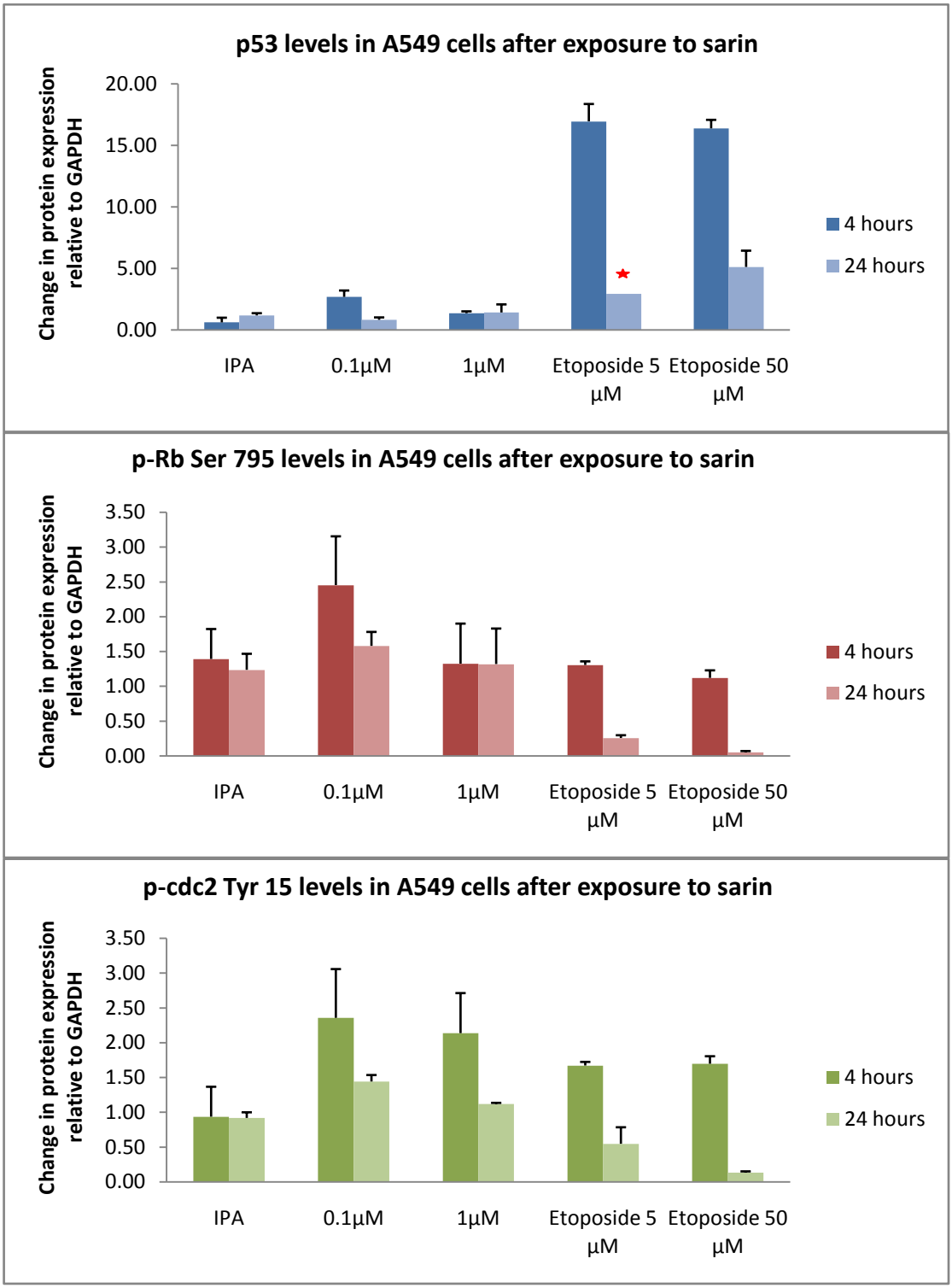


**Figure 5.12. Differing levels expression of p53, p-cdc2 (tyr15), p-Rb (ser795) in A549 cells.** Cells were exposed to the indicated concentrations of Sarin for 4 and 24 hours prior to western blot analysis. Etoposide was used as a positive control for the activation of DNA damage signalling and cell cycle effects. Values were calculated using Syngene software and normalised against GAPDH levels. Error bars are ± STD error. ★ Only one result of the pair used due to erroneous result

The data was quantified in exactly the same manner as with TK6 cells and figure 5.12 shows that sarin and etoposide have different effects upon the cell cycle of A549 cells. Sarin shows a clear increase in phosphorylated cdc2 protein with the amount of phosphorylated protein doubling after 4 hours of treatment with both doses of sarin, this is consistent with a G2/M block of the cell cycle but has no effect on p-Rb795. Etoposide demonstrates a block at G2/M at 4 hours with an in increase in p-cdc2 protein and at 24 hours a block at G1/S with a decrease in the phosphorylated p-Rb795 protein.

## 5.4 Discussion

The comet assay demonstrated that sarin induced DNA damage in TK6 cells in a dose-dependent manner. Although there was an increase in DNA damage in TK6 cells relative to control, the actual extent of DNA damage was still low. In general, OTM values <1 are classed as 'undamaged' and values of 1-2 are classed as low level damage (Collins et al., 1997). In addition, the maximum level of DNA damage was observed after 1 hour suggesting that sarin is able to modify DNA quickly. After 1hour the increase in DNA damage was associated with a 10% loss in cell viability after 0.01 and 0.1µM sarin and a 15% loss after 1µM sarin, therefore it cannot be excluded that the DNA damage occurred due to cell loss, although the mode of cell death is unclear. After 24 hours, the levels of DNA damage had decreased compared to the values at 1 hour. This may be due to the sarin rapidly disappearing from the in vitro system due to its instability in aqueous solution and the cell beginning to repair the DNA damage. Ewing et al. (2001) suggested that at pH 7.0 at ambient temperature the half life of sarin can vary from 10-100 hours; however this time would be expected to increase at 37$^{o}$C. Data obtained with the comet assay showed that exposure to sarin induced DNA damage, though at relatively low levels when considering the mean. However when considering damage on an individual cell basis, approximately 20% of cells treated with 1µM had an OTM value of >5 this is much higher than seen with dichlorvos compared with 2µM at 1 hour. It shows a similar distribution of damage to chlorpyrifos and chlorpyrifos oxon at the same concentration and time. Damage to DNA should result in the activation of DNA damage signalling pathways, mediated by the activity of the ATM/ATR and Chk1/2 protein kinases. Central to this signalling cascade is the tumour suppressor protein p53, which is induced and activated after DNA damage. In TK6 cells, p53

was increased at 0.1 and 1µM sarin after 1 hour. At 4 and 24 hours a similar expression to that of the IPA samples was observed. This would suggest that these concentrations of sarin caused a rapid and transient increase in p53 and would correlate with rapid DNA damage observed with the comet assay.

Cytotoxicity studies showed that sarin has low cytotoxic potential at nM-µM concentrations. The cytotoxicity of sarin, demonstrated in the MTT assay, was investigated further by analysing the cleavage of PARP-1 as an indicator of apoptotic cell death. Sarin (0.1 and 1µM) caused an increase in full length PARP-1 and the cleaved fragment of 89kDa after 1 hour. As described in the results section, the apparent increase in cleaved PARP-1 is likely an artefact, caused by an increase in the levels of full length PARP-1. However the fact that full length PARP-1 is increased is an interesting observation. Previous studies have demonstrated that enzymatic activity of PARP-1 is increased in the presence of DNA damage, with the actual protein levels remaining unchanged (Williams et al., 2008). However, there are no previous studies showing an increase in PARP-1 protein levels. This observation warrants further investigation, initially by identifying whether the increase is due to increased transcription of the PARP-1 gene or due to increased protein stability. The functional significance of this increase should then be investigated. No further PARP-1 cleavage is seen at 4 or 24 hours suggesting that sarin is able to cause its unidentified toxic effect within 1 hour but it is unlikely that it is apoptosis. This hypothesis is corroborated as during apoptosis pro-caspase 9 is cleaved from 45kDa to 35 kdA and 10 kdA fragment. Neither sarin nor etoposide showed the cleaved pro-caspase 9 fragment of 35kDa after 4 hours. The cleaved fragment was clearly seen with etoposide at 24 hours but not with sarin, suggesting that the cell death that occurred at 24 hours after treatment with sarin (according to the MTT assay) was not due to apoptosis. It is also possible that due to the small decrease in cell viability after exposure to sarin, the assay may not be sensitive enough to detect apoptosis in the small number of cells that die. Further investigation is required to identify the mode of cell death. To investigate apoptotic cell death further, other apoptotic markers should be investigated, for example the use of Annexin V assays that detects the expression of phosphatidylserine on the outer leaflet of the plasma membrane, (occurs early in apoptosis) and caspase cleavage. In addition markers of necrosis and other forms of cell death should be investigated due to the lack of evidence of apoptosis. For example

the Annexin V treatment can be coupled with propidium iodide and this will display any cells that have started to become necrotic.

A549 cells were used to study any cell cycle effects seen after exposure to sarin. Sarin was not responsible for a significant increase of p53 levels after 4 or 24 hours and this was the same as seen with TK6 cells. Sarin did not cause a decrease in Rb phosphorylation after 4 or 24 hours, suggesting that sarin does not cause cell cycle arrest at G1/S phase. However, there was an increase in the phosphorylated cdc2 protein with both 0.1 and 1µM sarin at 4 and 24 hours, suggesting cell cycle arrest at the G2/M boundary. The G2/M checkpoint is regulated by a complex of cdc2-cyclinB1; the initiation of cell cycle arrest is mediated by increased phosphorylation of cdc2. Cdc25 phosphatase is inactivated (by phosphorylation) in response to DNA damage which results in the accumulation of p-cdc2-tyr15. Etoposide was shown by Dan and Yamori 2001 to cause an initial increase in cdc-2 phosphorylation at 4 hours but this disappears at 24 hours and suggests that the G2 arrest is due, most likely, to cyclin b1 repression rather than inactivation of cdc2 phosphatase. It is possible that sarin works by a different mechanism and may phosphorylate cdc25 phosphatase which allows for a longer G2/M block. Whilst the measurement of protein biomarkers provides good evidence for cell cycle arrest, these studies should be corroborated using FACS analysis to measure the DNA content of cells thus giving an indication of cell cycle phase.

### 5.5. Chapter summary

Sarin caused low levels of DNA damage after 1 hour, which was partially repaired at 24 hours. This resulted in low level cytotoxicity and a rapid but transient increase in p53 and a G2/M cell cycle arrest. Further studies are required to confirm the mode of cell death after sarin.

# *Chapter 6*

# *General discussion*

# 6.0 Discussion

This study aimed to investigate whether organophosphates were able to damage DNA and the DNA damage responses were also investigated as a further marker of genotoxicity. The evidence presented suggests that dichlorvos and chlorpyrifos, currently used as OP pesticides and the nerve agent sarin tested in an in vitro system were able to cause DNA damage. A summary of the evidence to support this statement is presented for each OP and cell line (Table 6.1).

| Compound | Cell type | Effects |
|---|---|---|
| Dichlorvos | TK6 | • 2-100µM caused an increase in DNA damage at 1 and 24 hours.<br>• 100µM caused an increase in p53 protein levels at 2 and 4 hours, returning to background levels at 24 hours.<br>• At 24 hours 2- 100µM caused an increase in DNA damage and a loss in cell viability (2-100µM) associated with PARP-1 cleavage (100µM), suggesting apoptosis as a mechanism of cell death |
| | A549 | • Increased phosphorylation of histone H2AX, associated with DNA damage.<br>• Decreased Rb phosphorylation after 4 hours and 24 hours, indicating G1 cell cycle arrest (100µM).<br>• Decreased cdc2 phosphorylation at 4 hours, indicating a G2 cell cycle arrest (100 µM). |
| | SHSY5Y | • DNA damage after only ten minutes at nM concentrations. DNA damage at 0.01-100µM after 1 hour. |
| | Lymphocytes | • DNA damage at 0.01-100µM after 1 hour. |
| Chlorpyrifos | TK6 | • 0.01-10µM caused DNA damage after 1 hour, without a significant loss in cell viability. |

| | | |
|---|---|---|
| | | • After 1 hour 100µM caused an increase in DNA damage, associated with a loss in cell viability and PARP-1 cleavage, suggesting apoptosis as a mechanism of cell death<br>• At 24 hours, there was no difference between untreated cells and cells treated with 0.01 and 0.1µM, suggesting repair of the initial damage seen at 1 hour.<br>• 1-100µM caused an increase in DNA damage and decrease in cell viability after 24 hours. This was not associated with PARP-1 cleavage and this may be due to necrosis being the major pathway by which cell death is occurring.<br>• No increase in p53 protein levels at 4 or 24 hours. |
| | A549 | • No cell cycle effects at 24 hours (no change in Rb or cdc2 phosphorylation. |
| Chlorpyrifos oxon | TK6 | • 0.01-10µM caused an increase in DNA damage after 1 hour, without a significant loss in cell viability.<br>• 100µM caused an increase in DNA damage, with a loss in cell viability but no PARP-1 cleavage, suggesting that apoptosis was not the mechanism of cell death.<br>• 0.01-100µM Increase in DNA damage after 24 hour 0.01-100µM, with a significant loss in cell viability.<br>• 100µM caused an increase in DNA damage, with a loss in cell viability as well as PARP-1 cleavage, suggesting that apoptosis was a possible mechanism of cell death.<br>• A small increase in p53 levels was seen after 24 hours |

| | | |
|---|---|---|
| | | (100µM). |
| Sarin | TK6 | • 0.01 -1µM caused an increase in DNA damage after 1 hour (0.01-1µM), with a 10% loss in cell viability. 1µM caused an increase in DNA damage and a loss in cell viability with an apparent increase PARP-1 cleavage.<br>• Increase in p53 levels after 1 hour suggesting a transient p53 effect.<br>• 0.1 and 1µM caused an increase in DNA damage after 24 hours and a 10% loss in cell viability. |
| | A549 | • Decreased cdc2 phosphorylation at 4 and 24 hours, indicating a G2 (100µM).<br>• No effect on the phosphorylation of Rb-Ser795 at 4 and 24 hours. |

Table 6.1. A Summary of all results for the effects of OP in each of the cell lines used.

Dichlorvos caused DNA damage as assessed by the comet assay. Dichlorvos caused damage to DNA at nM concentrations that showed little to no signs of cytotoxicity. The comet assay only measures DNA damage but not the mechanism by which it occurs and damage may result from the direct effect of a chemical or its metabolite on DNA, as the result of oxidative stress or from apoptosis. At higher µM doses DNA damage is accompanied by cytotoxicity and dichlorvos (100µM) caused the cleavage of PARP-1 after 24 hours which is indicative of apoptosis. It is important to measure the effect of dichlorvos on other markers of apoptosis such as cleavage of pro-caspase9 and the expression of pro-apoptotic proteins such as Bax and cytochrome c, to confirm the importance of apoptosis at low and high concentrations. The DNA damage observed at high concentrations may in part be due to a direct mechanism such as methylation of bases, direct adduct formation or oxidative stress but it may also be a consequence of apoptosis and degradation of chromosomal DNA, which is detected by the comet assay. A recent study by Patel et al. (2007) demonstrated that

dichlorvos was cytotoxic and can cause DNA damage in Chinese hamster ovary (CHO) cells at concentrations of 0.01 to 10µM. The corresponding concentrations to those used in these experiments showed similar levels of cytotoxicity and they reported slightly lower levels of DNA damage than presented here. Doherty et al. (1996) have also demonstrated that the incidence of micronuclei increases after exposure to dichlorvos in human lymphoblastoid cells which suggests that dichlorvos is potentially genotoxic. Preliminary studies undertaken in primary lymphocytes showed that dichlorvos caused similar levels of DNA damage measured by the alkaline comet assay. The findings were supported by Atherton et al. (2006) who reported that dichlorvos was able to damage DNA in freshly isolated lymphocytes, at shorter exposure time and lower concentrations than the experiments conducted here. Primary lymphocytes isolated from human blood samples can be used to monitor biomarkers of DNA damage in vivo such as Comet assay and H2AX phosphorylation after exposure to OPs. DNA damage was detected by the Comet assay in blood samples from farm workers occupationally exposed to OPs in Spain corroborating the use of lymphocytes for biomonitoring of DNA damage (Atherton et al. (2009).

Studies in TK6 and A549 cells showed that dichlorvos caused an increase in p53 protein levels and increased H2AX phosphorylation, further suggesting that dichlorvos caused DNA damage and corroborating the comet assay data. It was also demonstrated that dichlorvos caused cell cycle arrest and apoptosis. As cytotoxicity occurred after exposure to dichlorvos in TK6 cells this would suggest that a proportion of cells are too extensively damaged and are being directed towards cell death. Other cells that have been damaged by dichlorvos have initiated cell cycle arrest and repair of the damaged DNA. It is unclear whether the cytotoxicity is a direct response to the DNA damage or whether dichlorvos is reducing cell viability via an alternative mechanism such as ROS production. Yamano et al. (1996) showed that dichlorvos did cause lipid peroxidation and single strand breaks in DNA in isolated rat hepatocytes and suggested that this occurred by two separate mechanisms. Further investigation to assess whether dichlorvos can directly adduct with DNA should be conducted by mass spectrometry to definitively identify what type of damage is occurring after exposure to dichlorvos. In addition 8-oxodeoxyguanosine (8-oxo-dG) is a product of oxidative DNA damage by ROS and serves as an established marker of oxidative stress.

Increased ROS will result in increased levels of 8-oxo-dG which if unrepaired can be genotoxic. Measuring ROS (for example by the fluorescence based nitroblue tetrazolium (NBT) assay) and levels of 8-oxo-dG by liquid chromatography mass spectrometry in vitro after dichlorvos would provide further evidence of the mechanism by which dichlorvos is able to cause DNA damage.

Dichlorvos did cause a decrease in Rb phosphorylation after 4 hours, this returned to background levels at 24 hours, which suggested that dichlorvos, does cause cell cycle arrest at G1/S phase but the block was lifted after 24 hours. There was an increase in the phosphorylated cdc2 protein with dichlorvos at 4 hours. This would suggest a G2/M block in the cell cycle. These effects would allow for cell cycle arrest and allow for repair of the DNA damage. Preliminary studies were conducted in TK6 cells on the role of specific DNA repair pathways after dichlorvos treatment. These studies involved treatment of TK6 cells with specific enzyme inhibitors to inhibit the DNA repair pathways BER and NHEJ, followed by treatment with dichlorvos and measurement of cell viability. Preliminary results suggested that both pathways were involved in the repair of DNA damage caused by dichlorvos, suggesting that dichlorvos was able to cause more than one type of lesion. BER repairs simple adducts and single strand breaks whereas NHEJ repairs double strand breaks. These finding could be explained by an ROS based mechanism as ROS are capable of forming all these types of lesion. These results, along with the comet assay data, indicate that dichlorvos causes damage to DNA which the cell responds to by initiating DNA repair mechanisms. Future work should include studies of other DNA repair pathways, for example, the role of NER can be studied using cells from individuals with Xeroderma Pigmentosum. In addition, cells are available that are deficient in ATM and ATR, from individuals with ataxia telangiectasia and seckel syndrome, respectively. By using these cells, it is possible to further understand DNA damage signalling after exposure to dichlorvos.

Chlorpyrifos and chlorpyrifos oxon both damaged DNA as assessed by the alkaline comet assay but this damage did not result in an increase in p53 following chlorpyrifos treatment

although a small increase followed chlorpyrifos oxon. Cell cycle effects were seen at 24 hours with a reduction in Rb and cdc2 phosphorylation after treatment with chlorpyrifos. It is possible that the p53 induction was rapid and transient as seen with sarin and not detected. There is evidence to suggest that the mode of cell death by chlorpyrifos or its oxon is apoptosis as PARP-1 cleavage was seen, but other cell death mechanisms or even a convergence of several cell death pathways cannot be ruled out without further investigation. The results presented here are in contrast with the findings of the In vitro results by Gollaupdi et al. (1995) who reported that chlorpyrifos did not induce chromosomal aberrations in Chinese hamster cells in vitro or in fresh lymphocytes from a rat pre-dosed with chlorpyrifos. Cui et al. 2006) reviews the potential of chlorpyrifos and cypermethrin to form DNA adducts in mouse hepatocytes was evaluated. It was found that chlorpyrifos was unable to form such adducts. In addition Cui et al. (2011) reported that chlorpyrifos induced no excision-repairable DNA damage (measured by the incorporation of radio labelled DNA) but did cause DNA strand breakage (measured by the comet assay) in ICR mouse hepatocytes. Therefore it is possible that chlorpyrifos as suggested by the above studies did not directly cause DNA damage but only following cytotoxicity unlike dichlorvos. However DNA damage did occur in the present study when there was little or no cytotoxicity. Rahman et al. (2002) concluded that chlorpyrifos was able to cause DNA damage in mice leucocytes in a dose dependant manner; with DNA damage measured using the alkaline comet assay. The study also noted that the DNA was repaired 48 hours after exposure. This provides some support for the results presented here as low nM concentrations of chlorpyrifos caused higher levels of DNA damage at 1 hour than 24 hours, suggesting that DNA repair was occurring. More recent studies by Salazar-Arredono et al. (2008) support that chlorpyrifos and its oxon are damaging to spermatoza.

Sarin was also able to cause DNA damage as assessed by the comet assay. Sarin possibly caused direct DNA damage as there was a rapid and transient p53 response after exposure to sarin at nM concentrations and the damage was repaired over the course of 24 hours. DNA damage did occur in parallel with a loss in cell viability (albeit only 10%), so it cannot be ruled out that some of the increase in DNA damage was due to cell death. There was no sign of apoptosis at low doses as PARP-1 and pro-caspase 9 cleavage was not increased and it is

possible the cell loss was by another mechanism such as necrosis. It is also possible that at higher doses, similar to those studied for dichlorvos and chlorpyrifos, sarin would cause apoptosis. There was evidence of a G2/M cell cycle arrest after sarin treatment, allowing for repair of DNA and providing further evidence that sarin was able to cause damage to DNA. As with dichlorvos, it was not possible to conclude that sarin caused direct DNA damage without evidence of adduct formation and the damage could be due to the production of ROS. Goldman et al. (1987) have reported that sarin is not genotoxic or mutagenic in *in vivo* and *in vitro* assays although in parallel with the results presented here Dave et al. (2007), showed that low level exposure to sarin in guinea pigs caused an initial increase in DNA damage at 1 and 4 days but after 17 days the damage had been repaired.

Dichlorvos was chosen as it is an oxon and in addition it also has small leaving groups like nerve agents. As previously discussed (see section 1.2) ageing of an OP determines how effective it is as an inhibitor of AChE. Dichlorvos was a good surrogate for a nerve agent as it has a similar structure and had been classed as possibly carcinogenic by the WHO and was available to use within the University laboratories. The genotoxic and mutagenic potential of dichlorvos has been the subject of a recent review (Booth et al., 2007). Chlorpyrifos was selected for study as it is available as both a phosphorothioate and the oxon metabolite allowing comparison between the toxicity of the two molecules. Sarin was chosen as the nerve agent for comparison

Initial studies were conducted using SHSY-5Y neuroblastoma cell lines. These were selected as they would be a target cell line after exposure to OP poisoning and were known to have AChE activity. However these cells did not produce spherical “heads” in the comet assay which made DNA damage difficult to quantitate accurately using the image analysis software. The study was then adapted to use TK6 lymphoblastoid cell line. This had many advantages as they were a suspension cell and could be grown in very large numbers relatively quickly. Because they were an immortalised lymphoblastoid they remained

spherical during the processing component of the comet assay and allowed for more accurate analysis. In addition, these cells serve as a model for freshly isolated blood lymphocytes.

OP oxons such as studied here (dichlorvos and sarin) are rapidly hydrolysed following absorption in to systemic circulation by PON1, Carboxylesterases (CaE) and the Mn-dependent esterase (Sogorb et al., 2002). The predominant esterase depends on the molecule and the nature of the bond. Chlorpyrifos oxon formed by oxidative metabolism in the liver is also hydrolysed. This rapidly removes the oxon reducing the direct toxic effect on acetylcholinesterase.

If DNA damage is dependent upon a direct mechanism then rapid hydrolysis in vivo allows for cellular recuperation and repair. If the DNA damage is due to oxidative stress induced by the oxon (via undetermined mechanism) then the damage might be observed after hydrolytic removal of the oxon, therefore OPs via an indirect mechanism are still able to exert a toxic effect even after hydrolysis and removal.

In vitro when the oxon is added to the medium the OP will enter the cell by passive diffusion. There is no evidence that oxons are substrates for active transporters but some evidence that they are for efflux transporters, with chlorpyrifos increasing the expression of MDR-1 (Agarwala et al., 2004*)*. Within the cell the OP could bind to acetylcholinesterase and other sequestering esterases, or become rapidly hydrolysed in aqueous conditions or by PON-1 (if present). In vivo Dichlorvos rapidly hydrolyses to dimethyl phosphate and dichloroacetaldehyde, or to o-demethyldichlrovos and methanol (Gan et al., 2006). Benoit-Marquie et al. (2003) suggest that dichlorvos when applied to an aqueous system will lose approximately 30% of the applied dose after ten minutes. Sarin will hydrolyse in neutral conditions to isopropyl methylphosphonate (degrading to methylphosphonic acid); this is affected by temperature and pH. Ewing et al. (2001) suggested that at pH 7.0 at ambient temperature the half life of sarin can vary from 10-100 hours; however this time would be

expected to decrease at systemic temperature. It is therefore possible that the levels of oxon to which cells are exposed in vitro for a specific dose will be higher than those in vivo, however due to the rapid rate of hydrolysis of these chemicals the concentration available in the in vitro system may still be low. Future work should be based on not only measuring the amount of dichlorvos in the media but in addition measuring the types and amount of adduct within the cell after exposure to OPs using tandem mass spectrometry. There is no published work that has looked at measuring the internal and external levels of OP in an in vitro system.

Phosphorothioates such as chlorpyrifos will not inhibit acetylcholinesterase until converted to chlorpyrifos oxon by cytochrome P450s. These enzymes are most abundant in the liver. The oxon will then be removed by hydrolysis. In vitro studies of the fate of chlorpyrifos indicate that following formation of the oxon, it is rapidly removed by hydrolysis. Chlorpyrifos at pH6.9 at 25$^{o}$C has a half life 35.3 days (Meikle et al., 1978). Chlorpyrifos is therefore more stable than the oxon metabolite (and dichlorvos and sarin) and is therefore able to remain in the in vitro system for longer if oxidative metabolising enzymes are low. Therefore as DNA damage is seen with chlorpyrifos in a lymphoblastoid cell line where there are no active cytochrome P450 enzymes (Shirnamé-Moré et al., 1991) the effect is most likely due to the parent molecule rather than conversion to chlorpyrifos oxon inducing oxidative stress by cytochrome P450 activity. There was greater damage with chlorpyrifos oxon than the parent molecule. On a molar basis at high concentrations both caused extensive cell death and therefore it is hard to interpret the DNA damage data at this concentration. It is likely that the DNA damage and cytotoxicity is due to availability of compound. The parent molecule causes extensive damage faster than the oxon as it is not bound to as many proteins and is free to exert a cytotoxic effect, whilst the unstable oxon binds to proteins within the cell and is not as available. It is likely that the toxic effect seen with these compounds is via the same mechanism and whether it is a phosphorothioate or an oxon either has the same effect or is not important in the mechanism for DNA damage or cytotoxicity.

Systemic µM doses of OP (0.1, 1, 10 and 100µM) would cause complete inhibition of AChE and the death of any organism exposed to that concentration in vivo. Therefore acute AChE inhibition is the primary toxic effect leading to death and the DNA damage seen at these levels would be less important in vivo. However DNA damage is more important at the lower concentrations where recovery from AChE inhibition is possible. Commercial formulations of organophosphates contain active ingredients at high molar concentrations, e.g. dichlorvos is present at 3.4 M in Nuvan 50 EC (Amvac Chemical Company) and chlorpyrifos is present at 594 mM in Dursban 480 EC (Dow Agrosciences), based on information given in manufacturers' safety data sheets (Amvac Chemical Company, 2011; Dow Agrosciences, 2011. Therefore any worker who is using these chemicals and is accidentally exposed to these via a splash to the skin could have a local exposure relevant to the concentrations used in these experiments. A finite dose of dichlorvos in isopropyl myrisate would result in a skin concentration of 450µM in the epidermis assuming that the dichlorvos remains there and does not move further into the dermis (Craig Moore- PhD thesis). The mechanisms observed at high µM concentrations could still be initiated by the cell in response to exposure to lower doses. The mechanisms were not detected at lower doses in these studies, as these concentrations of OP did not cause enough DNA damage to result in cellular changes detectable by western blotting analysis.

Initial experiments showed very low DNA damage in response to nM and low µM doses. The levels of DNA damage were not sufficient to induce any p53 response, as measured by western blotting. The experiments were expanded to include higher concentrations of OP and therefore allow for the mechanisms in response to DNA damage to be observed. At higher concentrations, OPs did cause higher levels of DNA damage. What became clear was that after exposure to dichlorvos and sarin, not all cells were affected to the same extent; some cells showed high levels of damage and others remained at back ground levels. However with chlorpyrifos and chlorpyrifos oxon the levels of DNA damage was more evenly distributed throughout the 50 cells scored. This could mean that sarin and dichlorvos are only able to cause DNA damage at certain points during the cell cycle. In order to establish this, cells can be synchronised in the cell cycle by the removal of FBS, this allows for the

synchronisation of cells in G0 and re-enter G1 upon addition of FBS. Treatment with OP can then occur at certain points in the cell cycle and allow for the comparison of DNA damage.

It is important to determine whether the DNA damage is due to a direct mechanism or as an artefact of cell death. In order to determine if the OPs used in this study were able to have direct effect the DNA would need to be analysed by mass spectrometry, this would establish if any adduct were occurring and the type of adduct formed. The best method for this is a general, non targeted screen for DNA adducts, and would use a mass spectrometry procedure called Data Dependent Constant Neutral Loss. This takes advantage of the mass spectrometry properties of the nucleosides which loose the deoxyribose group, a mass of 116 when damaged. The parent ion is measured by mass spectrometry. As the mass of non adducted nucleosides are known, a higher mass would predict the presence of a DNA adduct. The same procedure can be used for a more targeted approach, if the nature of the adducted compound is known or trying to detect a specific alkylation, where the mass of the parent DNA adduct can be specified.

Further investigation is required to determine which type of cell death is occurring and whether there is a switch between modes of cell death after exposure to OPs. Markers of apoptosis such as caspase 3, 8 and 9 and of other forms of cell death such as markers for necrosis like propidium Iodine should be investigated. Autophagy can be investigated using western blot analysis and tracking the change of the protein complex LC3-I to LC3-II. MAP-LC3 is a major constituent of the autophagosome, a double membraned structure that sequesters the target organelle/protein and then fuses with endo/lysosomes where the contents and LC3 are degraded. During autophagy, the cytoplasmic form (LC3 I) is processed and recruited to the autophagosome's, where LC3 II is generated by site specific proteolysis and lipidation near to the C-terminus. The hallmark of autophagic activation is thus the formation of cellular autophagosome containing LC3 II, while autophagic activity is measured biochemically as the amount of LC3 II that accumulates in the absence or presence of lysosomal activity (Tanidia et al., 2005) Parthantos can be studied by looking for the over activation of the PARP-1 enzyme using western blot analysis accompanied with

fluorescence microscopy of the PAR polymer formed. In order to ensure that no mechanistic changes are missed a more expansive time point regime is required and earlier time points of 1, 4, 8, 12, 16 and 24 hours should be included.

Although western blotting was a good technique for measuring protein levels in the cell cycle, there was little change in total protein levels after OP exposure. In future studies it may be useful to employ a more sensitive technique such as flow cytometry. Briefly, the DNA content of a cell can be quantitatively measured by flow cytometry. A permeabilized single cell solution has a fluorescent dye added to it. The dye binds stoichiometrically to the DNA meaning that the amount of stained material that is incorporated into the cell will be in proportion to the amount of DNA. The stained material is then measured in the flow cytometer and the emitted fluorescent signal yields an electronic pulse with amplitude proportional to the total fluorescence emission from the cell. Thereafter, such fluorescence data are considered a measurement of the cellular DNA content. Since the data obtained is not a direct measure of cellular DNA content, reference cells with various amounts of DNA should be included in order to identify the position of the cells with the normal diploid amount of DNA. In addition to determining the relative cellular DNA content, flow cytometry also enables the identification of the cell distribution during the various phases of the cell cycle. Four distinct phases could be recognized in a proliferating cell population: the G1-, S- (DNA synthesis phase), G2- and M-phase (mitosis). In addition to cell cycle effects flow cytometry could be used to measure and quantify γ-H2AX, this would be useful as this would allow for an accurate percentage of cells showing DNA damage.

To relate in vitro results to the in vivo exposure situation it is important to look at the effects of chronic exposure of cells to nM concentrations of OPs. This would allow for comparison with the acute effects reported here, to see if the rapid DNA damage seen here has lasting effect over a longer period of time. For example the relatively small level of cytotoxicity observed with nM concentrations of OP at 1 and 24 hours increased over time could be the initial signs of cell death or show signs of recovery when monitored for a longer

time period. In the case of DNA damage it would be interesting to see if the damage seen at 1 and 24 hours was repaired during a chronic exposure.

These studies have confirmed that two organophosphate pesticides with differing structures and the nerve agent sarin could induce DNA damage in cells in culture but to differing degrees and duration. Further investigations of cell signalling and repair indicated that the damage could either be repaired or the damage leads to cell death. These studies have shown that comparative studies using less toxic and available organophosphates can be extrapolated to understand the toxic effects of nerve agents. The concentration of organophosphate to which cells might be exposed in vivo in individuals on the periphery of an accidental exposure scenario for whom the acute effects of acetylcholinesterase inhibition would not be fatal due to metabolism and in the case of accidental exposure only primary exposure sites such as lung and skin would be exposed to high concentrations of OP where DNA damage might be induced. Further investigation is required to confirm the relation between exposure and effect in target tissues both in vitro and in vivo in animal models

These studies have shown that in vitro exposure of cells in culture to sarin at nM to µM concentrations could cause low level DNA damage. These observations may have implications for the exposure of the civilian population at the periphery of a release incident who does not suffer acute effects. An important future aim is to answer the question; will sub-lethal sarin exposure cause genotoxic effects? This would best be further investigated using comparative in vitro and in vivo studies, conducted in animals, with relevant concentrations of sarin. These studies could assess the risk to the population of DNA damage and development of cancer; however selection of an appropriate dose will be crucial. The most highly exposed cells in vivo would be in skin or airways and these should be investigated. The results present here suggest that cells may be able to repair low levels of DNA damage and the repair enzymes involved should be investigated in vivo. The type of DNA damage caused needs to be investigated and whether DNA damage may be induced by oxidative stress or as the result of direct formation of a DNA adduct. Newly synthesised OPs

should have genotoxicity tests included in the screening evaluation as these studies here have demonstrated that OPs can cause DNA damage and increased incidence of cancer has been seen in end users such as farmers and crop sprayers.

# *References*

Abu-Qare, A. W., and Abou-Donia, M. B. (2002). Sarin: Health effects, metabolism, and methods of analysis. *Food and Chemical Toxicology* **40**, 1327-1333.

Agarwala, S., Chen, W., and Cook, T. J. (2004). Effect of chlorpyrifos on efflux transporter gene expression and function in Caco-2 cells. *Toxicology in Vitro* **18**, 403-409.

Allinson, S. L., Sleeth, K. M., Matthewman, G. E., and Dianov, G. L. (2004). Orchestration of base excision repair by controlling the rates of enzymatic activities. *DNA Repair* **3**, 23-31.

Amer, S. M., and Fahmy, M. A. (1982). Cytogenetic effects of pesticides. I. Induction of micronuclei in mouse bone marrow by the insecticide Dursban. *Mutation Research* **101**, 247-255.

Andrabi, S. A., Kim, N. S., Yu, S. W., Wang, H., Koh, D. W., Sasaki, M., Klaus, J. A., Otsuka, T., Zhang, Z., Koehler, R. C., Hurn, P. D., Poirier, G. G., Dawson, V. L., and Dawson, T. M. (2006). Poly(ADP-ribose) (PAR) polymer is a death signal. *Proc Natl Acad Sci U S A* **103**, 18308-18313.

Atherton-Fessler, S., Liu, F., Gabrielli, B., Lee, M. S., Peng, C. Y., and Piwnica-Worms, H. (1994). Cell cycle regulation of the p34(cdc2) inhibitory kinases. *Molecular Biology of the Cell* **5**, 989-1001.

Atherton, K. M., Williams, F. M., Egea GonzÃ¡lez, F. J., Glass, R., Rushton, S., Blain, P. G., and Mutch, E. (2009). DNA damage in horticultural farmers: A pilot study showing an association with organophosphate pesticide exposure. *Biomarkers* **14**, 443-451.

Atherton, K. M., Williams, F. M., Jameson, S., and Mutch, E. (2006). DNA damage by dichlorvos and repair profiles in human lymphocytes, in vitro. *Toxicology* **226**, 53-53.

Bagchi, D., Bagchi, M., Hassoun, E. A., and Stohs, S. J. (1995). In vitro and in vivo generation of reactive oxygen species, DNA damage and lactate dehydrogenase leakage by selected pesticides. *Toxicology* **104**, 129-140.

Barr, D. B., Allen, R., Olsson, A. O., Bravo, R., Caltabiano, L. M., Montesano, A., Nguyen, J., Udunka, S., Walden, D., Walker, R. D., Weerasekera, G., Whitehead Jr, R. D., Schober, S. E., and Needham, L. L. (2005). Concentrations of selective metabolites of organophosphorus pesticides in the United States population. *Environmental Research* **99**, 314-326.

Bartek, J., and Lukas, J. (2007). DNA damage checkpoints: from initiation to recovery or adaptation. *Curr Opin Cell Biol* **19**, 238-245.

.

Batty, D. P., and Wood, R. D. (2000). Damage recognition in nucleotide excision repair of DNA. *Gene* **241**, 193-204.

Benoit-Marquié, F., De Montety, C Gilard, V. Martino, R. Maurette, M. T. and Malet-Martino, M. (2003) Dichlorvos degradation studied by $^{31}$P-NMR Environmental Chemistry Letters Volume 2, Number 2, 93-97.

Ben-Yehoyada, M., Gautier, J., and DuprÃ©, A. (2007). The DNA damage response during an unperturbed S-phase. *DNA Repair* **6**, 914-922.

Blattner, C., Tobiasch, E., Litfen, M., Rahmsdorf, H. J., and Herrlich, P. (1999). DNA damage induced p53 stabilization: no indication for an involvement of p53 phosphorylation. *Oncogene* **18**, 1723-1732

Booth, E. D., Jones, E., and Elliott, B. M. (2007). Review of the in vitro and in vivo genotoxicity of dichlorvos. *Regul Toxicol Pharmacol* **49**, 316-326.

Bouchard, V. J., Rouleau, M., and Poirier, G. G. (2003). PARP-1, a determinant of cell survival in response to DNA damage. *Experimental Hematology* **31**, 446-454.

Boulton, S., Pemberton, L. C., Porteous, J. K., Curtin, N. J., Griffin, R. J., Golding, B. T., and Durkacz, B. W. (1995). Potentiation of temozolomide-induced cytotoxicity: a comparative

study of the biological effects of poly(ADP-ribose) polymerase inhibitors. *Br J Cancer* **72**, 849-856.

Bowman, K. J., White, A., Golding, B. T., Griffin, R. J., and Curtin, N. J. (1998). Potentiation of anti-cancer agent cytotoxicity by the potent poly(ADP-ribose) polymerase inhibitors NU1025 and NU1064. *Br J Cancer* **78**, 1269-1277.

Bridges, B. A., Mottershead, R. P., Green, M. H. L., and Gray, W. J. H. (1973). Mutagenicity of dichlorvos and methyl methane sulphonate for Escherichia coli WP2 and some derivatives deficient in DNA repair. *Mutation Research* **19**, 295-303.

Brzak, K. A., Harms, D. W., Bartels, M. J., and Nolan, R. J. (1998). Determination of chlorpyrifos, chlorpyrifos oxon, and 3,5,6-trichloro- 2-pyridinol in rat and human blood. *Journal of Analytical Toxicology* **22**, 203-210.

Bullman, T. A., Mahan, C. M., Kang, H. K., and Page, W. F. (2005). Mortality in US Army Gulf War veterans exposed to 1991 Khamisiyah chemical munitions destruction. *American Journal of Public Health* **95**, 1382-1388.

Buratti, F. M., Volpe, M. T., Meneguz, A., Vittozzi, L., and Testai, E. (2003). CYP-specific bioactivation of four organophosphorothioate pesticides by human liver microsomes. *Toxicology and Applied Pharmacology* **186**, 143-154.

Burma, S., Chen, B. P., and Chen, D. J. (2006). Role of non-homologous end joining (NHEJ) in maintaining genomic integrity. *DNA Repair (Amst)* **5**, 1042-1048.

Chambers, J. E., and Oppenheimer, S. F. (2004). Organophosphates, serine esterase inhibition, and modeling of organophosphate toxicity. *Toxicological Sciences* **77**, 185-187.

Cho, C. M. H., Mulchandani, A., and Chen, W. (2004). Altering the substrate specificity of organophosphorus hydrolase for enhanced hydrolysis of chlorpyrifos. *Applied and Environmental Microbiology* **70**, 4681-4685.

Chunyuan, L., Saxena, A., Smith, M., Garcia, G., RadicÌ, Z., Taylor, P., and Doctor, B. P. (1999). Phosphoryl oxime inhibition of acetylcholinesterase during oxime reactivation is prevented by edrophonium. *Biochemistry* **38**, 9937-9947.

Colin, J., Gaumer, S., Guenal, I., and Mignotte, B. (2009). Mitochondria, Bcl-2 family proteins and apoptosomes: of worms, flies and men. *Front Biosci* **14**, 4127-4137

Collins, A. R., Dobson, V. L., DusÌŒinskaÌ , M., Kennedy, G., and SÌŒteÌŒtina, R. (1997). The comet assay: What can it really tell us? *Mutation Research - Fundamental and Molecular Mechanisms of Mutagenesis* **375**, 183-193.

Costa, L. G. (2006). Current issues in organophosphate toxicology. *Clinica Chimica Acta* **366**, 1-13.

Costa, L. G., Cole, T. B., Vitalone, A., and Furlong, C. E. (2005). Measurement of paraoxonase (PON1) status as a potential biomarker of susceptibility to organophosphate toxicity. *Clin Chim Acta* **352**, 37-47.

Costa, L. G., Cole, T. B., and Furlong, C. E. (2003). Polymorphisms of paraoxonase (PON1) and their significance in clinical toxicology of organophosphates. *J Toxicol Clin Toxicol* **41**, 37-45.

Costa, L. G., Richter, R. J., Li, W. F., Cole, T., Guizzetti, M., and Furlong, C. E. (2003). Paraoxonase (PON 1) as a biomarker of susceptibility for organophosphate toxicity. *Biomarkers* **8**, 1-12.

Crumpton, T. L., Seidler, F. J., and Slotkin, T. A. (2000). Is oxidative stress involved in the developmental neurotoxicity of chlorpyrifos? *Brain Res Dev Brain Res* **121**, 189-195.

Cuadrado, M., Martinez-Pastor, B., and Fernandez-Capetillo, O. (2006). "ATR activation in response to ionizing radiation: Still ATM territory". *Cell Division* **1**.

Cui, Y., Guo, J., Xu, B., and Chen, Z. (2011) Genotoxicity of chlorpyrifos and cypermethrin to ICR mouse hepatocytes. *Toxicol Mech Methods* **21**, 70-74.

Cui, Y., Guo, J., Xu, B., and Chen, Z. (2006). Potential of chlorpyrifos and cypermethrin forming DNA adducts. *Mutation Research - Genetic Toxicology and Environmental Mutagenesis* **604**, 36-41.

Dan, S., and Yamori, T. (2001). Repression of cyclin B1 expression after treatment with adriamycin, but not cisplatin in human lung cancer A549 cells. *Biochemical and Biophysical Research Communications* **280**, 861-867.

Dave, J. R., Connors, R. A., Genovese, R. F., Whipple, R. A., Chen, R. W., DeFord, S. M., Moran, A. V., and Tortella, F. C. (2007). DNA fragmentation in leukocytes following repeated low dose sarin exposure in guinea pigs. *Cellular and Molecular Life Sciences* **64**, 2823-2828.

Davies, H. G., Richter, R. J., Keifer, M., Broomfield, C. A., Sowalla, J., and Furlong, C. E. (1996). The effect of the human serum paraoxonase polymorphism is reversed with diazoxon, soman and sarin. *Nature genetics* **14**, 334-336.

Doherty, A. T., Ellard, S., Parry, E. M., and Parry, J. M. (1996). A study of the aneugenic activity of trichlorfon detected by centromere-specific probes in human lymphoblastoid cell lines. *Mutat Res* **372**, 221-231.

DrablÃ¸s, F., Feyzi, E., Aas, P. A., VaagbÃ¸, C. B., Kavli, B., Bratlie, M. S., PeÃ±a-Diaz, J., Otterlei, M., Slupphaug, G., and Krokan, H. E. (2004). Alkylation damage in DNA and RNA - Repair mechanisms and medical significance. *DNA Repair* **3**, 1389-1407.

Dreiher, J., Novack, V., Barachana, M., Yerushalmi, R., Lugassy, G., and Shpilberg, O. (2005). Non-Hodgkin's lymphoma and residential proximity to toxic industrial waste in southern Israel. *Haematologica* **90**, 1709-1710.

Dudas, A., and Chovanec, M. (2004). DNA double-strand break repair by homologous recombination. *Mutat Res* **566**, 131-167.

Dumaz, N., and Meek, D. W. (1999). Serine15 phosphorylation stimulates p53 transactivation but does not directly influence interaction with HDM2. *EMBO J* **18**, 7002-7010.

Eguchi, Y., Shimizu, S., and Tsujimoto, Y. (1997). Intracellular ATP levels determine cell death fate by apoptosis or necrosis. *Cancer Research* **57**, 1835-1840.

Evans, M. D., Dizdaroglu, M., and Cooke, M. S. (2004). Oxidative DNA damage and disease: Induction, repair and significance. *Mutation Research - Reviews in Mutation Research* **567**, 1-61.

Ewing, K. J., and Lerner, B. (2001). Infrared detection of the nerve agent Sarin (isopropyl methylphosphonofluoridate) in water using magnesium oxide for preconcentration. *Applied Spectroscopy* **55**, 407-411.

Fotakis, G., and Timbrell, J. A. (2006). In vitro cytotoxicity assays: Comparison of LDH, neutral red, MTT and protein assay in hepatoma cell lines following exposure to cadmium chloride. *Toxicology Letters* **160**, 171-177.

Friedberg, E. C. (2004). The discovery that xeroderma pigmentosum (XP) results from defective nucleotide excision repair. *DNA Repair (Amst)* **3**, 183, 195.

Furlong, C. E., Suzuki, S. M., Stevens, R. C., Marsillach, J., Richter, R. J., Jarvik, G. P., Checkoway, H., Samii, A., Costa, L. G., Griffith, A., Roberts, J. W., Yearout, D., and Zabetian, C. P (2010). Human PON1, a biomarker of risk of disease and exposure. *Chemico-Biological Interactions* **187**, 355-361.

Furlong, C. E., Cole, T. B., Jarvik, G. P., and Costa, L. G. (2002). Pharmacogenomic considerations of the paraoxonase polymorphisms. *Pharmacogenomics* **3**, 341-348.

Gan, Q., Singh, R. M., Wu, T., and Jans, U. (2006). Kinetics and mechanism of degradation of dichlorvos in aqueous solutions containing reduced sulfur species. *Environmental Science and Technology* **40**, 5717-5723.

Giordano, G., Afsharinejad, Z., Guizzetti, M., Vitalone, A., Kavanagh, T. J., and Costa, L. G. (2007). Organophosphorus insecticides chlorpyrifos and diazinon and oxidative stress in neuronal cells in a genetic model of glutathione deficiency. *Toxicol Appl Pharmacol* **219**, 181-189.

Goldman, M., A. K., Klein, Kawakami, and L.S. Rosenblatt, 1987, DTIC AD-A187841, Subject: "Toxicity studies on agents GB and GD," Ft Detrick, MD: Laboratory for Energy-Related Health Research, US Army Medical Research and Development Command.

Gollapudi, B. B., Mendrala, A. L., and Linscombe, V. A. (1995). Evaluation of the genetic toxicity of the organophosphate insecticide chlorpyrifos. *Mutation Research - Genetic Toxicology* **342**, 25-36.

Green, M. H. L., Medcalf, A. S. C., Arlett, C. F., Harcourt, S. A., and Lehmann, A. R. (1974). DNA strand breakage caused by dichlorvos, methyl methanesulphonate and iodoacetamide in Escherichia coli and cultured chinese hamster cells. *Mutation Research/Fundamental and Molecular Mechanisms of Mutagenesis* **24**, 365-378.

Griffin, D. E., and Hill, W. E. (1978). In vitro plasmid DNA breakage by mutagens and pesticides. *Mutation Research* **53**.

Gupta, S. C., Mishra, M., Sharma, A., Deepak Balaji, T. G. R., Kumar, R., Mishra, R. K., and Chowdhuri, D. K. Chlorpyrifos induces apoptosis and DNA damage in Drosophila through generation of reactive oxygen species. *Ecotoxicology and Environmental Safety* **73**, 1415-1423.

Ha, H. C., and Snyder, S. H. (1999). Poly(ADP-ribose) polymerase is a mediator of necrotic cell death by ATP depletion. *Proc Natl Acad Sci U S A* **96**, 13978-13982.

Hatjian, B. A., Mutch, E., Williams, F. M., Blain, P. G., and Edwards, J. W. (2000). Cytogenetic response without changes in peripheral cholinesterase enzymes following exposure to a sheep dip containing diazinon in vivo and in vitro. *Mutat Res* **472**, 85-92.

Heacock, M. L., Stefanick, D. F., Horton, J. K., and Wilson, S. H. (2010). Alkylation DNA damage in combination with PARP inhibition results in formation of S-phase-dependent double-strand breaks. *DNA Repair* **9**, 929-936.

Holstege, C. P., Kirk, M., and Sidell, F. R. (1997). Chemical warfare. Nerve agent poisoning. *Crit Care Clin* **13**, 923-942.

Ichihashi, M., Ueda, M., Budiyanto, A., Bito, T., Oka, M., Fukunaga, M., Tsuru, K., and Horikawa, T. (2003). UV-induced skin damage. *Toxicology* **189**, 21-39.

Jacobberger, J. W., Sramkoski, R. M., Zhang, D., Zumstein, L. A., Doerksen, L. D., Merritt, J. A., Wright, S. A., and Shults, K. E. (1999). Bivariate analysis of the p53 pathway to evaluate Ad-p53 gene therapy efficacy. *Cytometry* **38**, 201-213.

Jackson, S. P. (2002). Sensing and repairing DNA double-strand breaks. *Carcinogenesis* **23**, 687-696.

Jeggo, P. A., and Lobrich, M. (2006). Contribution of DNA repair and cell cycle checkpoint arrest to the maintenance of genomic stability. *DNA Repair (Amst)* **5**, 1192-1198.

Jowsey, P. A., Williams, F. M., and Blain, P. G. (2009). DNA damage, signalling and repair after exposure of cells to the sulphur mustard analogue 2-chloroethyl ethyl sulphide. *Toxicology* **257**, 105-112.

Kinner, A., Wu, W., Staudt, C., and Iliakis, G. (2008). Gamma-H2AX in recognition and signaling of DNA double-strand breaks in the context of chromatin. *Nucleic Acids Res* **36**, 5678-5694.

Kitazumi, I., and Tsukahara, (2010) M. Regulation of DNA fragmentation: the role of caspases and phosphorylation. *Febs J* **278**, 427-441.

Klein, A. K., Nasr, M. L., and Goldman, M. (1987). The effects of in vitro exposure to the neurotoxins sarin (GB) and soman (GD) on unscheduled DNA synthesis by rat hepatocytes. *Toxicol Lett* **38**, 239-249.

Kligerman, A. D., Erexson, G. L., and Wilmer, J. L. (1985). Induction of sister-chromatid exchange (SCE) and cell-cycle inhibition in mouse peripheral blood B lymphocytes exposed to mutagenic carcinogens in vivo. *Mutat Res* **157**, 181-187.

Knudsen, E. S., and Wang, J. Y. J. (1997). Dual mechanisms for the inhibition of E2F binding to RB by cyclin- dependent kinase-mediated RB phosphorylation. *Molecular and Cellular Biology* **17**, 5771-5783.

Kroemer, G., and Levine, B. (2008). Autophagic cell death: The story of a misnomer. *Nature Reviews Molecular Cell Biology* **9**, 1004-1010.

Kumaravel, T. S., Vilhar, B., Faux, S. P., and Jha, A. N. (2009). Comet Assay measurements: A perspective. *Cell Biology and Toxicology* **25**, 53-64.

Lawley, P. D., Shah, S. A., and Orr, D. J. (1974). Methylation of nucleic acids by 2,2-dichlorovinyl dimethyl phosphate (dichlorvos, DDVP). *Chem Biol Interact* **8**, 171-182.

Lehmann, A. R. (2003). DNA repair-deficient diseases, xeroderma pigmentosum, Cockayne syndrome and trichothiodystrophy. *Biochimie* **85**, 1101-1111.

Leist, M., Single, B., Castoldi, A. F., Kuhnle, S., and Nicotera, P. (1997). Intracellular adenosine triphosphate (ATP) concentration: a switch in the decision between apoptosis and necrosis. *J Exp Med* **185**, 1481-1486.

Levine, B., and Yuan, J. (2005). Autophagy in cell death: An innocent convict? *Journal of Clinical Investigation* **115**, 2679-2688.

Li, Q., Hirata, Y., Kawada, T., and Minami, M. (2004). Elevated frequency of sister chromatid exchanges of lymphocytes in sarin-exposed victims of the Tokyo sarin disaster 3 years after the event. *Toxicology* **201**, 209-217.

Li, Q., Hirata, Y., Piao, S., and Minami, M. (2000). The by-products generated during sarin synthesis in the Tokyo sarin disaster induced inhibition of natural killer and cytotoxic T lymphocyte activity. *Toxicology* **146**, 209-220.

Locksley, R. M., Killeen, N., and Lenardo, M. J. (2001). The TNF and TNF receptor superfamilies: Integrating mammalian biology. *Cell* **104**, 487-501.

Lorenzo, H. K., and Susin, S. A. (2007). Therapeutic potential of AIF-mediated caspase-independent programmed cell death. *Drug Resistance Updates* **10**, 235-255.

Luo, C., Saxena, A., Smith, M., Garcia, G., Radic, Z., Taylor, P., and Doctor, B. P. (1999). Phosphoryl oxime inhibition of acetylcholinesterase during oxime reactivation is prevented by edrophonium. *Biochemistry* **38**, 9937-9947.

Matsuda, Y., Nagao, M., Takatori, T., Niijima, H., Nakajima, M., Iwase, H., Kobayashi, M., and Iwadate, K. (1998). Detection of the sarin hydrolysis product in formalin-fixed brain tissues of victims of the Tokyo subway terrorist attack. *Toxicol Appl Pharmacol* **150**, 310-320.

Meeker, J. D., Singh, N. P., Ryan, L., Duty, S. M., Barr, D. B., Herrick, R. F., Bennett, D. H., and Hauser, R. (2004). Urinary levels of insecticide metabolites and DNA damage in human sperm. *Human Reproduction* **19**, 2573-2580.

Meikle, R. W., Kurihara, N. H., and De Vries, D. H. (1983). Chlorpyrifos: The photodecomposition rates in dilute aqueous solution and on a surface, and the volatilization rate from a surface. *Archives of Environmental Contamination and Toxicology* **12**, 189-193.

Minami, M., Hui, D. M., Katsumata, M., Inagaki, H., and Boulet, C. A. (1997). Method for the analysis of the methylphosphonic acid metabolites of sarin and its ethanol-substituted analogue in urine as applied to the victims of the Tokyo sarin disaster. *Journal of Chromatography B: Biomedical Applications* **695**, 237-244.

Moretto, A., Lotti, M., and Ramesh, C. G. (2006). Peripheral Nervous System Effects and Delayed Neuropathy. In *Toxicology of Organophosphate & Carbamate Compounds*, pp. 361-370. Academic Press, Burlington.

Munro, N. B., Talmage, S. S., Griffin, G. D., Waters, L. C., Watson, A. P., King, J. F., and Hauschild, V. (1999). The sources, fate, and toxicity of chemical warfare agent degradation products. *Environmental Health Perspectives* **107**, 933-974.

Munoz, I. M., Jowsey, P. A., Toth, R., and Rouse, J. (2007). Phospho-epitope binding by the BRCT domains of hPTIP controls multiple aspects of the cellular response to DNA damage. *Nucleic Acids Res* **35**, 5312-5322.

Muscarella, D. E., Keown, J. F., and Bloom, S. E. (1984). Evaluation of the genotoxic and embryotoxic potential of chlorpyrifos and its metabolites in vivo and in vitro. *Environmental Mutagenesis* **6**, 13-23.

Mutch, E., Kelly, S. S., Blain, P. G., and Williams, F. M. (1995). Comparative studies of two organophosphorus compounds in the mouse. *Toxicol Lett* **81**, 45-53.

Mutch, E., and Williams, F. M. (2006). Diazinon, chlorpyrifos and parathion are metabolised by multiple cytochromes P450 in human liver. *Toxicology* **224**, 22-32.

Nagata, S., Nagase, H., Kawane, K., Mukae, N., and Fukuyama, H. (2003). Degradation of chromosomal DNA during apoptosis. *Cell Death Differ* **10**, 108-116.

Nehez, M., Toth, C., and Desi, I. (1994). The effect of dimethoate, dichlorvos, and parathion-methyl on bone marrow cell chromosomes of rats in subchronic experiments in vivo. *Ecotoxicol Environ Saf* **29**, 365-371.

Nilsen, H., and Krokan, H. E. (2001). Base excision repair in a network of defence and tolerance. *Carcinogenesis* **22**, 987-998.

Nolan, R. J., Rick, D. L., Freshour, N. L., and Saunders, J. H. (1984). Chlorpyrifos: Pharmacokinetics in human volunteers. *Toxicology and Applied Pharmacology* **73**, 8-15.

Opresko, Dr. Dennis M., R.A. Young, A.P. Watson, R.A. Faust, S.S. Talmage, R.A. Ross, K.A. Davidson, J. King, and Veronique Hauschild, (2001), "Chemical Warfare Agents: Current Status of Oral Reference Doses," Review of Environmental Contamination and Toxicology, Springer-Verlag, 2001, Vol. 172, p. 65-85.

Patel, S., Bajpayee, M., Pandey, A. K., Parmar, D., and Dhawan, A. (2007). In vitro induction of cytotoxicity and DNA strand breaks in CHO cells exposed to cypermethrin, pendimethalin and dichlorvos. *Toxicology in Vitro* **21**, 1409-1418.

Paulsen, R. D., and Cimprich, K. A. (2007). The ATR pathway: Fine-tuning the fork. *DNA Repair* **6**, 953-966.

Paz-y-Mino, C., Davalos, M. V., Sanchez, M. E., Arevalo, M., and Leone, P. E. (2002). Should gaps be included in chromosomal aberration analysis? Evidence based on the comet assay. *Mutat Res* **516**, 57-61.

Perlow-Poehnelt, R. A., Zharkov, D. O., Grollman, A. P., and Broyde, S. (2004). Substrate discrimination by formamidopyrimidine-DNA glycosylase: Distinguishing interactions within the active site. *Biochemistry* **43**, 16092-16105.

Perrotta, D.M., 1996, "Long-term health effects associated with sub-clinical exposures to GB and mustard: A Review by the Environment Committee," Armed Forces Epidemiological Board, Washington, DC.

Rami, A. (2009). Review: autophagy in neurodegeneration: firefighter and/or incendiarist? *Neuropathol Appl Neurobiol* **35**, 449-461.

Rahman, M. F., Mahboob, M., Danadevi, K., Saleha Banu, B., and Grover, P. (2002). Assessment of genotoxic effects of chloropyriphos and acephate by the comet assay in mice leucocytes. *Mutation Research - Genetic Toxicology and Environmental Mutagenesis* **516**, 139-147.

Reinhardt, H. C., and Yaffe, M. B. (2009). Kinases that control the cell cycle in response to DNA damage: Chk1, Chk2, and MK2. *Current Opinion in Cell Biology* **21**, 245-255.

Sasaki YF, Sekihashi K, Izumiyama F, Nishidate E, Saga A, Ishida K, tsuda S. (2000). The Comet Assay with multiple mouse organs: comparison of Comet Assay results and carcinogenicity with 208 chemicals selected from the IARC monographs and U.S. NTP carcinogenicity database. Critical Reviews in Toxicology, **30**, 629-799.

Salazar-Arredondo, E., de Jesus Solis-Heredia, M., Rojas-Garcia, E., Hernandez-Ochoa, I., and Quintanilla-Vega, B. (2008). Sperm chromatin alteration and DNA damage by methyl-parathion, chlorpyrifos and diazinon and their oxon metabolites in human spermatozoa. *Reprod Toxicol* **25**, 455-460.

Schop, R. N., Hardy, M. H., and Goldberg, M. T. (1990). Comparison of the activity of topically applied pesticides and the herbicide 2,4-D in two short-term in vivo assays of genotoxicity in the mouse. *Fundam Appl Toxicol* **15**, 666-675.

Sherr, C. J. (1996). Cancer cell cycles. *Science* **274**, 1672-1677.

Shirname-More, L. (1991). Smokeless tobacco extracts mutate human cells. *Carcinogenesis* **12**, 927-930.

Sirivarasai, J., Kaojarern, S., Yoovathaworn, K., and Sura, T. (2007). Paraoxonase (PON1) polymorphism and activity as the determinants of sensitivity to organophosphates in human subjects. *Chem Biol Interact* **168**, 184-192.

Sogorb, M. A., and Vilanova, E. (2002). Enzymes involved in the detoxification of organophosphorus, carbamate and pyrethroid insecticides through hydrolysis. *Toxicol Lett* **128**, 215-228.

Susin, S. A., Lorenzo, H. K., Zamzami, N., Marzo, I., Snow, B. E., Brothers, G. M., Mangion, J., Jacotot, E., Costantini, P., Loeffler, M., Larochette, N., Goodlett, D. R., Aebersold, R., Siderovski, D. P., Penninger, J. M., and Kroemer, G. (1999). Molecular characterization of mitochondrial apoptosis-inducing factor. *Nature* **397**, 441-446.

Tanida, I., Minematsu-Ikeguchi, N., Ueno, T., and Kominami, E. (2005). Lysosomal turnover, but not a cellular level, of endogenous LC3 is a marker for autophagy. *Autophagy* **1**, 84-91.

Tungul, A., Bonin, A. M., He, S., and Baker, R. S. U. (1991). Micronuclei induction by dichlorvos in the mouse skin. *Mutagenesis* **6**, 405-408.

Vale, A. (2005). What lessons can we learn from the Japanese sarin attacks? *Przegl Lek* **62**, 528-532.

Wellman, S. E., and Kramer, R. E. (2004). Absence of DNA binding activity of methyl parathion and chlorpyrifos. *Toxicology Mechanisms and Methods* **14**, 247-251.

Wessels, D., Barr, D. B., and Mendola, P. (2003). Use of biomarkers to indicate exposure of children to organophosphate pesticides: Implications for a longitudinal study of children's environmental health. *Environmental Health Perspectives* **111**, 1939-1946.

Williams, B. L., Hornig, M., Yaddanapudi, K., and Lipkin, W. I. (2008). Hippocampal poly(ADP-ribose) polymerase 1 and caspase 3 activation in neonatal bornavirus infection. *Journal of Virology* **82**, 1748-1758.

Wooder M. F, Wright, A.S. and King L.J., 1977.In vivo alkylation studies with dichlorvos at practical use concentrations. Chem.-Biol. Interactions 19 (1977) 25-46. *Chemico-Biological Interactions* **20**, 262.

Worek, F., Koller, M., Thiermann, H., and Szinicz, L. (2005). Diagnostic aspects of organophosphate poisoning. *Toxicology* **214**, 182-189.

Yamano, T. (1996). Dissociation of DDVP-induced DNA strand breaks from oxidative damage in isolated rat hepatocytes. *Toxicology* **108**, 49-56.

Yang, C. C., and Deng, J. F. (2007). Intermediate syndrome following organophosphate insecticide poisoning. *J Chin Med Assoc* **70**, 467-472.

Yu, S. W., Wang, H., Poitras, M. F., Coombs, C., Bowers, W. J., Federoff, H. J., Poirier, G. G., Dawson, T. M., and Dawson, V. L. (2002). Mediation of poly(ADP-ribose) polymerase-1-dependent cell death by apoptosis-inducing factor. *Science* **297**, 259-263.

# *Bibliography*

Amvac Chemical Company (2011) Nuvan 50 EC Material Safety Data Sheet. http://www.amvac-chemical.com/nuvan_labels.html, accessed 14th April 2011

Dow Agrosciences (2011) Dursban 480 EC Material Safety Data Sheet. http://www.dowagro.com/za/product/, accessed 14th April 2011

Craig Moore, PhD thesis: "In vitro modelling of dermal absorption following environmental or accidental exposure". Submitted October 2010. Newcastle University